

IP and Broadcasting Systems Convergence

Guest Editors: Georgios Gardikis, George Xilouris, Marie-Jose Montpetit,
Alessandro Vanelli-Coralli, and Daniel Negru





IP and Broadcasting Systems Convergence

International Journal of Digital Multimedia Broadcasting

IP and Broadcasting Systems Convergence

Guest Editors: Georgios Gardikis, George Xilouris,
Marie-Jose Montpetit, Alessandro Vanelli-Coralli,
and Daniel Negru



Copyright © 2010 Hindawi Publishing Corporation. All rights reserved.

This is a special issue published in volume 2010 of “International Journal of Digital Multimedia Broadcasting.” All articles are open access articles distributed under the Creative Commons Attribution License, which permits unrestricted use, distribution, and reproduction in any medium, provided the original work is properly cited.

Editorial Board

S. S. Agaian, USA

Jörn Altmann, Republic of Korea

Ivan Bajic, Canada

John Buford, USA

Stefania Colonnese, Italy

Gerard Faria, France

Borko Furht, USA

Rajamani Ganesh, India

Yifeng He, Canada

Jukka Henriksson, Finland

Shuji Hirakawa, Japan

Y. Hu, USA

Jenq-Neng Hwang, USA

Daniel Iancu, USA

T. Kaiser, Germany

Dimitra Kaklamani, Greece

Markus Kampmann, Germany

Alexander Korotkov, Russia

Harald Kosch, Germany

Massimiliano Laddomada, USA

Jaime Lloret, Spain

Steven Loh, USA

Fa-Long Luo, USA

Thomas Magedanz, Germany

Guergana S. Mollova, Austria

Marie-Jose Montpetit, USA

Beatrice Pesquet-Popescu, France

K. R. Rao, USA

Marco Rocchetti, Italy

Ravi S. Sharma, Singapore

Wanggen Wan, China

Fujio Yamada, Brazil

Xenophon Zabulis, Greece

Liangpei Zhang, China

Chi Zhou, USA

Contents

IP and Broadcasting Systems Convergence, Georgios Gardikis, George Xilouris, Marie-Jose Montpetit, Alessandro Vanelli-Coralli, and Daniel Negru
Volume 2010, Article ID 382931, 2 pages

Hybrid Terrestrial-Satellite DVB/IP Infrastructure in Overlay Constellations for Triple-Play Services Access in Rural Areas, E. Pallis, D. Negru, and A. Bourdena
Volume 2010, Article ID 913421, 11 pages

Video Quality Prediction Models Based on Video Content Dynamics for H.264 Video over UMTS Networks, Asiya Khan, Lingfen Sun, Emmanuel Ifeakor, Jose-Oscar Fajardo, Fidel Liberal, and Harilaos Koumaras
Volume 2010, Article ID 608138, 17 pages

Cross-Layer Optimization of DVB-T2 System for Mobile Services, Lukasz Kondrad, Vinod Kumar Malamal Vadakital, Imed Bouazizi, Miika Tupala, and Moncef Gabbouj
Volume 2010, Article ID 435405, 13 pages

Design of an IPTV Multicast System for Internet Backbone Networks, T. H. Szymanski and D. Gilbert
Volume 2010, Article ID 169140, 14 pages

A Framework for an IP-Based DVB Transmission Network, Nimbe L. Ewald-Arostegui, Gorry Fairhurst, and Ana Yun-Garcia
Volume 2010, Article ID 394965, 13 pages

On the QoS of IPTV and Its Effects on Home Networks, Dongyu Qiu
Volume 2010, Article ID 253495, 5 pages

Performance Evaluation of Triple Play Services Delivery with E2E QoS Provisioning, Nikolaos Zotos, Evangelos Pallis, and Anastasios Kourtis
Volume 2010, Article ID 836501, 14 pages

Network Performance Evaluation of Abis Interface over DVB-S2 in the GSM over Satellite Network, S. B. Musabekov, P. K. Srinivasan, A. S. Durai, and R. R. Ibrahimov
Volume 2010, Article ID 381526, 8 pages

Editorial

IP and Broadcasting Systems Convergence

**Georgios Gardikis,^{1,2} George Xilouris,² Marie-Jose Montpetit,³
Alessandro Vanelli-Coralli,⁴ and Daniel Negru⁵**

¹*Institute of Informatics and Telecommunications, NCSR “Demokritos”, Agia Paraskevi 15310, Greece*

²*Technological Educational Institute of Crete, Heraklion 71500, Greece*

³*Research Laboratory of Electronics, MIT, Cambridge, MA 02139-4307, USA*

⁴*ARCES, University of Bologna, 40136 Bologna, Italy*

⁵*LaBRI-CNRS, University of Bordeaux, 33405 Talence Cedex, France*

Correspondence should be addressed to Georgios Gardikis, gardikis@iit.demokritos.gr

Received 31 December 2010; Accepted 31 December 2010

Copyright © 2010 Georgios Gardikis et al. This is an open access article distributed under the Creative Commons Attribution License, which permits unrestricted use, distribution, and reproduction in any medium, provided the original work is properly cited.

The vision of the Internet of the Future for service ubiquity dictates that end users should be able to access services—mostly media-oriented ones—at any time from a variety of networks, including mobile, broadband, and broadcast. In order to achieve network interworking and service ubiquity, IP arises as a key element for the realisation of a unified/fusion environment which enables the convergence/synergy between traditional and emerging technologies. In this context, IP can be also seen as the “gluing factor” in the rapidly progressing convergence between the technologically different sectors of Networking and Broadcasting.

This convergence, witnessed both at technological and service levels, is mainly empowered by the evolution of broadcasting standards (DVB, ISDB, ATSC, CMMB) and the recent advances in IP networking.

In this way, a broadcasting platform is no longer restricted to transmitting “bouquets” of TV programs. The ability to include IP services into the broadcast multiplex, along with the large coverage area and the high bit rate capabilities, allows broadcasting systems to constitute flexible broadband IP networking infrastructures, complementing existing and emerging wireless access networks such as 3G, WiMAX, and LTE.

Conversely, the provision of broadcast TV services over IP networks and over the Internet is further fading the borders between the IP/Networking and Broadcast worlds.

The aim of this special issue has been to include recent research efforts focusing on the convergence between the IP and Broadcasting systems, that is, the provision of IP services

over broadcasting platforms and vice versa, the streaming of A/V broadcasting services over IP networks.

An interesting aspect is the use of broadcasting platforms for regional-area IP networking, focusing on rural/underdeveloped areas. In this context, the paper entitled “*Hybrid terrestrial-satellite DVB/IP infrastructure in overlay constellations for triple-play services access in rural areas*” presents the concept, implementation, and experimental evaluation of a novel, dual-layer architecture, where rural customers are served by an interactive DVB-T platform. As an overlay, DVB-T service networks are interconnected by a satellite DVB-S2/DVB-RCS network, which acts as backhaul.

Video traffic is dominant across convergent IP/broadcast networks, and its proper transport and presentation is critical for end user satisfaction. The paper with the title “*Video quality prediction models based on video content dynamics for H.264 video over UMTS networks*” introduces an emulated loss model for H.264 video over data networks, focusing on 3G, and proposes an Adaptive Neural Fuzzy Inference System (ANFIS) and also a second model based on nonlinear regression analysis in order to predict the quality of the video, as perceived by the viewer.

DVB-T2 is the new cutting-edge technology in digital media terrestrial broadcasting. Its Physical Layer Pipes (PLP) feature enables the transmission of different streams with different physical-layer characteristics. The paper entitled “*Cross-layer optimization of DVB-T2 system for mobile services*” combines the PLP feature with Scalable Video Coding

in order to achieve cross-layer optimisation, with a variety of options, and maximise the efficiency of video delivery over DVB-T2 to diverse reception environments.

Delivery of IPTV streams in multicast environments is examined in “*Design of an IPTV multicast system for internet backbone networks.*” The authors present the design of an IPTV multicast system for the Internet backbone network and study it through extensive simulations. Traffic scheduling, shaping, and regeneration techniques are employed at the source and the destination nodes to achieve optimal delivery and a near-perfect end-to-end QoS.

The issue of transporting IP data over a DVB platform is investigated in “*A framework for an IP-based DVB transmission network.*” The paper studies the GS (Generic Stream) and GSE (Generic Stream Encapsulation) schemes which allow direct transport of IP traffic, eliminating the use of the legacy MPEG-2 Transport Stream. Novel approaches are introduced, which replace MPEG-2 signalling with GSE-compliant methods and allow the DVB network to be seamlessly included in an all-IP architecture and act as part of the Internet.

Network-level Quality of Service (QoS) is a critical factor for user satisfaction in IPTV systems. In the paper titled “*On the QoS of IPTV and its effects on home networks.*” the authors propose a queuing model for IPTV systems and use it to analyze the impact of IPTV traffic on other home-network applications. Results show that standard TCP congestion control is not adequate for this purpose and a tuning/optimisation procedure is proposed.

In the same context (i.e., QoS assurance in media delivery), the paper with the title “*Performance evaluation of triple play services delivery with E2E QoS provisioning.*” presents an enhanced core and access network architecture, featuring a WiMAX access network and allowing end-to-end QoS provision. Traffic-class mapping in the core network, following a DiffServ/MPLS approach, is extended to the access part, using native WiMAX QoS support. The efficiency of the mechanism is validated in a real demonstrator environment, where media streams are prioritised over background traffic and properly delivered.

Satellite broadcast networks can be remarkably efficient when used for data backhaul connectivity. The paper entitled “*Network performance evaluation of abis interface over DVB-S2 in the GSM over satellite network.*” investigates the use of a satellite broadcast DVB-S2 channel for interconnecting a GSM Base Station Controller (BSC) with a remote Base Transceiver Station (BTS), that is, for implementing the Abis interface. Extensive ns2-based simulations are employed to optimise transmission parameters and to determine satellite bandwidth and cost requirements for different network setups.

Acknowledgments

We would like to thank all the authors who submitted their work to this special issue and the reviewers for their timely and valuable assistance. We are also grateful to the editing and support personnel of the Journal who helped make this

special issue a reality and especially to the Editor-in-Chief, Dr. Luo, for his invitation and his support throughout the entire process.

Georgios Gardikis
George Xilouris
Marie-Jose Montpetit
Alessandro Vanelli-Coralli
Daniel Negru

Research Article

Hybrid Terrestrial-Satellite DVB/IP Infrastructure in Overlay Constellations for Triple-Play Services Access in Rural Areas

E. Pallis,¹ D. Negru,² and A. Bourdena¹

¹ Applied Informatics and Multimedia Department, Technological Educational Institute of Crete, Estavromenos, Heraklion, 71004 Crete, Greece

² CNRS-LaBRI Laboratory, University of Bordeaux, 351 Cours de la Libération, 33405 Talence Cedex, Bordeaux, France

Correspondence should be addressed to E. Pallis, pallis@iit.demokritos.gr

Received 19 November 2009; Accepted 10 February 2010

Academic Editor: Georgios Gardikis

Copyright © 2010 E. Pallis et al. This is an open access article distributed under the Creative Commons Attribution License, which permits unrestricted use, distribution, and reproduction in any medium, provided the original work is properly cited.

This paper discusses the convergence of digital broadcasting and Internet technologies, by elaborating on the design, implementation, and performance evaluation of a hybrid terrestrial/satellite networking infrastructure, enabling triple-play services access in rural areas. At local/district level, the paper proposes the exploitation of DVB-T platforms in regenerative configurations for creating terrestrial DVB/IP backhaul between the core backbone (in urban areas) and a number of intermediate communication nodes distributed within the DVB-T broadcasting footprint (in rural areas). In this way, triple play services that are available at the core backbone, are transferred via the regenerative DVB-T/IP backhaul to the entire district and can be accessed by rural users via the corresponding intermediate node. On the other hand, at regional/national level, the paper proposes the exploitation of a satellite interactive digital video broadcasting platform (DVB S2/RCS) as an overlay network that interconnects the regenerative DVB-T/IP platforms, as well as individual users, and services providers, to each other. Performance of the proposed hybrid terrestrial/satellite networking environment is validated through experimental tests that were conducted under real transmission/reception conditions (for the terrestrial segment) and via simulation experiments (for the satellite segment) at a prototype network infrastructure.

1. Introduction

Triple-play services provision depends not only on the access network that is usually considered as the last mile network, but also on the connection from the local “point of presence” (e.g., local exchange building) to the core high-capacity backbone network. This connection, which is known as “backhaul”, or the “middle mile” network, constitutes a significant issue for accessing triple-play services especially in dispersed, rural, and less developed areas, that is, those that are far away from the high-capacity core network. The backhaul connection to the nearest available main network node for triple-play services provision can be currently addressed by a variety of proprietary technologies, such as fibre optical, satellite, and microwave radio links [1, 2], the cost of which is proportionally increased to the remoteness, while decreasing as the number of customers is escalated. As a result, and especially in the case of highly

remote/rural communities, and/or low population areas, these technological solutions prove to be unprofitable for the services/network provider, and therefore deployment of backhaul for triple-play services provision still remains an issue in these regions.

While proprietary technologies prohibit individual investments in rural and less developed regions (and therefore backhaul connections for triple-play services access), it is foreseen that technology/services convergence could alleviate these obstacles and pave the way towards cost/economically efficient backhaul solutions. By encouraging synergetic activities among the various technology/service sectors, convergence could play a key role in the realisation of fusion environments that exploit and avail the particularities and complementarities among them, besides being fairly shared and commonly exploited by existing and potential service/network providers. In this context, the paper anticipates that convergence among the Broadcasting and Internet

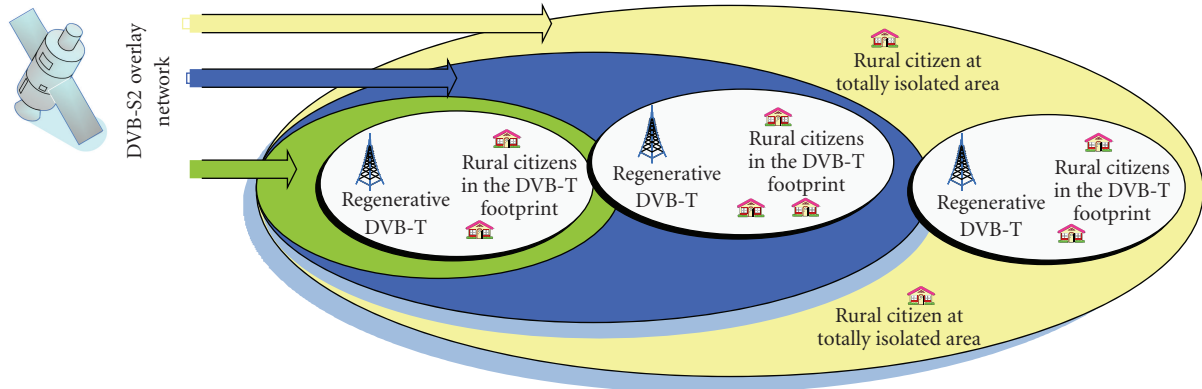


FIGURE 1: Overall architecture of the hybrid terrestrial/satellite infrastructure.

sectors may provide a very promising and cost-effective alternative backhaul solution. Building upon the advances of digital video broadcasting (DVB), and by exploiting their convergence with emerging wired/wireless telecommunication/Internet technologies (xDSL, WLAN, etc.), the paper proposes a hybrid terrestrial/satellite DVB/IP infrastructure capable of providing triple-play services in rural areas, at regional and national level (see Figure 1).

By exploiting the terrestrial digital video broadcasting (DVB-T) stream in regenerative configurations, it designs and implements a unified decentralised networking infrastructure at regional level, which is present and available within the entire broadcasting area. This decentralised infrastructure enables (i) urban citizens to distribute their own content/services to the entire network and (ii) with marginal cost, rural citizens to access/consume triple-play services and to be always-on connected to this unified infrastructure. More specifically, and in respect to rural citizens, the regenerative DVB-T stream acts as backhaul connection (middle-mile network) for extending the core backbone (present at urban areas) till the local PSTN/ISDN exchanger of a rural area, enabling in this way the deployment of xDSL networks as last-mile connections that provide for always-on connectivity.

Towards expanding the proposed concept at national level, the paper proposes the deployment of a number of these DVB/IP platforms at various rural areas and their interconnection via DVB-S2/RCS technology-based satellites. Exploiting the intrinsic characteristic of the DVB-S2 for carrying heterogeneous IP traffic over the same platform, the paper presents the design and implementation of a satellite backhaul connection that acts as an overlay network upon the terrestrial segments (i.e., upon the regenerative DVB-T platforms) for triple-play services provision, besides being able not only to interconnect each other but also individual citizens located at totally isolated rural areas (e.g., dispersed islands, or users outside a DVB-T broadcasting footprint).

Following this introductory section, the rest of this paper is structured as follows. Section 2 describes the overall architecture of the terrestrial segment in the proposed hybrid terrestrial/satellite infrastructure, utilizing regenerative DVB-T platforms as backhaul connections for triple-

play services provision mainly in rural areas, while Section 3 elaborates on its performance. Section 4 presents the overall architecture of the satellite segment that acts as an overlay network upon the terrestrial segments, while Section 5 elaborates on its performance as a matter of system and network scalability, network throughput, and packet loss, for national/international exploitation. Finally Section 6 concludes this paper.

2. Terrestrial DVB/IP Segment

The advent of digital video broadcasting (DVB) technology and its exploitation over terrestrial links (DVB-T), along with its inherent characteristic to combine heterogeneous traffic into the same data stream (i.e., MPEG-2 and IP data) [3], presents the possibility for the creation of a converged DVB/IP networking infrastructure [4, 5], able to provide triple-play services everywhere within the broadcasting footprint. Typical DVB-T broadcast channels send megabits or tens of megabits per second in a shared and unidirectional mode. Bidirectional operation, which is required for personalised and unicast services (e.g., triple-play services), can be achieved either by making use of a centralised approach where the user is directly communicating with the broadcasting station over a return path channel [6, 7] making use of any access technology such as WLAN, PSTN, and GSM [8], or in a decentralised approach through a subsystem of distributed Cell Main Nodes (CMNs). The overall architecture of such a decentralised infrastructure is depicted in Figure 2. It consists of two core subsystems: (a) a central broadcasting point (regenerative DVB-T) and (b) a number of distributed Cell Main Nodes (CMNs) located within the broadcasting area. Each CMN enables a number of users/citizens (geographically neighbouring to the specific CMN) to access IP unicast services that are hosted by the entire infrastructure (e.g., by the ISP and Multimedia provider as depicted in Figure 2). The communication between the users and the corresponding CMN (access network) is achieved via broadband point-to-multipoint links (i.e., WLAN, xDSL). The CMN gathers all IP traffic stemming from its own users and forwards it to the central broadcasting point (UHF transmission point visible

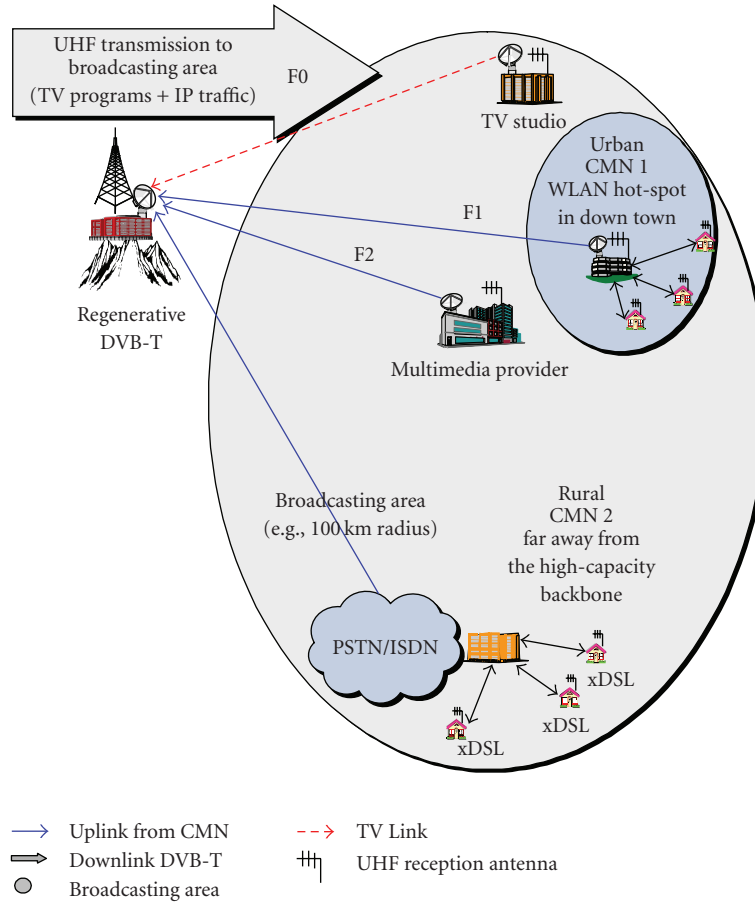


FIGURE 2: Overall architecture of the terrestrial DVB/IP segment.

by all CMNs) via dedicated point-to-point uplinks. IP traffic stemming from all CMNs is received by the broadcasting point, where a process unit filters, regenerates, and multiplexes them into a single transport stream (IP-multiplex) along with the digital TV programme(s) stemming from the TV broadcaster(s) (TV studio), towards forming the final DVB-T “bouquet”.

Each user receives the appropriate IP reply signals indirectly via the corresponding CMN, while receiving custom digital TV programme (e.g., MPEG-2) and IP multicast data (e.g., IP-TV) directly via the common DVB-T stream (by utilising a simple/custom UHF antenna). In such configuration, both reverse and forward IP data traffic are encapsulated into the common DVB-T stream, thus improving the flexibility and performance of the networking infrastructure. Furthermore, the cellular conception that is adopted utilises the DVB-T stream in a backbone topology, which interconnects all cells that are located within the broadcasting area. Thus, a unique virtual common IP backbone is created, which is present at every cell via its CMN. The IP traffic of this IP backbone is supplied by the DVB-T bit stream. Users access the network via the appropriate CMN.

2.1. Configuration of the Regenerative DVB-T. The configuration of the regenerative DVB-T broadcasting point

(depicted in Figure 3) is capable of (a) receiving the users IP traffic over the uplinks (via the appropriate CMN—see PSTN/ISDN uplink and F1 in Figure 2), (b) receiving any local digital TV program(s) with IP multicast and Internet services, stemming from the TV studio broadcaster and the ISP/multimedia provider, respectively (see TV Link and F2 in Figure 2), and (c) creating and broadcasting a common UHF downlink that carries the digital TV program(s) and the IP data.

According to the configuration depicted in Figure 3, the multiplexing device receives any type of data (IP and/or digital TV programs), adapts them into a DVB-T transport stream (IP to MPEG-2 encapsulation), and finally broadcasts this DVB-T stream to the entire broadcasting area following the DVB-T standard (COFDM scheme in the UHF band). In this respect, triple-play services providers contribute to the creation of a backbone (DVB-T stream) that is present and available within the entire broadcasting area. An actual exploitation of this architecture can be realized for the deployment of xDSL infrastructures that enable not only triple-play services and access, but also always-on connectivity. The deployment of xDSL access networks require the head-end unit (i.e., DSLAM) to be placed close to a high-capacity core backbone (i.e., fiber), while the end user’s equipment must be located no further than a few

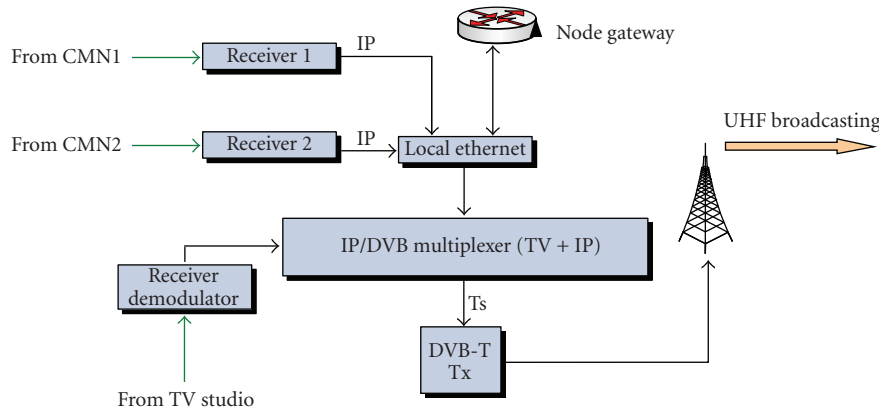


FIGURE 3: Configuration of regenerative DVB-T.

kilometers from the point-of-presence (i.e., 5 km from the DSLAM). As a result, in rural areas and in areas of dispersed population, that are far away from the core backbone, xDSL deployment cannot be realized unless extension of the high-capacity backbone is achieved to reach these areas. However, this is a matter of installation and operational costs.

In this context and by taking into account that DVB-T transmissions utilize coverage areas of many kilometers (e.g., 100 km) the proposed configuration (Figure 3) can be exploited for realizing the common DVB-T stream in middle-mile/backhaul configurations, extending the core backbone within the entire broadcasting area and making it available or present at any CMN within the coverage footprint. This type of networking solution, which conforms to the proposed architecture, is presented next, with a description of a rural-based CMN that is placed away from the national backbone, providing users with always-on connectivity and access to triple-play services. An urban-based CMN is also presented, enabling users to actively participate in the creation of the final DVB-T stream and provide their own content/services.

2.2. Configuration of Urban-Based Cell Main Node. Although access to triple-play services and always-on connectivity can be easily achieved in urban and developed areas (due to the widespread availability of ICT in these regions), the realization of a networking architecture constitutes a major factor in the active participation of users in the information society (in the context of not only consuming custom and predefined content) but also in the capability of creating, manipulating, and distributing their own content and services over a commonly exploited infrastructure. The active participation of these potential content and application providers (stemming from traditional, passive users) is the key to generate revenues, create rich activity in the market chain, and spearhead new progress in the broadcasting, Internet, and telecommunication sectors. The realization of a networking architecture decouples the service provision function from the network operators and offers this privilege to all potential interested players, changing the traditional passive users to active ones. In the previous

context, urban users who wish to become active participants in the information society, can access the entire infrastructure for distributing their own services via a CMN (urban-based CMN), the configuration of which is depicted in Figure 4. This infrastructure utilizes a broadband uplink for realizing the communication between this CMN and the regenerative DVB-T (e.g., microwave RF link) and WLAN technology in the access network, consisting of an access point (AP) at the CMN site, which maintains a full duplex communication with the station adapters (SAs) at the users' sites. The CMN gathers all IP traffic stemming from its users (custom and active users, potential content providers, etc.), and forwards it to the central broadcasting point (i.e., regenerative DVB-T). This IP traffic is processed, regenerated and multiplexed with all other IP traffic (stemming from other CMNs) into a single transport stream (i.e., IP-plex), with the digital TV program(s) stemming from the TV broadcaster, participating in this way in the creation of the final DVB-T bouquet. In this respect, an active user exploits the common DVB-T stream for maintaining his own e-business, which is virtually present at any place within the entire broadcasting area (via the common DVB-T stream). Such an e-business may be the realization of an IP-TV multicast, capable of targeting customers in a radius of 100 km, located both in urban and rural areas.

2.3. Configuration of Rural-Based Cell Main Node. In rural areas where the population is dispersed that are far away from a core backbone network (e.g., fiber) and only custom PSTN/ISDN is currently available, access to triple play services and always-on connectivity cannot be realized, unless diffusion of ICT is achieved and/or extension of the core backbone to these regions is accomplished. Cost mainly constitutes the major obstacle for such ICT diffusion and extension of the core backbone in these areas. For these regions or cases, the exploitation of the proposed networking architecture is a very promising solution, enabling not only the provision of triple-play services but also of always-on connectivity via cost-effective (marginal cost) extension of the core backbone. Primarily, the common DVB-T stream enables broadcast and multicast data (such as digital TV

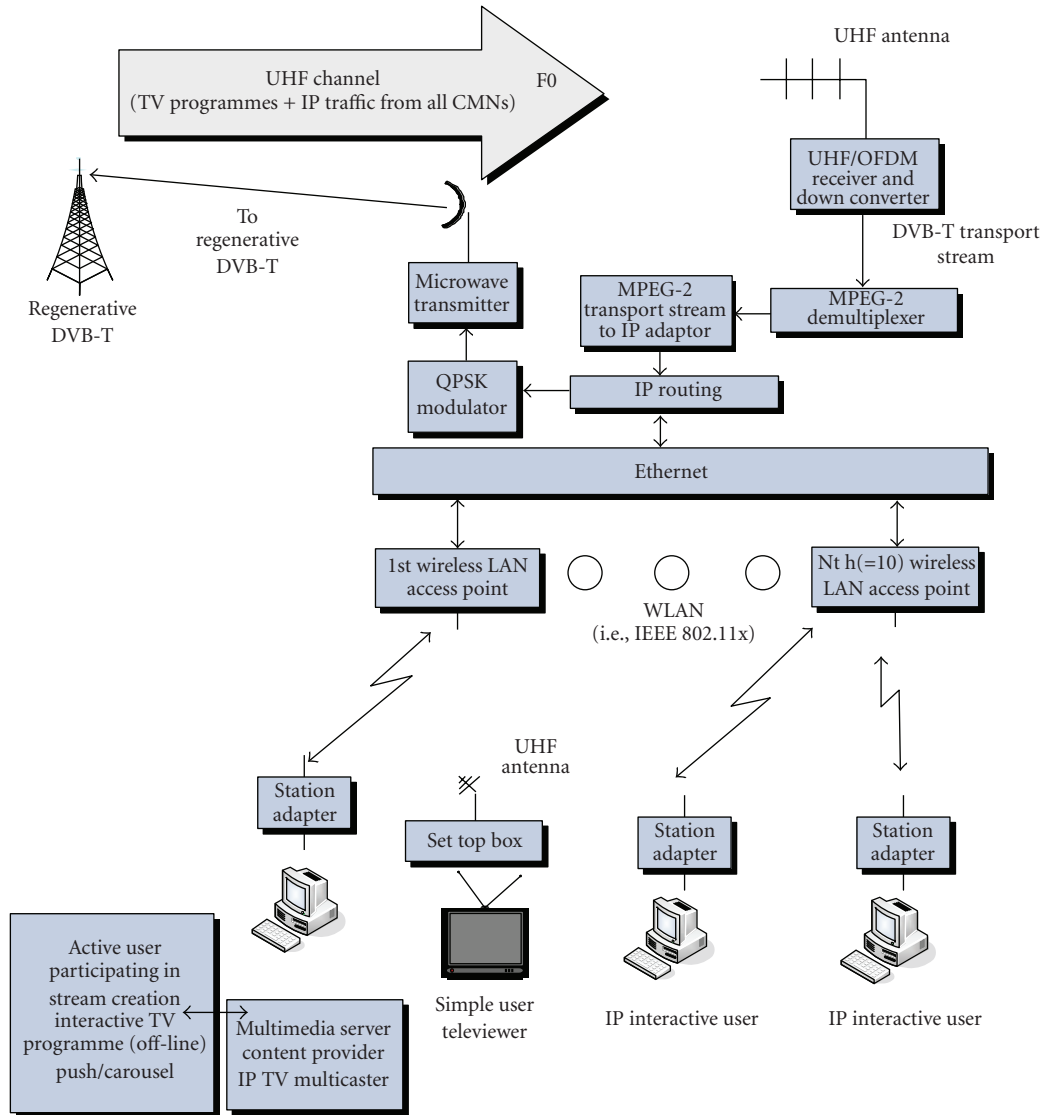


FIGURE 4: Urban-based CMN.

MPEG-2 and IP-TV services) to be present and available within the entire coverage area. Users located even in rural and regions, where the population is dispersed, can easily and cost effectively access services by utilizing a simple/custom UHF reception antenna and a corresponding DVB-T reception equipment on their premises. In addition, the exploitation of the common DVB-T stream in backhaul/middle-mile configurations enables the fast/immediate interconnection between the core backbone and any CMN within the entire broadcasting footprint. With such an approach, in a way, the core backbone is transferred to rural-based CMNs, enabling the deployment of ICT that provides for always-on connectivity (e.g., ADSL). The overall configuration of such a rural-based CMN is depicted in Figure 4. At this point, it should be noted that the deployment of the ADSL technology in the access network would not have been feasible due to high costs for the backhaul connection (physical connection between this rural-based CMN and the

nearest optical backbone network). However, the proposed configuration enables the low cost and fast deployment of an ADSL network, by exploiting the common DVB-T stream as a backhaul and middle-mile infrastructure, capable of interconnecting the core backbone (present in urban areas) with the rural-based CMN. Such an approach enables rural users to maintain always-on connectivity (over the ADSL network) and triple-play services access over the common UHF beam.

3. Performance Evaluation of the Terrestrial DVB/IP Segment

In order to evaluate the network performance of the proposed terrestrial system, several experimental tests were conducted by emulating the provision of bulk TCP data streams under a specific use case scenario (i.e., when a

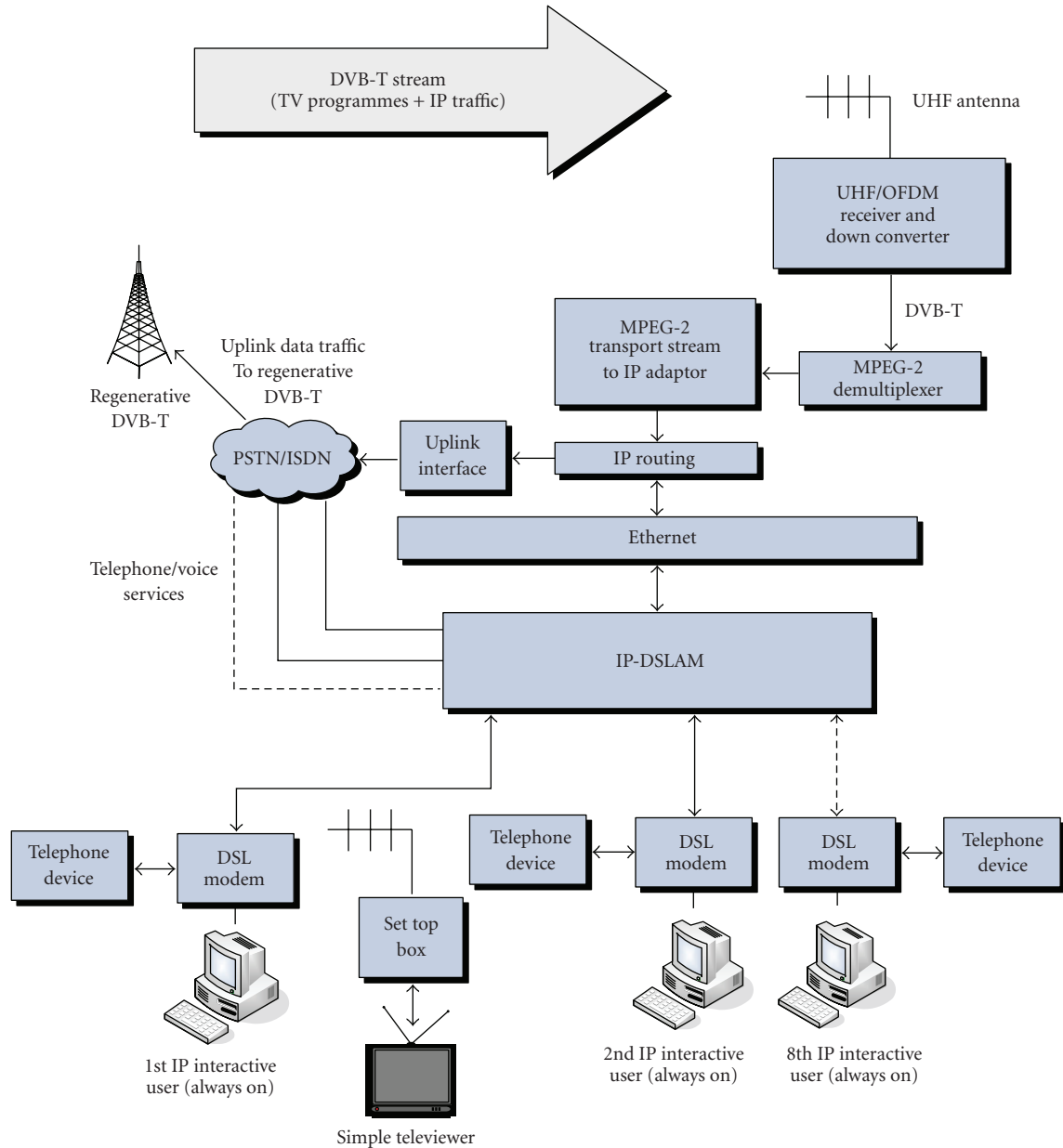


FIGURE 5: Rural-based CMN.

user located in CMN2 is accessing content hosted by an active user located in CMN1—see Figure 6). The overall system architecture regarding this preliminary experimental test is depicted in Figure 6, 8 Mbps of the total available bandwidth of the common DVB-T stream (i.e., 21.11 Mbps) were allocated for the provision of TCP/IP traffic, and the rest of the available networking resources were dedicated to provide a number of digital television programs.

During the experimental process (i.e., 180 s) Iperf application [9] was utilized to generate TCP/IP data traffic between an end user located in CMN2 and an active user located in CMN1 (see Figure 6). The reverse data traffic stemming from the end user is received by CMN2 and forwarded to the regenerative DVB-T platform, where it is

then broadcasted together with multiple digital television programs. CMN1 is then able to receive this traffic and forward it to the active user's terminal. The forward data traffic and reply signals, originated from the active user, are received by the regenerative DVB-T platform through CMN1 and the IEEE802.11g uplink. This traffic is then broadcasted to the entire DVB-T coverage area, enabling CMN2 to receive the reply signals and forward them to the end user's terminal. Tcpdump application [10] was utilized, running both at the end user's and active user's terminals, for capturing the headers of the transmitted/received data packets, besides storing them as "dump" files. Upon completion of the TCP connection, the data stored within the "dump" files were collected and analysed by the TCPTrace tool [11], providing

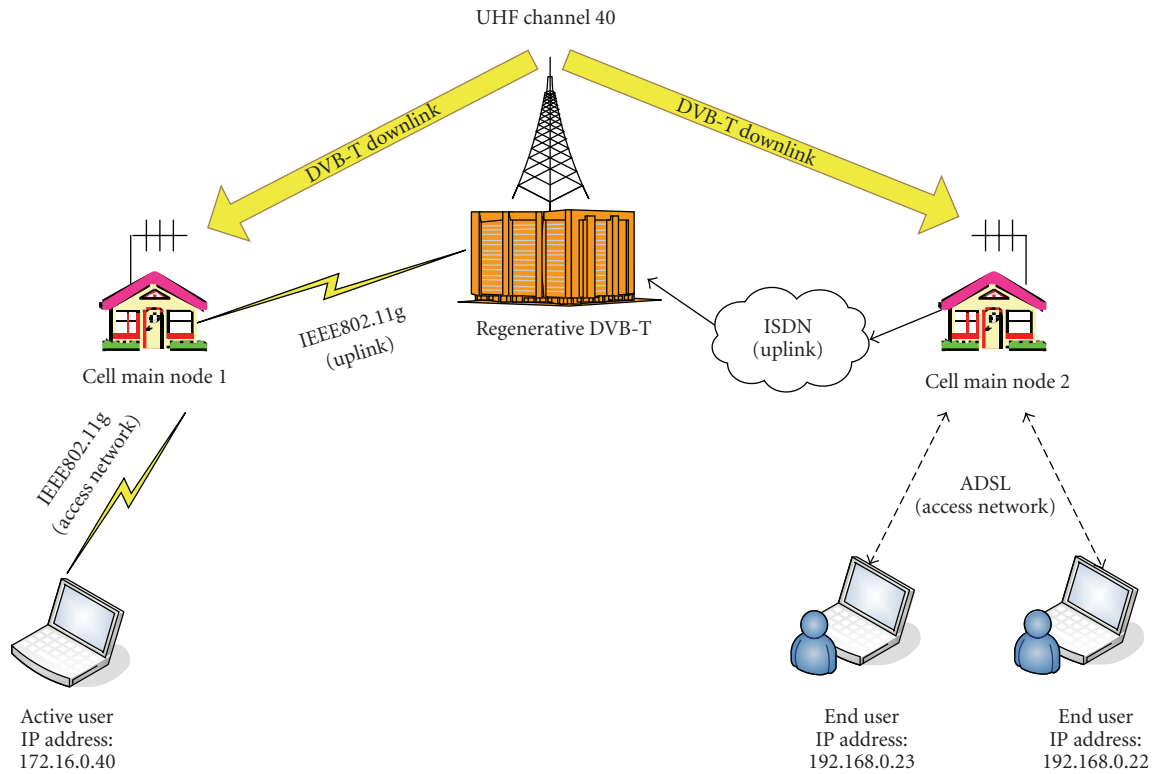


FIGURE 6: Experimental test bed.

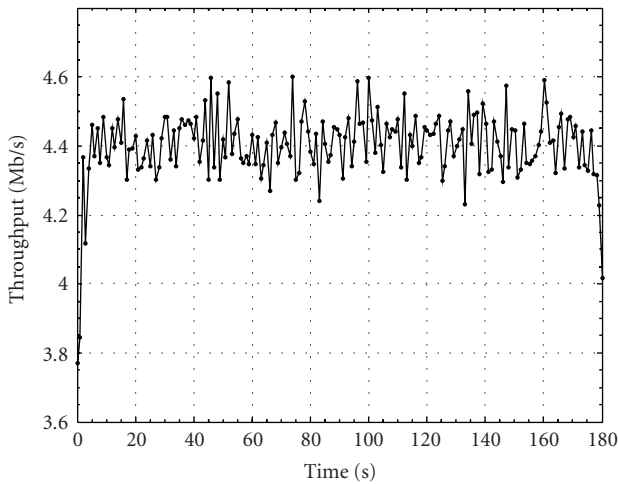


FIGURE 7: Useful throughput for end-to-end communication.

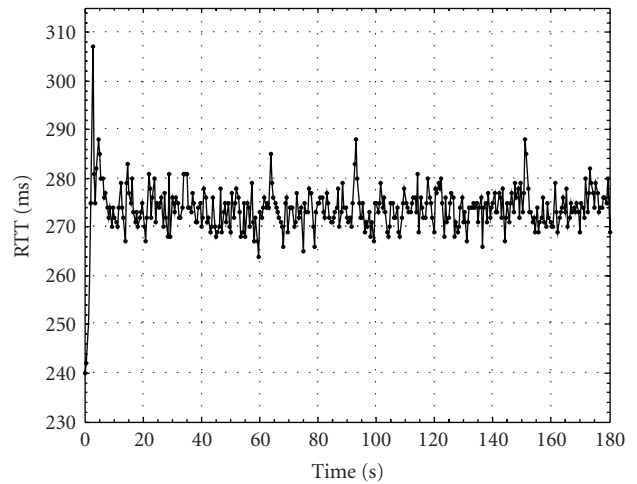


FIGURE 8: Round trip time for end-to-end communication.

results regarding the instantaneous useful throughput, TCP Round Trip Time (RTT), and retransmitted packets. The experimental results indicated an average useful throughput of 4.4 Mb/s and an average RTT of 273.69 ms, during this end-to-end TCP communication, while no retransmissions were observed. Figures 7 and 8 depict the graphical representations of useful throughput and RTT versus time, respectively.

4. Satellite DVB/IP Segment

The previous sections presented the design, implementation, and performance evaluation of the terrestrial DVB/IP segment of the proposed hybrid infrastructure, exploiting DVB-T in regenerative configurations for the realisation of backhaul connections in order to enable local/regional access (i.e., within the DVB-T footprint) to triple-play services even by rural citizens. In order to expand the proposed concept at national level, so that triple-play services would

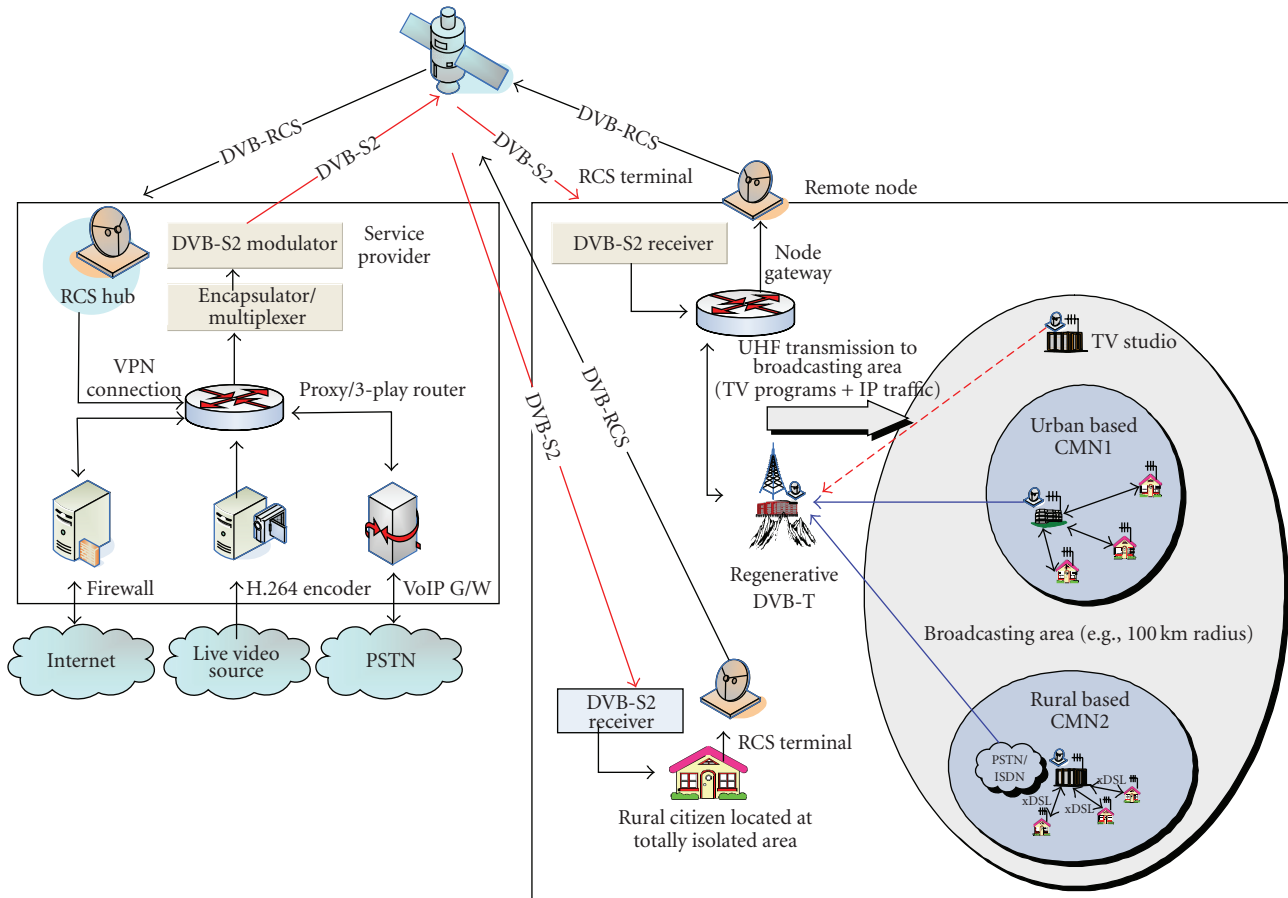


FIGURE 9: Overall architecture and configuration of the satellite DVB/IP segment.

be accessed by any user/citizen, a number of such DVB/IP platforms must be deployed at the various rural areas and be interconnected to each other. Towards these, DVB-S2/RCS technology-based satellites can be exploited for the creation of an overlay network upon the terrestrial segments, capable not only of interconnecting but also complementing the regenerative DVB-T coverage, especially in cases of users located in totally isolated rural areas (i.e., where no regenerative DVB-T platform exists, or users outside a DVB-T broadcasting footprint). The same holds for citizens on the move, such as passengers in trains, airplanes, or ships. For all these cases, the DVB-S2/RS satellite access solution is very promising for the delivery of ubiquitous triple-play integrated services.

The overall configuration of the satellite DVB/IP segment, depicted in Figure 9, provides a flexible and viable broadband architecture for triple-play services provision to individual users and small wired or wireless local networks which are geographically isolated or, in general, are in a condition which prevents them from connecting to terrestrial network infrastructures. The proposed system is based on a DVB-S2 communication chain (IP-to-DVB encapsulator, multiplexer, and modulator) and a remote DVB-RCS Hub (i.e., RCS Hub in Figure 9), located at the regenerative DVB-T or at individual user's premises

for collecting and transmitting the uplink data. A VPN (Virtual Private Network) tunnel from the RCS Hub feeds the data into the provider platform. A Proxy/3-play Router feeds the triple-play streams (destined to the end users) to the Encapsulator for processing and transmission and routes appropriately the IP datagrams, which arrive via RCS Hub from the terrestrial sites. The Encapsulator/multiplexer operates in compliance to [12] and treats each traffic stream individually and can apply different queuing priorities to each service. This differentiation is performed in a static manner. In case that dynamic bandwidth management is required, a mechanism like the one described in [13] can be employed. Video streams are served by a real-time H.264 encoder fed by a live source, and a VoIP Gateway utilizing H.323/SIP acts as an interface to the public PSTN network. Internet connections are firewalled and served via a Web proxy.

At the remote node (e.g., regenerative DVB-T or individual user's premises), the reception and transmission is undertaken by two separate modules—a DVB-S2 receiver and a separate DVB-RCS terminal. A Node Gateway undertakes the routing and the policing of the traffic within the node. In this infrastructure (Figure 9), each regenerative DVB-T platform utilizes a DVB-S2/DVB-RCS satellite terminal, in order to be interconnected with other terrestrial segments.

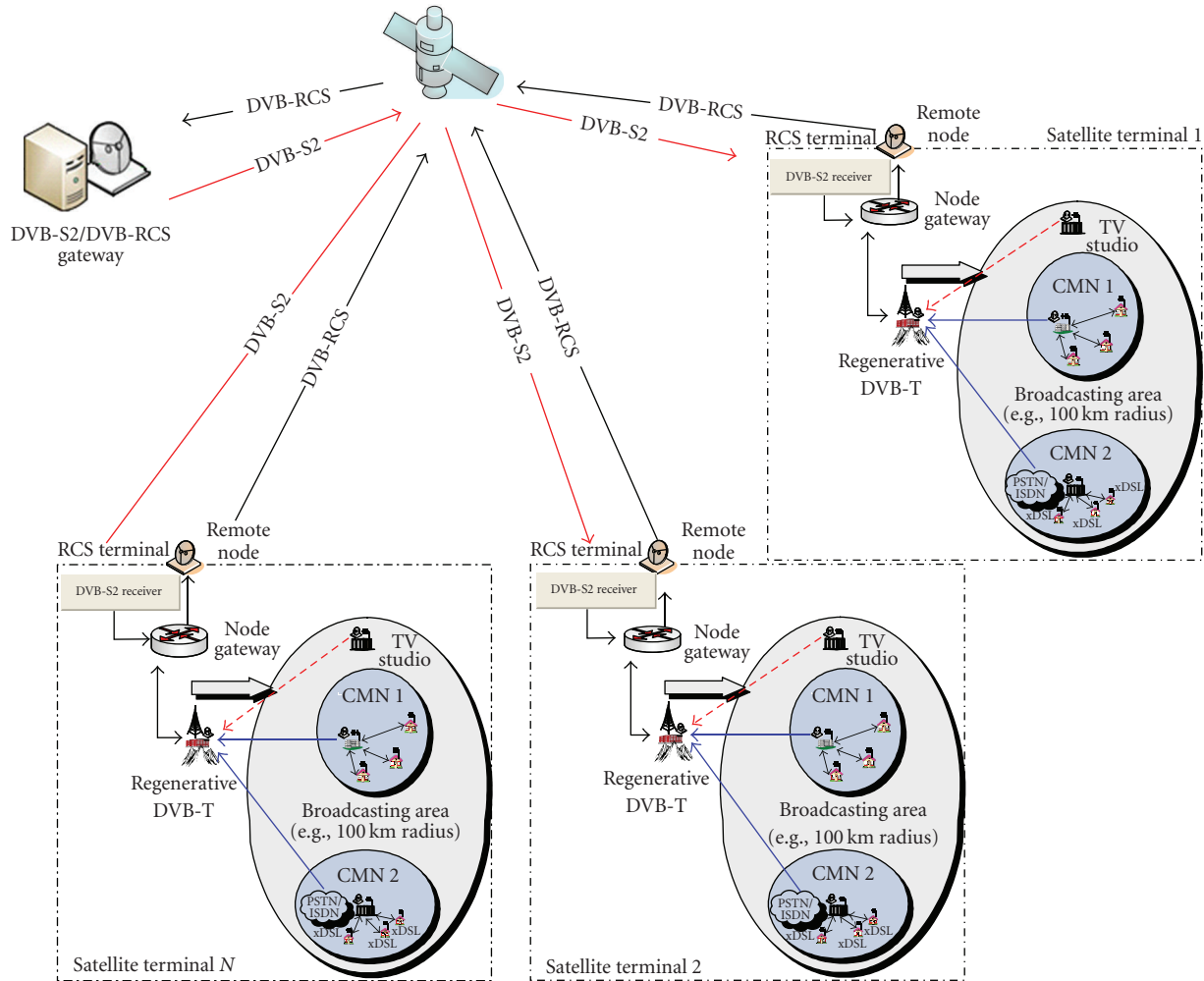


FIGURE 10: Configuration of the simulation test-bed for evaluating the performance of the hybrid terrestrial/satellite DVB/IP infrastructure.

IP traffic and triple-play services stemming/targeting from/to the regenerative DVB-T platforms are forwarded by the individual DVB-RCS uplinks to the satellite. The networking services, that are provided by the DVB-S.2 satellite downlink, are encapsulated into the common terrestrial television bouquet and finally broadcasted via the UHF channel at high data rates following the DVB-T standard.

5. Performance Evaluation of the Hybrid Terrestrial/Satellite Infrastructure

This section presents the scenario used to validate the capabilities and potentialities of the proposed hybrid terrestrial/satellite infrastructure, in terms of scalability and maximum number of supported terminal/nodes, network throughput, and packet loss. The simulation framework was constructed by using Opnet 11.5 [14], and the study included the core network performance of the overall system.

More specifically, the sets of simulation tests were designed in order to evaluate the performance of the uplink-downlink communication chain, which uses DVB-S2 technology in the downlink and DVB-RCS in the uplink.

The overall configuration of this experimental test-bed is depicted in Figure 10.

In the first simulation scenario a shared uplink of 2 Mb/s and a downlink of 4 Mb/s were considered. By varying the signaling overhead as well as the interval between two successive signaling packets, the maximum number of supported satellite terminals was obtained (see Figure 11). It should be noted that during these simulation experiments “satellite terminal” was considered the reception/transmission modules both at the regenerative DVB-T terrestrial segments, and at individual user’s premises. Following the simulation results it was verified that for the recommended signaling overhead (5% of the total bandwidth) and for an interval between two successive signaling packets of five seconds (which presents a good trade-off between reactivity and overhead), a maximum number of 1736 satellite terminals can be supported.

In Figures 12 and 13 the average throughput and the packets loss are, respectively, presented in relation to the number of multimedia flows. In these simulations, the scalability and efficiency are emphasized by using variable number of multicast multimedia MPEG-4 communication

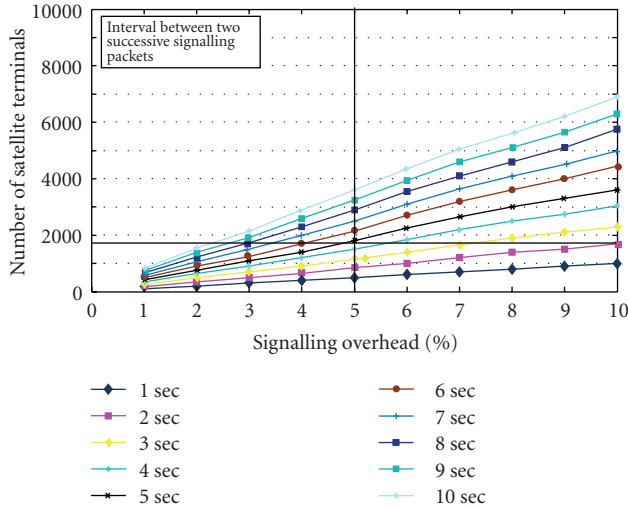


FIGURE 11: Scalability of the proposed framework in terms of supported terminals.

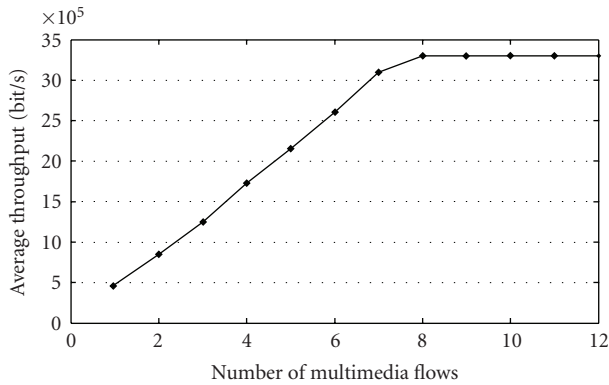


FIGURE 12: Average throughput versus number of multimedia flows.

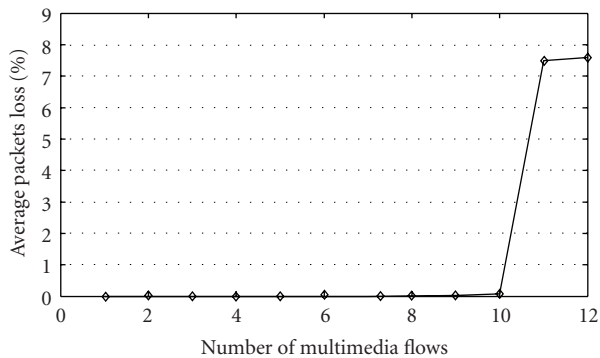


FIGURE 13: Average packets loss versus number of multimedia flows.

sessions (the average bit rate is about 480 kb/s). It is clearly shown in Figure 12 that the proposed configuration supports a maximum number of 10 parallel sessions. For this number of sessions, throughput is maximized (as it is observed in Figure 13) and the packets loss is insignificant ($\ll 1\%$). However, additional flows impact very badly the system.

Indeed, the loss ratio increases rapidly to value greater than 7%, which deteriorates the perceived quality of service.

6. Conclusions

This paper elaborated on the convergence of digital broadcasting and Internet technologies, by designing, implementing, and evaluating the performance of a hybrid terrestrial/satellite networking infrastructure, enabling triple-play services access in rural areas, both at local and national levels. At local/district level, the paper proposed the exploitation of terrestrial digital video broadcasting platforms (DVB-T) in regenerative configurations in order to create terrestrial DVB/IP backhaul between the core backbone (present in urban areas) and a number of intermediate communication nodes distributed within the DVB-T broadcasting footprint (in rural areas). Triple-play services, that are available at the core backbone, are transferred via the regenerative DVB-T/IP backhaul to the entire district (DVB-T coverage area) and can be accessed by rural users/citizens via the corresponding intermediate node, utilising broadband technologies only in the access network (e.g., WLAN, xDSL). At regional/national level and in the case of totally isolated users (e.g., located outside a regenerative DVB-T footprint), the paper discussed the exploitation of satellite interactive digital video broadcasting platform (DVB-S2/RCS) as an overlay network that interconnects the terrestrial DVB-T/IP platforms (located within the DVB-S2 footprint), as well as individual users, services providers, and ISPs to each other. Performance of the proposed hybrid terrestrial/satellite networking environment verified the validity of the proposed architecture, through experimental tests that were conducted under real transmission/reception conditions (for the terrestrial segment) and via simulation experiments (for the satellite segment) at a prototype infrastructure that conforms to the proposed architectural design issues.

Acknowledgments

Part of the work presented in this paper was undertaken within the framework of the IST-FP6-507312 ATHENA project (Digital Switchover: Developing infrastructures for broadband access) and the IST-FP6-027457 IMOSAN project (Integrated Multilayer Optimization in broadband DVB-S.2 Satellite Networks).

References

- [1] M. Philpott, "Broadband technologies and rural areas," *Journal of the Communications Network*, vol. 2, no. 1, pp. 9–16, 2003.
- [2] C. Boscher, N. Hill, P. Lainé, and A. Candido, "Providing always-on broadband access to under-served areas," *Alcatel Telecommunications Review*, no. 4-1, pp. 127–132, 2003.
- [3] ETSI, "ETSI TR 101 202 v1.2.1 Digital Video Broadcasting (DVB): implementation guidelines for data broadcasting," 2003.
- [4] G. Mastorakis, G. Kormentzas, and E. Pallis, "A fusion IP/DVB networking environment for providing always-on

- connectivity and triple-play services to urban and rural areas,” *IEEE Network*, vol. 21, no. 2, pp. 21–27, 2007.
- [5] E. Pallis, C. Mantakas, G. Mastorakis, A. Kourtis, and V. Zacharopoulos, “Digital switchover in UHF: the ATHENA concept for broadband access,” *European Transactions on Telecommunications*, vol. 17, no. 2, pp. 175–182, 2006.
- [6] ETSI, “ETSI EN 301 958 v.1.1.1 Digital Video Broadcasting (DVB): Interaction Channel for Digital Terrestrial Television (RCT) Incorporating Multiple Access OFDM,” 2002.
- [7] ETS 300 801—Digital Video Broadcasting (DVB), “Interaction channel through Public Switched Telecommunications Network (PSTN)/Integrated Services Digital Networks,” (ISDN).
- [8] G. Xilouris, G. Gardikis, E. Pallis, and A. Kourtis, “Reverse Path Technologies in Interactive DVB-T Broadcasting,” in *Proceedings of the IST Mobile and Wireless Telecommunications Summit*, pp. 292–295, Thessaloniki, Greece, June 2002.
- [9] “NLANR/DAST Iperf Version 2.0.2: The TCP/UDP Bandwidth Measurement Tool,” <http://www.noc.ucf.edu/Tools/Iperf/>.
- [10] TCPdump, <http://www.tcpdump.org/>.
- [11] “TCPTrace, a TCP analysis tool,” <http://www.tcptrace.org/>.
- [12] ETSI EN 301 192, “Digital Video Broadcasting (DVB): DVB Specification for data broadcasting,” ETSI European Standard; v.1.4.1; November 2004 Standard.
- [13] G. Gardikis, A. Kourtis, and P. Constantinou, “Dynamic bandwidth allocation in DVB-T networks providing IP services,” *IEEE Transactions on Broadcasting*, vol. 49, no. 3, pp. 314–318, 2003.
- [14] <http://www.opnet.com/>.

Research Article

Video Quality Prediction Models Based on Video Content Dynamics for H.264 Video over UMTS Networks

Asiya Khan,¹ Lingfen Sun,¹ Emmanuel Ifeakor,¹ Jose-Oscar Fajardo,² Fidel Liberal,² and Harilaos Koumaras³

¹Centre for Signal Processing and Multimedia Communication, School of Computing, Communications and Electronics, University of Plymouth, Plymouth PL4 8AA, UK

²Department of Electronics and Telecommunications, University of the Basque Country (UPV/EHU), 48013 Bilbao, Spain

³Institute of Informatics and Telecommunications, NCSR Demokritos, 15310 Athens, Greece

Correspondence should be addressed to Asiya Khan, asiya.khan@plymouth.ac.uk

Received 30 October 2009; Accepted 18 February 2010

Academic Editor: Daniel Negru

Copyright © 2010 Asiya Khan et al. This is an open access article distributed under the Creative Commons Attribution License, which permits unrestricted use, distribution, and reproduction in any medium, provided the original work is properly cited.

The aim of this paper is to present video quality prediction models for objective non-intrusive, prediction of H.264 encoded video for all content types combining parameters both in the physical and application layer over Universal Mobile Telecommunication Systems (UMTS) networks. In order to characterize the Quality of Service (QoS) level, a learning model based on Adaptive Neural Fuzzy Inference System (ANFIS) and a second model based on non-linear regression analysis is proposed to predict the video quality in terms of the Mean Opinion Score (MOS). The objective of the paper is two-fold. First, to find the impact of QoS parameters on end-to-end video quality for H.264 encoded video. Second, to develop learning models based on ANFIS and non-linear regression analysis to predict video quality over UMTS networks by considering the impact of radio link loss models. The loss models considered are 2-state Markov models. Both the models are trained with a combination of physical and application layer parameters and validated with unseen dataset. Preliminary results show that good prediction accuracy was obtained from both the models. The work should help in the development of a reference-free video prediction model and QoS control methods for video over UMTS networks.

1. Introduction

Universal Mobile Telecommunication System (UMTS) is a third generation (3G), wireless cellular network based on Wideband Code Division Multiple Access technology, designed for multimedia communication. UMTS is among the first 3G mobile systems to offer wireless wideband multimedia communications over the Internet Protocol [1]. Multimedia contents on the Internet can be accessed by the mobile Internet users at data rates between 384 kbps and up to 2 Mbps in a wide coverage area with perfect static reception conditions.

Video streaming is a multimedia service, which is recently gaining popularity and is expected to unlock new revenue flows for mobile network operators. Significant business potential has been opened up by the convergence of communications, media, and broadcast industries towards

common technologies by offering entertainment media and broadcast content to mobile user. However, for such services to be successful, the users Quality of Service (QoS) is likely to be the major determining factor. QoS of multimedia communication is affected by parameters both in the application and physical layer. In the application layer, QoS is driven by factors such as resolution, frame rate, sender bitrate, and video codec type. In the physical layer, impairments such as the block error rate, jitter, delay, and latency, are introduced. Video quality can be evaluated either subjectively or based on objective parameters. Subjective quality is the users' perception of service quality (ITU-T P.800) [2]. The most widely used metric is the Mean Opinion Score (MOS). Subjective quality is the most reliable method. However, it is time consuming and expensive and hence, the need is for an objective method that produces results comparable with those of subjective testing. Objective measurements can

be performed in an intrusive or nonintrusive way. Intrusive measurements require access to the source. They compare the impaired videos to the original ones. Full reference and reduced reference video quality measurements are both intrusive [3]. Quality metrics such as Peak Signal-to-Noise Ratio (PSNR), SSIM [4], VQM [5], and PEVQ [6] are full reference metrics. VQM and PEVQ are commercially used and are not publicly available. Nonintrusive methods (reference-free), on the other hand, do not require access to the source video. Nonintrusive methods are either signal- or parameter-based. Nonintrusive methods are preferred to intrusive analysis as they are more suitable for online quality prediction/control.

Recently, there has been work on video quality prediction. Authors in [7–9] predicted video quality for mobile/wireless networks taking into account the application level parameters only, whereas authors in [10] used the network statistics to predict video quality. In [11] authors have proposed a model to measure temporal artifacts on perceived video quality in mobile video broadcasting services. We proposed in [12] video quality prediction models over wireless local area networks that combined both the application and network level parameters. In UMTS Radio Link Control (RLC), losses severely affect the QoS due to high error probability. The RLC is placed on top of the Medium Access Control and consists of flow control and error recovery after processing from the physical layer. Therefore, for any video quality prediction model, it is important to model the RLC loss behaviour appropriately. In this paper only RLC Acknowledged Mode (AM) is considered as it offers reliable data delivery and can recover frame losses in the radio access network. Recent work in [13–16] has focused on the impact of UMTS link layer errors on the quality of H.264/MPEG4 encoded videos. In [17] the impact of H.264 video slice size on end-to-end video quality is investigated. In [18] authors have shown that RLC AM mode outperforms the unacknowledged mode and proposed a self-adaptive RLC AM protocol. In [19] performance evaluation of video telephony over UMTS is presented. Most of the current work is either limited to improving the radio channel or evaluation of parameters that impact on QoS of video transmission over UMTS networks. However, very little work has been done on predicting end-to-end video quality over UMTS networks considering both the different content types and the impact of RLC loss models.

As the convergence of broadcast/multicast and the Internet becomes a reality, delivery of multimedia content to large audiences will become very cost-effective using wireless access networks such as UMTS, WiFi, WiMax, or DVB-H. Therefore, provisioning of multimedia services can easily be offered over several access technologies. Hence, there is a need for an efficient, nonintrusive video quality prediction model for technical and commercial reasons. The model should predict perceptual video quality to account for interactivity. In this paper, we have looked at the UMTS access network. The error rate simulated in the physical layer is employed to generate losses at the link layer modelled with a 2-state Markov model [20–22] with variable Mean Burst Lengths (MBLs) [23]. Hence, we evaluate the impact

of different loss models on end-to-end video quality as it was shown in [24] that there is a strong impact of second-order error characteristics of the channel onto the performance of higher layer protocols. Furthermore, based on the content types, we are looking for an objective measure of video quality simple enough to be calculated in real-time at the receiver side. We present two new reference-free approaches for quality estimation for all content types. The contributions of the paper are twofold

- (1) investigation of the combined effects of physical and application layer parameters on end-to-end perceived video quality over UMTS networks for all content types,
- (2) development of learning models for video quality prediction as (a) a hybrid video quality prediction model based on an Adaptive Neural Fuzzy Inference System (ANFIS), as it combines the advantages of a neural network and fuzzy system [25] for all content types and (b) a regression-based model for all content types.

The model is predicted from a combination of parameters in the application layer, that is, Content Type (CT), video Sender Bitrate (SBR), and Frame Rate (FR), and in the physical layer, that is, Block Error Rate (BLER) and Mean Burst Length (MBL). The video codec used was H.264/AVC [26] as it is the recommended codec for video transmission over UMTS 3G networks. All simulations were carried out in the OPNET Modeler [27] simulation platform.

The rest of the paper is organised as follows. The video quality assessment problem is formulated in Section 2. Section 3 presents the background to content-based video quality prediction models. In Section 4, the proposed content-based video quality models are presented, whereas, Section 5 outlines the simulation set-up. Section 6 describes the impact of QoS parameters on end-to-end video quality. The evaluation of the proposed models is presented in Section 7. Conclusions and areas of future work are given in Section 8.

2. Problem Statement

In multimedia streaming services, there are several parameters that affect the visual quality as perceived by the end users of the multimedia content. These QoS parameters can be grouped under application layer QoS and physical layer QoS parameters. Therefore, in the application layer perceptual QoS of the video bitstream can be characterized as

$$\text{Perceptual QoS} = f(\text{content type, SBR, frame rate, codec type, resolution, etc.})$$

whereas, in the physical layer it is given by

$$\text{Perceptual QoS} = f(\text{PER, delay, latency, jitter, etc.}).$$

It should be noted that the encoder and content dimensions are highly conceptual. In this research we chose H.264 as the encoder type as it is the recommended codec for

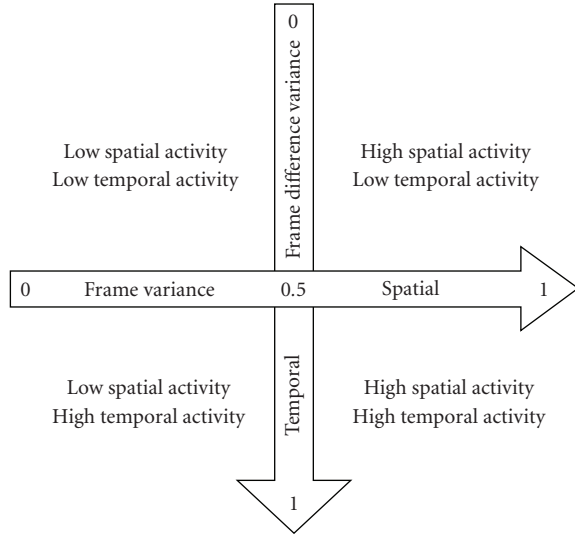


FIGURE 1: The Spatiotemporal grid.

low bitrates. We used our previously defined classification function [12] to classify the video contents based on their spatial and temporal features. In the application layer we chose Sender Bitrate (SBR), Frame Rate (FR), and Content Type (CT) and in the physical layer we chose Block Error Rate (BLER) and Mean Burst Length (MBL) as QoS parameters. A single Mean Opinion Score (MOS) value is used to describe the perceptual quality. Therefore, MOS in the application layer is given as MOS^A , whereas, MOS in the physical layer is given by MOS^P as

$$MOS^A = \{CT, SBR, FR\} \text{ and } MOS^P = \{BLER, MBL\}$$

The overall MOS is given by $MOS = f(MOS^A, MOS^P)$.

In this paper we evaluated the impact of QoS parameters both in the application and physical layer and hence confirmed the choice of parameters in the development of the learning models. Video quality is affected by parameters in the application and physical layer. Therefore, video quality prediction model should take into account parameters in both layers. The relationships of QoS parameters are thought to be nonlinear. Therefore, an ANFIS-based neural network model is chosen for video quality prediction because it combines the advantages of fuzzy systems (based on human reasoning) and neural networks. In addition to ANFIS-based prediction models, we have also predicted video quality based on nonlinear regression. This method is chosen as it is easy to implement in QoS control, for example, video SBR adaptation. ANFIS-based models are more complex and to implement them in real-time for QoS control is not as straightforward as a regression-based model which is light weighted and easily implementable. The purpose of this paper is to highlight the two methods for video quality prediction.

3. Background to Content-Based Video Quality Prediction

In this section we present the background literature on content classification and its impact on video quality prediction.

3.1. Two-Dimensional Content Classification. The content of each video clip may differ substantially depending on its dynamics (i.e., the spatial complexity and/or the temporal activity of the depicted visual signal). The quantification of this diversity is of high interest to the video coding experts, because the spatiotemporal content dynamics of a video signal specify and determine the efficiency of a coding procedure.

From the perceptual aspect, the quality of a video sequence is dependent on the spatiotemporal dynamics of the content. More specifically, it is known from the fundamental principles of the video coding theory that action clips with high dynamic content are perceived as degraded in comparison to the sequences with slow-moving clips, subject to identical encoding procedures.

Thus the classification of the various video signals according to their spatiotemporal characteristics will provide to the video research community the ability to quantify the perceptual impact of the various content dynamics on the perceptual efficiency of the modern encoding standards.

Towards this classification, a spatiotemporal plane is proposed, where each video signal (subject to short duration and homogeneous content) is depicted as Cartesian point in the spatiotemporal plane, where the horizontal axis refers to the spatial component of its content dynamics and the vertical axis refers to the temporal one. The respective plane is depicted on Figure 1.

Therefore, according to this approach, each video clip can be classified to four categories depending on its content dynamics, namely,

- (i) Low Spatial Activity-Low Temporal Activity (upper left),
- (ii) High Spatial Activity-Low Temporal Activity (upper right),
- (iii) Low Spatial Activity-High Temporal Activity (lower left),
- (iv) High Spatial Activity-High Temporal Activity (lower right).

The accuracy of the proposed spatiotemporal content plane is subject to the duration of the video signal and the homogeneity of the content. For short duration and homogeneous content video clips, the classification is representative and efficient. However, for video clips of longer duration and heterogeneous content, spatiotemporal classification is becoming difficult.

We propose to use two discrete metrics, one for the spatial component and one for the temporal one in order to cover the spatiotemporal plane and the needs of this paper. The averaged frame variance is proposed for the spatial component of the video signal. This objective metric permits



FIGURE 2: Snapshots of the training and validation content types.

the quantification of the spatial dynamics of a video signal short in duration and homogeneous. Considering that a frame y is composed of N pixels x_i , then the variance of a frame is defined in

$$\sigma_{\text{frame},y}^2 = \frac{1}{N} \sum_{i=1}^N (x_i - \bar{x})^2. \quad (1)$$

Derived from (1), (2) presents the averaged frame variance for the whole video duration. K represents the number of frames in the video

$$\frac{1}{K} \sum_{k=1}^K \sigma_{\text{frame},y}^2 = \frac{1}{K} \frac{1}{N} \sum_{k=1}^K \sum_{i=1}^N (x_{k,i} - \bar{x}_k)^2. \quad (2)$$

The averaged variance of the successive y frame luminance difference is proposed as a metric for the quantification of the temporal dynamics of a video sequence. Considering that a frame contains N pixels x_i and K , the number of frames in the video, then the averaged frame difference of the successive frame pairs is defined in

$$\frac{1}{K-1} \sum_{k=2}^K \frac{1}{N} \sum_{i=1}^N (x_{k,i} - x_{k-1,i}). \quad (3)$$

Therefore, the averaged variance for the overall duration of the test signal is defined in

$$\frac{1}{K-1} \sum_{k=2}^K \left(\frac{1}{N} \sum_{i=1}^N (x_{k,i} - x_{k-1,i}) - \frac{1}{K-1} \sum_{k=2}^K \frac{1}{N} \sum_{i=1}^N (x_{k,i} - x_{k-1,i}) \right)^2. \quad (4)$$

The scale in both axes refers to the normalized measurements (considering a scale from 0 up to 1) of the spatial and temporal component, according to the aforementioned metrics. The normalization procedure applied in this paper, sets the test signal with the highest spatiotemporal content to the lower right quarter and specifically to the Cartesian (Spatial, Temporal) values (0.75, 0.75). This hypothesis, without any loss of generality, allows to our classification grid the possibility to consider also test signals that may have higher spatiotemporal content in comparison to the tested ones.

For the needs of this paper six short sequences (three for training and three for validation) are used. Snapshots of these sequences are depicted in Figure 2. All sequences are available to download from [28].

Applying the described spatial and temporal metrics on the sequences used, their classification on the proposed

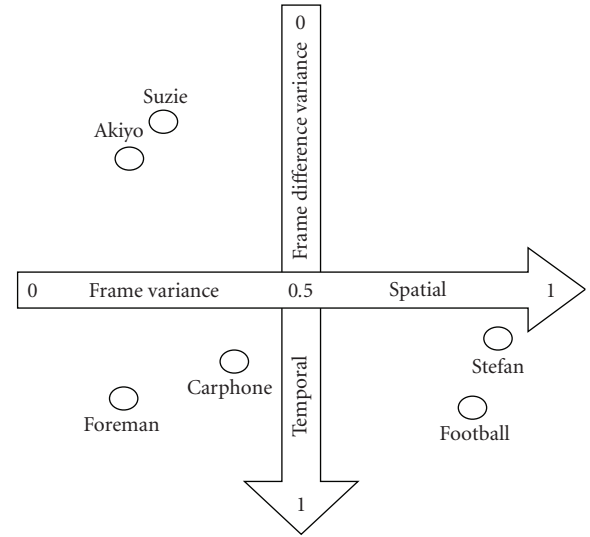


FIGURE 3: Spatiotemporal classification of the training and validation sequences.

spatiotemporal grid is depicted on Figure 3. According to Figure 3, it can be observed that the spatiotemporal dynamics of the selected sequences are distributed to the three quarters of the spatiotemporal grid, indicating their diverse nature of the content dynamics. Moreover, the validity of the proposed metrics is certified by these experimental results, showing that they provide adequate differentiation among the dynamics of the signals under test.

3.2. Video Quality Prediction Method. Figure 4 illustrates how the video quality is predicted nonintrusively. At the top of Figure 4, intrusive video quality measurement block is used to measure video quality at different network QoS conditions (e.g., different packet loss, jitter, and delay) or different application QoS settings (e.g., different codec type, content type, sender bitrate, frame rate, and resolution). The measurement is based on comparing the reference and the degraded video signals. Peak Signal-to-Noise Ratio (PSNR) is used for measuring video quality in the paper to prove the concept. MOS values are obtained from PSNR to MOS conversion [29]. The video quality measurements based on MOS values are used to derive nonintrusive prediction model based on artificial neural networks and nonlinear regression methods. The derived prediction model can predict video quality (in terms of MOS) from the physical layer QoS parameters of block error rate and mean burst

length and the application layer QoS parameters of content type, SBR, and frame rate. In Figure 4 the video content classification is carried out from raw videos at the sender side by extracting their spatial and temporal features. The spatio-temporal metrics have quite low complexity and thus can be extracted from videos in real-time. Video contents are classified as a continuous value from 0 to 1, with 0 as content with no movement, for example, still pictures and 1 as a very fast moving sports type of content. The content features reflecting the spatiotemporal complexity of the video go through the statistical classification function (cluster analysis) and content type is decided based on the Euclid distance of the data [12]. Therefore, video clips in one cluster have similar content complexity. Hence, our content classifier takes the content features as input observations while content category as the output. For larger video clips or movies the input will be segment-by-segment analysis of the content features extracted. Therefore, within one movie clip there will be a combination of all content types.

3.3. Content Dynamics and Video Quality Prediction. In this subsection, we discuss the spatiotemporal content dynamics impact on (i) the video quality acceptance threshold (i.e., the perceptual quality level below which the user considers that an encoded video is of unacceptable quality), (ii) the highest achievable video quality level, and (iii) the pattern of video quality versus sender bitrate.

In order to examine the impact of the content dynamic on the deduced video quality versus the sender bitrate pattern, respective curves of PQoS versus sender bitrate and PQoS versus frame rate should be derived. Such curves can be derived using an audience of people, who are watching the video (e.g., a short video clip) and score its quality, as perceived by them. Such curves are shown in Figures 5(a) and 5(b). Figure 5(a) represents PQoS versus sender bitrate curves which follow the typical logarithmic/exponential pattern that can be met at the literature. More specifically, curve A represents a video clip with low temporal and spatial dynamics, that is, whose content has “poor” movements and low picture complexity. Such a curve can be derived, for example, from a talk show. Curve C represents a short video clip with high dynamics, such as a football match. Curve B represents an intermediate case. Each curve—and therefore each video clip—can be characterized by (a) the low sender bitrate (SBR_L), which corresponds to the lower value of the accepted PQoS (PQ_L) by the audience, (b) the high sender bitrate (SBR_H), which corresponds to the minimum value of the sender bitrate for which the PQoS reaches its maximum value (PQ_H) (see BR_H for curve A in Figure 5(a)), and (c) the mean inclination of the curve, which can be defined as $ME = (PQ_H - PQ_L)/(SBR_H - SBR_L)$. From the curves of Figure 5(a), it can be deduced that video clips with low dynamics have lower SBR_L than clips with high dynamics.

In comparison to Figure 5(a), the curves in Figure 5(b) represent PQoS versus frame rates for the three types of video clips. As mentioned before curve A represents video clip with low spatiotemporal activity, curve B represents an intermediate case and curve C represents video with high

spatio-temporal activity. We observe from Figure 5(b) that for video with low spatio-temporal activity, frame rates do not have any impact on quality. However, as the spatio-temporal activity increases, for example, from intermediate to high, then for low frame rates quality degrades significantly depending on the spatio-temporal complexity.

In the literature, the specific curves are characterized as Benefit Functions, because they depict the perceptual efficiency of an encoded signal in relevance to the encoding bitrate. The differentiation among these curves comes from their slope and position on the benefit-resource plane, which depend on the S-T activity of the video content. Thus, the curve has low slope and transposes to the lower right area of the benefit-resource plane, for audiovisual content of high S-T activity. On the contrary, the curve has high slope and transposes to the upper left area, for low S-T activity content.

Practically, the transposition of the curve to the upper left area means that content with low S-T activity (e.g., a talk show) reaches a better PQoS level at relatively lower sender bitrate in comparison with a video content with high S-T activity. In addition, when the encoding bitrate decreases below a threshold, which depends on the video content, the PQoS practically “collapses”. On the other hand, the transposition of the curve to the lower right area means that content with high S-T activity (e.g., a football match) requires higher sender bitrate in order to reach a satisfactory PQoS level. Nevertheless, it reaches its maximum PQoS value more smoothly than in the low S-T activity case.

Practically, it can be observed from Figure 5(a) that in low sender bitrates curve A reaches a higher perceptual level compared to curve B depicting a sequence with higher spatiotemporal content. On the other hand, curve C requires higher sender bitrate in order to reach a satisfactory PQoS level. Nevertheless, curve (C) reaches its maximum PQoS value more smoothly than in the low activity case.

Following the general pattern in Figures 5(a) and 5(b), it can be observed that the impact of the spatiotemporal activity on the sender bitrate pattern is depicted very clearly. It also shows two more important outcomes:

- (i) For video signals with low spatiotemporal activity, a saturation point appears, above which the perceptual enhancement is negligible even for very high encoding bitrates. However, frame rates do not have an impact on quality for the same videos.
- (ii) As the spatiotemporal activity of the content becomes higher, the respective perceptual saturation point (i.e., the highest perceptual quality level) becomes lower, which practically means that video of high dynamics never reaches a very high perceptual level. The low frame rates reduce the perceptual quality for the same videos.

4. Proposed Video Quality Prediction Models

4.1. Introduction to the Models. The aim is to develop learning models to predict video quality for all content types from both application and physical layer parameters for video streaming over UMTS networks as shown in

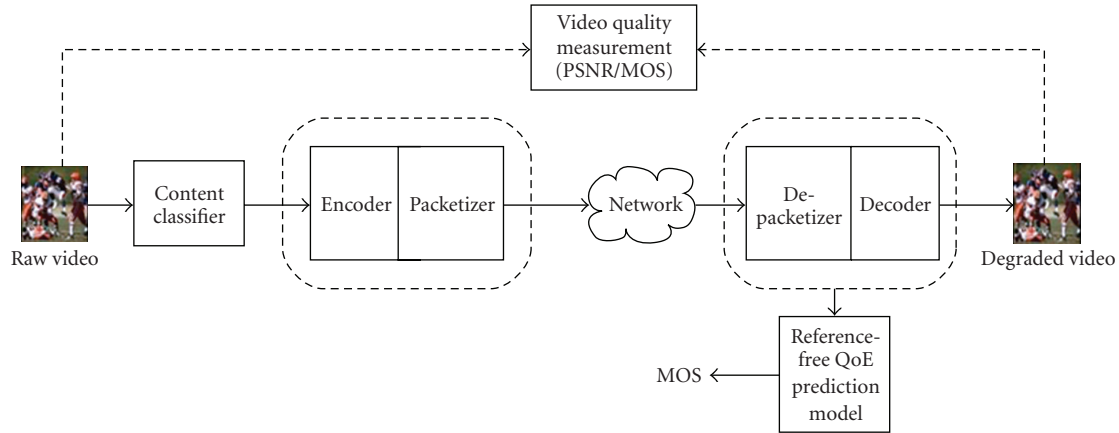


FIGURE 4: Conceptual diagram to illustrate video quality prediction.

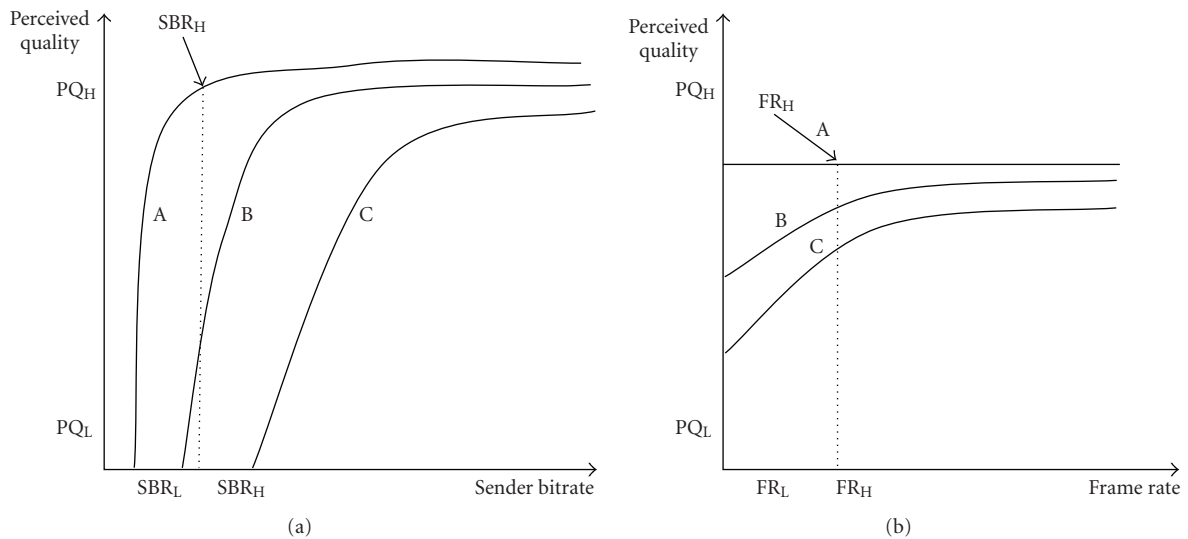


FIGURE 5: (a) Impact of dynamics on the video quality versus sender bitrate curves. (b) Impact of dynamics on the video quality versus frame rate curves.

Figure 6. For the tests we selected three different video sequences representing slow moving content to fast moving content as classified in our previous work [12]. The video sequences were of QCIF resolution (176×144) and encoded in H.264 format with an open source JM software [26] encoder/decoder. The three video clips were transmitted over simulated UMTS network using OPNET simulator. The application layer parameters considered are CT, FR, and SBR. The physical layer parameters are BLER and MBL modelled with 2-state Markov model.

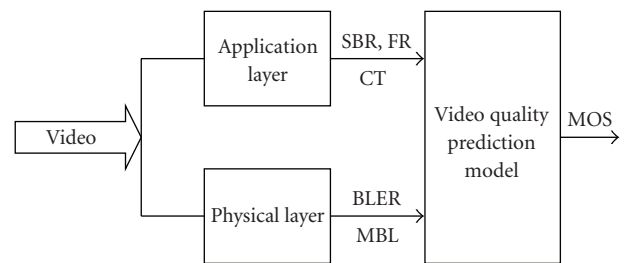
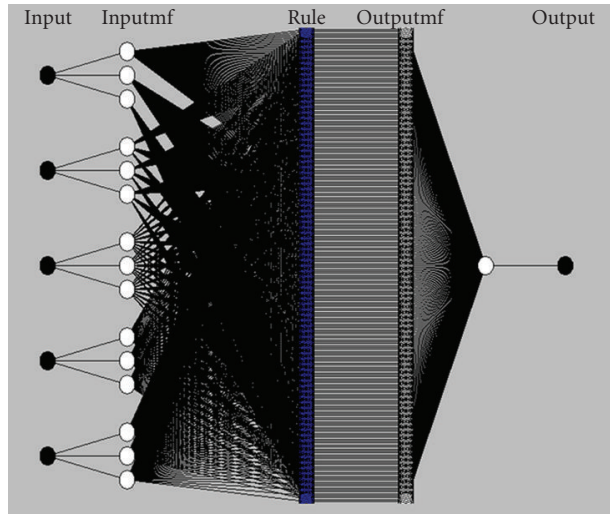
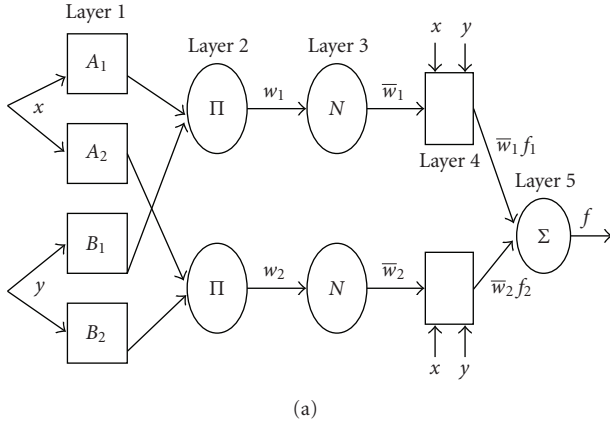


FIGURE 6: Functional block of proposed video quality prediction model.

4.2. ANFIS-Based Video Quality Prediction Model. ANFIS uses a hybrid learning procedure and can construct an input-output mapping based on both human knowledge (in the form of fuzzy if-then rules) and stipulated input-output data pairs. A two-input ANFIS [25] architecture as shown in Figure 7(a) is an adaptive multilayer feedforward network in which each node performs a particular function on incoming signals as well as a set of parameters pertaining to this node.

The entire system architecture in Figure 7(a) consists of five layers, namely, a fuzzy layer, a product layer, a normalized layer, a defuzzy layer, and a total output layer. The two inputs are x and y . The output is f . For a first-order Sugeno fuzzy model, a typical rule set with two fuzzy if-then rules can be



Logical operations

- And
- Or
- Not

(b)

FIGURE 7: (a) ANFIS architecture [25]. (b) ANFIS architecture.

expressed as

Rule 1: If x is A_1 and (y is B_1), then $f_1 = p_1x + q_1y + r_1$,

Rule 2: If x is A_2 and (y is B_2), then $f_2 = p_2x + q_2y + r_2$,

where p_1, p_2, q_1, q_2, r_1 , and r_2 are linear parameters, and A_1, A_2, B_1 , and B_2 are nonlinear parameters

$$f = \frac{w_1 f_1 + w_2 f_2}{w_1 + w_2}. \quad (5)$$

The corresponding equivalent ANFIS architecture for our model is shown in Figure 7(b).

The five chosen inputs in Figure 7(b) are Frame Rate (FR), Sender Bitrate (SBR), Content Type (CT), Block Error Rate (BLER), and Mean Burst Length (MBL). Output is the MOS score. The degree of membership of all five inputs is shown in Figure 8.

The number of membership function is two for all five inputs and their operating range depends on the five inputs.

For example for input of SBR the operating range is (50–250).

4.3. Regression-Based Video Quality Prediction Model. The relationship of MOS and the 5 selected inputs is shown in Figure 9. From Figure 9 we can obtain the range of MOS values obtained for each input, for example, from MOS versus FR, the range of MOS is from 1 to 4.5 for FRs of 5, 10, and 15. Once the relationship between MOS and the five selected inputs was found for the three content types representing low spatio-temporal to high ST features, we carried out nonlinear regression analysis with the MATLAB function *nlintool* to find the nonlinear regression model that best fitted our data.

4.4. Training and Validation of the Proposed Models. For artificial neural networks, it is not a challenge to predict patterns existing on a sequence with which they were trained. The real challenge is to predict sequences that the network did not use for training. However, the part of the video sequence to be used for training should be “rich enough” to equip the network with enough power to extrapolate patterns that may exist in other sequences. The three content types used for training the models were “akiyo”, “foreman”, and “Stefan”, whereas, the model was validated by three different content types of “suzie”, “carphone”, and “football” reflecting similar spatio-temporal activity [12]. Snapshots of the training and validation sequences are given in Figure 2. The data selected for validation was one third that of testing. The parameter values are given in Table 1. In total, there were around 600 sequences for training and around 250 test sequences for validation for the proposed models.

5. Simulation Set-Up

5.1. Network Topology. The UMTS network topology is modeled in OPNET Modeler and is shown in Figure 10. It is made up of a Video Server, connected through an IP connection to the UMTS network, which serves to the mobile user.

With regard to the UMTS configuration, the video transmission is supported over a Background Packet Data Protocol (PDP) Context with a typical mobile wide area configuration as defined in 3GPP TR 25.993 [1] for the “Interactive or Background/UL:64 DL:384 kbps/PS RAB”. The transmission channel supports maximum bitrates of 384 kbps Downlink/64 kbps Uplink over a Dedicated Channel (DCH). Since the analyzed video transmission is unidirectional, the uplink characteristics are not considered a bottleneck in this case. Table 1 shows the most relevant parameters configured in the simulation environment.

The RLC layer is configured in Acknowledge Mode (AM) and without requesting in-order delivery of Service Data Units (SDUs) to upper layers. Additionally, the Radio Network Controller (RNC) supports the concatenation of RLC SDUs, and the SDU Discard Timer for the RLC AM recovery function is set to 500 ms. As a result of all these

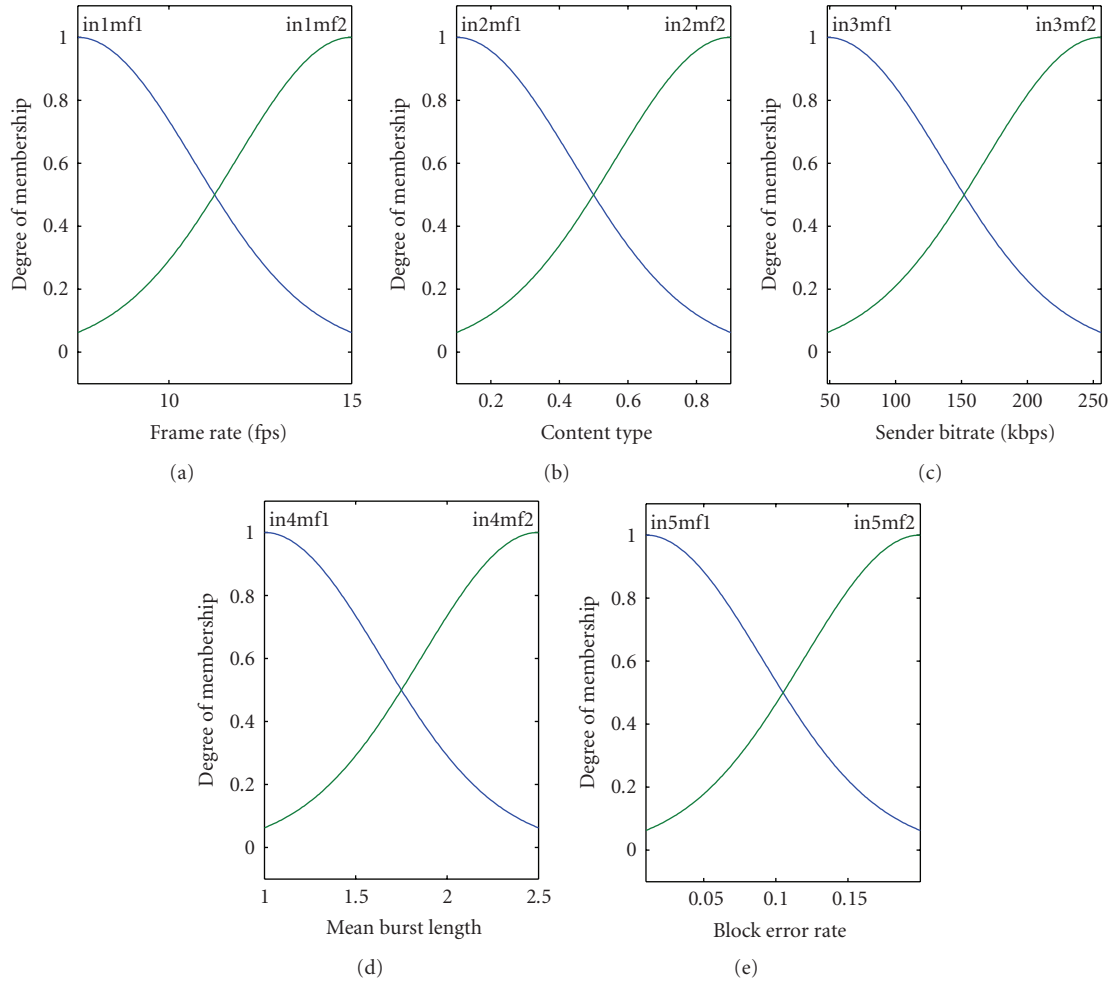


FIGURE 8: Membership function for the 5 selected inputs.

TABLE 1: DL UTRAN Configuration.

UTRAN Feature	Value
Max. bitrate at RLC level	384 kbps
RLC PDU size	320 bits
RLC Mode	Acknowledged Mode (AM)
Delivery order of SDUs	No In-Order Delivery
Allowed Transport Format Set (TFS)	Six possible TFs: 0-1-2-4-8-12 TB/TBS
SDU discard mode	Timer Based, Discard Timer = 500 ms
SDU concatenation	Enabled
Transport Block (TB) size	336 bits
PHY layer	
Transmission Time Interval (TTI)	10 ms
Transmission Channel (TrCH) type	Dedicated Channel (DCH)

configuration parameters, the behavior of the UTRAN is as follows.

- (i) The RNC keeps sending RLC SDUs to the UE at the reception rate.
- (ii) When an RLC PDU is lost, the RNC retransmits this PDU.

(iii) When all the PDUs of an RLC SDU are correctly received, the UE sends it to the upper layer regardless the status of the previous RLC SDUs.

(iv) If a retransmitted RLC PDU is once again lost, the RNC tries the retransmission until the SDU Discard Timer expires.

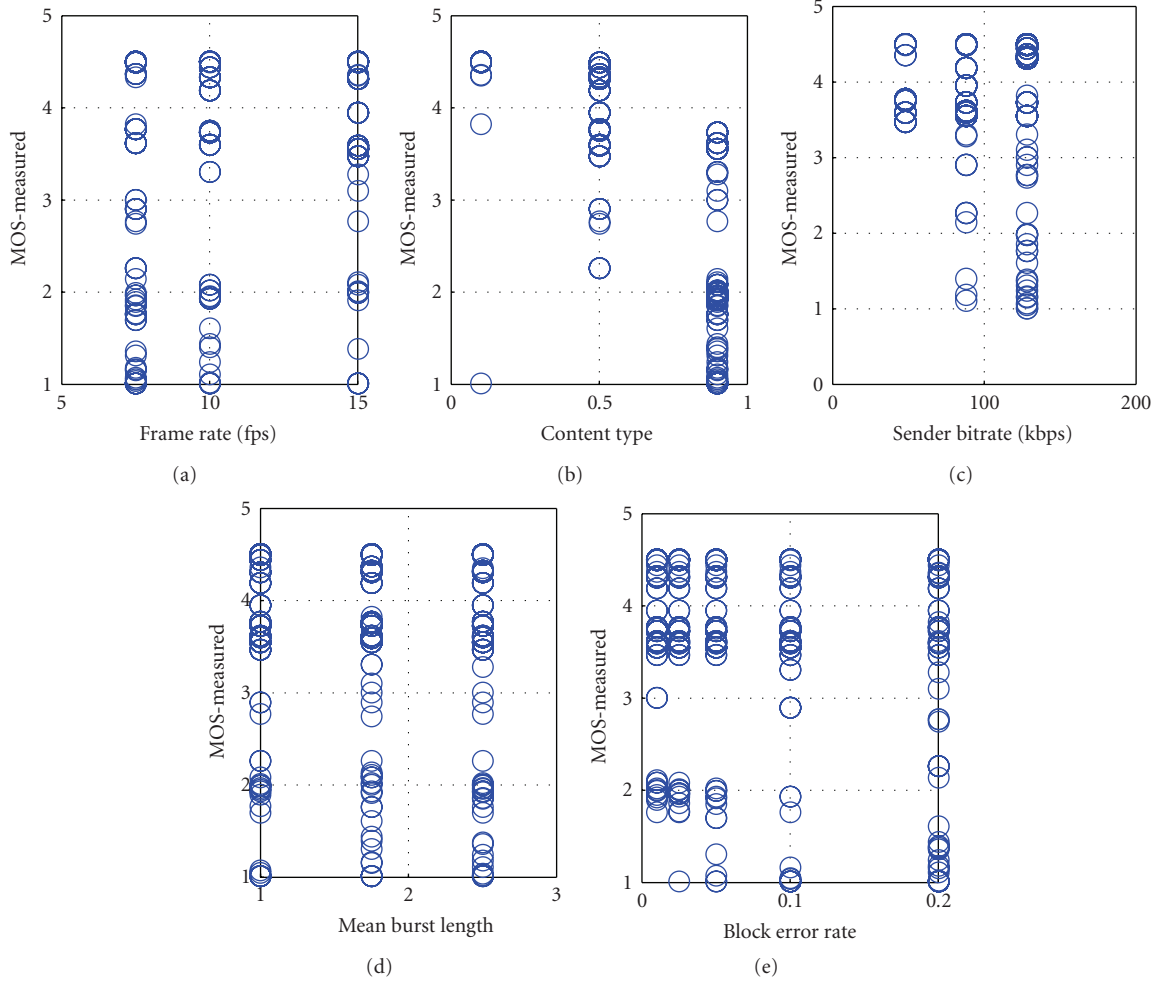


FIGURE 9: Relationship between the 5 selected inputs and MOS.

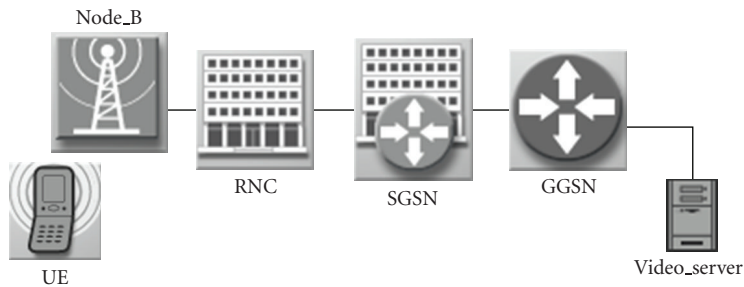


FIGURE 10: OPNET network scenario.

Although the considered UMTS service supports the recovery of radio errors in the UTRAN, the quality of the video reception may be impacted in several ways. The local recoveries introduce additional delays, which may lead to frame losses in the application buffer. As well, the local recoveries are limited by a counter, so in severe radio degradations some frames may be actually lost in the UTRAN. Additionally, these recoveries increase the required bitrate in the radio channel, which in high usage ratios may further degrade the

video transmission. As a result of all these considerations, we can state the great relevance of the combined impact of the video encoding parameters and the specific UMTS error conditions.

The implemented UMTS link layer model is based on the results presented in [23], which analyzes the error traces from currently deployed 3G UMTS connections. Specifically, the error model at RLC layer indicates that, for mobile users, the radio errors can be aggregated at Transmission Time Interval

(TTI-) level. This error model leads to possible losses of RLC SDUs, which lead to losses at RTP layer and finally to frame losses at video layer.

5.2. Transmission of H.264 Encoded Video. The transmission of H.264 encoded video over UMTS network is illustrated in Figure 11. The original YUV sequences are encoded with the H.264/AVC JM Reference Software with varying SBR and FR values. H.264 is chosen as it is the recommended codec to achieve suitable quality for low bitrates. The resulting 264 video track becomes the input of the next step, which emulates the streaming of the mp4 video over the network based on the RTP/UDP/IP protocol stack. The maximum packet size is set to 1024 bytes in this case. The resulting trace file feeds the OPNET simulation model. For the aims of this paper, the video application model has been modified to support the incoming trace file (st) and generate the RTP packet traces in the sender module (sd) and in the receiver module (rd). Finally, the last step is in charge of analyzing the quality of the received video sequences against the original quality and the resulting PSNR values are calculated with the ldecod tool included in the H.264/AVC JM Reference Software. MOS scores are calculated based on the PSNR-to-MOS conversion from Evalvid [29].

Instead of setting up a target BLER value for the PDP Context, the UE model is modified in order to support the desired error characteristics. The implemented link loss model is special case of a 2-state Markov model [20, 21] and its performance is provided by two parameters: the BLER and the MBL. The 2-state Markov Model is depicted in Figure 12. According to this model, the network is either in good (G) state, where all packets are correctly delivered, or in bad (B) state, where all packets are lost. Transitions from G to B and vice versa occur with probability $1 - \beta$ and $1 - \alpha$. The average block error rate and mean burst length can be expressed as $MBL = (1 - \alpha)^{-1}$ and $BLER = (1 - \beta)/(2 - \alpha - \beta)$. If $\alpha = 0$, this reduces to random error model with the only difference that loss of two consecutive packets is not allowed.

The $MBL = 1.75$ is selected based on the mean error burst length found in [23] from real-world UMTS measurements. The $MBL = 2.5$ depicts a scenario where more bursty errors are found, while the $MBL = 1$ depicts random uniform error model.

5.3. Test Sequences and Variable Test Parameters. The video encoding process was carried out using the H.264 codec as the most prominent alternative for low bandwidth connections. From the 3GPP recommendations we find that for video streaming services, such as VOD or unicast IPTV services, a client should support H.264 (AVC) Baseline Profile up to Level 1.2. [26]. As the transmission of video was for mobile handsets, all the video sequences are encoded with a QCIF resolution. The considered frame structure is IPP for all the sequences, since the extensive use of I frames could saturate the available data channel. From these considerations, we set up the encoding features as shown in Table 2.

The variable encoding parameters of the simulations are the video sequence, the encoding frame rate, and the target

TABLE 2: Encoding parameter set.

Encoding parameter	Value
Profile/level IDC	(66,11) baseline profile, level 1.1
Target BR	Variable (see Table 3)
Frame Skip (resulting FR)	Variable (see Table 3)
Spatial resolution	QCIF (176 × 144)
Sequence type	IPPP
Entropy coding method	CAVLC
RD-optimized mode decision	Enabled
Data partitioning mode	1 partition
FMO	No FMO
Slice mode	Not used
Total number of reference frames	5
Output type	Annex B [26]

bitrate at the Video Coding Layer (VCL). The experiment takes into account six test sequences, divided in two groups: akiyo, foreman, and stefan are used for training the model, while carphone, suzie, and football are devoted to the validation of results. The selected frame rates and bitrates are considered for low resolution videos, targeted at a mobile environment with a handset reproduction.

For the UTRAN configuration, the 2-state Markov model is set up at different BLER values and different burst patterns in order to study the effect into the application layer performance. The video sequences along with the combination of parameters chosen are given in Table 3.

6. Impact of QoS Parameters on End-to-End Video Quality

In this section, we study the effects of the five chosen QoS parameters on video quality. We chose three-dimensional figures in which two parameters were varied while keeping the other three fixed. The MOS scores are computed as a function of the values of all five QoS parameters.

6.1. Impact of BLER and MBL on Content Type (CT). The impact of MBL and BLER on our chosen content types is given in Figures 13(a) and 13(b).

The content type is defined in the range of [0, 1] from slow moving to fast moving sports type of content. From Figure 13(a), we observe that as the activity of the content increases the impact of BLER is much higher. For example, for 20% BLER, CT of slow to medium type gives very good MOS; whereas as the content activity increases, MOS reduces to 3. From Figure 13(b) we observe that the MBL similar to BLER has greater impact for content types with higher S-T activity.

Similarly, the impact of SBR and FR on CT is given by Figures 14(a) and 14(b). Again we observe that as the activity of content increases for very low SBRs (20 kb/s) and low FRs (5 f/s) the MOS is very low. However, for slow to medium content activity the impact of SBR and FR is less obvious.

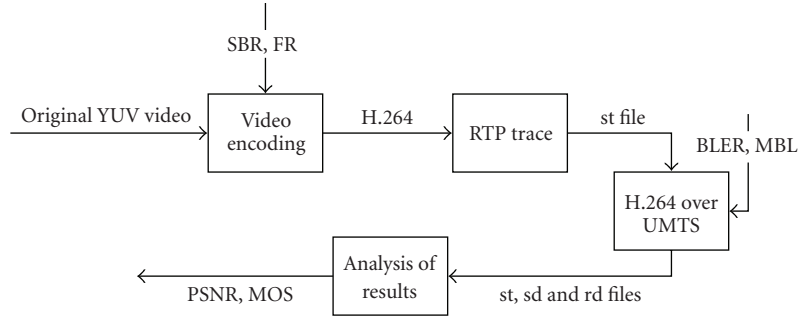


FIGURE 11: Simulation methodology.

TABLE 3: Simulation parameters.

Video sequences	FR (fps)	SBR (kbps)	BLER (%)	MBL
Akiyo, Foreman	7.5, 10, 15	48, 88, 128		
Suzie, Carphone	10, 15	90, 130	1, 5, 10, 15, 20, 30, 50	1, 1.75, 2.5
Stefan	7.5, 10, 15	88, 130, 256		
Football	10, 15	130, 200		

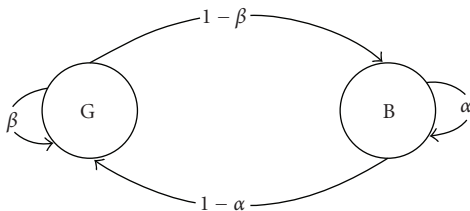


FIGURE 12: 2-state Markov loss model.

The lower value of MOS for higher SBR is due to network congestion.

6.2. *Impact of BLER and MBL on SBR.* The combined impact of SBR and BLER/MBL is given in Figure 15. As expected, with increasing BLER and MBL the quality reduces. However, for increasing SBR the quality improves up to a point (SBR \sim 80 kb/s) then increasing the SBR results in a bigger drop of quality due to network congestion. From Figure 15(b) we observe that the best quality in terms of MOS was for an MBL of 1 (depicted random uniform scenario). This would be expected because the BLER was predictable. The worst quality was for BLER of 2.5 (very bursty scenario). Again this substantiates the previous findings on 2-state Markov model. It was interesting to observe how MBLs impact on quality; however it is captured by the QoS BLER. Similar to Figure 15(a) for high SBR, quality collapse for all values of MBLs due to network congestion.

6.3. *Impact of BLER and MBL on FR.* Figures 16(a) and 16(b) show the impact of BLER and MBL on FR for all content types. We observe that for faster moving contents very low frame rates of 7.5 fps impair quality. Again, we observe that both BLER and MBL impact on the overall quality. The impact of frame rate is more obvious for low

TABLE 4: Five-way ANOVA on MOS.

Parameters	Sum of Squares	Degrees of Freedom	Mean Squares	F statistic	P-value
CT	29.508	2	14.754	109.27	0
FR	1.017	2	1.016	7.53	.0069
SBR	9.559	2	4.7797	35.4	0
BLER	1.152	4	0.3839	2.84	.0402
MBL	0.361	2	0.1807	1.34	.2659

FRs and high BLER. However, when BLER is low quality is still acceptable. This is shown in Figure 16(a). Figure 16(b) shows that for low FRs quality is acceptable for MBL of 1.5. However, for MBL of 1 it starts to deteriorate. This is mainly for high spatio-temporal contents. However, quality completely collapses for MBL of 2.5 (very bursty scenario). Again the impact is much greater on contents with high spatio-temporal activity compared to those with low ST activity.

6.4. *Analysis of Results.* In order to thoroughly study the influence of different QoS parameters on MOS we perform ANOVA (analysis of variance) [30] on the MOS data set. Table 4 shows the results of the ANOVA analysis.

We performed 5-way ANOVA to determine if the means in the MOS data set given by the 5 QoS parameters differ when grouped by multiple factors (i.e., the impact of all the factors combined). Table 4 shows the results, where the first column is the Sum of Squares, the second column is the Degrees of Freedom associated with the model, and the third column is the Mean Squares, that is, the ratio of Sum of Squares to Degrees of Freedom. The fourth column shows the F statistic and the fifth column gives the P-value, which is derived from the cumulative distribution function (cdf) of F [30]. The small P-values ($P \leq .01$) indicate that the

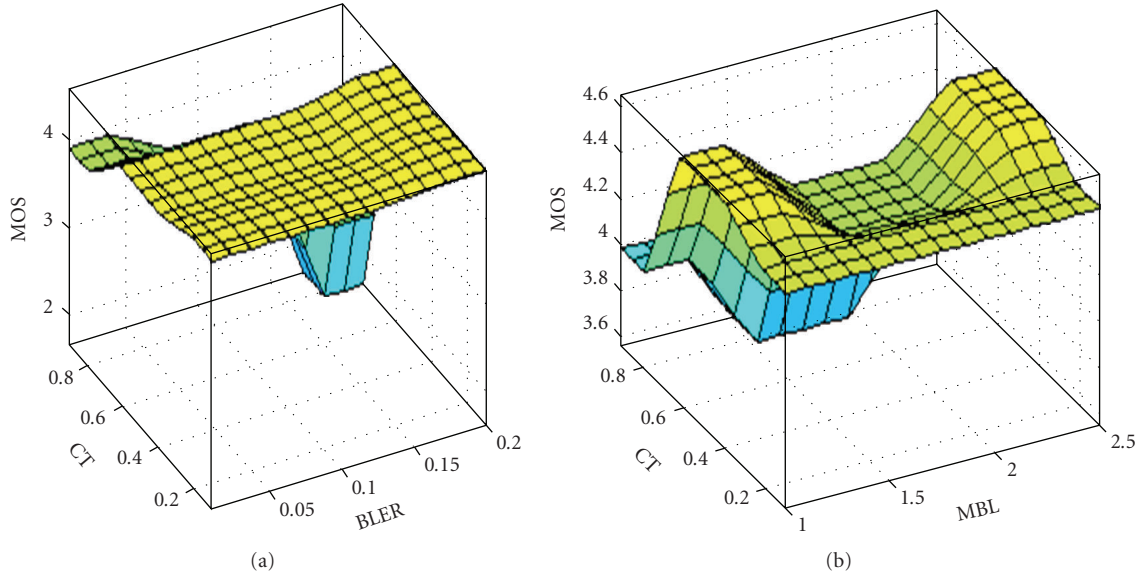


FIGURE 13: (a) MOS versus CT versus BLER. (b) MOS versus CT versus MBL.

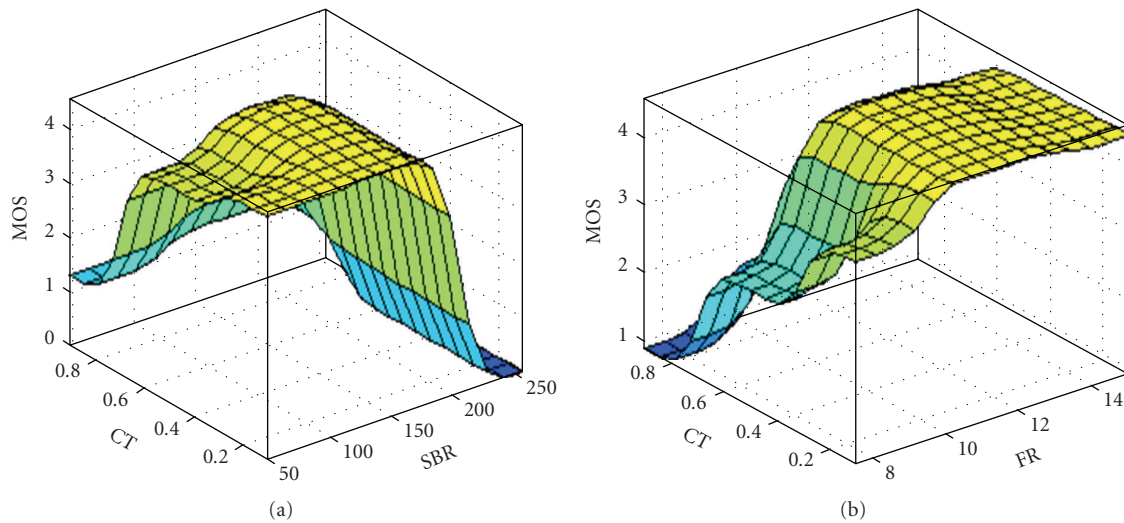


FIGURE 14: (a) MOS versus CT versus SBR. (b) MOS versus CT versus FR.

MOS is substantially affected by at least four parameters. Furthermore, based on the magnitudes of P -values, we can make a further claim that CT and SBR (P -value = 0) impact the MOS results the most, followed by FR and then BLER, while MBL has the least influence. As the MOS is found to be mostly affected by CT and SBR, we further categorize the CT and SBR using the multiple comparison test based on Tukey-Kramer's Honestly Significant Difference (HSD) criterion [31]. The results of comparison test for CT and SBR are shown in Figures 17(a) and 17(b), where the centre and span of each horizontal bar indicate the mean and the 95% confidence interval, respectively. The different colours in Figure 17 highlight similar characteristics and are very useful in grouping similar attributes together. In Figure 17(a) (CT versus MOS), CT is classified as [0.1 0.9], 0.1 is slow

moving content, for example, Akiyo and 0.9 are Stefan. Therefore, from Figure 17(a), we can see that MOS is from 2.5 to 2.7 for Stefan as compared to MOS between 4.3 to 4.6 for slow moving content (Akiyo) and 3.8–4.0 for medium ST activity (Foreman). Therefore, from Figure 17(a), we observe that content types with medium-to-high S-T activity show similar attributes, compared to that with low S-T activity. Similarly, in Figure 17(b), the impact of higher SBR (i.e., 128 and 256) have similar impact on quality due to network congestion issues compared to that of low SBR values.

Our studies (Figures 13–17) numerically substantiate the following observations of video quality assessment.

- (i) The most important QoS parameter in the application layer is the content type. Therefore, an accurate

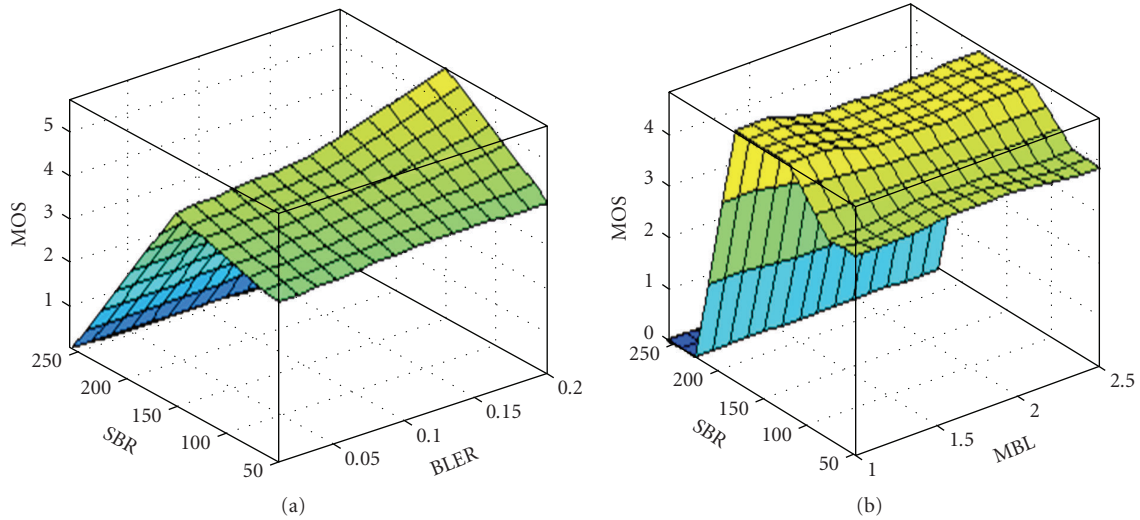


FIGURE 15: (a) MOS versus SBR versus BLER. (b) MOS versus SBR versus MBL.

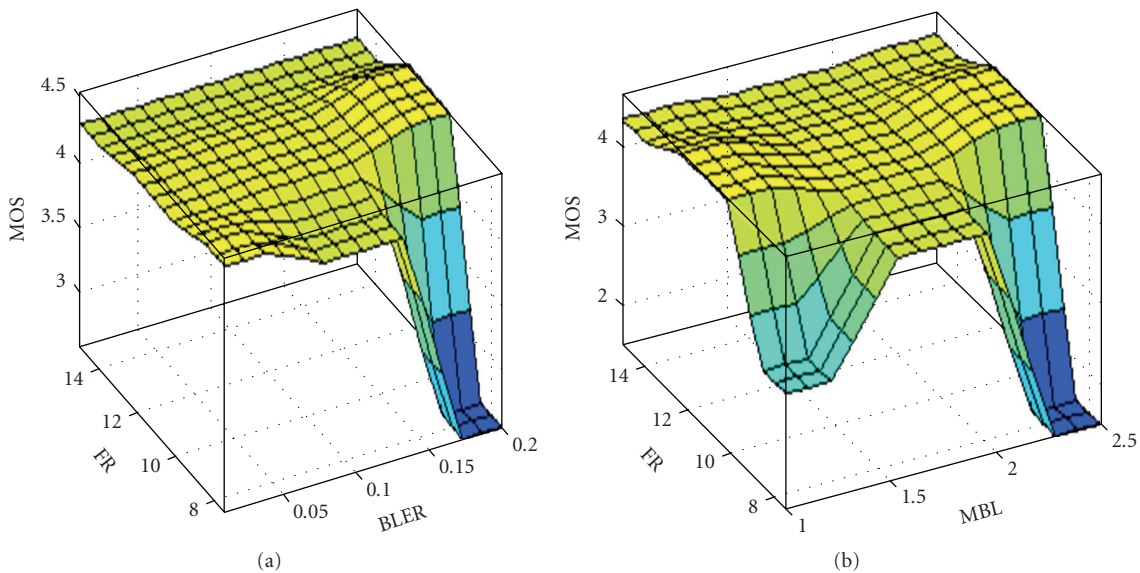


FIGURE 16: (a) MOS versus FR versus BLER. (b) MOS versus FR versus MBL.

video quality prediction model must consider all content types. Application layer parameters of SBR and FR are not sufficient in predicting video quality.

- (ii) The optimal combination of SBR and FR that gives the best quality is very much content dependent and varies from sequence to sequence. We found that for slow moving content $FR = 7.5$ and $SBR = 48$ kbps gave acceptable quality; however, as the spatio-temporal activity of the content increased this combination gave unacceptable quality under no network impairment.
- (iii) The most important QoS parameter in the physical layer is BLER. Therefore, an accurate video quality prediction model must consider the impact of physical layer in addition to application layer parameters.

- (iv) The impact of physical layer parameters of MBL and BLER varies depending on the type of content. For slow moving content, BLER of 20% gives acceptable quality; however, for fast moving content for the same BLER, the quality is completely unacceptable. Therefore, the impact of physical layer QoS parameters is very much content dependent.

7. Evaluation of the Proposed Video Quality Prediction Models

The aim was to develop learning models to predict video quality considering all content types and RLC loss models (2-state Markov) with variable MBLs of 1, 1.75, and 2.5 for H.264 video streaming over UMTS networks.

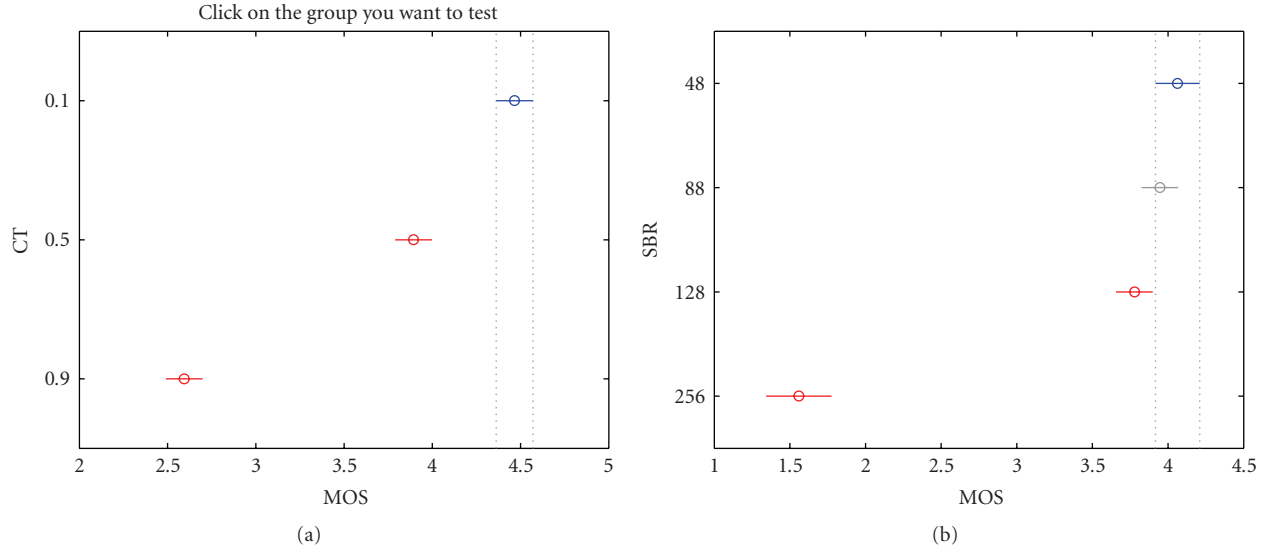


FIGURE 17: (a) Multiple comparison test for CT versus MOS. (b) Multiple comparison test for SBR versus MOS.

TABLE 5: Coefficients of metric models.

a	b	c	d	E	f	g	h
4.3911	$3.9544e - 08$	0.0447	8.8501	-2.1381	-0.3631	-10.1177	0.3442

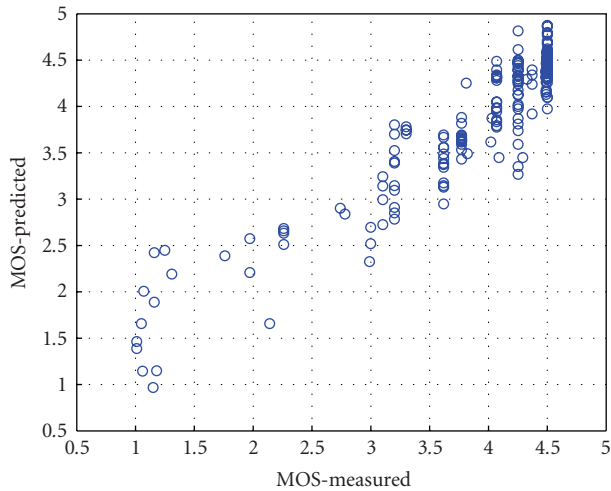


FIGURE 18: Predicted versus measured MOS results (ANFIS-based).

The models were trained with three distinct video clips (Akiyo, Foreman, and Stefan) and validated with video clips of Suzie, Carphone, and Football. The application layer parameters were FR, SBR and CT and physical layer parameters were BLER and MBL. The accuracy of the proposed video quality prediction models is determined by the correlation coefficient and the RMSE of the validation results. MATLAB *nlintool* is used for the nonlinear regression modeling

7.1. ANFIS-Based. The accuracy of the proposed ANFIS-based video quality prediction model is determined by

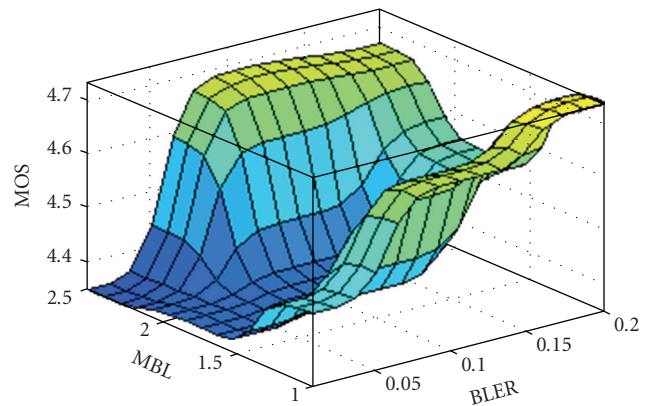


FIGURE 19: MOS versus BLER versus MBL for the three content types.

the correlation coefficient and the RMSE of the validation results. The model is trained with three distinct content types from parameters both in the application and physical layers over UMTS networks. The model is predicted in terms of the Mean Opinion Score (MOS). The predicted versus measured MOS for the proposed ANFIS-based prediction model is depicted in Figure 18.

7.2. Regression-Based. The procedure for developing the regression-based model is outlined below.

Step 1 (Select content types). We selected three video sequences with different impact on the user perception for training and three different video sequences for validation

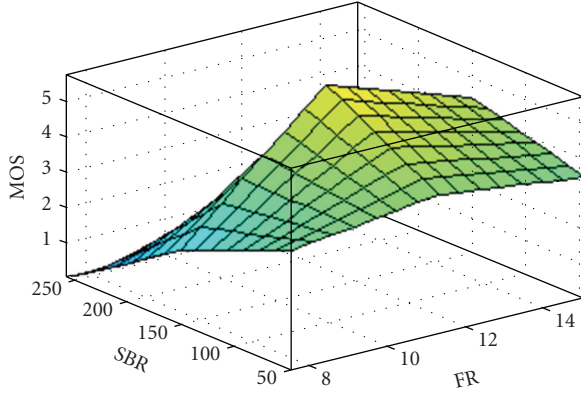


FIGURE 20: MOS versus SBR versus FR for the three content types.

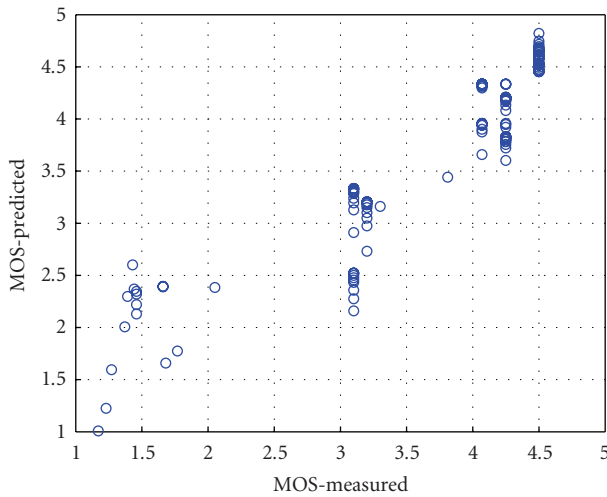


FIGURE 21: Predicted versus measured MOS results (regression-based).

as shown in Figure 2. The video sequences ranged from very little movement to fast moving sports type of clips to reflect the different spatio-temporal features. Hence, the proposed model is for all content types.

Step 2 (Obtain MOS versus BLER versus MBL). The impact of BLER and MBL on MOS is shown in Figure 19. From Figure 19, we observe that the higher the BLER and MBL values, the greater loss in overall quality. However, MBL of 1 gives the best quality for all values of BLER. Introducing burstiness reduces quality as would be expected.

Step 3 (Obtain MOS versus SBR versus FR). The relationship between MOS, SBR, and FR is shown in Figure 20. From Figure 20, we observe that at higher SBRs the video quality degrades rapidly due to the UMTS network congestion at downlink bandwidth. Similarly, at lower FRs, video quality degrades. The impact is greater on videos with higher spatio-temporal activity.

Step 4 (Surface fitting for nonlinear mapping from BLER, MBL, CT, SBR, and FR to MOS). A nonlinear regression

TABLE 6: Comparison of the models.

Models	R^2	RMSE
Regression-based	86.52%	0.355
ANFIS-based	87.17%	0.2812

analysis was carried out with the MATLAB function *nlintool*. We obtained the nonlinear equation given in (6) with a reasonable fitting goodness. The coefficients of the proposed model given in (6) are given in Table 5. Figure 21 shows the MOS-measured versus MOS predicted for the proposed model

$$\text{MOS} = a + \frac{be^{\text{FR}} + c \log(\text{SBR}) + \text{CT}(d + e \log(\text{SBR}))}{1 + (f(\text{BLER}) + g(\text{BLER})^2)h\text{MBL}} \quad (6)$$

7.3. Comparison of the Models. The models proposed in this paper are reference-free. The comparison of the two models in terms of the correlation coefficient (R^2) and Root Mean Squared Error (RMSE) is given in Table 6.

The performance of both the ANFIS-based and regression-based models over UMTS network is very similar in terms of correlation coefficient and RMSE as shown in Table 5. The model performance compared to a recent work given in [32] where the authors have used a tool called Pseudo-Subjective Quality Assessment (PSQA) based on random neural networks performs well. In [32], the authors train the random neural networks with network parameters, for example, packet loss and bandwidth. In addition they have used their tool to assess the quality of multimedia (voice and video) over home networks—mainly WLAN. Our proposed tool can be modified in the future to assess voice quality. However, our choice of parameters includes a combination of application and physical layer parameters and our access network is UMTS where bandwidth is very much restricted. Also compared to our previous work [12], where we proposed three models for the three content types, both the models perform very well.

We feel that the choice of parameters is crucial in achieving good prediction accuracy. Parameters such as MBL in link layer allowed us to consider the case of less bursty or more bursty cases under different BLER conditions. Also, in the application level, the content type has a bigger impact on quality than sender bitrate and frame rate. However, if frame rate is reduced too low, for example, 7.5 f/s, then frame rate has a bigger impact on quality than sender bitrate for faster moving content. Similarly, if the sender bitrate is too high, then quality practically collapses. This is due to the bandwidth restriction over UMTS network causing network congestion. Also contents with less movement require low sender bitrate compared to that of higher movement. Finally, to predict video quality, content type is very important.

8. Conclusions

This paper presented learning models based on ANFIS and nonlinear regression analysis to predict video quality over UMTS networks nonintrusively. We, further, investigated the combined effects of application and physical layer parameters on end-to-end perceived video quality and analyzed the behaviour of video quality for wide-range variations of a set of selected parameters over UMTS networks. The perceived video quality is evaluated in terms of MOS. Three distinct video clips were chosen to train the models and validated with unseen datasets.

The results demonstrate that it is possible to predict the video quality if the appropriate parameters are chosen. Our results confirm that the proposed models both ANFIS-based ANN and regression-based learning model are a suitable tool for video quality prediction for the most significant video content types.

Our future work will focus on extensive subjective testing to validate the models and implement them in our Internet Multimedia Subsystem-based test bed, and further applying our results to adapt the video sender bitrate and hence optimize bandwidth for specific content type.

Acknowledgment

The research leading to these results has received funding from the European Community's Seventh Framework Programme FP7/2007-2013 under grant agreement no. 214751/ICT-ADAMANTIUM/.

References

- [1] 3GPP TS 25.322, "Third Generation Partnership Project: Technical Specification Group Access network; Radio Link Control," RLC Specification (Release 5).
- [2] ITU-T. Rec P.800, "Methods for subjective determination of transmission quality," 1996.
- [3] Video quality experts group, "Multimedia group test plan," Draft version 1.8, December 2005, <http://www.vqeg.org/>.
- [4] Z. Wang, L. Lu, and A. C. Bovik, "Video quality assessment based on structural distortion measurement," *Signal Processing: Image Communication*, vol. 19, no. 2, pp. 121–132, 2004.
- [5] <http://compression.ru/video/index.htm>.
- [6] <http://www.pevq.org/>.
- [7] M. Ries, O. Nemethova, and M. Rupp, "Video quality estimation for mobile H.264/AVC video streaming," *Journal of Communications*, vol. 3, no. 1, pp. 41–50, 2008.
- [8] H. Koumaras, A. Kourtis, C.-H. Lin, and C.-K. Shieh, "A theoretical framework for end-to-end video quality prediction of MPEG-based sequences," in *Proceedings of the 3rd International Conference on Networking and Services (ICNS '07)*, June 2007.
- [9] K. Yamagishi, T. Tominaga, T. Hayashi, and A. Takahashi, "Objective quality evaluation model for videophone services," *NTT Technical Review*, vol. 5, no. 6, 2007.
- [10] P. Calyam, E. Ekici, C.-G. Lee, M. Haffner, and N. Howes, "A "GAP-model" based framework for online VVoIP QoE measurement," *Journal of Communications and Networks*, vol. 9, no. 4, pp. 446–456, 2007.
- [11] Q. Huynh-Thu and M. Ghanbari, "Temporal aspect of perceived quality in mobile video broadcasting," *IEEE Transactions on Broadcasting*, vol. 54, no. 3, pp. 641–651, 2008.
- [12] A. Khan, L. Sun, and E. Ifeachor, "Content-based video quality prediction for MPEG4 video streaming over wireless networks," *Journal of Multimedia*, vol. 4, no. 4, pp. 228–239, 2009.
- [13] W. Karner, O. Nemethova, and M. Rupp, "The impact of link error modeling on the quality of streamed video in wireless networks," in *Proceedings of the 3rd International Symposium on Wireless Communication Systems (ISWCS '06)*, pp. 694–698, Valencia, Spain, September 2006.
- [14] M. Rossi, L. Scaranari, and M. Zorzi, "Error control techniques for efficient multicast streaming in UMTS networks: proposals and performance evaluation," *Journal on Systems, Cybernetics and Informatics*, vol. 2, no. 3, 2004.
- [15] H. Peteghem, L. Schumacher, and C. De Vleeschouwer, *UMTS Parameterization for Real-Time Flows*, Qshine, Vancouver, Canada, August 2007.
- [16] A. Panchaem, S. Kamolpiwong, M. Unhawiwat, and S. Sae-wong, "Evaluation of UMTS RLC parameters for MPEG4 video streaming," *ECTI Transactions on Computer and Information Technology*, vol. 3, no. 1, 2007.
- [17] J. O. Fajardo, F. Liberal, and N. Bilbao, "Impact of the video slice size on the visual quality for H.264 over 3G UMTS services," in *Proceedings of the 6th International Conference on Broadband Communications, Networks and Systems, (BROAD-NETS '09)*, Madrid, Spain, September 2009.
- [18] A. Lo, G. J. Heijenk, and I. G. M. M. Niemegeers, "Performance evaluation of MPEG-4 video streaming over UMTS networks using an integrated tool environment," in *Proceedings of the International Symposium on Performance Evaluation of Computer and Telecommunication Systems (SPECTS '05)*, pp. 676–682, Philadelphia, Pa, USA, July 2005.
- [19] M. Malkowski and D. ClaBen, "Performance of video telephony services in UMTS using live measurements and network emulation," *Wireless Personal Communications*, vol. 46, no. 1, pp. 19–32, 2008.
- [20] E. N. Gilbert, "Capacity of a burst-noise channel," *Bell Systems Technical Journal*, vol. 39, pp. 1253–1265, 1960.
- [21] R. W. Lucky, "Automatic equalization for digital communication," *Bell Systems Technical Journal*, vol. 44, no. 4, pp. 547–588, 1965.
- [22] ITU-T Rec. M.60, 3008; ITU-T Rec.Q.9, 0222.
- [23] W. Karner, O. Nemethova, P. Svoboda, and M. Rupp, "Link error analysis and modeling for video streaming cross-layer design in mobile communication networks," *ETRI Journal*, vol. 29, no. 5, pp. 569–595, 2007.
- [24] M. Zorzi and R. R. Rao, "Perspectives on the impact of error statistics on protocols for wireless networks," *IEEE Personal Communications*, vol. 6, no. 5, pp. 32–40, 1999.
- [25] J.-S. R. Jang, "ANFIS: adaptive-network-based fuzzy inference system," *IEEE Transactions on Systems, Man and Cybernetics*, vol. 23, no. 3, pp. 665–685, 1993.
- [26] "JM H.264 Software," <http://iphome.hhi.de/suehring/tml/>.
- [27] "OPNET for research," <http://www.opnet.com/>.
- [28] "Raw video sequences," <http://trace.eas.asu.edu/yuv/index.html>.
- [29] J. Klaue, B. Rathke, and A. Wolisz, "EvalVid—a framework for video transmission and quality evaluation," in *Proceedings of the 13th International Conference on Modelling Techniques and Tools for Computer Performance Evaluation*, vol. 2794, pp. 255–272, Urbana, Ill, USA, 2003.

- [30] G. W. Snedecor and W. G. Cochran, *Statistical Methods*, Iowa State University Press, Iowa, Iowa, USA, 8th edition, 1989.
- [31] Y. Hochberg and A. C. Tamhane, *Multiple Comparison Procedures*, John Wiley & Sons, New York, NY, USA, 1987.
- [32] G. Rubino, M. Varela, and J.-M. Bonnin, "Controlling multimedia QoS in the future home network using the PSQA metric," *Computer Journal*, vol. 49, no. 2, pp. 137–155, 2006.

Research Article

Cross-Layer Optimization of DVB-T2 System for Mobile Services

Lukasz Kondrad,¹ Vinod Kumar Malamal Vadakital,¹ Imed Bouazizi,² Miika Tupala,³
and Moncef Gabbouj¹

¹Department of Signal Processing, Tampere University of Technology, 33720 Tampere, Finland

²Nokia Research Center, 33720 Tampere, Finland

³Nokia, 24100 Salo, Finland

Correspondence should be addressed to Lukasz Kondrad, lukasz.kondrad@tut.fi

Received 30 September 2009; Accepted 29 March 2010

Academic Editor: Georgios Gardikis

Copyright © 2010 Lukasz Kondrad et al. This is an open access article distributed under the Creative Commons Attribution License, which permits unrestricted use, distribution, and reproduction in any medium, provided the original work is properly cited.

Mobile broadcast services have experienced a strong boost in recent years through the standardization of several mobile broadcast systems such as DVB-H, ATSC-M/H, DMB-T/H, and CMMB. However, steady need for higher quality services is projected to surpass the capabilities of the existing mobile broadcast systems. Consequently, work on new generations of mobile broadcast technology is starting under the umbrella of different industry consortia, such as DVB. In this paper, we address the question of how DVB-T2 transmission can be optimized for improved mobile broadcast reception. We investigate cross-layer optimization techniques with a focus on the transport of scalable video (SVC) streams over DVB-T2 Physical Layer Pipes (PLP). Throughout the paper, we propose different optimization options and verify their utility.

1. Introduction

The success of the DVB family of standards over the last decade and the constant development of new technologies resulted in the creation of a second generation of DVB standards that is expected to bring significant improvements in performance and to cater for the evolving market needs for higher bandwidth. One of the standards is DVB-T2 [1], a new digital terrestrial TV standard, which is an upgrade for the widely used DVB-T system. The initial tests show that the new standard brings more than 40% bit-rate improvement compared to DVB-T [2].

The second generation of DVB standards also benefits from the latest state of the art coding technologies. The Scalable Video Coding (SVC) standard [3] was developed as an extension of the H.264 Advanced Video Coding (H.264/AVC) [3] codec. The new standard is advantageous especially as an alternative to the simulcast distribution mode, where the same service is broadcasted simultaneously to multiple receivers with different capabilities. Instead of sending two or more independent streams to serve user groups of different quality requirements as in simulcast, an

SVC encoded bit-stream, consisting of one base layer and one or more enhancements layers, may be transmitted to address the needs of those user groups. The enhancement layers improve the video in temporal, spatial, and/or quality domain. DVB recognized the potential of the SVC standard and adopted it as one of the video codecs used for DVB broadcast services [4].

In addition to the efficient simultaneous serving of heterogeneous terminals, building DVB services that make use of SVC may bring additional benefits. Among others benefits, deployment of SVC will enable providing conditional access to particular video quality levels, ensure graceful degradation using unequal error protection for higher reliability of the base layer that acts as a fallback alternative, as well as the introduction of new backwards-compatible services [5].

The recent DVB-T2 standard, on the other hand, provides a good baseline for the future development of a new mobile broadcast system. The new system would be able to reuse the infrastructure and components that would be available for DVB-T2. At the same time, it would benefit from the significantly increased channel capacity to achieve high quality mobile multimedia services.

When targeting mobile devices, different challenges, such as power consumption limitations and mobility-incurred transmission errors, need to be addressed. Handheld mobile terminals operate on a limited power. Therefore, power optimization becomes an important issue to be considered, when designing algorithms for handheld mobile devices. The DVB-T2 standard allows for data transmission in bursts in one T2 frame. However, when H.264/SVC is transmitted not all receivers are interested in the enhancement layers. To solve the problem, a novel signalling method and a data scheduler for H.264/SVC are proposed. Due to the proposed solution a portable receiver would be able to receive only the relevant data and consequently switch off the receiver for longer periods of time and hence save battery life.

Another challenge arises from the high-bit error rates that a mobile transmission channel is subject to. The DVB-T2 standard was already developed with portable receivers as one of the target user groups. Time interleaving, subslicing, and Forward Error Correction (FEC) are tools that constitute part of the DVB-T2 standard.

This basic support for mobile terminals may be tailored further to optimize mobile reception. As an example, service specific error robustness is enabled by the DVB-T2 standard. Each service may be configured to use a different Forward Error Correction (FEC) code rate, thus resulting in different protection levels. Unfortunately, this differentiation is only possible at service level, but not among the components of the same service. The same drawbacks apply to the time slicing approach that is specified in DVB-T2.

Finally, bandwidth is a crucial resource which should be used efficiently when transmitting to mobile devices. DVB-T2 comes with many possible ways of IP data encapsulation and transmission. Each method brings different overheads. Therefore, it is important to know when and how to choose a particular encapsulation method. This paper discusses the data overhead problem and provides a conceptual solution. Furthermore, an optimal cross-layer scheduling method for IP transmission over DVB-T2 is also proposed. This cross layer optimization takes into consideration the dependencies of data parts within a H.264/SVC coded bit-stream for unequal error protection.

The rest of this paper is organized as follows. Background information about the DVB-T2 broadcast system is presented in Section 2. The Scalable Video Coding standard is described in Section 3. In Section 4, we address the power consumption issues in mobile broadcast. An approach for minimizing power consumption during reception of SVC over DVB-T2 is presented. Subsequently, the challenges of the mobile channel and the increased error rates are examined in Section 5. Further optimizations to the DVB-T2 system are presented in Section 6. The paper is concluded in Section 7.

2. DVB-T2

Digital television is steadily gaining a large interest from users all over the world, and in order to satisfy growing demands DVB organization decided to design a new physical layer for

digital terrestrial broadcast television. The main goals of the new standard were to achieve more bit-rate compared to the first generation DVB-T standard, targeting HDTV services, improve single frequency networks (SFN), provide service specific robustness, and target services for fixed and portable receivers. As a result of the work carried inside the DVB organization the DVB-T2 specification was released in June 2008.

2.1. Physical Layer. The DVB-T2 standard specifies mainly the physical layer structure and defines the construction of the over-the-air signal which is produced at the T2 modulator. Figure 1 depicts the high level architecture of the DVB-T2 system.

The DVB-T2 physical layer data channel is divided into logical entities called the physical layer pipe (PLP). Each PLP carries one logical data stream. An example of such a logical data stream would be an audio-visual multimedia stream along with the associated signalling information. The PLP architecture is designed to be flexible so that arbitrary adjustments to robustness and capacity can be easily done. Data within a PLP is organized in the form of baseband (BB) frames and within a PLP the content formatting of BB frames remains the same.

PLPs are further organized as slices in a time-frequency frame structure, and this structure is shown in Figure 2. Data that is common to all PLPs is carried in a “common PLP”, located at the beginning of each T2 frame. PSI/SI tables carrying, for example, EPG information for the whole multiplex is an example of such common data.

The input preprocessor module though not a part of the DVB-T2 system may be included to work as a service splitter, scheduler, or demultiplexer for Transport Streams (TS) to prepare data to be carried over T2.

The preprocessor module is not defined as a part of the T2 system. However, functionally, it could perform tasks such as service splitting, scheduling or transport stream (TS) demultiplexing and preparing the incoming data for T2 processing.

The input processing module is responsible for constructing a BB frame. It operates individually on the contents of each PLP. The input data from the preprocessor module is first sliced into data fields. A data field can include an optional padding or in-band signalling data. A BB header is included at the start of each data field. The data field along with the BB header form a BB frame. The FEC code rate applied on the BB frame dictates the payload size of a BB frame. A BB frame can be classified into one of two frame size categories: short and long. A short BB frame has data length varying from 3072 to 13152 bits and a long BB frame has data length varying from 32208 to 53840 bits. The structure of a BB frame is depicted in Figure 3.

FEC coding is handled by the bit interleaving, coding and modulation unit. It uses chain codes. The outer code is a Bose-Chaudhuri-Hocquenghem (BCH) [6] code while the inner code is Low Density Parity Check (LDPC) [7]. The FEC parity bits are appended at the end of the BB frame to create the FEC frame. A short FEC frame is 16200 bits in size and

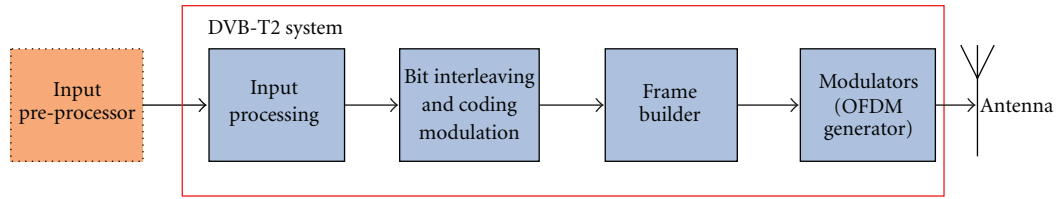


FIGURE 1: High level architecture of DVB-T2 system.

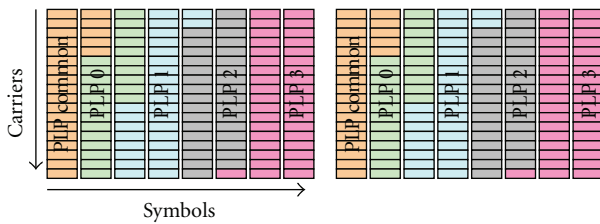


FIGURE 2: Different PLP's occupying different slices of individual modulation, code rate, and time interleaving.

a long FEC frame is 64800 bits in size. The structure of an FEC frame is shown in Figure 4. The FEC code construction is followed by bit interleaving, followed by mapping of the interleaved bits to constellation symbols.

The next block in the DVB-T2 system is the frame builder block, which is responsible for creating superframes. Each super frame is 64 seconds long. The super frames are further subdivided into T2 frames. A T2 frame consists of one P1 preamble symbol followed by one or more P2 preamble symbols. Data symbols obtained from the bit interleaving, coding and modulation module are appended after the P2 symbols. The preamble symbols are explained in detail the next paragraph. The T2 frames are further divided into OFDM symbols. These OFDM symbols are then passed on to the OFDM generator module. The structural composition of a super frame is shown in Figure 5.

Two types of signalling symbols are used in DVB-T2. They are (a) P1 symbols and (b) P2 symbols. P1 signalling symbols are used to indicate the transmission type and the basic transmission parameters. The content of P2 signalling symbols can be further subclassified as L1 presignalling and the L1 postsignalling. The L1 presignalling enables the reception and decoding of the L1 postsignalling, which in turn conveys the parameters needed by the receiver to access the physical layer pipes. The L1 postsignalling can be further subclassified into two parts: configurable and dynamic, and these may be followed by an optional extension field. CRC and padding ends the L1 post signalling field. The structure is depicted in Figure 6. Configurable parameters cannot change during the transmission of a super-frame while dynamic parameters can be changed within one super-frame.

DVB-T2 demodulator module receives one, or more, RF signals and outputs one service stream and one signalling stream. Based on the information in the signalling stream the client can choose which service to receive. Then a decoder module depending on the received service stream and signalling stream outputs the decoded data to a user.

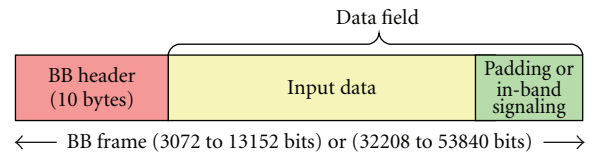


FIGURE 3: BB frame structure.

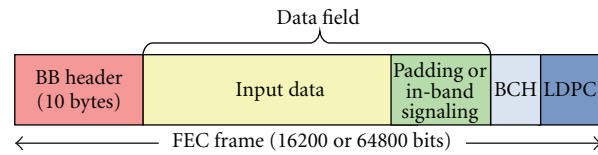


FIGURE 4: FEC frame structure.

2.2. *IP over DVB-T2.* DVB-T2 provides two main encapsulation protocols, the MPEG-2 TS [8] packetization, which has been the classical encapsulation scheme for DVB services, and the Generic Stream Encapsulation (GSE) [9], which was designed to provide appropriate encapsulation for IP traffic.

The standard ways to carry IP datagrams over MPEG2-TS are Multiprotocol Encapsulation (MPE) [10] and Unidirectional Lightweight Encapsulation (ULE) [11]. However, their design was constrained by the fact that DVB protocol suite used MPEG2-TS at the link layer. MPEG-2 TS is a legacy technology optimized for media broadcasting and not for IP services. Furthermore, the MPEG2 TS MPE/ULE encapsulation of IP datagrams adds additional overheads to the transmitted data, thus reducing the efficiency of the utilization of the channel bandwidth.

An alternative to MPEG2 TS is GSE which was design mainly to carry IP content. GSE is able to provide efficient IP datagrams encapsulation over variable length link layer packets, which are then directly scheduled on the physical layer BB frames. Using GSE to transport IP datagrams reduces the overhead by a factor of 2 to 3 times when compared to MPEG-TS transmission

3. Scalable Video Coding (SVC)

Scalable Video Coding (SVC) concept has been widely investigated in academia and industry for the last 20 years. Almost every video coding standards, such as H.262 [12], H.263 [13], and MPEG-4 [14], supports some degree of scalability. However, before H.264/SVC standard, scalable video coding was always linked to increased complexity and a drop

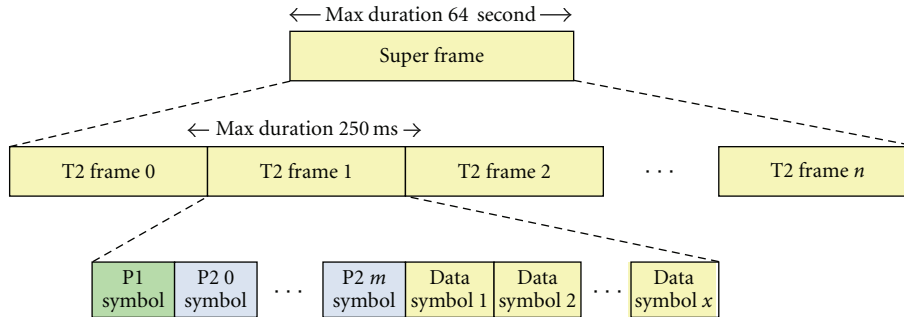


FIGURE 5: Superframe structure.

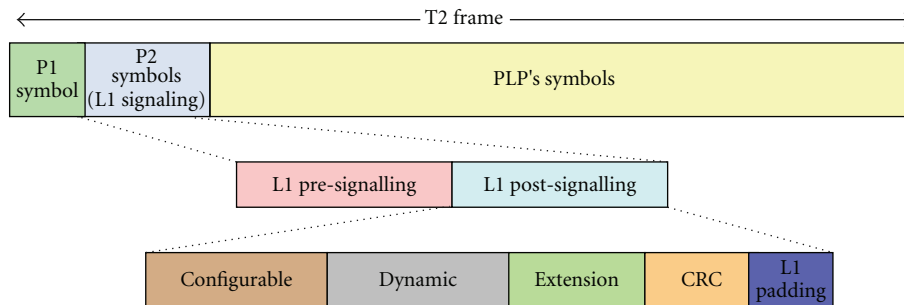


FIGURE 6: L1 signalling.

in coding efficiency when compared to non-scalable video coding. Hence, SVC was rarely used and it was preferred to deploy simulcast, which provides similar functionalities as an SVC bit-stream by transmission of two or more single layer streams at the same time. Though simulcast causes a significant increase in the resulting total bit rate, there is no increase in the complexity.

The new H.264/SVC standard is an extension of H.264/AVC standard. It enables temporal, spatial, and quality scalability in a video bit-stream. However, in contrary to the previous implementations of scalability, H.264/SVC is characterized by good coding efficiency and moderate complexity, and hence it can be seen as a superior alternative to the simulcast. Moreover, simulations [15] show better savings in bandwidth when using H.264/SVC in comparison to simulcast.

The idea behind SVC is that the encoder produces a single bit-stream containing different representations of the same content with different characteristics. An SVC decoder can then decode a subset of the bit-stream that is most suitable for the use case and the decoder capabilities. A scalable bit stream consists of a base layer and one or more enhancement layers. The removal of enhancement layers leads to a decoded video sequence with reduced frame rate, picture resolution, or picture fidelity. The base layer is an H.264/AVC bit-stream which ensures backwards compatibility to existing receivers. Through the use of SVC we can provide spatial resolution, bit rate, and/or even power adaptation. Additionally, by exploiting the intrinsic media data importance (e.g., based on the SVC layer to which those media units belong) higher error and loss resilience may be achieved. As a result, the

enhanced service consumers (those consuming the base and enhancement layers) may then benefit from graceful degradation in the case of packet losses or transmission errors which was proven in [16].

When temporal scalability is used, frames from higher layers can be discarded, which results in a lower frame rate, but does not introduce any distortion during play out of the video. This results from the fact that hierarchical bipredictive frames are used. Other modes of scalability that SVC supports are spatial scalability and quality scalability. In the case of spatial scalability, the encoded bit-stream contains substreams that represent the same content at different spatial resolutions. Spatial resolution is a major motivation behind the introduction of SVC to mobile TV services. It addresses a heterogeneous receiver population, where terminals have different display capabilities (e.g., QVGA and VGA displays). Coding efficiency in spatial scalability is achieved by exploiting interlayer dependencies while maintaining low complexity through a single loop decoder requirement. Quality scalability enables the achievement of different operation points each yielding a different video quality. Coarse Granular Scalability (CGS) [17] is a form of quality scalability that makes use of the same tools available for the spatial scalability. Medium Granular Scalability (MGS) [17] achieves different quality encodings by splitting or refining the transform coefficients.

For detailed information about architecture, system, and transport interface for SVC, the reader is referred to the Special Issue on Scalable Video Coding in IEEE Transactions on Circuits and Systems for Video Technology [18].

4. Power Consumption

Handheld mobile terminals operate on a limited power. Therefore, power optimization becomes an important issue to be considered when designing transmission technologies for handheld mobile devices. One solution to optimize power consumption for data transmission to handheld devices is Time Division Multiplexing (TDM). The idea is to send data in bursts so that a receiver can switch off when data is not transmitted, thus saving power. In DVB-T2 the concept of TDM is introduced by subslicing PLPs data within one T2 frame or by time interleaving. PLP may not appear in every T2 frame of the superframe, and this is signalled by a frame interleaving parameter. However, the interval between successive frames is fixed and can not change within one super frame. Therefore, time slicing is not as flexible as in the case of DVB-H [19]. Furthermore, since in the DVB-T2 system, data is transmitted over fully transparent PLP, in order for a receiver to decode, it first needs to parse the signalling information associated with the data and then parse the proper PLP. The type of data in the PLP in a given T2 frame is unknown to the receiver, until data is parsed by upper layers.

If Scalable Video Coding (SVC) transmission is used, receivers with lower capabilities, interested only in the base layer data, are also forced to receive other enhancement layers transmitted on dedicated PLPs. Only when the data is parsed by upper layers, the receiver may discard irrelevant data which belongs to the enhancement layers. The lack of information about the type of data that is delivered in the PLP leads to high penalty of processing power on power constrained terminals.

The problem could be solved by signalling the type of data contained in each T2 frame for each specific PLP. This information would then be used by receiver to skip data of PLPs in a frame that does not contain the required information. This solution would also allow the use of a single PLP for the whole service, including all related SVC layers, while avoiding the penalty on power constrained receivers. DVB-T2 allows dynamic signalling. Therefore, this additional information may be included in L1 signalling carried in each T2 frame. The signalling information may change in every T2 frame, and it would indicate the data type carried by PLP symbols in a T2 frame.

A comparative example of how data is currently transmitted (without specifying methods of scheduling input data to BB frame) and how it may be transmitted if scheduling is applied is shown in Figures 7 and 8, respectively.

The scheduler or data preprocessor assigns the data from different SVC layers to different T2 frames. As an example, data from the base layer as well as the audio streams could be mapped to odd T2 frames, while the data of the enhancement layer could be mapped to even T2 frames. The L1 signalling that is included in each T2 frame would carry an indication of the frame with the highest importance.

Due to the data type information carried in PLP symbols in any given T2 frame, the receiver could discard the frame if it is not needed, without any further processing. Additionally, if a delta time concept is used, as in DVB-H, the receiver

would be able to know the time to the next T2 frame that comprises the needed data, thus enabling more power saving through longer switch-off time.

As an example, the well-known City sequence, encoded using SVC and where the base layer has a resolution of QVGA at 15 fps and the enhancement layer has a resolution of VGA at 30 fps, gives a base layer to enhancement layer bit-rate ratio of 1 to 3 [20], which is necessary to maintain similar video quality levels at base and enhancement layers. Accordingly, the usage of the proposed scheduling method at the transmitter yields savings of 75% of the on-time for receivers that are only interested in consuming the base layer stream.

The drawback of transmitting all SVC layers over one PLP is that modulations and physical layer FEC code rates are the same for all SVC layers. Therefore, unequal error protection (UEP) scheme for different layers may be implemented only on upper layers, which might be not as strong as a differentiation of robustness by using different modulations and FEC codes on physical layer.

An alternative solution would be to deliver different layers of SVC bit-stream on separate PLPs. As a result service component specific robustness could be applied by using different coding and modulation setting for each PLP. Moreover, needed data could be extracted by a receiver by parsing only the required PLP. However, complexity issue should be considered for this use case. As a receiver would need to reserve resource for each PLP separately it would require more processing power, memory, and energy which could minimize battery lifetime. Moreover, additional circuitry essential for the simultaneous reception of multiple PLPs could increase the cost of the receiver in comparison to one PLP model. Finally, this solution would imply that receivers interested in higher quality/resolution are able to receive multiple data PLPs simultaneously, which is currently not required by the DVB-T2 specification.

5. Mobile Transmission Channel

A mobile transmission channel is highly error prone. Many contributions have been made in the literature to address the issue of robustness against packet loss in mobile data transmission over a fading channel. One of the main techniques to cope with the problem is Forward Error Correction (FEC). FEC is a technique where the transmitter adds redundancy, known as repair symbols, to the transmitted data, enabling the receiver to recover the transmitted data, even if there were transmission errors. No feedback channel is needed to recover the lost data in this technique, which makes it well suited for broadcast transmission.

Besides FEC, DVB-T2 standard introduced other tools to cope with channel errors, interleaving of T2 frames over time and subslicing of PLP data inside one T2 frame. The purpose of time interleaving is to protect a transmission against burst errors. subslicing has two consequences. First, it divides the data into slices that are transmitted in different parts of a T2 frame, which gives tolerance to short burst errors and to some extent also against slow fading. On the other hand,

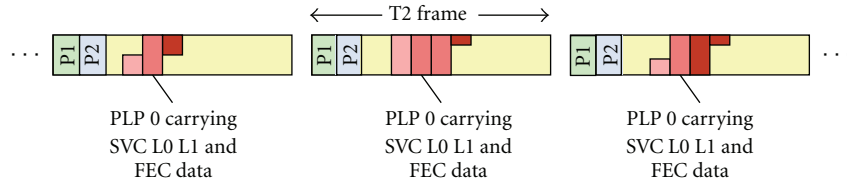


FIGURE 7: Transmission of data over one PLP.

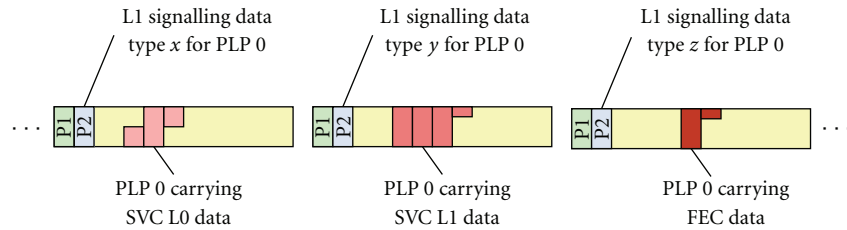


FIGURE 8: Transmission of scheduled data over one PLP with additional L1 signalling.

increasing the number of sub-slices increases the number of used OFDM symbols. This gives extra time diversity which is important in mobile channels.

To fully understand how and what benefits these tools bring when a mobile channel is considered, simulations of DVB-T2 physical layers were performed. The simulation description and the results obtained are presented in the next subsection. Subsequently, in Section 5.2 the improvement which could be introduced at the link layer is discussed.

5.1. Physical Layer. To study the suitability of the DVB-T2 standard for mobile and handheld reception and to find the relevant parameter combinations a set of simulation was performed. The simulation analyzed how time interleaving, subslicing, and FEC cope with channel errors. For the simulation a DVB-T2 physical layer model implemented in Matlab was utilized. The model uses ideal synchronization with ideal channel estimation and an ideal demapper benefiting from error-free a priori information for the rotated constellations. The model was verified by comparing the performance to the results presented in the DVB-T2 Implementation Guidelines [21].

The simulations were carried for transmission of twelve identical PLPs with 1 Mbit/s service bit rate which cover mobile broadcasting scenario. For simulation, the maximum length T2 frames (250 ms) comprising the short 16200 bits long FEC frames were used. The modulation parameters were set to 16 QAM, 8 k FFT size, and 1/4 guard interval. Moreover, P1 (not-boosted) pilot pattern and constellation rotation were used. As a transmission channel, the TU6 80 Hz model was employed. All the error calculations were performed by averaging the individual error rates to minimize variations due to dynamic channel.

In Figure 9, results for different time interleaving and subslicing settings are presented. It can be clearly seen that by increasing the interleaving length and number of sub-slices the performance of the system can be improved.

TABLE 1: Average on-time.

$N_{\text{sub-slices}}$	Avg. on-time [%]	Avg. on-time per frame [ms]
1	8.0	20.0
2	8.5	21.2
3	8.9	22.3
5	9.8	24.5
9	11.6	29.0
270	92.4	230.0

The highest possible number of sub-slices, 270, is greater than the number of OFDM symbols in a T2 frame, which effectively means continuous transmission. This “full subslicing” scenario always gives a better performance compared to the single sub-slice case. It is also understandable that increasing the time interleaving length does not significantly improve the performance with full subslicing because most of the time diversity is already there even with the shortest interleaver. Additionally, in Figure 10, subslicing without time interleaving comparison is presented.

The performance of different FEC code rates with different time interleaving is presented in Figure 11. The results clearly show that DVB-T2 is well equipped with tools which can improve the mobile broadcasting. However, it is important to properly choose the parameters. The use of subslicing should be carefully considered due to power consumption. A high number of sub-slices means longer on-the-air transmission. In Table 1, the average on-time number of sub-slices is presented. It can be seen that, for example, using nine sub-slices results in 45% increase in on-time compared to one sub-slice, consequently leading to higher power consumption by a mobile receiver. One possibility to achieve good time diversity and low power consumption is to use the full subslicing scheme, and transmit the PLPs in T2 frames periodically with some interval. In the T2 specification, this is enabled by the frame interval parameter.

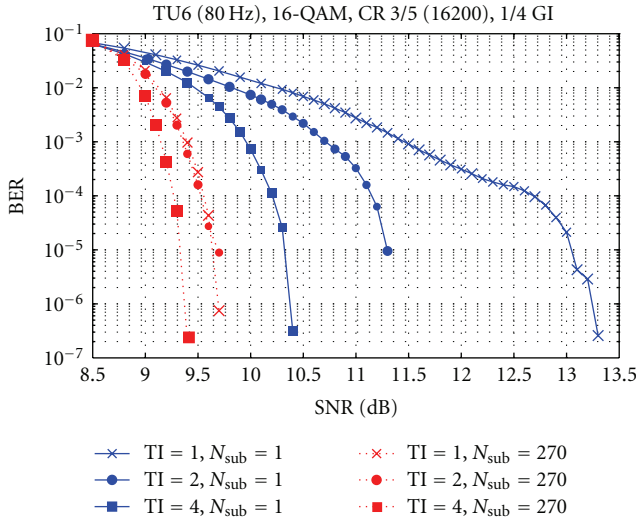


FIGURE 9: TU6 80 Hz: time interleaving and subslicing comparison.

Moreover, for real-time services the total interleaving length is limited by the required channel zapping time, which plays an important role in the user experience [22]. Furthermore, stronger FEC code rate consumes more bandwidth. It is known that time-interleaving as well as error correction can be performed also by upper layers and thus brings more flexibility to the system. In [23] authors show that Upper Layer FEC (UL-FEC) may bring improvement in DVB-S2, which uses similar physical layer FEC codes to DVB-T2. The UL-FEC is discussed in the next subsection.

5.2. Link Layer (BB-FEC (Base Band—FEC)). DVB-T2 standard uses FEC codes at the physical layer by introducing the FEC-FRAME concept described in Section 2. Accordingly, it may be said that transmission errors after physical layer decoding are reflected at the BB frame level. Moreover, it may be assumed that if the combined BCH/LDPC FEC decoding fails, then the whole BB frame is marked as lost. However, the corrupted data from the BB frame may be recovered if any UL-FEC method was applied on the transmitted data.

There are many UL-FEC methods tailored for different types of content delivery and different receiver groups. As an example, if a file needs to be delivered to a set-top box then Application Layer FEC (AL-FEC) which employs Raptor Code [24] may be used. On the other hand, if a streaming content needs to be delivered to portable/handset receivers then MPE-FEC [19], MPE-IFEC [25], or Link Layer FEC (LL-FEC) may be applied.

MPE-FEC scheme was shown to bring benefits for mobile transmission in DVB-H standard [26]. Similarly, a LL-FEC could be applied in DVB-T2 to combat errors caused by the mobile fading channel. However, data in DVB-T2 may be transmitted by using MPE/TS, ULE/TS or by using GSE. When MPE/TS is used for data transmission, the MPE-FEC technology used in DVB-H may be used. If IP data is transmitted over ULE/TS or GSE then a new method for constructing LL-FEC along with a new method

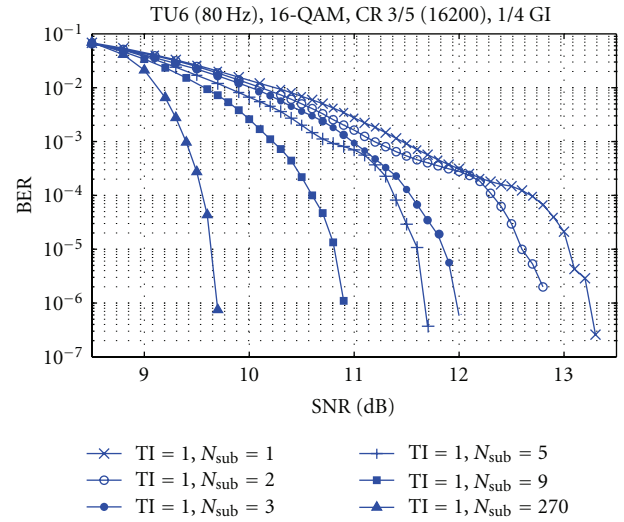


FIGURE 10: TU6 80 Hz: subslicing comparison.

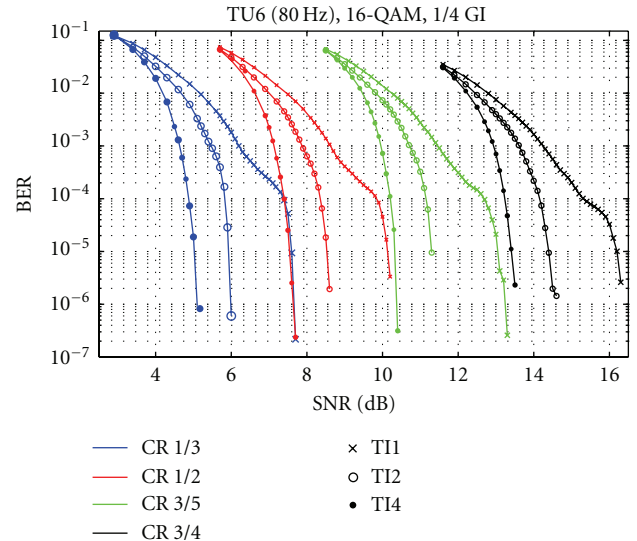


FIGURE 11: TU6 80 Hz: Code rate and time interleaving comparison.

of signalling is needed. To avoid diversification of FEC correction methods depending on the data transmission technology used, this paper proposes to shift the MPE-FEC paradigm to lower layer, that is, BB frame layer which is called BB-FEC.

In BB-FEC, the FEC source block is created from data in k BB frames. The number of rows, where each row is one byte, is equal to the data field size of the BB which corresponds to the data of a BB frame, excluding the BB header, BCH, and LDPC repair bits. This means that the payload of a BB frame (without FEC repair bits) gets mapped to a FEC source symbol. Next, FEC encoding is performed rowwise to generate the repair symbols. The resulting repair symbols are put to a new columnwise BB frames where exactly one column of repair symbol is put in one BB frame. The FEC table construction is presented in Figure 12.

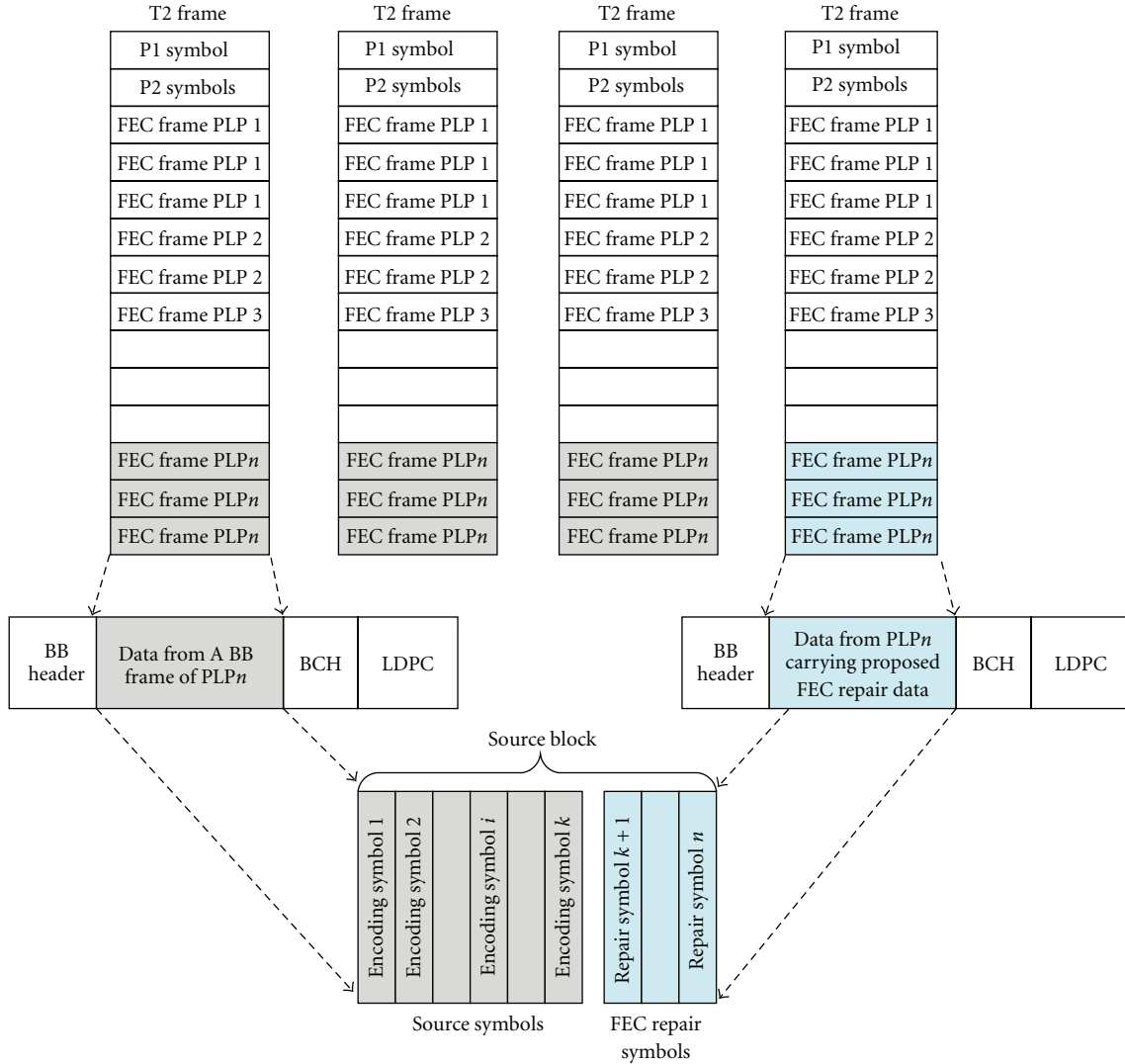


FIGURE 12: Example of a construction of a link layer FEC table.

The advantage of BB-FEC over MPE-FEC is that due to the mapping of one column to exactly one FEC frame the fragmentation of errors between many columns is avoided.

Additionally, if transmission of scalable service presented in Section 4 is considered, BB-FEC can be employed to enable unequal error protection. Two separate source blocks, as depicted on Figure 12, can be constructed one containing a BB frame with a base layer data and one containing a BB frame with enhancement layers. Next, in each of the source blocks different FEC code rates can be applied, and thus unequal error protection can be achieved.

Deciding which specific FEC code, for example, Reed-Solomon [27], Raptor, LDPC or other, to use in BB-FEC requires further studies. Moreover, it is important to specify the proper technique of decoding as it was shown in [28]. Therefore, the BB-FEC is presented here only as a concept and will be investigated in future work.

6. Further Optimization

In the previous sections it was shown that using FEC correction, and by proper data scheduling, efficiency in transmission can be achieved. However, it is also important to save the bandwidth where possible and use expensive resources efficiently. The data throughput is maximized by reducing overhead without losing functionality or by minimizing padding by proper data scheduling. In this section we show how IP/UDP header may be compressed which leads to a gain in the bandwidth.

6.1. Header Compression. Channel bandwidth is a scarce resource which should be utilized in the most efficient way. When source data is prepared for transmission each layer adds its own header to help properly decode the received data. Parts of the header data may be redundant depending on the transmission scenario. These protocol overheads can

TABLE 2: UDP header.

Bits Offset	0–15	16–31
0	Source Port	Destination Port
32	Length	Checksum

TABLE 3: IPv6 header.

Bits Offset	0–7	8–15	16–23	24–31
0	Version	Traffic Class	Flow Label	
32	Payload Length		Next Header	Hop Limit
64	Source Address			
96				
128				
160				
192	Destination Address			
224				
256				
288				

be minimized, without sacrificing functionality, by tailoring the headers to the bearer needs, which consequently would lead to network throughput improvement.

Data is transmitted over the Internet using protocols which allow routing over a path with multiple hops. Thus, protocol headers are important to ensure reliable interchange of data over a communication channel with multiple hops. However, in hop-to-hop case where only one link exists, such as DVB-T2, many of the header fields, which are used in traditional Internet, serve no useful purpose and are redundant.

In DVB system the overhead of transmitted data usually comprises 8 bytes of UDP header, presented in Table 2, 40 bytes of IP header, presented in Table 3, and 7 to 10 bytes of GSE header, 2 bytes of MPE header and 4 bytes of CRC, or 4 bytes of ULE header and 4 bytes of CRC check. If MPE or ULE is used as an IP carrier then, additionally, 4 bytes of TS header for every 184 bytes of data is added. If the average protocol data unit (PDU), for example RTP packet, size is assumed to be 1000 bytes, the overhead is 55 or 58 bytes when GSE is used, 88 bytes when MPE over TS is used, and 84 bytes when ULE over TS is used. Choosing GSE instead of MPE over TS may already bring a 35 to 37% overhead reduction with similar error performance. However, in all of the cases the largest part of the overhead is IP/UDP header which is 48 bytes for each data packet irrespective of its size. IP/UDP data header information is hardly used for point-to-point broadcast transmission. The information transmitted by IP header may be extracted from lower layer or from out of the band signalling. The large part of the IP header and UDP header fields are constant and repeated from packet to packet.

There are many header compression schemes [29] which are adopted by various standardization bodies including 3GPP [30] and 3GPP2 [31]. However, these technologies assume an existence of the return channel which excludes their use in DVB-T2 broadcast scenario. Therefore, a new scheme dedicated to DVB-T2 should be created.

The fields of the IPv6 header such as Traffic Class, Flow Label, Next Header, Hop Limit, and Source Address are static for each packet and could be transmitted out of band. The functionality of the remaining three fields, Version, Payload Length, and Destination Address, could be shifted to lower layers. If this is done, then the whole IP header would be redundant and could be deleted. Similar to IPv6 header, in UDP header, source port field value could be transmitted out of band and the length value extracted from lower layers. In Table 4, a possible gain, when IP/UDP header deletion is used, is presented.

From Table 4 it can be seen that the size of the transmitted PDU should be as large as possible. Moreover, if the overhead is taken as a criterion then GSE should be used as the encapsulation method. By properly choosing the average packet size (APS) as well as the used encapsulation method the gain can be significant, from 41% when the APS is 100 bytes and MPE is used to 3.98% when the APS is 1400 and GSE is used. Further, if IP/UDP header is compressed the overhead goes below 1%. If two extreme cases are compared the data throughput difference is about 40%.

6.2. IP Encapsulation. Transmission errors after physical layer decoding are seen at the BB frame level. It is assumed that if the combined BCH/LDPC FEC decoding fails, then the whole BB frame is marked as lost. To minimize the effects of a BB frame loss, a scheduling algorithm for optimized mapping of service data to the data field of the BB frames is now presented. The scheduler constitutes a part of the preprocessor in the DVB-T2 transmission chain. One scheduler is allocated for each PLP in order to operate on the data packets of that PLP.

In [32], we proposed a scheduling algorithm that avoids fragmentation of the IP packets containing media data of higher importance. By avoiding fragmentation of important media units, improved error resilience is achieved. Additionally, restricted time interleaving is applied to IP packets that contain media units of a higher importance access unit. Time interleaving spreads the media units of an access unit across multiple T2 frames. Consequently, losses which are typically of a bursty nature would most likely not affect the complete access unit. As an example, an intradecoder refresh IDR picture that consists of several slices would ultimately be mapped into several BB frames that are spread over multiple T2 frames. Transmission errors may corrupt a set of consecutive BB frames depending on the burst length. Due to the time interleaving, the impact of loss of a set of consecutive BB frames would less likely result in significant loss to the random access points.

As mentioned earlier, the time interleaving is restricted to limit the required initial buffering time and to keep the channel switch time within an acceptable range. The number of T2 frames that are used for the time interleaving of the random access point and the related group of pictures is restricted to 1 to 1.5 seconds. With a typical T2 frame duration of 250 ms, the total number of T2 frames used for time interleaving a group of pictures is then 4 to 6 T2 frames.

TABLE 4: Transmission overheads.

Average Packet Size [bytes]	Uncompressed IP/UDP headers			Compressed IP/UDP headers		
	MPE [%]	ULE [%]	GSE [%]	MPE [%]	ULE [%]	GSE [%]
100	41,52	38.65	36,71	21,26	15.97	12,28
200	28,06	25.93	22,48	14,53	11.50	6,54
400	17,53	16.14	12,66	9,30	7.62	3,38
600	13,29	12.28	8,81	7,41	6.25	2,28
800	11,01	10.21	6,76	6,43	5.55	1,72
1000	9,58	8.93	5,48	5,84	5.12	1,38
1200	8,61	8.05	4,61	5,44	4.84	1,15
1400	7,89	7.41	3,98	5,15	4.63	0,99

TABLE 5: PSNR and Packet error rate (crew).

BB frame error rate [%]	Generic		Proposed Scheduling Algorithm	
	Packet error rate [%]	PSNR [dB]	Packet error rate [%]	PSNR [dB]
7.33	9.12	28.72	9.03	29.19
3.32	4.42	32.48	4.43	32.74
1.80	2.22	34.93	2.14	35.63
1.55	2.03	35.26	2.01	35.66
0.00	0.00	39.85	0.00	39.85

The size of the data field in a BB frame for a specific service depends on the selected modulation scheme and the physical layer FEC code rate. Upon determining the size of the payload of a BB frame, the number of BB frames needed to transmit the set of pictures of the video stream can be calculated based on the total size of the media units to be transmitted. The number, M , of BB frames allocated for the service in each T2 frame can be dynamically determined according to the following equation:

$$M = \frac{S}{(PS \times N)}, \quad (1)$$

where PS is a payload size of the BB frame allocated for the service, N is number of T2 frames, S is a total size of media units over the duration of N T2 frames.

After determining the BB frame allocation over the set of T2 frames, the scheduling algorithm proceeds by mapping media data packets to BB frames. The target thereby is manifold. First, the mapping algorithm avoids fragmentation of important media units over more than one BB frame. Secondly, it aims at providing maximum error resilience through time interleaving. Finally, the algorithm aims at increasing bandwidth usage efficiency by avoiding total fragmentation overhead and padding operations.

The problem discussed above is equivalent to the bin packing problem (packing objects of different sizes and weights/importance into bins of equal sizes) [33] and is an NP-hard problem. A heuristic solution to keep the complexity within a still manageable range while achieving a close to optimal solution is followed. The algorithm is described below.

- (1) Arrange media packets in descending order of importance.
- (2) Start from higher importance media packets (e.g., those containing base layer IDR pictures) and assign them to maximally distant BB frames.
- (3) For the rest of the media packets, order media packets according to their size in decreasing order.
- (4) Loop through the set of media packets and
 - (a) assign packet to the best fitting BB frame (the BB frame that leaves the least free space after adding the media packet);
 - (b) if no fitting BB frame is found queue the media packet at the tail of the set of media packets;
 - (c) stop if no media packet can be mapped to available free space;
 - (d) end Loop.
- (5) Fragment the left-over media packets starting from the first BB frame.

The proposed scheduling algorithm is well-suited for handling scalable media such as an SVC media stream. The scheduler complexity is limited to the handling of the RTP packet header and the RTP payload format. Given that the set of media encoding options in a broadcast scenario is limited, this additional functionality would not significantly increase the complexity of the scheduler.

Now, a comparison of the scheduling method described above and the generic approach without scheduling is presented.

TABLE 6: PSNR and Packet error rate (crowd).

BB frame error rate [%]	Generic		Proposed Scheduling Algorithm	
	Packet error rate [%]	PSNR [dB]	Packet error rate [%]	PSNR [dB]
7.33	8.81	23.81	8.67	24.04
3.32	4.48	26.15	4.45	26.00
1.80	2.23	27.48	2.18	27.99
1.55	2.07	27.95	2.04	28.09
0.00	0.00	30.88	0.00	30.88

TABLE 7: Number of erroneous packets (crew).

BB frame error rate [%]	Generic			Proposed Scheduling Algorithm			
	I	P	B	I	P	B	
7.33	169	1034	236	139	913	373	Error packets
	72	419	91	0	246	342	Error packets due to fragmentation
3.32	88	481	129	54	470	175	Error packets
	43	229	67	0	154	174	Error packets due to fragmentation
1.80	38	255	58	36	204	97	Error packets
	13	94	20	0	27	95	Error packets due to fragmentation
1.55	33	219	68	21	184	112	Error packets
	16	92	32	0	39	101	Error packets due to fragmentation

For the simulations, the crew and crowd sequences, with a resolution of 1280×720 and 600 and 500 frames, respectively, were used. The sequences were encoded using the main profile of H.264/AVC. To create a simple temporal scalability structure, every second picture was encoded as a nonreference B picture. This meant that a base layer with 15 fps and an enhancement layer with 30 fps were created. The encoding parameters were set as follows. Bitrate ~ 8 Mbits/s, an IDR picture was inserted once every 30 pictures and the maximum slice size was set to 1300 bytes.

To conduct the simulations, an Input preprocessor (IPP) was implemented. The physical layer transmission over a DVB-T2 bearer was simulated to generate BB frame error patterns that were used for evaluating the optimization approaches. Four different error patterns, containing 1.55%, 1.80%, 3.32%, and 7.33% lost BB frames respectively, were used throughout the simulations. Based on the bit-error patterns, a BB frame was marked as lost if the BCH/LDPC decoding process fails to recover from the bit errors at that BB frame.

Each NAL unit of the encoded sequence is packetized as a GSE packet, where an additional 67 bytes header is added to correspond to the GSE/IP/UDP/RTP headers. The subsequent scheduling is performed by the scheduler submodule of the IPP module, which operates on sets of packets that belong to a single group of pictures (GoP).

At the receiver side, the resulting errors at the BB frames were mapped on the data packets, where the loss of one or more data fragments of a data packet would result in discarding of the whole packet as it would be useless for the media decoder. Next, the lost NAL units were discarded from the error-free sequence, and erroneous bit-stream was decoded using H.264/AVC decoder with motion vector copy error concealment method.

The following configurations of the scheduler have been analyzed in the simulations.

- (1) A generic approach without scheduling. The scheduler based on data field length of BB frame fragments the packets as they come and adds new GSE header and CRC check to fragmented packet.
- (2) A cross-layer approach where the scheduler uses information from the physical layer (data field length of a BB frame) and application layer (priority of the packet). Based on that information an algorithm, described in this subsection, was examined.

In Tables 5 and 6 PSNR values and packet loss rates are depicted for each of the tested configuration for crew and crowd sequences, respectively. It can be seen that thanks to the proposed cross layer scheduling approach, the packet loss rate can be reduced and consequently around 0.5 dB PSNR gain was achieved.

The gain in PSNR is achieved not only by packet loss reduction but also due to spreading errors through less important packets. In Tables 7 and 8, the number of erroneous packets as well as the number of erroneous packets as a result of the fragmentation process are presented.

The results show that due to scheduling none of the packets belonging to I frames is lost because of fragmentation. Additionally, due to the time interleaving applied to the I packets, a reduced number of these packets are affected by errors. Moreover, it is shown that the proposed scheduling method move most of the errors to the packets belonging to the less important B frames.

In Figures 13 and 14, PSNR plots for the first 120 frames of both sequences crew and crowd, after transmission over the channel with highest BB frame error rate, are presented.

TABLE 8: Number of erroneous packets (crowd).

BB frame error rate [%]	Generic			Proposed Scheduling Algorithm			
	I	P	B	I	P	B	
7.33	142	801	210	137	707	291	Error packets
	57	321	82	0	183	287	Error packets due to fragmentation
3.32	93	427	66	75	368	140	Error packets
	47	204	32	0	165	121	Error packets due to fragmentation
1.80	27	226	39	33	161	91	Error packets
	10	85	13	0	26	81	Error packets due to fragmentation
1.55	31	201	39	34	141	92	Error packets
	14	88	18	0	17	90	Error packets due to fragmentation

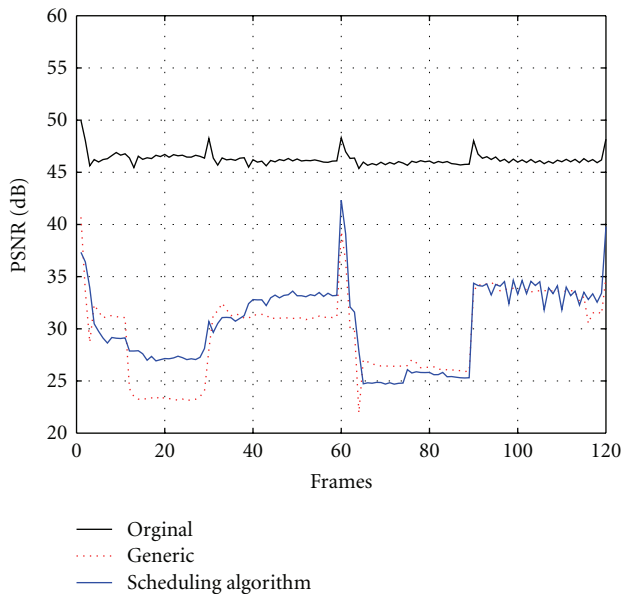


FIGURE 13: PSNR of crew sequence for the first 120 frames.

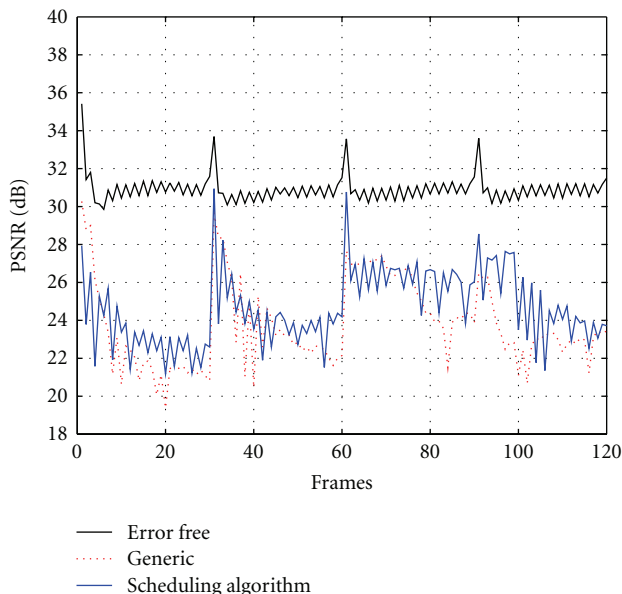


FIGURE 14: PSNR of crowd sequence for the first 120 frames.

It can be seen that due to the spread of errors among packets rapid quality change can be avoided, as for example, in the first 30 frames of the crew sequence. Additionally, it can be observed that on both plots almost all I frames (30th, 60th, 90th, and 120th frames) have higher PSNR value when scheduling algorithm is used. Consequently, it should lead to less prediction errors which would be visible during playback of the decoded video. Even scheduling algorithm may sometimes show a weaker performance than that of the generic transmission, for example, it can be seen on Figure 13, frames 60 to 90, that the overall results proved that due to the scheduling algorithm the errors are moved to the less important data packets which lead to unequal error resilience of the transmitted stream. Finally, it should be noted that the 0.5 dB gain on average achieved by scheduling algorithm does not fully reflect the subjective gain which may be achieved by a viewer.

7. Conclusions

This paper discussed the use of DVB-T2 system as a bearer for mobile data using H.264/SVC. Three important challenges for mobile transmission: power consumption, transmission errors, and data throughput were discussed. A scheduling method exploiting H.264/SVC bit-stream characteristics so as to reduce power consumption was proposed. Due to the grouping of each scalable layer into separate transmission data bursts, a receiver with lower capabilities would be able to reduce power consumption by receiving only relevant data. Furthermore, a bursty transmission introduces further time interleaving on application layer data and consequently makes the transmitted data more robust to errors. Since DVB-T2 was developed with portable receivers as one of the target user groups, it comes with dedicated tools to cope with an error-prone mobile transmission channel. The performance of these tools was investigated, and the results showed that they can bring significant gain. To bring additional flexibility to the DVB-T2 transmission system, a BB-FEC concept was proposed. The introduction of BB-FEC enables unequal error protection on transmitted data even if one PLP is used for service transmission. Finally, when mobile channels are considered, bandwidth is a scarce resource which has to be utilized optimally. Three popular encapsulation methods were compared from an overhead

perspective, and IP/UDP overhead compression was discussed. A novel packet scheduling method, which uses the bandwidth efficiently and provide unequal error resilience for transmitted packet, was described and supported by simulation results.

Acknowledgment

This work was partially supported by Nokia and the Academy of Finland, Project No. 129657 (Finish Centre of Excellence program 2006–2011).

References

- [1] ETSI EN 302 755 V 1.1.1, "Digital Video Broadcasting (DVB): frame structure channel coding and modulation for a second generation digital terrestrial television broadcasting system (DVB-T2)," Draft, July 2008.
- [2] "DVB-T2—the HDTV generation of terrestrial DTV," DVB-TM-3997, March 2008.
- [3] ITU-T Recommendation, H.264, "Advance Video Coding for generic audiovisual services," November 2007.
- [4] ETSI TS 102 005 V1.4.1, "Digital Video Broadcasting (DVB); specification for the use of Video and Audio Coding in DVB services delivered directly over IP protocols," Working Draft.
- [5] T. Schierl, C. Hellge, S. Mirta, K. Grüneberg, and T. Wiegand, "Using H.264/AVC-based scalable video coding (SVC) for real time streaming in wireless IP networks," in *Proceedings of the IEEE International Symposium on Circuits and Systems (ISCAS '07)*, pp. 3455–3458, May 2007.
- [6] R. C. Bose and D. K. Ray-Chaudhuri, "On a class of error correcting binary group codes," *Information and Control*, vol. 3, no. 1, pp. 68–79, 1960.
- [7] R. G. Gallager, "Low-density parity-check codes," *IRE Transactions on Information Theory*, vol. 8, no. 1, pp. 21–28, 1962.
- [8] ISO/IEC IS 13818-1, "Information technology—generic coding of moving pictures and associated audio information: systems".
- [9] ETSI TS 102 606 V1.1.1, "Digital Video Broadcasting (DVB); Generic Stream Encapsulation (GSE) Protocol," October 2007.
- [10] ETSI EN 301 192 V 1.4.2, "Digital Video Broadcasting (DVB); DVB specification for data broadcasting," April 2008.
- [11] IETF RFC 4326, G. Fairhurst, and B. Collini-Nocker, "Unidirectional Lightweight Encapsulation (ULE) for Transmission of IP Datagrams over an MPEG-2 Transport Stream (TS)," December 2005.
- [12] ISO/IEC IS 13818-2, "Information Technology—generic coding of moving pictures and associated audio information: video".
- [13] ITU-T Recommendation, "H.263: Video Coding for Low Bit Rate Communication," 1998.
- [14] ISO/IEC IS 14496-2, "Information Technology—Coding of Audio-Visual Objects—Part 2: Visual," 1998.
- [15] M. Wien, H. Schwarz, and T. Oelbaum, "Performance analysis of SVC," *IEEE Transactions on Circuits and Systems for Video Technology*, vol. 17, no. 9, pp. 1194–1203, 2007.
- [16] C. Hellge, T. Schierl, and T. Wiegand, "Mobile TV using scalable video coding and layer-aware forward error correction," in *Proceedings of the IEEE International Conference on Multimedia and Expo (ICME '08)*, pp. 1177–1180, 2008.
- [17] H. Schwarz, D. Marpe, and T. Wiegand, "Overview of the scalable video coding extension of the H.264/AVC standard," *IEEE Transactions on Circuits and Systems for Video Technology*, vol. 17, no. 9, pp. 1103–1120, 2007.
- [18] "Special issue on scalable video coding-standardization and beyond," *IEEE Transactions on Circuits and Systems for Video Technology*, vol. 17, no. 9, pp. 1097–1269, 2007.
- [19] ETSI EN 302 304 V 1.1.1, "Digital Video Broadcasting (DVB); Transmission System for Handheld Terminals (DVB-H)," November 2004.
- [20] L. Kondrad, I. Bouazizi, and M. Gabbouj, "Media aware FEC for scalable video coding transmission," in *Proceedings of the IEEE Symposium on Computers and Communications*, pp. 7–12, Sousse, Tunisia, July 2009.
- [21] ETSI TR 102 831 V1.1, "Implementation guidelines for a second generation digital terrestrial television broadcasting system (DVB-T2)," February 2009.
- [22] M. Rezaei, M. M. Hannuksela, and M. Gabbouj, "Tune-in time reduction in video streaming over DVB-H," *IEEE Transactions on Broadcasting*, vol. 53, no. 1, part 2, pp. 320–328, 2007, special issue on *Mobile Multimedia Broadcasting*.
- [23] J. Lei, M. A. Vazquez Castro, F. Vieira, and T. Stockhammer, "Application of link layer FEC to DVB-S2 for railway scenarios," in *Proceedings of the 10th International Workshop on Signal Processing for Space Communications (SPSC '08)*, October 2008.
- [24] A. Shokrollahi, "Raptor codes," *IEEE Transactions on Information Theory*, vol. 52, no. 6, pp. 2551–2567, 2006.
- [25] DVB BlueBook A131, "Digital Video Broadcasting (DVB); MPE-IFEC," November 2008.
- [26] V. K. M. Vadakital, M. Hannuksela, H. Pekkonen, and M. Gabbouj, "On datacasting of H.264/AVC over DVB-H," in *Proceedings of the 7th IEEE Workshop on Multimedia Signal Processing (MMSP '05)*, p. 4, Shanghai, China, October–November 2005.
- [27] L. Rizzo, "Effective erasure codes for reliable computer communication protocols," *ACM Computer Communication Review*, vol. 27, pp. 24–36, 1997.
- [28] J. Paavola, H. Himmanen, T. Jokela, J. Poikonen, and V. Ipatov, "The performance analysis of MPE-FEC decoding methods at the DVB-H link layer for efficient IP packet retrieval," *IEEE Transactions on Broadcasting*, vol. 53, no. 1, pp. 263–275, 2007.
- [29] IETF RFC 1144 and V. Jacobson, "Compressing TCP/IP Headers for Low-Speed Serial Links," February 1990.
- [30] <http://www.3gpp.org/>.
- [31] <http://www.3gpp2.org/>.
- [32] L. Kondrad, I. Bouazizi, V. K. M. Vadakital, M. M. Hannuksela, and M. Gabbouj, "Cross-layer optimized transmission of H.264/SVC streams over DVB-T2 broadcast system," in *Proceedings of the IEEE International Symposium on Broadband Multimedia Systems and Broadcasting (BMSB '09)*, pp. 1–5, May 2009.
- [33] S. Martello and P. Toth, "A mixture of dynamic programming and branch-and-bound for the subset-sum problem," *Management Science*, vol. 30, no. 6, pp. 765–771, 1984.

Review Article

Design of an IPTV Multicast System for Internet Backbone Networks

T. H. Szymanski^{1,2} and D. Gilbert¹

¹Department of Electrical and Computer Engineering, McMaster University, Hamilton, ON, Canada L8S 4K1

²Bell Canada Chair in Data Communications, McMaster University, Hamilton, ON, Canada L8S 4K1

Correspondence should be addressed to T. H. Szymanski, teds@mcmaster.ca

Received 2 November 2009; Revised 3 March 2010; Accepted 23 March 2010

Academic Editor: Daniel Negru

Copyright © 2010 T. H. Szymanski and D. Gilbert. This is an open access article distributed under the Creative Commons Attribution License, which permits unrestricted use, distribution, and reproduction in any medium, provided the original work is properly cited.

The design of an IPTV multicast system for the Internet backbone network is presented and explored through extensive simulations. In the proposed system, a resource reservation algorithm such as RSVP, IntServ, or DiffServ is used to reserve resources (i.e., bandwidth and buffer space) in each router in an IP multicast tree. Each router uses an Input-Queued, Output-Queued, or Crosspoint-Queued switch architecture with unity speedup. A recently proposed *Recursive Fair Stochastic Matrix Decomposition* algorithm used to compute near-perfect transmission schedules for each IP router. The IPTV traffic is shaped at the sources using *Application-Specific Token Bucket Traffic Shapers*, to limit the burstiness of incoming network traffic. The IPTV traffic is shaped at the destinations using *Application-Specific Playback Queues*, to remove residual network jitter and reconstruct the original bursty IPTV video streams at each destination. All IPTV traffic flows are regenerated at the destinations with essentially zero delay jitter and essentially-perfect QoS. The destination nodes deliver the IPTV streams to the ultimate end users using the same IPTV multicast system over a regional Metropolitan Area Network. It is shown that all IPTV traffic is delivered with essentially-perfect end-to-end QoS, with deterministic bounds on the maximum delay and jitter on each video frame. Detailed simulations of an IPTV distribution system, multicasting several hundred high-definition IPTV video streams over several essentially saturated IP backbone networks are presented.

1. Introduction

Multimedia traffic such as IPTV and video-on-demand represent a rapidly growing segment of the total Internet traffic. According to Cisco [1, 2], global Internet traffic is nearly doubling every 2 years, and global capacity will have to increase 75 times over the decade 2002–2012 to keep up with the demand. Furthermore, video-based traffic such as IPTV [3] will represent 90% of global network loads in 2012. The US Federal Communication Commission (FCC) has required that all TV broadcasts occur in digital format in 2009, and the growing fraction of multimedia traffic threatens to overwhelm the current Internet infrastructure. According to [4], “*The United States will not be the first country to complete the transition to digital television... Luxembourg, the Netherlands, Finland, Andorra, Sweden, and Switzerland have all completed their transitions, utilizing the*

Digital Video Broadcasting—Terrestrial (DVB-T) standard. Transitions are now under way in more than 35 other countries.” According to Cisco [5]: “*With the deployment of these new IPTV services, existing network infrastructures will be pushed to their limits.*” The congestion problems are already visible: “*Video is clogging the internet. How we choose to unclog it will have far-reaching implications*” [6]. Recognizing the problems, the US National Science Foundation initiated a major project called “*Global Initiative for Network Investigations*” (GENI), which is open to a complete “*clean slate*” redesign of Internet if necessary, in an attempt to address the problems [7, 8]. In summary, new technologies which support the efficient multicasting and broadcasting of multimedia services such as IPTV are essential.

In this paper, the design of an IPTV multicast system for Internet backbone networks is presented and explored

through extensive simulations. An IPTV multicast system was first proposed in [9] based upon a theoretical foundation established in [10, 11]. Extensive simulations were presented for an 8-node multicast tree in [9], however the design or simulation of a multicast system for a real IP network topology was not presented.

In this paper, the design of a realistic IPTV multicast system for several real backbone IP networks described in [12] is presented. Exhaustive simulations confirm that the system can deliver several hundred IPTV packet streams over the Internet backbone networks with essentially zero delay jitter, essentially zero packet loss rate, and essentially-perfect end-to-end QoS for every provisioned multicast tree. In the proposed system, a resource-reservation algorithm such as RSVP, IntServ, or DiffServ is used to reserve resources such as buffer space and transmission capacity in each multicast router in each multicast tree. Each IP router then uses a recently proposed *Recursive Fair Stochastic Matrix Decomposition* scheduling algorithm [9, 10] to schedule the IPTV traffic streams through the router while meeting rigorous QoS guarantees, under the constraint of unity speedup.

Internet routers can use three basic switch architectures, the *Input-Queued (IQ)* switch, the *Output-Queued (OQ)* switch, or the *Combined Input and Crosspoint Queued (CIXQ)* switch. OQ switches can achieve optimal throughput but they require an internal speedup of $O(N)$, which renders them impractical for large sizes. *Combined Input and Output Queued (CIOQ)* switches have also been proposed. These switches can also achieve 100% throughput, but they also require a speedup typically by a factor of 2 or 4, which is difficult to realize and which increases costs. CIXQ switches can also achieve 100% throughput with simpler scheduling algorithms, but they require many crosspoint queues in the switching matrix which increase costs. To minimize costs, many high capacity routers exploit some form of Input Queueing. Figure 1 illustrates a packet-switched IP router using an $N \times N$ *Input-Queued (IQ)* switch architecture. Each input port has N “*Virtual Output Queues (VOQs)*”, and the switch has a total of N^2 VOQs. Figure 2 illustrates a packet-switched IP multicast tree, which consists of a tree of packet-switched IP routers as shown in Figure 1.

Many IP routers exploit a fixed-sized cell switching architecture. Variable-sized IP packets containing video data arrive at the input ports. Each IP packet is disassembled into small fixed-sized cells, which are stored in the appropriate VOQ at the input side of the switch. Typical cells can be between 64 and 256 bytes in length. At each input port j , each $VOQ(j,k)$ stores cells destined for output port k . The fixed-sized cells are scheduled for transmission across the switch in a series of time slots. The variable-sized IP packets are reconstructed at the output side of the router and are then transmitted to the next router in the multicast tree. In each time slot, a scheduling algorithm is used to compute a set of up to N cells to transfer across an IQ switch, subject to two constraints: (1) each input port transmits at most 1 cell from its N VOQs, and (2) each output port receives at most 1 cell from any VOQ. The set of cells to transmit per time slot can be represented as a permutation.

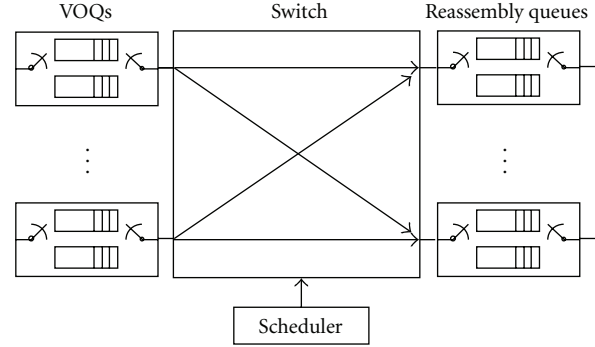


FIGURE 1: IQ switch.

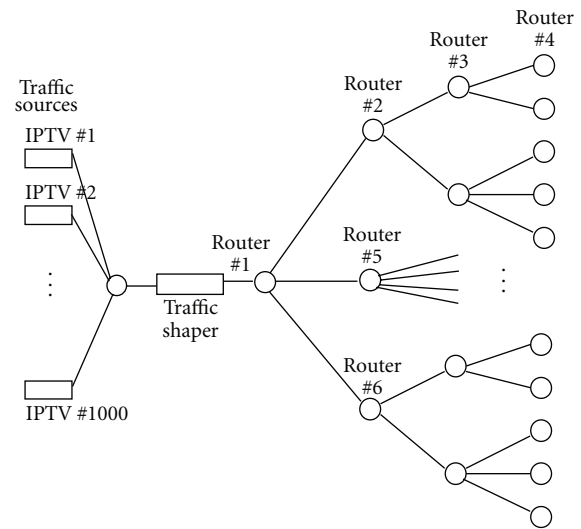


FIGURE 2: IPTV Multicast tree.

Scheduling for IQ switches is known to be a difficult problem [13–27]. The difficulty is compounded when Quality-of-Service (QoS) constraints are added to the scheduling problem. It has been shown that effective IPTV delivery requires low jitter [28–30]. The selection of a set of N cells to transfer per time-slot in an IQ switch is equivalent to finding a matching in a bipartite graph. Assuming link rates of 40 or 160 Gbps, the durations of a time-slot for a 64-byte cell are 12.8 and 3.2 nanoseconds, respectively. Therefore, schedulers for IQ switches must compute new bipartite graph matchings very quickly, typically at rates of 100–300 million matchings per second. Existing switch schedulers can be classified into two classes: (1) “*Dynamic schedulers*” which compute new bipartite matchings in every time-slot without any a priori knowledge of the long-term traffic demands on the switch, and (2) “*Guaranteed-Rate (GR) schedulers*” which periodically compute a sequence of F matchings to be used in F consecutive time slots called a “*scheduling frame*”. The schedules can be reused repeatedly, and the schedule is recomputed when the long-term traffic demands of the switch are modified.

It is known that dynamic schedulers for IQ switches can achieve 100% throughput, if a *Maximum Weight Matching*

(*MWM*) algorithm is used to compute the matching for each time-slot, where the largest queues receive preferential service [13]. However, the *MWM* algorithm has complexity $O(N^3)$ work per time-slot and is considered intractable for use in real IP routers [13]. Therefore, existing dynamic schedulers typically use sub optimal heuristic schedulers, such as Parallel Iterative Matching or iSLIP [14]. However, due to the severe time constraints all heuristic schedulers have sub optimal throughput efficiencies and exhibit significant delay and jitter at high loads. The iSLIP algorithm used in the Cisco 1200 series routers is an iterative heuristic scheduler which can achieve throughput efficiencies as high as 80% for non uniform traffic patterns. However, the average queuing delay per cell can approach several thousand time slots at high loads, and the delay jitter can be equally high.

In this paper, a recently proposed *Recursive Fair Stochastic Matrix Decomposition* algorithm is used to schedule multicast IPTV traffic in each router in an IP multicast tree in a fully saturated IP network, and the performance is examined through extensive simulations. A resource-reservation protocol such as RSVP, IntServ, or DiffServ is used to maintain a traffic rate matrix for each IP router. (We note that while DiffServ does not use explicit resource reservation, DiffServ does use class-based weighted fair queueing, which effectively reserves bandwidth for each DiffServ traffic class.) Each traffic rate matrix is doubly sub stochastic or stochastic, and specifies the guaranteed traffic rates between every pair of *Input-Output* (IO) ports of the router. The traffic matrix in each router can then be mathematically decomposed to yield a sequence of bipartite graph matchings or permutations. Each matching configures the switch for one time-slot, and the sequence of matchings is guaranteed to deliver the IPTV stream through the IP router while providing rigorous QoS guarantees, under the constraint of unity speedup.

The *Recursive Fair Stochastic Matrix Decomposition* (RFSMD) algorithm proposed in [10] converts an admissible traffic rate matrix for a router into a quantized (integer) matrix with integer-valued elements, assuming a scheduling frame of length F time slots. The algorithm then recursively partitions the quantized matrix in a recursive and relatively fair manner, yielding a sequence of permutation matrices, also called permutations. The resulting sequence of permutations forms a “*frame transmission schedule*”, for transmitting cells through the packet-switched IP router. The sequence of permutations in a frame transmission schedule can be repeatedly reused, as long as the traffic rate matrix remains unchanged. When the traffic rate matrix is updated by the RSVP, IntServ, or DiffServ algorithm, the frame transmission schedule can be recomputed. The RFSMD algorithm, along with appropriate traffic shaping at the sources, rigorously guarantees that every provisioned traffic flow achieves near-minimal delay and jitter and essentially-perfect end-to-end QoS, for all networks loads up to 100%. By “essentially-perfect QoS”, we mean that every provisioned traffic flow can be delivered with zero packet loss rate, near-minimal end-to-end delay and zero network-introduced delay jitter. Theoretical bounds on the delay, jitter and QoS are presented in [10, 11] and are summarized in Section 4 of this paper.

In this paper, we apply the RFSMD scheduling algorithm to the problem of multicasting real IPTV traffic through multicast trees in several real IP backbone networks, to explore the feasibility of large-scale IPTV multicasting in IP networks.

Section 2 describes video traffic model. Section 3 describes some prior guaranteed-rate scheduling algorithms. Section 4 describes the low-jitter RFSMD scheduling algorithm in more depth. Section 5 describes the IP backbone networks and the IPTV multicast trees, and presents detailed simulation statistics. Section 6 contains concluding remarks.

2. Video Traffic Model

Cisco Systems estimates that several hundred video channels requiring up to 1 Gbps bandwidth may be distributed over the IP backbone to support emerging IPTV applications [5]. To gather realistic data for our simulations, a high-definition video stream entitled “*BBC Blue Planet*” available at the University of Arizona [31] website was processed. The video stream includes 61 K video frames which arrive at the rate of 24 video frames/sec. The minimum, mean, and maximum video frame sizes are 81, 21 K, 495 K bytes respectively, illustrating a very bursty behaviour.

We assume these video frames are disassembled into fixed-sized 64-byte cells before transmission into the IP multicast tree. These video frame sizes correspond to a mean of 328 cells per video frame, with a minimum and maximum of 2 and 7,735 cells per video frame, respectively. The single video stream has a compression ratio of 151, with a mean bit rate of about 4 Mbps, and a peak bit rate of 95 Mbps. To simplify the terminology, define this data to represent a single “*video channel*”. A “*video stream*” consists of the aggregation of 1 or more video channels.

The Arizona website [31] provides video frame size statistics for a few high-definition video channels. In this paper, we assume 100 high-definition video channels are to be multicast in each multicast tree, each with a 4 Mbps average rate, for an aggregate stream traffic rate of approximately 404 Mbps. To achieve the statistics for the 100 video channels used in our network simulations, the data for the video “*BBC Blue Planet*” was reused in a circular manner, with a randomly selected starting video frame for each channel.

Table 1 lists some properties of the single video channel and several aggregated video traffic streams. In Table 1, the ratio of the peak-to-mean rates is an indication of the burstiness of the traffic. The single channel has a peak-to-mean ratio of 23.5, indicating a high degree of burstiness. Referring to Table 1, the aggregated stream of 100 channels has an aggregate data rate of 404 Mbps, with a peak rate of 700 Mbps. The ratio of peak-to-mean rates is 1.73, indicating a considerable reduction in burstiness.

Figure 3 illustrates visually the effect of aggregation of multiple video channels on the burstiness of the aggregated video stream. Figure 3 illustrates the instantaneous normalized bandwidth versus time for the same aggregated streams. The mean rate of each stream has been normalized to 1, and the reduction in burstiness when many video channels are aggregated is evident.

TABLE 1: Statistics on aggregated traffic.

Channels	Mean Rate(Mbps)	Max Rate	Max/Mean	Standard Deviation	10% extra cap delay (sec)
1	4.04	95	23.5	6.68	97.1
10	40.4	165	4.08	21	45.4
100	404	700	1.73	69	4.35

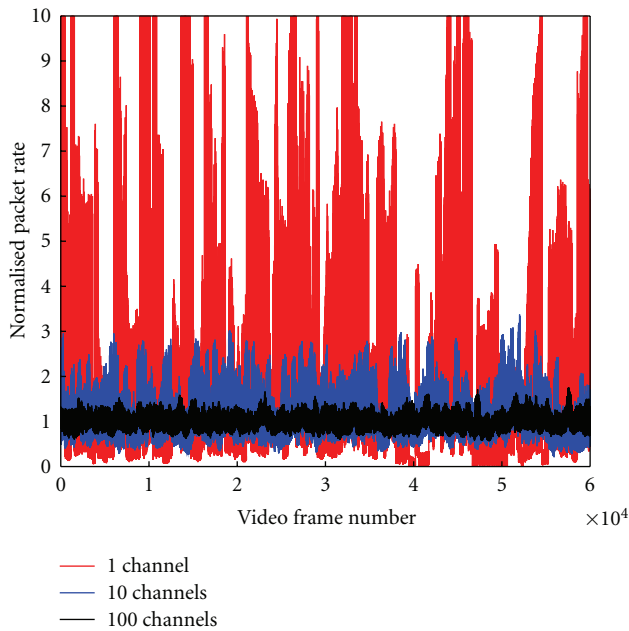


FIGURE 3: Burstiness of aggregated traffic.

Assume that video frames for any one video channel arrive at the root of a multicast tree at the fixed rate of 24 video frames per second. The arrival rate of video frames for the aggregated stream of 100 channels is therefore 2,400 video frames per second. The arriving traffic is quite bursty, as shown in Figure 3.

In this paper, we assume an *Application-Specific Token Bucket Traffic Shaper (ASTS)* module [9, 11] is used at the source to smoothen incoming bursty IPTV traffic to conform to an appropriate mean traffic rate with bounded burstiness. Cells are allowed to depart the ASTS at the maximum rate of 440 Mbps, when cells are available. The ASTS will introduce an *application-specific* delay at the source which is independent of the network. Referring to Figure 2, assume that the 100 video channels are available at the root of each IP multicast tree for distribution. The aggregated stream of 100 channels has an average data rate of 404 Mbps, and each IP multicast tree must be provisioned to support this traffic. In this paper, we assume that each IP multicast tree is provisioned such that the average data rate of the aggregated video stream consumes 90% of the provisioned tree link capacity, thereby providing 10% excess bandwidth for bursts. Therefore, each IP multicast tree must be provisioned to support about 440 Mbps of guaranteed rate traffic on every link in the tree. Given the line rate of 40 Gbps, the use

of 64-byte cells, and a scheduling frame of length $F = 1$ K, then each time-slot reservation represents a bandwidth of approximately 40 Mbps. Therefore, a guaranteed rate of 440 Mbps requires the reservation of 11 cells per scheduling frame, or about 1% of the line rate. However, each backbone network has multiple IPTV multicast trees, between 9 and 16 trees in our simulations, so the fraction of multicast traffic on each link will be typically between 4% and 7% of the link capacity in our models. When bursts of cells arrive at the ASTS module, these cells will be temporarily stored, and will be released into the network at an average rate of 400 Mbps and a maximum data rate of 440 Mbps.

Referring to Figure 2, the router no.1 is the root of a multicast tree and implements a 1-to-3 multicasting of the cells. There are many nodes in an IP multicast tree, distributing content to potentially millions of end-users (i.e., households). Each destination node of the multicast tree has an *Application-Specific Playback Queue (ASPQ)* [9, 11] which receives the fixed-sized cells corresponding to the aggregated video stream. The purpose of the ASPQ is to filter out residual network-introduced jitter and reconstruct the original bursty video frames. The destination nodes in an Internet backbone network may represent a Central Office in a city. The Central Office node must deliver the IPTV streams to the ultimate end-users, which are the residential homes or mobile phones, and so forth, over a regional Metropolitan Area Network. The delivery of the IPTV traffic over the regional Metropolitan Area Network can use the same IPTV multicast design described in this paper. Therefore, bursty IPTV traffic flows can be delivered to the ultimate end-users in a hierarchical manner, with essentially zero delay jitter, with essentially zero packet loss rates and with essentially-perfect end-to-end QoS.

IP networks typically transmit variable-sized IP packets. Packets are typically disassembled into fixed-sized cells at the input size of each IP router, and IP packets are reassembled at the output size of the IP router, before they are transmitted to the next IP router. The use of variable-sized IP packets typically leads to delays associated with disassembling and reassembling IP packets in each IP router. In this paper, we assume an IP/MPLS technology, where all IP packets carrying video data have a fixed size, for example 64 bytes, 1024 bytes, or 1500 bytes. IP packets are disassembled once at the ingress router and reassembled once at the egress router of an MPLS domain. This assumption eliminates the need to repeatedly disassemble and re-assemble variable-sized IP packets at each IP router within one domain, and removes the packet reassembly delay in each IP router. However, the main results hold even if large fixed-sized packets are used

(i.e., 1500 bytes), or if variable size packets are used. In this case, the packet reassembly delay must be added to each router. The important point is that all variable queueing delays and jitter have been removed.

3. Prior Guaranteed-Rate Scheduling Algorithms

Several schemes have been proposed for scheduling guaranteed-rate (GR) traffic through an IQ packet switch, which are briefly reviewed. All of the schemes discussed in this section assume that every router maintains a traffic rate matrix, which specifies the requested traffic rates between all IO pairs in the router.

In the Birkoff von-Neuman (BVN) scheme proposed in [17, 18], a doubly stochastic traffic rate matrix is decomposed into a sequence of permutation matrices and associated weights. Each matrix represents a switch configuration, that is, a matching or permutation of input ports onto output ports. These matrices are then scheduled to appear in proportion to their weights using the GPS or WFQ algorithm, to determine the sequence of switch configurations which meet the GR traffic requirements. Each switch configuration is used to configure the packet switch for one time-slot. Best-Effort IP traffic can then use any switching capacity not used by GR traffic. The BVN decomposition can achieve 100% throughput through a router, that is, it does not introduce “speedup” at any router. However, the BVN decomposition has a time complexity of $O(N^{4.5})$ in a serial processor and is generally considered too slow for use in real-time packet-switched IP routers.

An algorithm to schedule traffic through an IQ packet-switched IP router, while attempting to minimize the “service lag” amongst multiple competing IP flows and to minimize the speedup, was developed at MIT [16]. A doubly stochastic traffic rate matrix is first quantized to contain integer values and then is decomposed into a series of permutation matrices and associated weights, which then must be scheduled. With speedup $S = 1 + sN$ between 1 and 2, the maximum service lag (defined ahead) over all IO pairs is bounded by $O((N/4)(S/(S-1)))$ time slots. According to [16]; “with a fairly large class of schedulers a maximum service lag of $O(N^2)$ is unavoidable for input queued switches. To our knowledge, no scheduler which overcomes this $O(N^2)$ has been developed so far. For many rate matrices, it is not always possible to find certain points in time for which the service lag is small over all IO pairs simultaneously.”

A greedy scheduling algorithm which attempts to minimize the delay jitter amongst simultaneous competing IP flows through an IQ packet switch was developed at Bell Labs [19, 20]. The traffic demand is specified in an $N \times N$ traffic rate matrix. The low-jitter GR traffic is constrained to be a relatively small fraction of the total traffic. The delay and jitter minimization problem is first formulated as an integer programming problem. The traffic rate matrix must be decomposed into a set of permutation matrices and associated weights, such that each traffic flow is supported by exactly one permutation in the set. This

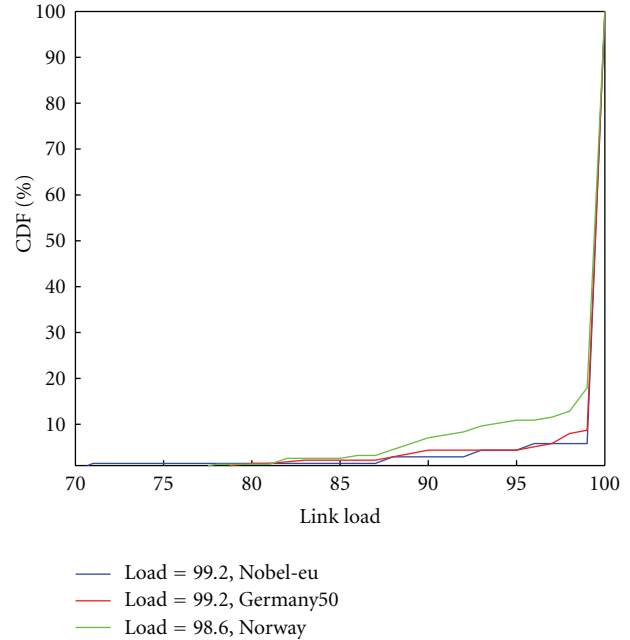


FIGURE 4: Average link loads.

matrix decomposition problem was shown to be NP-HARD. They then formulate a greedy low-jitter decomposition with complexity $O(N^3)$ time. The resulting schedule requires a worst-case speedup of $O(\log N)$, which renders it costly in practice. Hard analytic bounds on the jitter were not available.

A heuristic scheduling algorithm for scheduling packets in an IQ switch was developed at the UCR [21]. The algorithm attempts to decompose an admissible integer traffic rate matrix into the sum of integer matrices, where the maximum row or column sums of the matrices represent a decreasing geometric sequence. The authors establish a jitter bound which grows as the switch size N increases, and identify an open problem “to determine the minimum speedup required to provide hard guarantees, and whether such guarantees are possible at all” [21].

In summary, there is a considerable body of recent research into mathematical scheduling algorithms based upon the decomposition of traffic rate matrices. Unfortunately, tractable scheduling algorithms which achieve stability within the capacity region or which achieve bounded delays or jitter under the constraint of unity speedup, in one IP/MPLS router or a network of IP/MPLS routers, are unknown.

4. The Recursive Fair Stochastic Matrix Decomposition Algorithm

An $N \times M$ packet switch has N input and M output ports, and an associated traffic rate matrix. Each input port j for $0 \leq j < N$ has M Virtual Output Queues, one for each output port k , $0 \leq k < M$. The guaranteed-rate traffic requirements

for an $N \times N$ packet switch can specified in a doubly sub stochastic or stochastic traffic rate matrix Λ :

$$\Lambda = \begin{pmatrix} \lambda_{0,0} & \lambda_{0,1} & \cdots & \lambda_{0,N-1} \\ \lambda_{1,0} & \lambda_{1,1} & \cdots & \lambda_{1,N-1} \\ \cdots & \cdots & \cdots & \cdots \\ \lambda_{N-1,0} & \lambda_{N-1,1} & \cdots & \lambda_{N-1,N-1} \end{pmatrix}, \quad (1)$$

$$\sum_{i=0}^{N-1} \lambda_{i,j} \leq 1, \quad \sum_{j=0}^{N-1} \lambda_{i,j} \leq 1.$$

Each element $\lambda_{j,k}$ represents the fraction of the transmission line rate reserved for guaranteed-rate traffic between IO pair (j, k) . The transmission of cells through the switch is governed by the frame transmission schedule, also called a “frame schedule”. In an 8×8 crossbar switch with $F = 128$ time slots per frame, the minimum allotment of bandwidth is $1/F = 0.78\%$ of the line rate, which reserves one time-slot per frame on a recurring basis. Define a new quantized traffic rate matrix R where each traffic rate is expressed as an integer number times the minimum quota of reservable bandwidth:

$$R = \begin{pmatrix} R_{0,0} & R_{0,1} & \cdots & R_{0,N-1} \\ R_{1,0} & R_{1,1} & \cdots & R_{1,N-1} \\ \cdots & \cdots & \cdots & \cdots \\ R_{N-1,0} & R_{N-1,1} & \cdots & R_{N-1,N-1} \end{pmatrix}, \quad (2)$$

$$\sum_{i=0}^{N-1} R_{i,j} \leq F, \quad \sum_{j=0}^{N-1} R_{i,j} \leq F.$$

Consider two classic underlying theories from the field of graph theory and combinatorial mathematics, summarized in [10, 16–21]. Theorem 1 states that any integer matrix with a maximum row or column sum of F can be expressed as the sum of F permutation matrices. Theorem 2 states that any doubly sub stochastic or stochastic matrix can be decomposed into a convex set of permutations matrices and weights. All of the matrix decomposition algorithms reviewed in Section 3 attempt to exploit the above 2 theorems. They all are based upon the decomposition of a given traffic rate matrix into a convex set of constituent permutation matrices and associated weights, such that the weighted sum of the permutation matrices equals the original traffic rate matrix. Unfortunately, problems in combinatorial mathematics are difficult to solve efficiently, due to the large number of combinations that must be considered in any solution. As shown in Section 3, the problem of scheduling traffic to achieve zero jitter in minimum time is NP-HARD. All the algorithms reviewed in Section 3 (except for the BVN algorithm) require the introduction of “*speedup*” to the switches to achieve a decomposition, which limits their practical applicability. The BVN decomposition does not require a speedup, but its complexity is $O(N^{4.5})$ on a serial processor, which is considered intractable given that current Internet routers must compute decompositions at the rates of 100–300 million permutation matrices per second.

The *Recursive Fair Stochastic Matrix Decomposition* algorithm presented in [10] is an efficient deterministic

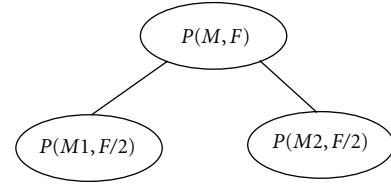


FIGURE 5: Recursive problem $P(M, F)$ of scheduling of matrix M into a scheduling frame with F time slots.

algorithm to decompose an admissible traffic rate matrix into a sum of permutation matrices under the constraint of unity speedup. Let $P(M, F)$ denote the problem of scheduling an admissible quantized traffic rate matrix M into a scheduling frame of length F time slots, as shown in Figure 5. In particular, an integer matrix M with a maximum row or column sum of F must be partitioned into two integer matrices $M1$ and $M2$, each with a maximum row or column sum of $F/2$. More specifically, the scheduling problem $P(M, F)$ must be recursively decomposed into 2 smaller scheduling problems $P(M1, F/2)$ and $P(M2, F/2)$, such that the integer matrices $M1 + M2 = M$, where $M1$ and $M2$ are admissible integer traffic rate matrices, and for all j and k where $0 \leq j \leq N$ and $0 \leq k \leq N$, then $M1(j, k) \leq M2(j, k) + c$ and $M2(j, k) \leq M1(j, k) + c$ for $c = 1$. This step of partitioning an integer matrix into 2 integer matrices is a problem in combinatorial mathematics. The RFSMD algorithm achieves the decomposition by transforming one combinatorial problem into another combinatorial problem with a recently proposed solution. In particular, the problem of decomposing an integer matrix relatively fairly into 2 integer matrices is transformed into the problem of routing permutations in a rearrangeably nonblocking switching network [10]. An efficient algorithm for the combinatorial problem of routing permutations in rearrangeable networks was proposed in [10].

The recursive nature of the RFSMD algorithm yields a very efficient decomposition. The decomposition of an $N \times N$ integer matrix with a maximum row or column sum of F can be accomplished in $O(NF \log(NF))$ time. The decomposition yields F permutations or bipartite graph matchings, which can configure the switch for F time slots. The computational complexity for each computed permutation of N elements is therefore $O(N \log(NF))$ time on a serial processor, which is near optimal.

The RFSMD algorithm also partitions each matrix M relatively fairly, so that the two smaller matrices $M1$ and $M2$ differ by at most 1 in any position. As a result, the traffic in the original scheduling problem is scheduled relatively fairly over the 2 smaller scheduling problems. This relatively fair recursive partitioning leads to a bound on the maximum jitter for any traffic flow, and a bound for the *maximum normalized service lead* or *maximum normalized service lag* for any scheduled traffic flow (these terms are formally defined in the next paragraphs). The bounded normalized service lead/lag can be used to create bounds on the end-to-end QoS for every scheduled traffic flow, as will be shown ahead.

One step in the decomposition for a 4×4 matrix operating at 99.2% load with unity speedup is shown in (3). Given an $N \times N$ switch and a fixed scheduling frame length F , the RFSMD matrix decomposition algorithm [10] bounds the *normalized service lead* and *service lag* for the aggregated traffic leaving any *node* to $\leq k \cdot \text{IIDT}$ time slots for constant K , where *IIDT* represents the “*Ideal Interdeparture Time*” for cells belonging to the aggregated traffic leaving an edge. Furthermore, the bound applies to all individual competing traffic flows traversing each edge, provided that cells are selected for service within each VOQ according to a GPS scheduling algorithm

$$\begin{bmatrix} 106 & 222 & 326 & 345 \\ 177 & 216 & 303 & 326 \\ 459 & 232 & 183 & 147 \\ 282 & 352 & 211 & 178 \end{bmatrix} = \begin{bmatrix} 53 & 111 & 163 & 172 \\ 88 & 108 & 152 & 163 \\ 230 & 116 & 91 & 74 \\ 141 & 176 & 105 & 89 \end{bmatrix} \quad (3)$$

$$+ \begin{bmatrix} 53 & 111 & 163 & 173 \\ 89 & 108 & 151 & 163 \\ 229 & 116 & 92 & 73 \\ 141 & 176 & 106 & 89 \end{bmatrix}.$$

Each smaller scheduling problem contains approximately one half of the original time-slot reservation requests, and has as smaller scheduling frame of length $F/2$ time slots to realize these reservation requests, as shown in Figure 5. Repeated application of the relatively fair recursive partitioning results in a sequence of partial or full permutation matrices which determine the IQ switch configurations, called the frame transmission schedule. Due to the relatively fair recursive partitioning, the service a traffic flow receives in each half of the frame schedule will be relatively fair, and the delay jitter will be relatively small.

Several of the following definitions from [10] will be useful to interpret the simulation results to be presented in Section 6.

Definition 1. A “*Frame transmission schedule*” of length F is a sequence of partial or full permutation matrices (or vectors) which define the crossbar switch configurations for F time slots within a scheduling frame. Given a line rate L , the frame length F is determined by the desired minimum quota of reservable bandwidth = L/F . To set the minimum quota of reservable bandwidth to $\leq 1\%$ of L , set $F \geq 100$, that is, $F = 128$.

Definition 2. The “*Ideal Interdeparture Time*” denoted *IIDT* (i, j) of cells in a GR flow between IO pair (i, j) with quantized rate $R(i, j)$ time-slot reservations in a frame of length F , given a line rate L in bytes/sec and fixed-sized cells of C bytes, is given by: $\text{IIDT}(i, j) = F/R(i, j)$ time slots, each of duration (C/L) sec. (The subscripts will be suppressed when possible.)

Definition 3. The “*Ideal Service Time*” (*ST*) of cell $0 \leq c \leq R(i, j)$ in a GR flow between IO pair (i, j) with an *Ideal Interdeparture Time* of $\text{IIDT}(i, j)$ is given by $ST = j \cdot \text{IIDT}(i, j)$ time slots.

Definition 4. The “*Received Service*” of a flow with quantized guaranteed rate $R(i, j)$ at time-slot t within a frame of length F , denoted $S_{ij}(t)$, equals the number of permutation matrices in time slots $1 \dots t$, where $1 \leq t \leq F$, in which input port i is matched to output port j .

Definition 5. The “*Service Lag*” of a flow between input port i and output port j , at time-slot t within a frame of length F , denoted $L_{ij}(t)$, equals the difference between the requested quantized GR prorated by t/F , and the received service at time-slot t , that is, $L_{ij}(t) = S_{ij}(t) - (t/F)R_{ij}(t)$. A positive Service Lag denotes the case where the received service is less than the requested service, that is, a cell arrives later than its ideal service time. A negative Service Lag is a Service Lead, where the received service exceeds the requested service, that is, a cell arrive sooner than its ideal service time. The *normalized service lead/lag* for a flow f equals the service lead/lag for flow f divided by the *IIDT* for flow f .

Consider a discrete time queueing model, where time is normalized for all flows and is expressed in terms of the *IIDT* for each flow. The following notations presented in [11] are used. The cumulative arrival curve of a traffic flow f is said to conform to $T(\lambda, \beta, \delta)$, denoted, $A_f : T(\lambda, \beta, \delta)$ if the average cell arrival rate is λ cells/sec, the burst arrival rate is $\leq \beta\lambda$ cells/sec, and the maximum normalized service lead/lag is δ . A similar notation is used for cumulative departures and cumulative service. In any IP router, the cumulative departure curve for f is said to “*track*” the cumulative service curve for f when cell departures are constrained by the scheduled service opportunities. This situation occurs when flow f has queued cells at $\text{VOQ}(j, k)$.

The following four theorems were established in [11]. Assume each traffic flow is admitted to an IP/MPLS network subject to an *Application-Specific Token-Bucket Traffic Shaper Queue (ASSQ)*, and has a maximum normalized service lead/lag of K cells. The traffic rate matrix for each router is updated by a resource reservation protocol such as RSVP, IntServ, or DiffServ. Each *IP router* is scheduled using the proposed RFSMD algorithm with a maximum normalized service lead/lag of K cells. We assume fixed size cells, with any reasonable cell size, however similar bounds apply for the case of variable-sized IP packet.

Theorem 1. Given a flow f traversing $\text{VOQ}(j, k)$ over an interval $t \in [0, \tau]$, with arrivals $A_f : T(\phi(f), \beta, K)$, with service $S_f : T(\phi(f)\beta, K)$ and $Q(0) \leq O(K)$, then $Q(t) \leq O(K)$.

Theorem 2. When all queues in all intermediate nodes have reached steady state, the maximum end-to-end queueing delay of a GR flow traversing H routers is $O(KH) \cdot \text{IIDT}$ time slots.

Theorem 3. In the steady state, the departures of traffic flow f at any IQ router along an end-to-end path of H routers are constrained by the scheduling opportunities, and will exhibit a maximum normalized service lead/lag of K , that is, $S_f : T(\phi(f)\beta, K)$. The normalized service lead/lag of a flow is not cumulative when traversing multiple routers.

Theorem 4. *A traffic flow which traverses H IQ routers along an end-to-end path can be delivered to the end-user with zero network-introduced delay jitter, when a playback buffer of size $4K$ cells is employed, that is, $S_f : T(\phi(f)\beta, K)$.*

According to Theorem 4, a bursty IPTV traffic flow which traverses H IQ routers along an end-to-end path can be delivered to the end-user with *zero network-introduced delay jitter*, when an appropriately-sized Application-Specific Token-Bucket Traffic Shaper Queue and Application-Specific Playback Queue are used, as described in Section 3.

Theorem 1 states that the number of cells buffered for any flow in any router in any network is limited to a small number for all loads up to 100%. Theorem 2 states that all end-to-end traffic flows will never experience any congestion, excessive delay or throughput degradation. Every end-to-end flow experiences a small but effectively negligible queueing delay at each router compared to current router technologies. Theorem 3 states that the normalized service lead/lag is not cumulative when traversing multiple routers in any network. Theorem 4 states that every end-to-end traffic flow can be delivered at every destination router with essentially-perfect end-to-end Quality of Service. In particular, a bursty IPTV traffic flow transmitted through an IP network using the RFSMD scheduling algorithm can be perfectly regenerated at every destination route, with zero packet loss rate and zero delay jitter. These 4 theorems demonstrate that traffic flows can be scheduled to achieve essentially-perfect end-to-end QoS in any Internet topology for all loads up to 100%. The simulation results reported in Section 6 will demonstrate these 4 theorems.

5. Backbone Topologies

The *Survivable Network Design Library (SNDlib)* is a library of telecommunication network designs [12]. The library contains data for 22 IP backbone networks and several optimization problems for each network. The SNDlib provides a series of real IP network topologies appropriate for reproducible case studies. In this paper, simulation results for three of the SDNlib networks are presented. We have followed the node placement and link assignments described by SNDlib, although we have made our own assumptions about the IPTV broadcast tree construction, session demands, and link capacities.

We selected the NOBEL-EU, GERMANY50, and the NORWAY network models from [12], as shown in Figure 6. The NOBEL-EU network covers Europe and has 28 nodes and 41 edges. It is a reference network originating from the European project NOBEL, where a detailed cost model was developed for various kinds of SDH and WDM equipment [12]. The GERMANY50 has 50 nodes and 88 edges provided by T-Systems International AG, and is an extension of the NOBEL-GERMANY network. The NORWAY network has 27 nodes and 51 edges and represents a backbone network from Norway.

We developed several heavily loaded IPTV *traffic specifications* for each network. In each traffic specification, one-third of the highest degree nodes are selected as roots of

the IPTV multicast trees. For example, in the NOBEL-EU network with 28 nodes there are 9 multicast trees, each broadcasting 100 IPTV traffic streams. To generate each traffic specification, a 2-step process was used. In the first step, the IPTV multicast trees were routed into the network. $N/3$ nodes with the highest degrees were selected as roots for the $N/3$ trees. Each multicast tree was then routed to every other node in the network, using a shortest distance spanning tree computed using Dijkstra's algorithm. Many links in the network, especially those in the center of the topology, carry traffic from each of the all $N/3$ multicast trees. In the second step, background traffic was added in an iterative manner between randomly selected pairs of nodes, to essentially saturate the network. In our traffic specifications, we achieve link loads of approx. 99%. In each iteration, a random pair of nodes was selected, and a shortest delay path between the nodes was computed using an OSPF routing algorithm. A traffic rate was selected for the flow to nearly saturate the end-to-end path, and the flow would be confirmed. As the network load approaches 100%, it becomes increasingly difficult to route any additional flows, as all links approach saturation. Therefore, in the last iteration, multiple 1-hop traffic flows are added between neighboring nodes to effectively saturate the network, so that every link has a load of approximately 99%. Referring to Figure 4, the link loads used in our 3 network simulations are 99.2%, 99.2%, and 98.6%.

Each traffic specification represents an extremely heavy load, not likely to be encountered in practice. A resource reservation protocol such as RSVP, IntServ, or DiffServ was then used to reserve buffer space and bandwidth along each router and link in the network. These reservations result in the creation of an admissible traffic rate matrix for every router in the network. The traffic rate matrices for each router were then scheduled using the RFSMD algorithm. The network was then simulated, to gather statistics on the end-to-end QoS for every traffic flow, including IPTV multicast traffic and background traffic.

Numerous traffic specifications were generated, routed and simulated for the three selected network topologies. Figure 6 illustrates typical multicast trees in the 3 topologies examined in this paper, that is, the NOBEL-EU, NORWAY, and the GERMANY50 topologies. All of network simulations indicated essentially identical results, so we present the detailed simulations of one traffic specification over two networks, the NOBEL-EU and GERMANY50 networks. The NOBEL-EU network has 28 nodes, 41 links, and 9 IPTV multicast trees, each multicasting 100 IPTV channels to all other nodes. The selected traffic specification results in 321 traffic flows in the NOBEL-EU network, with an average distance of 5 hops and a maximum distance of 14 hops. The average link load is about 99%. The GERMANY50 network has 50 nodes, 88 links, and 16 IPTV multicast trees, each multicasting 100 IPTV channels to all other nodes. The selected traffic specification results in 693 traffic flows in the GERMANY50 topology, with an average distance of 5 hops and a maximum distance of 18 hops.

The roots of the IPTV multicast trees are illustrated as a bold circle in Figure 6. The IPTV multicast trees are

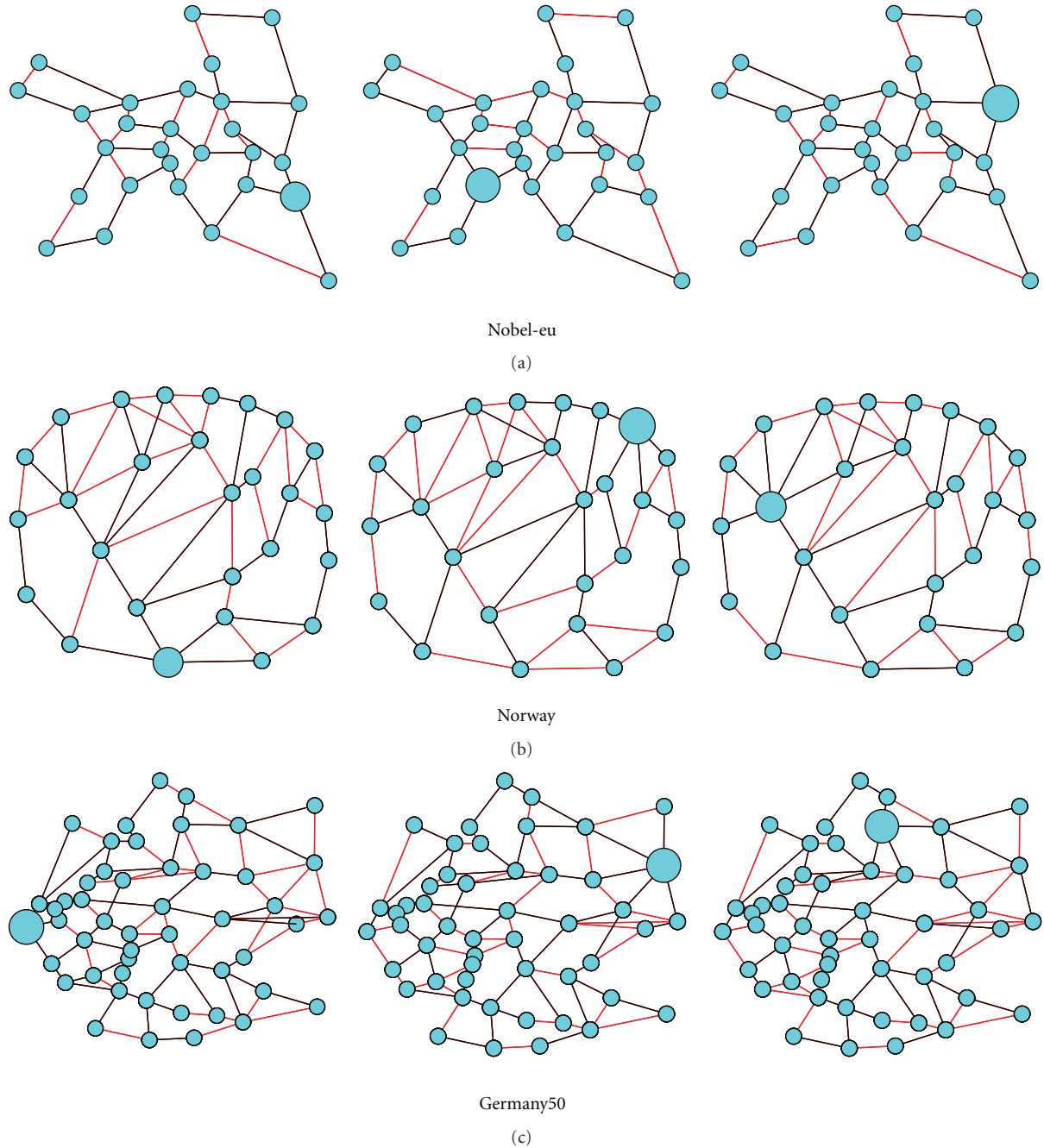


FIGURE 6: Three network topologies, each showing three typical multicast trees. Bold nodes are the roots of IPTV multicast trees.

routed according to Dijkstra's shortest path algorithm. As a result, links near the center of the network will tend to carry more IPTV traffic than those near the edge. Each multicast tree for a given source node is not unique, since in many cases each tree has several equal length shortest paths from which to select an edge. In our traffic specifications, a typical link will devote between 4% and 7% of its allocated bandwidth of 40 Gbps to IPTV multicast data, with a maximum of 20%. The remaining bandwidth is used for background traffic between randomly selected pairs of nodes.

6. Results of IPTV Multicasting

Assume an IP/MPLS backbone network with 40 Gbps links, with a scheduling frame length $F = 1.024$ (where 1 Gbps denotes 2^{30} bps and 1 Mbps denotes 2^{20} bps). The minimum quota of reservable bandwidth is one time-slot reservation per scheduling frame, or equivalently 4 Mbps. The provisioned GR rate of 440 Mbps per multicast tree established in Section 2 requires 11 time-slot reservations per scheduling frame. Each IP router in Figure 6 must reserve and schedule 11 cell transmissions per scheduling frame between the

appropriate IO pairs, per IPTV multicast tree. In our traffic specifications, every incoming and outgoing link in each IP router is essentially saturated with additional background traffic. Given this worst-case load, the IP routers should find it challenging to schedule the traffic to meet QoS guarantees.

The performance of the IP multicast trees in each IP backbone network was evaluated using a discrete-event simulator written in the C programming language, with over 20,000 lines of code. The simulator was written with the help of four graduate students, with funding provided by the Ontario Centers of Excellence. (Several independent simulators were actually written, to verify the experimental results.) The simulations were run on a large cluster-based supercomputing system in the Dept. of ECE at McMaster University, with 160 dual processing nodes running the LINUX operating system. Each dual-processor node has a clock rate of 1-2 GHz and between 1-2 GB of memory. A central dispatcher assigns tasks to processors to exploit parallelism.

Figure 7 illustrates the end-to-end delay (lifetime) PDF for (a) background traffic and (b) for multicast traffic in the GERMANY50 topology. Recall that there are 693 end-to-end paths and 16 IPTV multicast trees in this traffic specification. The multicast trees were routed first in the network using Dijkstra's shortest path algorithm, and therefore they have relatively low path lengths. The end-to-end delay for multicast traffic shown in Figure 7(b) varies from 1 IIDT up to about 9 IIDT. The background traffic is point-to-point, and was routed along shortest-delay paths using the OSPF routing algorithm. The shortest-delay paths generally do not equal the shortest-hop paths, and as a result the background traffic tends to be routed along longer paths. The end-to-end delays for background traffic shown in Figure 7(a) varies from about 1 IIDT up to 40 IIDT, indicating that some paths are very long.

Figure 8 illustrates the jitter of the traffic along each end-to-end path, for both background traffic and multicast traffic. The jitter along one path is defined as the deviation of each cell's delay along that path, relative to the mean value of the delay along a path. Figures 8(a) and 8(b) apply to the NOBEL-EU topology with 321 end-to-end paths. Figures 8(c) and 8(d) apply to the GERMANY50 topology with 693 end-to-end paths. Observe that 99% of all traffic flows arrive with less than 3 IIDTs of jitter, and 100% of all traffic flows arrive with less than 4 IIDTs of jitter. Observe from Figure 8 that the jitter for all point-to-point traffic and all multicast traffic is small and bounded by 4 IIDT, and the bound is network independent. These experimental results are consistent with the 4 theorems summarized in this paper. In [10], Theorems 5 and 8 establish that all jitter is bounded by 4 IIDT. Therefore, the experimental results in Figure 8 are perfectly consistent with the theorems in [10, 11].

Figure 9 illustrates the PDF for the distribution of the number of cells queued in each IP router in the GERMANY50 topology, for background traffic and multicast traffic. There are 3,465 individual plots in Figure 9, equal to 693 end-to-end paths passing through 5 routers on average. The number of cells queued per traffic flow in each router is small, less than 2 cells on average per multicast output

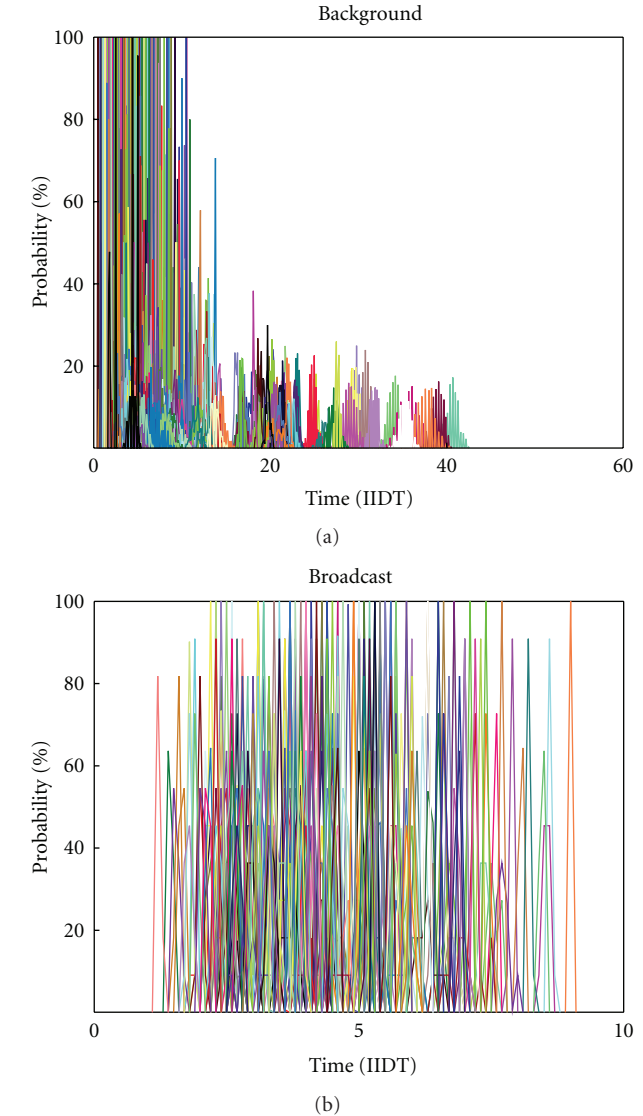


FIGURE 7: PDF of End-to-End Delay for Germany50 topology.

port. No router buffers more than 7 cells per flow per unicast output, as shown in Figure 9(a). No router buffers more than 3 cells per aggregated flow per multicast output port, as shown in Figure 9(b). The multicast cells are stored in a multicast queue, which is separate from the VOQs in each router. Figure 9 indicates that the cells move at a relatively consistent rate through the IP network. These experimental results are consistent with the 4 theorems summarized in this paper. In particular, Theorem 1 in [11] establishes that all queue sizes are bounded by a small number of cells (16 cells for these networks). Therefore, the experimental results in Figure 9 are perfectly consistent with the theorems in [10, 11]. The amount of memory required for buffering is several orders of magnitude lower when compared to traditional IP routers, as the next section will demonstrate.

Figure 10 illustrates the end-to-end delay for the IPTV multicast traffic, as a function of the excess bandwidth selected for each multicast tree. Recall that in our traffic

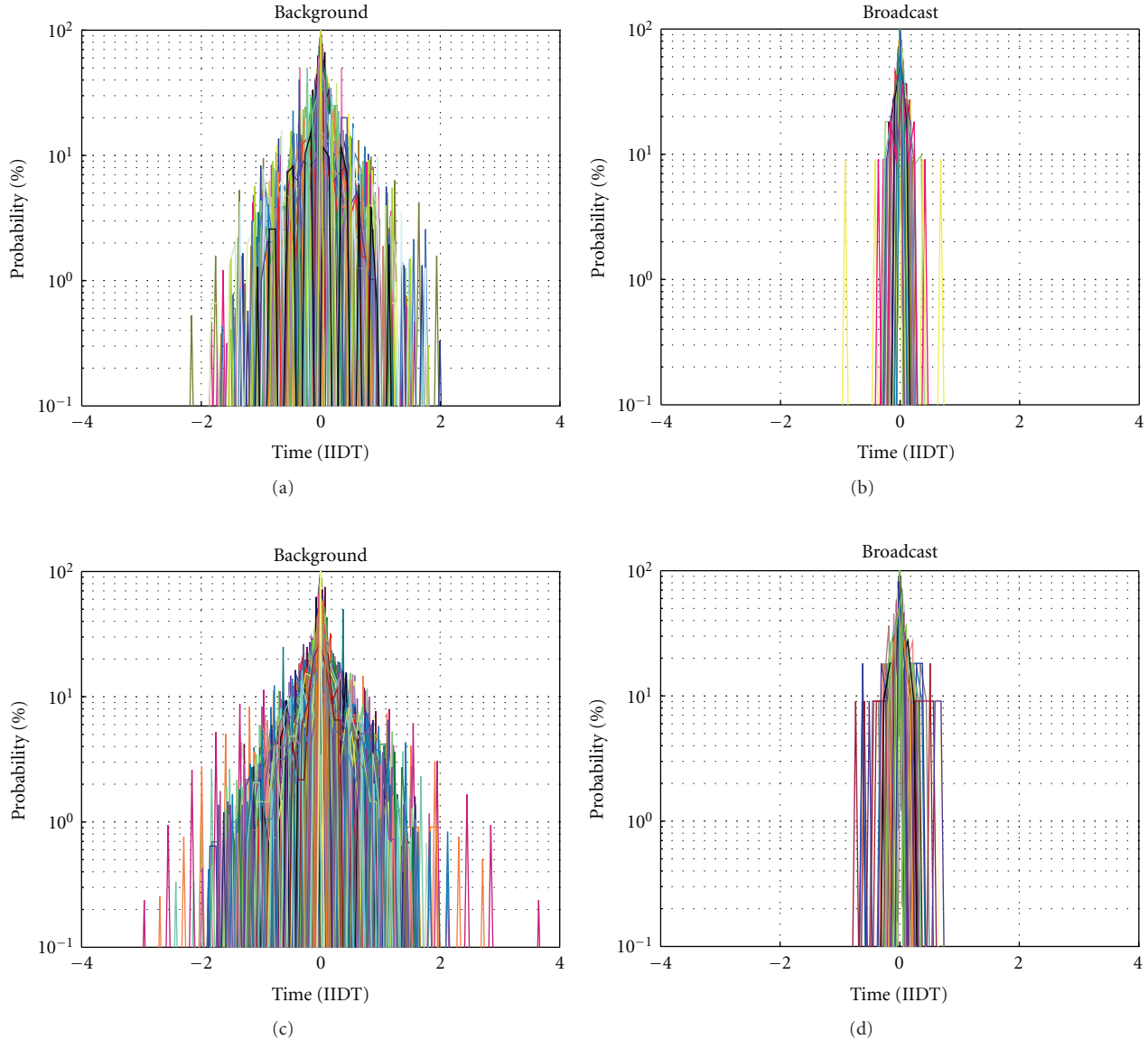


FIGURE 8: PDF of Delay Jitter. (a) and (b): Nobel-EU topology. (c) and (d): Germany50 topology.

specifications, an excess bandwidth of 10% was provisioned for every IPTV multicast tree. The excess bandwidth determines the end-to-end delay. According to Figure 10, an excess bandwidth of 10% yields an end-to-end queuing delay of about 3 seconds on each IPTV multicast tree. The *Application Specific Playback Queue* at each destination node has reconstructed the original bursty IPTV video frames, filtered out the residual network jitter and made all 100 video streams available at each destination IP router in the multicast tree with essentially zero delay jitter and essentially-perfect end-to-end QoS.

6.1. Buffer Sizing in IP Routers. In this section, we explore the issue of memory requirements in Internet routers. One well-established design rule for buffer sizing in IP networks using TCP flow-control is called the “*classical buffer rule*”, also called the “*bandwidth-delay-product*” buffer rule [31]. This

design rule states that *each link in each IP router* requires a buffer of $B = O(C \cdot T)$ bits, where C is the link capacity and T is the round-trip time of the flows traversing the link [31]. According to data in [31], a 40 Gbps link handling TCP flows with a round-trip time of 250 millisecond requires a buffer size B about five million IP packets per link. Each IP packet may contain up to 1500 bytes (or equivalently 24 fixed-sized cells). Therefore, each link buffer may require up to 7.5 Gigabytes of memory per link. A 16×16 router may require about 120 Gigabytes of high-speed memory. This large buffer size is partially due to the use of the traditional TCP flow-control protocol, which introduces a large jitter into the traffic flows, which in turn necessitates the use of large buffers. The large buffer size is also partially due to the use of sub optimal heuristic schedulers, which introduce a large and potentially unbounded jitter at every router, which in turn necessitates the use of large buffers.

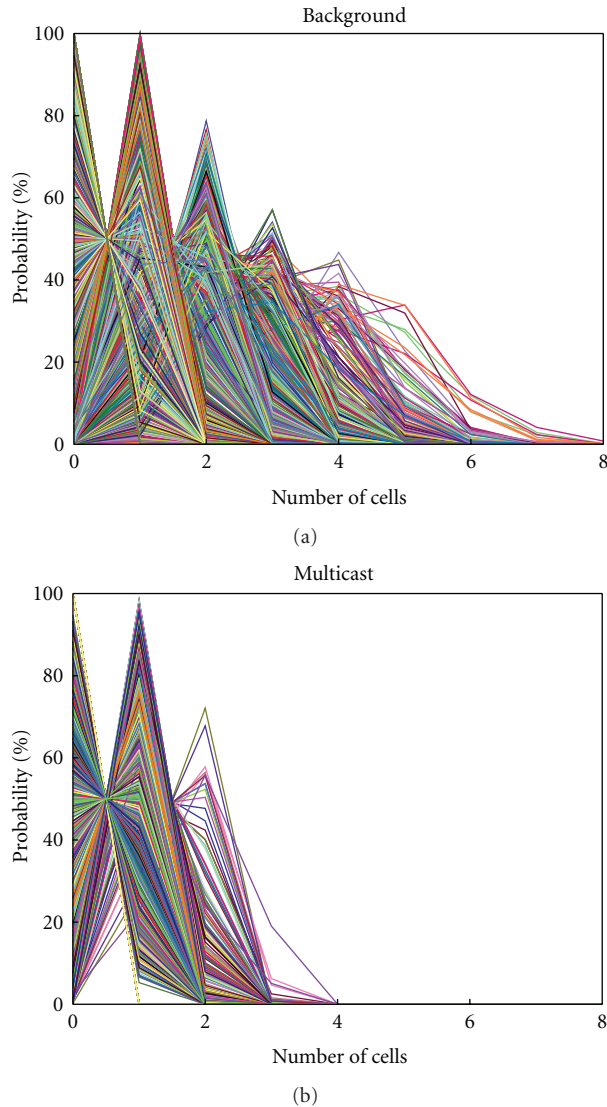


FIGURE 9: PDF for number of queued cells per traffic flow per router for Germany50 topology. (a) for background traffic. (b) for multicast traffic.

A “*small buffer rule*” was proposed in [32], where $B = O(C \cdot T/\sqrt{N})$, and where N is the number of long-lived TCP flows traversing the router. With the same parameters reported above, the buffer size B can be reduced to about fifty thousand IP packets [32]. Therefore, each link buffer may require up to 75 Megabytes of memory per link. A 16×16 router may require about 1.2 Gigabytes of high-speed memory.

More recently, [33] proposed a “*tiny buffer rule*” where $B = O(\log W)$, where W is the maximum TCP congestion window size. With the same parameters, [33] suggests that average buffer sizes of between 20–50 IP packets or equivalently about 30,000–75,000 bytes of memory may suffice if 3 important conditions can be met; (a) the jitter of incoming traffic at the source node is sufficiently small, (b) the IP routers introduce a sufficiently small jitter, and (c) 10–15% of the throughput is sacrificed. The paper in [33]

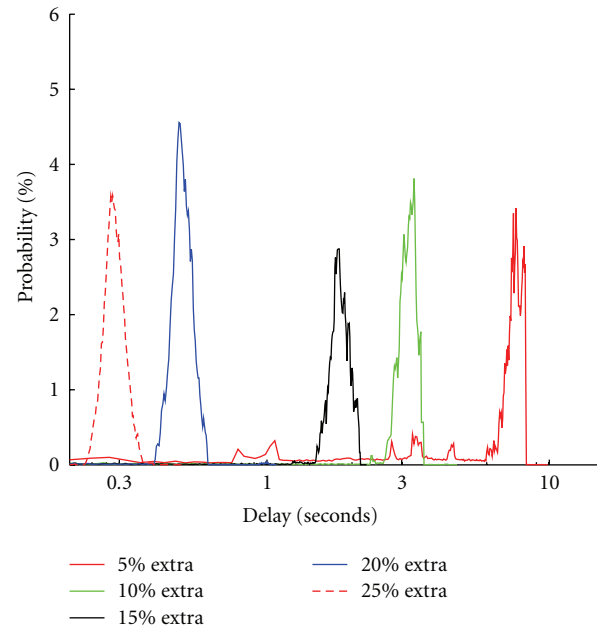


FIGURE 10: Plot of end-to-end delay versus excess bandwidth for multicast traffic.

however did not propose a low-jitter scheduling algorithm, which is in itself a major theoretical unsolved problem as Section 3 illustrates. Furthermore, [32, 34] have argued that small buffers may cause significant losses, instability or performance degradation at the application layer.

Our theorems in [10, 11] and our exhaustive simulations indicate that network memory requirements can be several orders of magnitude smaller than those in current IP routers, when a low-jitter scheduling algorithm with a bounded normalized service lead/lag is used, as established in Theorems 1–4. In our IP multicast system, each IP router needs to buffer on average about 2 cells (128 bytes) per flow per router to guarantee 100% throughput and essentially-perfect end-to-end QoS for all provisioned traffic flows, even at 100% network loads. In comparison, existing IP routers using the combination of heuristic schedulers, TCP flow control, and the classic bandwidth-delay-product buffer-sizing rule require buffers of about 5 million IP packets per link at 40 Gbps to achieve high throughput, without providing any rigorous QoS guarantees. The RFSMD algorithm and Theorems 1–4 allow for reductions in buffer sizes by several orders of magnitude compared to the existing IP multicast technology, while simultaneously meeting rigorous QoS constraints.

7. Conclusions

The design of an IPTV multicast system for packet-switched Internet backbone networks has been presented. Three real IP backbone network topologies, the NOBEL-EU European topology, and the GERMANY50 and the NORWAY topologies, were used to illustrate the design. Multiple IPTV multicast trees were provisioned into each network, each

carrying 100 IPTV channels. Additional background traffic was added between nodes to essentially fully saturate each network. Every link operates at loads of approximately 99%. A resource reservation algorithm was used to reserve resources for each IPTV multicast tree in the network. A recently proposed *Recursive Fair Stochastic Matrix Decomposition* algorithm was used to compute near-perfect low-jitter transmission schedules for each packet-switched IP router in each multicast tree. The low-jitter schedules remove most of the cell delay jitter associated with the sub optimal dynamic scheduling algorithms used in existing IP routers and minimize the amount of buffering required in the IP routers. Extensive simulations indicate that large-scale IPTV multicasting can be supported. The IPTV traffic is delivered to every destination node with near-minimal delays, near-minimal jitter, zero packet loss rates, and essentially-perfect end-to-end QoS, as confirmed by theory. Our extensive simulations indicate that each IP router typically buffers less than 2 cells (about 128 bytes) of video data per traffic flow per router, several orders of magnitude less buffering than current IP routers require. The multicast technology is also applicable to other multimedia streams over the Internet, including VOIP, Video-on-Demand, Telemedicine, and Telerobotic control over IP. The application of the technology to deliver telerobotic control systems over saturated Internet backbone networks is described in [35].

References

- [1] Cisco Systems White Paper, "Approaching the Zettabyte Era," 2008, <http://www.cisco.com>.
- [2] R. Lawler, "Cisco Sees a Zettaflood of IP Traffic-Driven by Video," Contentinople—Networking the Digital Media Industry, 2008, <http://www.contentinople.com>.
- [3] Y. Xiao, X. Du, J. Zhang, F. Hu, and S. Guizani, "Internet protocol television (IPTV): the killer application for the next-generation internet," *IEEE Communications Magazine*, vol. 45, no. 11, pp. 126–134, 2007.
- [4] J. M. Boyce, "The US digital television broadcasting transition," *IEEE Signal Processing Magazine*, vol. 26, no. 3, pp. 110–112, 2009.
- [5] Cisco Systems White Paper, "Optimizing Video Transport in your IP Triple Play Network," 2006, <http://www.cisco.com>.
- [6] L. Hardesty, "Internet gridlock: video is clogging the internet. How we choose to unclog it will have far-reaching implications," *MIT Technology Review*, 2008.
- [7] M. Baard, "NSF Preps New Improved Internet," *Wired*, August 2005.
- [8] BBN Technologies—GENI Project Office, "Global Environment for Network Innovations—GENI System Overview," December 2007.
- [9] T. H. Szymanski and D. Gilbert, "Internet multicasting of IPTV with essentially-zero delay jitter," *IEEE Transactions on Broadcasting*, vol. 55, no. 1, pp. 20–30, 2009.
- [10] T. H. Szymanski, "A low-jitter guaranteed-rate scheduling algorithm for packet-switched IP routers," *IEEE Transactions on Communications*, vol. 57, no. 11, 2009.
- [11] T. H. Szymanski, "Bounds on end-to-end delay and jitter in input-buffered and internally-buffered IP/MPLS networks," in *Proceedings of the IEEE Sarnoff Symposium (SARNOFF '09)*, Princeton, NJ, USA, 2009.
- [12] S. Orłowski, R. Wessaly, M. Pioro, and A. Tomaszewski, "SNDlib1.0-survivable network design library," ZIB report ZR-07-15, Networks, October 2009, <http://sndlib.zib.de/home.action>.
- [13] L. Tassiulas and A. Ephremides, "Stability properties of constrained queueing systems and scheduling policies for maximum throughput in multihop radio networks," *IEEE Transactions on Automatic Control*, vol. 27, pp. 1936–1948, 1992.
- [14] V. Anantharam, N. McKeown, A. Mekkittikul, and J. Walrand, "Achieving 100% throughput in an input-queued switch," *IEEE Transactions on Communications*, vol. 47, no. 8, pp. 1260–1267, 1999.
- [15] N. McKeown, "The iSLIP scheduling algorithm for input-queued switches," *IEEE/ACM Transactions on Networking*, vol. 7, no. 2, pp. 188–201, 1999.
- [16] C. E. Koksal, R. G. Gallager, and C. E. Rohrs, "Rate quantization and service quality over single crossbar switches," in *Proceedings of the IEEE Conference on Computer Communications (INFOCOM '04)*, pp. 1962–1973, 2004.
- [17] C.-S. Chang, W. J. Chen, and H.-Y. Huang, "On service guarantees for input buffered crossbar switches: a capacity decomposition approach by birkhoff and von neuman," in *Proceedings of the IEEE International Workshop on Quality of Service (IWQoS '99)*, pp. 79–86, 1999.
- [18] C.-S. Chang, W.-J. Chen, and H.-Y. Huang, "Birkhoff-von neumann input-buffered crossbar switches for guaranteed-rate services," *IEEE Transactions on Communications*, vol. 49, no. 7, pp. 1145–1147, 2001.
- [19] I. Keslassy, M. Kodialam, T. V. Lakshman, and D. Stiliadis, "On guaranteed smooth scheduling for input-queued switches," *IEEE/ACM Transactions on Networking*, vol. 13, no. 6, pp. 1364–1375, 2005.
- [20] M. S. Kodialam, T. V. Lakshman, and D. Stiliadis, "Scheduling of Guaranteed-bandwidth low-jitter traffic in input-buffered switches," *US patent application no. #20030227901*, 2003.
- [21] S. R. Mohanty and L. N. Bhuyan, "Guaranteed smooth switch scheduling with low complexity," in *Proceedings of the IEEE Global Telecommunications Conference (GLOBECOM '05)*, pp. 626–630, 2005.
- [22] N. McKeown and B. Prabhakar, "Scheduling multicast cells in an input-queued switch," in *Proceedings of the 15th Annual Joint Conference of the IEEE Computer and Communications Societies (INFOCOM '96)*, vol. 1, pp. 271–278, March 1996.
- [23] M. Marsan, A. Bianco, P. Giaccone, E. Leonardi, and F. Neri, "Multicast traffic in input-queued switches: optimal scheduling and maximum throughput," *IEEE/ACM Transactions on Networking*, vol. 11, no. 3, pp. 465–477, 2003.
- [24] J. F. Hayes, R. Breault, and M. K. Mehmet-Ali, "Performance analysis of a multicast switch," *IEEE Transactions on Communications*, vol. 39, no. 4, pp. 581–587, 1991.
- [25] J. Y. Hui and T. Renner, "Queueing analysis for multicast packet switching," *IEEE Transactions on Communications*, vol. 42, no. 2, pp. 723–731, 1994.
- [26] B. Prabhakar, N. McKeown, and R. Ahuja, "Multicast scheduling for input-queued switches," *IEEE Journal on Selected Areas in Communications*, vol. 15, no. 5, pp. 855–866, 1997.
- [27] M. Song, W. Zhu, A. Francini, and M. Alam, "Performance analysis of large multicast switches with multicast virtual output queues," *Computer Communications*, vol. 28, no. 2, pp. 189–198, 2005.
- [28] S. R. Gulliver and G. Ghinea, "The perceptual and attentive impact of delay and jitter in multimedia delivery," *IEEE Transactions on Broadcasting*, vol. 53, no. 2, pp. 449–458, 2007.

- [29] S. Chand and H. Om, "Modeling of buffer storage in video transmission," *IEEE Transactions on Broadcasting*, vol. 53, no. 4, pp. 774–779, 2007.
- [30] Y. Bai and M. R. Ito, "Application-aware buffer management: new metrics and techniques," *IEEE Transactions on Broadcasting*, vol. 51, no. 1, pp. 114–121, 2005.
- [31] Y. Ganjali and N. McKeown, "Update on buffer sizing in internet routers," *ACM SIGCOMM Computer Communication Review*, vol. 36, no. 5, pp. 67–70, 2006.
- [32] G. Vu-Brugier, R. S. Stanojevic, D. J. Leith, and R. N. Shorten, "A Critique of recently proposed buffer sizing strategies," *ACM/SIGCOMM Computer Communication Review*, vol. 37, no. 1, pp. 43–47, 2007.
- [33] M. Enachescu, Y. Ganjali, A. Goel, N. McKeown, and T. Roughgarden, "Routers with very small buffers," in *Proceedings of the 25th IEEE International Conference on Computer Communications (INFOCOM '06)*, Barcelona, Spain, April 2006.
- [34] A. Dhamdhere and C. Dovrolis, "Open issues in router buffer sizing," vol. 36, no. 1, pp. 87–92.
- [35] T. H. Szymanski and D. Gilbert, "Provisioning mission-critical telerobotic control systems in internet backbone networks with essentially-perfect QoS," *IEEE Journal on Selected Areas in Communications*, vol. 28, no. 5, pp. 630–643, 2010.

Research Article

A Framework for an IP-Based DVB Transmission Network

Nimbe L. Ewald-Arostegui,¹ Gorry Fairhurst,¹ and Ana Yun-Garcia²

¹ School of Engineering, University of Aberdeen, Aberdeen AB24 3UE, UK

² Thales Alenia Space, C/Einstein 7, Tres Cantos-Madrid 28760, Spain

Correspondence should be addressed to Nimbe L. Ewald-Arostegui, nimbe@erg.abdn.ac.uk

Received 14 December 2009; Accepted 29 March 2010

Academic Editor: Georgios Gardikis

Copyright © 2010 Nimbe L. Ewald-Arostegui et al. This is an open access article distributed under the Creative Commons Attribution License, which permits unrestricted use, distribution, and reproduction in any medium, provided the original work is properly cited.

One of the most important challenges for next generation all-IP networks is the convergence and interaction of wireless and wired networks in a smooth and efficient manner. This challenge will need to be faced if broadcast transmission networks are to converge with IP infrastructure. The 2nd generation of DVB standards supports the Generic Stream, allowing the direct transmission of IP-based content using the Generic Stream Encapsulation (GSE), in addition to the native Transport Stream (TS). However, the current signalling framework is based on MPEG-2 Tables that rely upon the TS. This paper examines the feasibility of providing a GSE signalling framework, eliminating the need for the TS. The requirements and potential benefits of this new approach are described. It reviews prospective methods that may be suitable for network discovery and selection and analyses different options for the transport and syntax of this signalling metadata. It is anticipated that the design of a GSE-only signalling system will enable DVB networks to function as a part of the Internet.

1. Introduction

The first generation of DVB standards [1–3] uses a time-division transmission multiplexing method derived directly from the Moving Pictures Expert Group-2 Transport Stream (MPEG-2 TS) standards [4]. The MPEG-2 specifications define the Program Specific Information (PSI), a Table-based signalling system that is multiplexed with the content and allows a receiver to identify MPEG-2 Programs and to demultiplex their Program Elements from the TS. These Tables are segmented in Sections and directly encapsulated into MPEG-2 TS packets, as shown in Figure 1. The Digital Video Broadcasting (DVB) project specified additional types of Table, DVB-Service Information (SI) [5] while the Advanced Television System Committee (ATSC) also defined a set of Tables for the US market [6].

Current signalling metadata relies on this TS packet format [4]. The 2nd generation of DVB systems, DVB-S2/C2/T2 [7–9], preserved this signalling framework utilising MPEG-2 encoded Tables. Some transmission systems use IP-based Service Discovery and Selection (SD&S) procedures to obtain content metadata, for example, acquisition of an Electronic Service Guide (ESG), the network signalling necessary for the initial bootstrapping is sent using MPEG

-2 encoded Tables, for example, in DVB-Handheld (DVB-H) and DVB-Satellite to Handheld (DVB-SH) systems [10, 11].

SD&S is a generic term that has been used to describe various discovery and selection procedures for, mainly, IP-based content metadata. The term Network Discovery and Selection (ND&S) is defined in this paper to describe the discovery and selection of network signalling metadata such as the acquisition of PSI/SI.

Figure 2 illustrates the process of ND&S and SD&S for an example transmission system. ND&S procedures are separated into two logical parts: network discovery starts by acquiring the network bootstrap information from a well-known link stream, followed by selection of the required network service.

First, when a multiplex has been identified at a receiver, the receiver will need to perform a bootstrap of the signalling system, network bootstrapping. The same transmission multiplex may carry bootstrap information for more than one network, if the multiplex supports multiple logical networks. Bootstrap information could also relate to other network services transmitted over other multiplexes, possibly using different transmission technologies. Once the bootstrap has been performed, the receiver has the basic information required to discover the signalling stream—that

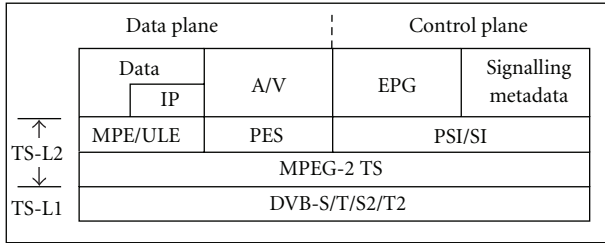


FIGURE 1: Current DVB MPEG-2 TS architecture.

is, the logical flow of signalling information relating to a network service from which it wishes to receive content. The receiver then needs to set a filter that extracts the appropriate signalling from the multiplex selected based on the required network service. The receiver can, then, be used to perform address/service resolution, identifying the required elementary streams or an IP stream that can be used to locate content.

In an all-IP system, the content may be directly accessed, or may be accessed via a content guide such as an ESG. The content guide may be discovered from content bootstrap information provided in a well-known IP stream. More than one network may reference the same content stream as in the case of duplicate multicast content. Similarly, more than one content guide may be active within a network service and the content bootstrap can then be used to select the appropriate content guide. DVB-H and DVB-SH systems follow this two-stage procedure once the PSI/SI information has been extracted.

Current broadcast transmission networks using the TS format can provide platforms for high-speed unidirectional IP transmission, not just for TV-based services. A convergent IP-oriented architecture will ease integration of transmission systems and enable development of multi-network service delivery platforms. The benefits of a DVB IP-based signalling architecture are discussed in Section 3.

The remainder of the paper is divided as follows: a brief description of the current DVB signalling is given in Section 2, GSE suitability, the envisaged IP/GSE signalling framework, and its potential benefits are discussed in Section 3. The requirements of the GSE-only signalling architecture will be identified in Section 4. Then, the different areas that comprise the GSE-only signalling system are analysed, and methods that may address them are discussed in Section 5. Finally, conclusions and future work are stated in Section 6.

2. Current Signalling Framework

In current DVB systems, key-signalling information is sent, in the Programme Association Table (PAT) of PSI, using its well-known 13-bit Packet Identifier (PID) value in the TS packet header. This allows a receiver to readily extract this PID from a received TS multiplex. Figure 3 shows a schematic diagram of this PID acquisition procedure.

In many cases, equipment has hardware support to filter PID values, initially, set to well-known values defined by

the MPEG standard, that is, the fixed PIDs of the PAT, the Conditional Access Table (CAT), and the Transport Stream Descriptor Table (TSDT). Once the PAT has been received and the respective PID of the Network Information Table (NIT) has been extracted (step 1 in Figure 3), the receiver filters this PID, accesses the NIT and re-tunes, if necessary (step 2). Next, the terminal can access the appropriate PAT from where the PIDs of the MPEG-2 Programs' Program Map Table (PMT) can be found (step 3). The receiver can, then, setup filters to receive other PIDs to acquire a full set of relevant signalling information. The receiver can acquire Audio/Video (A/V) Program Elements through their PIDs, which are also advertised in the PMT (step 4). The PID of the Forward Link Signalling (FLS) [12] is also advertised in the PMT.

As shown in Figure 1, alongside these signalling Tables directly encapsulated into TS packets, A/V and data services are adapted to the TS using adaptation protocols such as Packetised Elementary Stream (PES) and Multiprotocol Encapsulation (MPE). If required, data can be placed directly in TS packets using the Unidirectional Lightweight Encapsulation (ULE) [13] protocol.

3. An All-IP Second Generation Transmission Network

The 2nd generation of DVB standards [7–9] foresees the possibility of converged IP-based transmission that supports both broadcast applications and broadband access service by adopting a common IP-based infrastructure. This converged network would bridge the gap between broadcast transmission and traditional networks.

To support a converged approach, the 2nd generation of DVB transmission standards introduced the Generic Stream (GS) in addition to the TS. The GS may be used to carry packets of different sizes, eliminating the TS packet format. The GS is, primarily, expected to be used for network services, where IP packets and other network-layer protocols can be efficiently encapsulated using the Generic Stream Encapsulation, GSE, protocol [14, 15].

GSE provides a network-oriented adaptation layer. Each network layer Protocol Data Unit (PDU) is prefixed by a GSE header, which is shown in Figure 4. GSE supports flexible fragmentation, adapting the encapsulated data to a range of possible physical-layer frame sizes. GSE offers a higher encapsulation efficiency (2%–5% better than the TS counterpart when padding is used for data packets [14]). In addition, GSE is extensible, which allows implementing additional features through its extension headers [16], for example, security, header compression, and timestamps. The base header, present in every encapsulated packet, is 4 Bytes. The additional fields, present only in some packets, are shown shadowed in Figure 4.

While GSE defines the adaptation needed to support data transmission, there is no current specification for a signalling system that could replace the MPEG-2 TS signalling by a system using IP over GSE.

A transition to an IP-based content and signalling will enable common use of IP delivery techniques at the receiver,

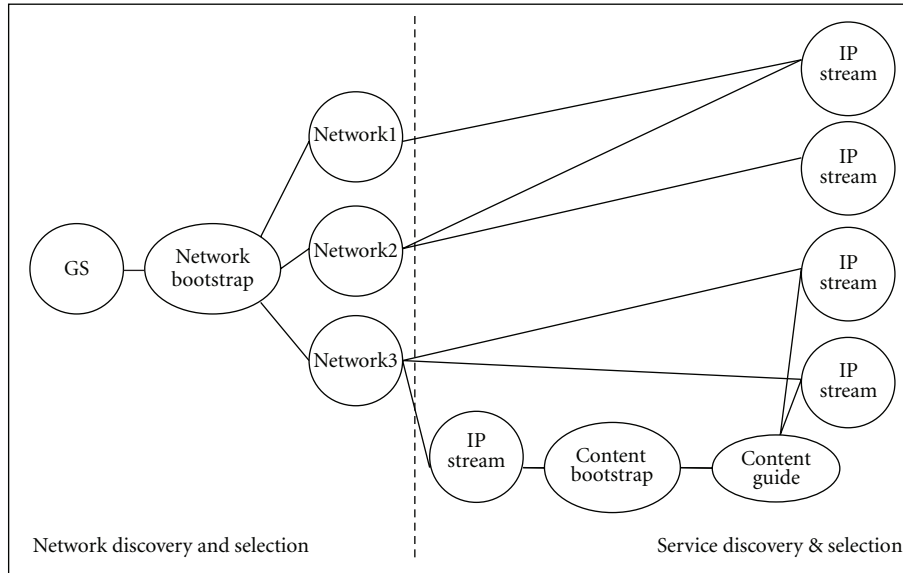


FIGURE 2: ND&S and SD&S procedures.

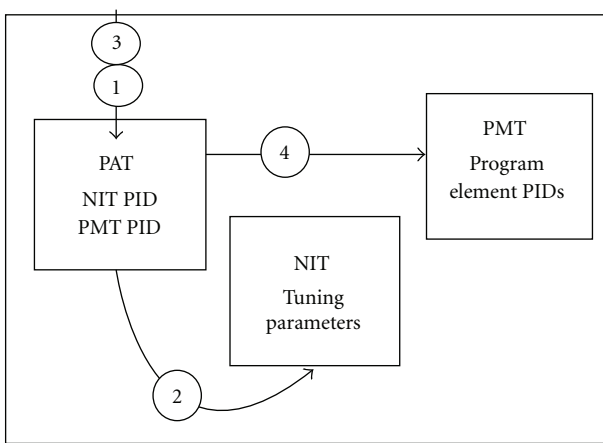


FIGURE 3: Initial acquisition of PIDs.

presenting new opportunities for integrating broadcast content with standard IP applications, and the introduction of value-added services. An IP-based transmission network design also enables the use of data networks (e.g., using wired/wireless Ethernet or mobile platforms) for onward delivery to the TV receiver. An IP-based approach allows reuse of existing techniques and protocol machinery (for configuration, management, accounting, encryption, authentication, etc.). This can support evolution of the services and be used to manage the network and monitor performance.

IP-based transmission products are already available for TV contribution networks and digital satellite news gathering. For example, IP satellite news gathering can significantly benefit from the improved efficiency of DVB-S2 while also utilising standards-based IP-based media codecs.

Broadcast transmission can supplement existing wireless infrastructure where sufficient capacity is not available,

provide a resilient alternate path, or be used to roll out new services. Broadcast networks are especially suited to services that can exploit cost-efficient wide-area delivery using IP multicast.

This paper proposes a framework based on the reference model shown in Figure 5, where we replace TS-L2 (in Figure 1) by the adaptation layer, GS-L2. The signalling metadata is placed at the application layer level, GS-L5, while IP at GS-L3 allows convergence with the Internet. ND&S procedures refer to an IP signalling system associating IP addresses and services with a stream and a specific transmission multiplex. The MPEG-2 TS format is also included to support legacy services.

One simple solution is to encapsulate TS packets in GSE through its TS-Concat extension header [16]. This format allows one or more TS packets to be sent within one GSE packet by combining the group of TS packets with a 4B GSE base header (Figure 4). For a single TS Packet this additional overhead is less than 2%.

Encapsulating the current TS-packed Tables into GSE packets could be an attractive transition method while both TS and GS multiplexes are in use. However, it is likely to constrain the evolution towards an all-IP network and it does not provide an efficient way to transmit PSI/SI Tables. The total overhead would consist of GSE and TS packet headers, and the TS packet padding. For example, if a 30B Table were sent in one TS Packet, the overhead comprised by the TS headers (5B), padding (153B), and the GSE base header (4B) would be 162B, if a Label field (Figure 4) is not used. The impact of overheads on the system efficiency should be considered (preliminary overhead analysis of different encapsulation methods is provided in Section 5.5.2).

However, this is only a partial solution. If signalling were transported using GSE packets instead of TS packets, there would not be a direct equivalent to the PID filters used for TS, that is, GSE does not contain a PID field. Thus, the receiver

S	E	LT	GSE length	Protocol type	Frag ID	Total length	Label	Extension headers
1b	1b	2b	12b	2B	1B	2B	$\frac{3}{6}B$	$\geq 2B$

FIGURE 4: GSE header.

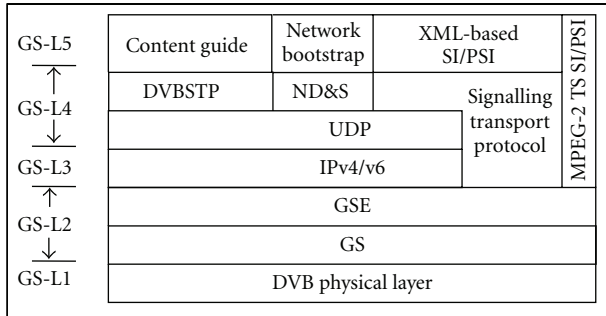


FIGURE 5: Envisaged DVB IP/GSE signalling framework.

will need to identify which physical-layer frames or GSE packets carry the required network signalling information. Potential procedures to recognise GSE packets conveying signalling are proposed and discussed in this paper.

4. GSE-Only Framework Requirements

This section derives a set of requirements for transition to a GSE-only signalling framework.

4.1. IP Interoperability. The signalling system needs to support the IP protocol stack, as the envisaged system depicted in Figure 5. It must be able to coexist with and provide metadata for IP-based protocols such as the Real-time Transport Protocol (RTP) [17] or the File Delivery over Unidirectional Transport (FLUTE) [18]. As DVB networks become an integral part of the Internet, the use of IP network signalling will allow all-IP delivery of services such as IPTV. Importantly, other supporting functions (including network management and related content) may utilise well-known IP-based tools, which may potentially reduce the cost of development and operation.

4.2. Coexistence with MPEG-2 TS Services. During transition, there is a need to allow the exchange of TS signalling information over a GS transmission network. Various options exist that may enable this transport, including the transmission of MPEG-2 Sections over UDP/IP using GSE encapsulation, or a direct mapping between MPEG-2 SI/PSI and GSE, for example, using the GSE TS-Concat extension [16]. In considering the need for coexistence, the cost of translation and the additional cost (if any) of transmission must be analysed.

4.3. Similar or Higher Efficiency as Current TS Signalling. The overhead arising from the protocols used in the envisaged IP-based signalling framework of Figure 5 must be mitigated.

Although the signalling traffic for typical MPEG-2 TS SI/PSI use-cases typically contributes a small fraction of the total available bandwidth, the performance of the system needs to be evaluated and compared to the efficiency achieved by current MPEG-2 TS SI/PSI systems. Methods must be examined to reduce the additional transmission overhead, such as header compression (e.g., techniques based on Robust Header Compression (ROHC) [19, 20]) or the use of link mechanisms, such as the GSE PDU-Concat extension [16]. This extension allows several IP packets to be delivered to the same destination (GS-L2 address) using a single GSE packet, up to the maximum GSE payload length of 64000B. For example, if ten IP packets were sent in a single GSE packet, this would save 35% of the GS-L2 overhead.

4.4. Signalling Security. When desired, signalling may be secured in an all-IP solution. The security requirements can be different for discovery functions (where all receivers may initially need access during bootstrap), and for individual signalling streams (which may be authorised to specific groups of users). Security of the signalling stream may be provided using a GSE security extension [16]. Alternatively, or in combination, the signalling information may be directly protected by authentication and encryption of the metadata.

4.5. Enabling Service Discovery and Service Description Metadata. The new signalling system should enable a receiver to perform a “network scan” to discover the network and content, equivalent to the current PAT functionality. That is, it would allow a receiver to determine which networks and what content is available by decoding the GS without a priori information. The network discovery methods should identify the multiplex and resolve to a Network Point of Attachment/Medium Access Control (NPA/MAC) address at the GSE level. Supporting a “network scan” will place requirements on the repetition rates of the network signalling stream.

4.6. Providing Easy Identification of Signalling in GSE Streams. A receiver must quickly and efficiently identify the GSE packets carrying network signalling information within the GS. This is needed to provide fast service acquisition and may help in changing to a different service (e.g., to provide fast acquisition of signalling information when zapping between channels). The chosen mechanisms also need to ensure this procedure is not processing intensive at the receiver.

4.7. Quality of Service (QoS) and Timing Reconstruction. The delivery requirements for network signalling need to be considered. It is assumed that packet loss due to link corruption may be disregarded, since in most cases the physical-layer

TABLE 1: Relationships among the proposal requirements and applicability to network/content discovery and selection.

No.	Requirement	Network discovery	Network selection	Service discovery & selection
4.1	IP interoperability		X	X
4.2	Coexistence with MPEG-2 TS services	X	X	X
4.3	Similar, or higher, bandwidth efficiency as current TS signalling	X	X	
4.4	Signalling security		X	
4.5	Enable service discovery and service description metadata		X	X
4.6	Provides easy identification of signalling in GSE streams	X	X	
4.7	QoS and timing reconstruction			X
4.8	Extensible syntax		X	X
4.9	Separation of network and content signalling	X	X	X

waveform will provide a quasi-error-free service using a combination of physical-layer parameters and Forward Error Correction (FEC) coding (e.g., a certain ModCod in DVB-S2). The repetition of signalling also improves robustness and allows fast PSI/SI bootstrap acquisition. The description syntax should allow easily inclusion of QoS descriptors for the network service. A/V timing needs to be synchronised, requiring mechanisms equivalent to the Program Clock Reference/Network Clock Reference (PCR/NCR), for example, using RTP timestamps. The GSE timestamp extension header [16] does not provide the required resolution for synchronisation, since it was designed to support functions with less stringent timing accuracy, such as monitoring and management operations.

4.8. Extensible Syntax. The network signalling metadata syntax should provide a “user-friendly” description to facilitate modification, extension and/or enhancement of the signalling to support new formats and methods from a network/content provider. It should also enable easy addition of new signalling schemes that may be needed to support new applications and new services (requiring new descriptors or Tables).

4.9. Separation of Network and Content Signalling. Network and content signalling should be organised and sent independently from each other, so that a receiver can acquire network signalling faster than that of its content counterpart. This can also permit a receiver to acquire appropriate signalling without the need to parse the entire GS. That is, the identification of GSE packets carrying network signalling should not involve the filtering of all frames at levels GS-L1 or GS-L2. In addition, the method to achieve this separation should be applicable to any DVB standard, allowing sending network signalling with the same technique over any DVB physical frame, making it bearer-agnostic.

4.10. Requirements for ND&S and/or SD&S. Together these requirements may be used to derive a new signalling framework. Requirements 4.2, 4.3, 4.6 and 4.9 involve network discovery procedures, while requirement 4.1 includes network selection and SD&S techniques. For a better

understanding, Table 1 identifies requirements applicable to network discovery, network selection and service discovery and selection.

5. GSE-Only Signalling Framework

This section analyses methods to provide GSE signalling identification and ND&S procedures. The signalling transport protocol and signalling syntax are also studied to identify which may be suitable for a GSE-only signalling framework and may meet the requirements stated in the previous section. Some methods are already used for IP-based signalling of content metadata, however, all current DVB systems use network signalling based on MPEG-2 encoded Tables.

5.1. GSE Signalling Identification. Since there are no PIDs in a GSE-only signalling architecture, the first step towards this framework is to provide ND&S by filtering of signalling information at the GS-L1 or GS-L2 layers, to identify which GSE packets convey signalling information. Procedures for identification of packets carrying signalling metadata are needed to minimise receiver processing. Appropriate techniques can also assist in meeting the requirements for separation of network and content signalling.

A range of techniques is available, as presented in Table 2 and described in detail below. This includes use of fields in the frame header and the allocation of protocol codepoints. Some of these procedures may be jointly used, for example, methods 5.1.4 and 5.1.5. The methods are organised by increasing amounts of information that would need to be parsed by a receiver joining the network. The final solution should preserve flexibility to use different higher layer protocols, introduce security when required, and provide flexibility to optimise the overhead (e.g., use of header compression).

5.1.1. Assignment of a Dedicated Transmission Stream. It is possible to reserve entire transmission frames at the physical-layer for use by a separate signalling stream. This stream could be identified by a physical-layer identifier, for example, a well-known Input Stream Identifier (ISI) value in DVB-

TABLE 2: Candidate methods for identifying GSE packets carrying network signalling.

No.	Candidate method	Filtering level
5.1.1	Assignment of a dedicated transmission stream (e.g., DVB ISI)	GS-L1
5.1.2	Assignment of fields in the transmission frame header	GS-L1
5.1.3	Alignment of signalling transmission to a time-slicing frame	GS-L1
5.1.4	Placement of a GSE packet at a known position within a frame	GS-L2
5.1.5	Assignment of a dedicated GSE Type field value	GS-L2
5.1.6	Assignment of a dedicated Label/NPA or IP address	GS-L2/GS-L3
5.1.7	Assignment of a well-known UDP port	GS-L4

S2/T2. A receiver performing a bootstrap may skip all frames with a different ISI, reducing the receiver information processing load. However, this method could reduce overall system efficiency when the frame size is large. Receivers need to be setup to process more than one ISI, this approach is being tested in some present systems.

5.1.2. Assignment of Fields in the Physical Frame Header. Rather than dedicate a specific channel to signalling, the control information in the physical-layer header may be extended to carry network signalling information. This approach resembles the use of the Fast Information Channel (FIC) in ATSC Mobile Digital Television systems [21]. The FIC channel provides a network bootstrap method that is specified outside the normal frame payload, and hence is independent of the data channel carrying Reed-Solomon (RS) FEC frames, shown in Figure 6. Its data unit is the FIC-Chunk, which provides the binding information between the Mobile/Handheld (M/H) services and the M/H ensembles. A M/H ensemble is a set of consecutive RS frames with the same FEC coding. Information such as the ensemble ID, Tables carried by the ensemble, the number of services carried and the service ID is carried by the FIC-Chunk. This approach is an optimisation of the physical-layer, which may be processed independently of the content. This enables fast tuning and simpler processing at the receiver.

The DVB physical-layer specifications do not provide an equivalent physical-layer signalling channel, although the DVB-S2/T2 frame headers currently have unallocated bits. A single bit in these frames could signal if a GSE packet conveying signalling is present in the frame, otherwise a receiver seeking signalling may ignore the frame. Additional bits could be used, if appropriate and available, to help define the type of signalling, for example, bootstrap or network services signalling. This would require an update to the present DVB transmission standards.

5.1.3. Alignment of Signalling Transmission to a Time-Slicing Frame. Time-slicing is a well-known method used for power-saving in DVB-H and DVB-SH systems. This technique could be applied to signalling to allow a receiver to know which frames may contain signalling information and allow a receiver to skip processing of frames that are known to not contain signalling PDUs. Timeslicing information (i.e., prior knowledge of times when signalling data is to

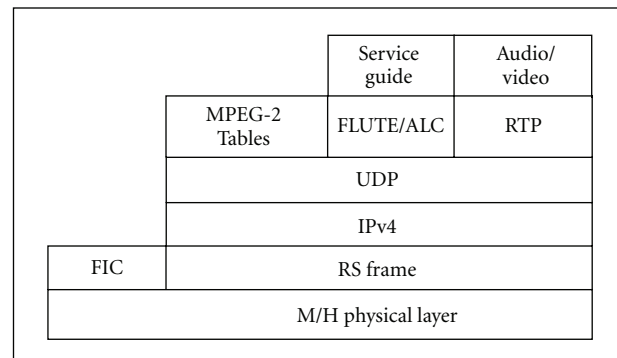


FIGURE 6: Simplified protocol stack for ATSC Mobile DTV.

be sent) would allow a synchronised receiver to disregard a proportion of physical-layer frames. Such an approach may be desirable for mobile applications, and could be extended to all signalling messages in any new system.

5.1.4. Placement of a GSE Packet at a Known Position in a Frame. Transmission frames are typically long compared to the PDUs (signalling or data) that they carry. Processing of a frame that may contain one or more signalling PDUs could be simplified if the signalling information was inserted at a known position within a frame. The flexibility in the fragmentation algorithm of GSE would allow signalling packets to always be placed at the start of the frame payload. Although a receiver would need to inspect all frames, it may then skip any remaining payload after finding the first GSE packet in the S2/T2 frame that does not contain signalling information. This method does not require any change to the present physical-layer or GSE standards.

5.1.5. Allocation of a Dedicated GSE Type Field Value. A receiver needs a simple way to demultiplex GSE signalling packets from data packets. One option is to use the GSE Type field. This may be performed in two ways:

(a) *Assign a Well-Known Mandatory Type Field [13, 14].* A mandatory Type field directly precedes the GSE PDU (Figure 4). One mandatory Type is required for each type of signalling information, for example, if IPv4 or IPv6 is used, the version of IP will need to be signalled, or if header

compression is used. GSE-level encryption would prevent visibility of a mandatory Type field prior to decryption.

(b) *Assign a Well-Known Optional Type Field.* An optional Type field [13] is a separate tag inserted after the GSE base header. In this case, the tag would be used to indicate that the encapsulated PDU carries signalling data. The original Type field would also be present (indicating the version of IP, use of encryption, etc.), so operation would resemble the Router Alert option in the IP header. This is the simplest method, but will add 2B of overhead to the GSE header.

The Internet Assigned Numbers Authority (IANA) assigns Mandatory and Optional Type values. The Institute of Electrical and Electronics Engineers (IEEE) also register EtherTypes that can be used as mandatory Type values.

5.1.6. *Allocation of a Dedicated Label/NPA or IP Address.* The demultiplexing of signalling from data packets may be aided by using well-known values of other protocol fields. Two methods have been identified at the GSE and IP levels that may assist in this process:

(a) *Assignment of a Well-Known Multicast NPA Address.* It is attractive to use well-known L2 addresses for bootstrapping, for example, an IANA DVB multicast IP address that maps to a MAC/NPA address [22], but this has limited use for discovery. After bootstrap, a receiver may move to one of several network services, and it may be natural to assign different address to each service. If this method were used to identify signalling, this would prevent suppression of the NPA address/label field in GSE. This suggests there can be no single address binding that applies to all scenarios.

(b) *Assignment of a Well-Known IP Address.* This method would allow suppression of the NPA/MAC address but requires an IP packet format. Filtering using the IP address is not recommended, since it would preclude the use of link header compression or encryption of the GSE packet payload (since all packets would have to be decompressed and/or decrypted before filtering). The system would also increase complexity when other GSE extensions are present (e.g., timestamps). Well-known IP multicast destination addresses are used in many IP bootstrap procedures, and when present, these would normally result in a mapping to well-known MAC addresses [22].

5.1.7. *Assignment of a Well-Known UDP Port.* This method requires an IP packet format, as in Section 5.1.6, and deep packet inspection (i.e., parsing of the IP and transport headers). It is not compatible with header compression and with other extension headers. This would not be recommended since the receiver would have to process all packets at GS and IP level to finally filter those conveying signalling at the transport layer level.

5.2. *Network Discovery and Selection.* This section proposes a two-stage approach which could be used for ND&S, in common with other IP-based systems to provide content

discovery and selection. Once the GSE packets carrying signalling metadata are filtered at the GS-L1 or GS-L2 layers, a bootstrap will be performed to select the appropriate network signalling information. The network signalling information can then be used to select the required network service. The procedures below are based on IP satisfying the requirement for IP interoperability when enabling service discovery.

A bootstrap method eliminates the need to manually enter a bootstrap entry point, for example, the need to configure IP/NPA addresses out of band or using device configuration. Instead the device only has to be configured with the logical name for the network to which it is attached.

The format of network bootstrap information could be a Table structure that maps logical names to appropriate discovery entry points, that is, IP addresses where the discovery information can be found. Such a Table may be equivalent to the IP/MAC Notification Table (INT) used by DVB-H systems to signal the availability and location of IP streams. Another format could use a multicast Domain Name Server Service (mDNS SRV) record [23] to specify the network service discovery entry points, similar to the procedure recommended for DVB-IPTV [24]. SRV records convey information about the service, such as the transport protocol used, its priority and the IP address of the server providing the service.

For broadcast networks, the bootstrap could be sent using a well-known IP multicast address. This approach is similar to that for DVB service discovery (*dvb-servdsc*) information, that is, *dvb-servdsc* information is provided, by default, on the IANA-registered well-known *dvb-servdsc* multicast address of 224.0.23.14 for IPv4 and FF0X:0:0:0:0:0:12D for IPv6, and on the IANA-registered well-known *dvb-servdsc* port 3937 via TCP and UDP [25].

For bidirectional networks, ND&S entry point addresses may be found through the following three options: the Simple Service Discovery Protocol (SSDP) over UDP, SRV records via DNS over UDP or SRV records via DHCP option 15 over UDP. SSDP, defined by Microsoft and Hewlett-Packard, is specified as the Universal Plug and Play (UPnP) discovery protocol [26]. It uses part of the header field format of HTTP1.1. Since it is only partially based on HTTP1.1, it is carried by UDP instead of TCP. A drawback is that SSDP is a proprietary standard. SRV records via DNS or via DHCP option 15 are SD&S procedures (for content metadata) recommended by DVB-IPTV [24] and also used by the Open IPTV Forum (OIPF) framework [27] as well as for the signalling of DVB interactive applications [28]. The methods described for bidirectional networks, are not suited to unidirectional broadcast since they rely on the existence of a return channel. A unidirectional solution applicable to both scenarios, broadcast and interactive, is desirable.

5.3. *Signalling Transport Protocol.* Selection of a transport protocol for the signalling metadata needs to take into consideration the requirements (similar efficiency than that of TS signalling) and characteristics (high repetition rates) of the metadata.

For unicast scenarios with bidirectional connectivity, HTTP over TCP is a commonly chosen method for unicast content metadata transport since it is used by DVB-IPTV, DVB-H, DVB-SH and OIPF architectures.

A/V data is transmitted over RTP via UDP/IP in DVB-IPTV and DVB-H systems. RTP with an extension header [17] carrying timestamps could be used for synchronisation, as the equivalent to PCR/NCR. Signalling metadata could potentially be sent in a new defined payload format for RTP. RTP can open up a set of media-related services, such as source identification, packet loss measure, jitter control, and reliability techniques. The extension header of RTP may also provide means of performing discovery, although it would also add an overhead of 12 or 16B per Section.

The DVB SD&S Transport Protocol (DVBSTP) [24] over UDP has been specified for reliable multicast SD&S content metadata delivery in architectures compliant with DVB-IPTV [24] and OIPF [27]. It transports eXtensible Markup Language (XML) [29] records and defines the type of payload carried through its Payload ID field (e.g., Content on Demand, Broadcast discovery information). A Compression field indicates the type of compression encoding, if any. A DVBSTP header adds an overhead of at least 12B per Section. The redundancy for network signalling may not be needed when Tables are transmitted at high repetition rates. Since the DVBSTP header provides signalling identification through its Payload ID field, it would allow the receiver to determine whether a signalling stream contains replicated metadata that has been already received or metadata that the receiver does not wish to receive.

The FLUTE [18] protocol has been used for content guide transport over UDP in DVB-H, DVB-SH and ATSC Mobile DTV [21]. FLUTE builds on the Asynchronous Layered Coding (ALC) specification to provide scalable, unidirectional, multicast distribution of objects. ALC/FLUTE was also recommended for the design of a new transport protocol for the delivery of Internet Media Guides (IMGs) by the IETF Multiparty Multimedia Session Control (MMUSIC) group, when seeking to provide a format for content metadata over the Internet [30].

Since the requirements for transport of network signalling metadata differ from those for content metadata, the transport protocols listed above may not be suitable. For example, ALC/FLUTE offers support for FEC-based reliability although this may increase processing overhead and is not required when data is repeated frequently. It also increases transmission cost. DVBSTP adds an overhead of at least 12B and provide reliability (also not required). DVBSTP does provide an indication of the type of XML-record carried through its 1B Payload ID field and the type of compression used through a 3-bit Compression field. These features, together with the ability to determine if content (Table) is encrypted before processing the payload are attractive for a transport protocol. Further work is needed to determine whether the overhead is justified and whether this choice of transport can be efficiently combined with the metadata encoding to optimise overall performance, or whether a new alternate lightweight protocol is preferable.

5.4. Signalling Syntax. This section reviews a set of candidate methods for representing the metadata. It discusses existing SI/PSI, the Session Description Protocol (SDP) [31] and SDP with negotiation capabilities (SDPng) [32], and finally use of XML [29].

5.4.1. Direct Encapsulation of PSI/SI. PSI, SI and FLS syntax has been standardised in MPEG-2 [4, 5, 12] and were outlined in Section 2. Even though this Table-based format is expected to continue for backwards compatibility, it is desirable the transition to a more flexible syntax to allow extensibility and evolution of signalling. Any new method should support MPEG-2 PSI/SI to satisfy the requirement for coexistence.

5.4.2. SDP and SDPng. The IETF MMUSIC group standardised SDP [31] for multimedia session description over IP. SDP defines a format for session description to announce sessions and their parameters to prospective receivers; it does not specify a transport protocol. In bidirectional networks, SDP is commonly transported using the Session Initiation Protocol (SIP), specified in RFC 3261, or the Real Time Streaming Protocol (RTSP), specified in RFC 2326. In a multicast IP network, RFC 2974 specifies how SDP may be transported over the Session Announcement Protocol (SAP) using a set of well-known multicast addresses.

The ESG in DVB-H, the OIPF framework and multicast sessions in ATSC use SDP records. Even though SDP is an IP-level method, it does not provide link-specific information to identify a network service or physical-layer tuning parameters for the transmission multiplex (e.g., frequency, transmission mode, and ISI). Hence, it would need to be extended to be suitable for network signalling.

The IETF started to develop an updated SDP protocol, SDPng. This was intended to address the lack of negotiation capabilities in SDP by providing alternatives for session parameter configurations. That is, an IP host would be able to negotiate session parameters according to its system capabilities. Proposals for SDPng used the XML syntax, Document Type Definitions (DTDs) and Schemas, to allow extensibility. It was one candidate method to convey session parameters for an IMG [30]. However, work on SDPng has not continued since 2003, with no specifications defined, and therefore is not applicable for a GSE-only signalling framework.

5.4.3. XML. The eXtensible Markup Language, XML [29], has been standardised by the Worldwide Web Consortium, W3C. It is now a common syntax for network control information and content metadata. The DVB-IPTV, DVB-H, DVB-SH, OIPF, UPnP and ATSC systems define XML Schemas, while DVB interactive application metadata is defined as XML DTDs [28]. XML Schemas have been developed to make it easier to create and enhance the encoded information and are preferred over DTDs, for example, XML Schemas defined for DVB-IPTV can also be used in the OIPF framework. In contrast to DTDs, XML Schemas provide support for namespaces, can constrain

TABLE 3: Potential methods for a GSE-only signalling framework.

GSE-only signalling framework area	Prospective methods	Section
GSE Signalling Identification	Assignment of a dedicated transmission stream	5.1.1
	Assignment of fields in physical frame header	5.1.2
	Alignment of signalling transmission to a time-slicing frame	5.1.3
	Placement of a GSE packet at a known position in a frame	5.1.4
	Allocation of a dedicated GSE Type field value	5.1.5
	Allocation of a dedicated Label/NPA or IP address	5.1.6
	Assignment of a well-known UDP port	5.1.7
ND&S	Bootstrap Table using well-known multicast addresses	5.2
	SRV record via DNS using well-known multicast addresses	
	SRV record via DHCP option*	
	SSDP	
Transport Protocol	HTTP/TCP*	5.3
	DVBSTP/UDP	
	FLUTE/ALC/UDP	
	RTP/UDP	
	New lightweight transport/UDP	
Syntax	MPEG-2	5.4.1
	XML	5.4.3
	Compressed XML	5.4.3

*This procedure requires bidirectional connectivity.

data based on common data types, and present object oriented features such as type derivation. In addition, XML allows encryption, which could be used to provide signalling security.

A Uniform Resource Name (URN) namespace has been defined for naming resources defined within DVB standards by [25]. DVB specifies XML Schemas and DTDs, namespaces and other types of resource [33]. XML network signalling, in parallel with classical SI/PSI Tables may be used in interactive DVB applications for hybrid broadcast/broadband environments [28].

In a GSE-only signalling framework, metadata syntax could be converted to XML. A simple, but effective method could retain the segmentation of the PSI/SI Tables, since the Section mechanism is an important element of the PSI/SI structure, to allow easy access to parts of the Table. In the XML encoding, the PID may be substituted by the IP destination address and UDP port number, similar to the approach proposed in [34]. This substitution also allows reuse of Tables after the PIDs are mapped to these IP addresses/ports within the PSI/SI.

Since encoding the signalling metadata in XML significantly increases the information rate (due to its inherent verbosity), this will decrease bandwidth efficiency. However, XML data may be readily compressed, for example, two compression algorithms are recommended for DVB-H content metadata: GZIP [35] and BiM [36]. The GZIP format uses

the deflate algorithm (RFC 1952). This combines an index (dictionary) approach together with Huffman compression. GZIP is effective on streams with recurring patterns of data, especially when used with large data sets. The ISO MPEG-7 group defined the Binary MPEG format for XML, BiM, as an alternative to text representation. BiM was proposed for TV-Anytime content metadata and afterwards recommended for DVB-IPTV and DVB-H ESG.

BiM compression can reduce the transmission cost up to 60% of the MPEG-2 encoded PSI/SI Tables [34]. However, this adds complexity to the system, since XML Schemas are needed at the receiver to decompress the encoded Sections.

GZIP presents lower complexity than BiM, since no Schemas are needed before decompression at the receiver. This makes it attractive for handheld terminals to minimise the processing requirements. However, its compression gain is typically much lower than for BiM; PSI/SI Sections converted into XML and compressed with GZIP can increase the overall volume of data by 30% compared to the original binary encoded size [34]. Section 5.5.2 provides some example comparison of overhead. As in many compression technologies patents need to be considered. Patents have been already registered for a tool for BiM compression.

Other XML compression algorithms are in the process of being developed. One is the Efficient XML Interchange (EXI) by W3C [37]. EXI not only achieves higher compression gains than GZIP, but also presents a lower decoding

TABLE 4: Potential methods to fulfill the GSE-only signalling requirements.

GSE-only signalling requirement	Prospective methods
IP interoperability	Encapsulation of an IP packet as GSE payload. Any of the ND&S methods described in Section 5.2. Any unidirectional transport protocol.
Separation of network and content signalling	Any methods for GSE signalling identification described in Section 5.1 enabling filtering at GS-L1/L2. Transport protocol with a payload type field.
Extensible syntax	XML syntax.
Similar, or higher, bandwidth efficiency to that of current TS signalling	GSE extension headers to indicate compression. IP/UDP header compression. XML compression. New optimised lightweight transport protocol.
Coexistence with MPEG-2 TS services	Encapsulation of TS packet over GSE. Encapsulation of TS packet over UDP/IP/GSE.
Signalling security	GSE security extensions. Transport protocol with a field to indicate payload encryption. XML encryption.
QoS and timing reconstruction	Timestamps in RTP extension header. QoS descriptors in XML. Signalling repetition rates.
Enable service discovery and service description metadata	Any of the ND&S methods described in Section 5.2. XML syntax.
Provides easy identification of signalling in GSE streams	Any methods for GSE signalling identification described in Section 5.1 enabling filtering at GS-L1/L2.

complexity since Schemas are not necessarily needed at the receiver when performing a network scan.

5.5. GSE/IP Signalling System Prospective Methods. Table 3 presents a summary of the prospective methods described in this section. For completeness, it includes methods currently specified for bidirectional links, which are indicated by an asterisk. While techniques may be combined, it is recommended that at least one technique is used at GS-L1 to identify signalling, in order to reduce processing requirements at the receiver.

Table 4 relates these methods to the requirements identified in Section 4. Overall, the processing cost of decoding at the receiver is important when analysing the use of any of the potential methods listed in Tables 3 and 4, in particular those for identification of signalling in GSE streams. We suggest using the extensible syntax XML for network service description metadata. XML encryption and compression would enable signalling security and are expected to result in similar bandwidth efficiency to that of TS, respectively.

5.5.1. Encapsulation. Several network signalling encapsulation options exist for a GSE-only system.

- (1) The GSE TS-Concat extension [16] may be used to enable the coexistence with TS services but increases overhead above the current MPEG-2 TS by adding

GSE headers. A method is, however, needed to relate the metadata to the IP address.

- (2) To reduce overhead, the SI Table may be directly encapsulated as a PDU in the GSE payload. Since a Section should not be larger than 1024B [5], a GSE payload may be able to carry more than one Section. A method is however need to relate the metadata to the IP address.
- (3) Network metadata may be encapsulated as UDP datagram's over IP, similar to the current encapsulation performed in DVB-H systems where ESG XML records are sent over FLUTE via UDP/IP. Recent techniques for IP/UDP header compression, such as ROHC [19, 20], may in future further reduce IP overhead.
- (4) The PDU-Concat extension [16] can improve system efficiency when transmitting small IP packets by combining several in a single GSE payload, subject to the maximum payload length of 64000B.

5.5.2. Overhead Analysis. This section compares the transmission cost for sending network signalling. The overhead respect to the Table size resulting from the candidate techniques is shown in Table 5. Three Tables sizes were analysed: one comprising a small section of 30B, a second

TABLE 5: Overhead for different combinations of syntax and encapsulation procedure.

DFL (B)	Overhead (%)								
	1 × 30B Section			1 × 1024B Section			4 × 1024B Section		
	384	3216	7274	384	3216	7274	384	3216	7274
MPEG-2 Section in TS		526			10.1			10.1	
MPEG-2 Section in TS with dedicated ISI	1146	10586	24113	119	213	609	22	63	84
MPEG-2 Section in TS/GSE with TS-Concat		540		11.8	10.5		11.3	10.5	10.1
XML GZIP Section over DVBSTP/UDP/IP/GSE		160		5.8	4.3		5.6	4.5	4.3
XML BiM Section over DVBSTP/UDP/IP/GSE		146		5.2	4.3		4.9	4.2	4.2
XML BiM Section over FLUTE/ ALC/UDP/IP/GSE		146		5.2	4.3		4.9	4.2	4.2
XML GZIP Section over DVBSTP/UDP/IP/GSE with HC		76		3.3	1.8		3.0	2.1	1.9
XML BiM Section over DVBSTP/UDP/IP/GSE with HC		63		2.8	1.8		2.7	2.0	1.8

with a 1024B Section and a final Table comprising four 1024B Sections. The overhead was calculated for a set of DVB-S2/T2 frame sizes (data field lengths, DFL). In DVB-S2, network signalling is expected to be sent using the most robust ModCod supported in the network to reduce the probability of loss and to allow signalling acquisition in all channel conditions. Hence, this will typically result in frames with a small DFL.

The methods were compared to native transmission of MPEG-2 encoded Sections using the TS, as in current DVB signalling. Padding is added to each TS packet, as necessary. Table 5 shows that this padding results in an overhead for a 30B Table that is more than fifty times higher than the corresponding value for the 1024 and 4096B Tables. Section overhead, only considering the TS headers, is 16.6% for the 30B Table and 2.4% for the 1024 and 4096B Tables, but since a whole TS packet needs to be sent, the overhead becomes 526 and 10.1%, respectively, as shown in Table 5.

Section 5.1.1 proposed a method in which the TS packets were sent on a separate stream using a dedicated stream (ISI value). The fixed size of the frame results in a significant overhead given that there is insufficient signalling data to fill the frame. It is assumed that the overall transmission rate allocated to signalling does not result in any empty frames (although the burst-nature of signalling data may be hard to match to a fixed transmission rate).

Encapsulation of TS packets in GSE, as a transition method, is also analysed. GSE TS-Concat is considered for Tables with multiple Sections. As expected, the overhead is higher than that for native TS transmission. This is also higher than the IP-based encapsulation methods.

The next set of methods considers IP-based protocols and XML-translated Sections. Each Section is encapsulated by DVBSTP/UDP/IP or FLUTE/ALC/UDP/IP, where the additional headers contribute 40B. The GSE PDU-Concat extension is used for the Table with four Sections. It is assumed that signalling identification is carried at GS-L1 (e.g., optional GSE Type fields are not considered).

The overhead for the medium and large Tables represents a trade-off with the benefits provided by an IP-based signalling system. Small Tables negatively impact the efficiency of an IP-based signalling framework regardless of

the encapsulation technique and frame size, however the overhead is always lower than that of native MPEG-2 TS. This overhead is further reduced when header compression (HC) is considered. Estimates of the compressed size using either GZIP or BiM algorithms are provided. This assumes that BiM compression of the XML-encoded Section results in a reduction of 40% with respect to the size of the MPEG-2 encoded Section [34]. In contrast, applying GZIP to a XML-encoded Section results in an increase of 30% with respect to the size of the MPEG-2 encoded Section [34]. Despite this, using XML with GZIP results in less than half the overhead of the native TS method for the 1024 and 4096B Tables.

DVBSTP and FLUTE resulted in the same overhead. Although, DVBSTP was designed to ease processing of SD&S XML records at the receiver, it results in significant overhead for small PDUs. The 12B of overhead introduced above the UDP layer is seen as an upper bound. This overhead could be reduced further by design of a lightweight transport protocol to replace the DVBSTP header, or by combined optimisation of content-encoding and transport protocol.

The UDP/IP headers are assumed to be compressed to 3B when using a form of header compression, although no method has currently been specified for use with DVB. The use of header compression for signalling should be analysed further given the positive effect on reducing the overhead.

6. Conclusions and Future Work

The convergence of DVB networks with IP infrastructure bridges the gap between broadcast transmission and traditional networks. Current MPEG-2 systems are already used to transmit IP packets, mostly using MPE or ULE, it is expected that future DVB transmission networks adopt an all-IP approach by gradually replacing the TS by the GS. Transition to IP-based content and signalling will enable common use of IP delivery techniques at the receiver, presenting new opportunities for integrating broadcast content with standard IP applications, and the introduction of value-added services.

One major challenge to transitioning broadcast services to the GS is the lack of a GSE-only signalling framework. IP-based procedures for content metadata exist in DVB systems,

but current signalling is implemented through MPEG-2 TS Tables. This paper explains the need for a GSE-only signalling framework and formulates a set of requirements, reviews a range of candidate methods, including current IP-based methods and has derived their potential benefits.

The proposed methods can identify GSE packets carrying signalling and replace the role of PIDs. In addition, current IP-based methods may be used as prospective techniques for ND&S procedures and for the signalling syntax. Options were also presented for a signalling transport protocol. Methods for encoding metadata that allow extensibility and easy modification were examined. XML Schemas are strong candidates because of their extensibility characteristics and current common use for content metadata. Indicative performance data is used to compare the anticipated overhead for the various approaches.

This work is intended to guide and inform future standardisation work. As future work, we intend to select the optimal candidate methods and propose a GSE-only signalling architecture. The high-level requirements in terms of signalling for different scenarios, for example, fixed broadcast, interactive, will be also defined, as well as the specification for mapping current SI/PSI/FLS MPEG-2 encoded Tables to their XML-based counterparts.

Acknowledgment

The authors acknowledge the support of the European Space Agency (ESA) Contract 22471/09/NL/AD.

References

- [1] ETSI EN 300 421, "Digital Video Broadcasting (DVB); Framing Structure, Channel Coding and Modulation for 11/12—GHz Satellite Services," October 1997.
- [2] ETSI EN 300 744, "Digital Video Broadcasting (DVB); framing structure, channel coding and modulation for digital terrestrial television," February 1997.
- [3] ETSI EN 300 429, "Digital Video Broadcasting (DVB); framing structure, channel coding and modulation for cable systems," April 1998.
- [4] ISO/IEC 13818-1, "Information technology—generic coding of moving pictures and associated audio information: systems," 1995.
- [5] ETSI EN 300 468, "Digital Video Broadcasting (DVB); Specification for Service Information (SI) in DVB systems, February 1998.
- [6] ATSC Standard A/65, "Program and System Information Protocol for Terrestrial Broadcast and Cable (PSIP)," December 1997.
- [7] ETSI EN 302 307, "Digital Video Broadcasting (DVB); second generation framing structure, channel coding and modulation systems for Broadcasting, Interactive Services, News Gathering and other broadband satellite applications (DVB-S2)," August 2009.
- [8] ETSI EN 302 755, "Digital Video Broadcasting (DVB); frame structure channel coding and modulation for a second generation digital terrestrial television broadcasting system (DVB-T2)," September 2009.
- [9] ETSI EN 302 769, "Digital Video Broadcasting (DVB); frame structure channel coding and modulation for a second generation digital transmission system for cable systems (DVB-C2)," January 2010.
- [10] ETSI TS 102 471, "Digital Video Broadcasting (DVB); IP Datacast over DVB-H: Electronic Service Guide (ESG)," April 2009.
- [11] ETSI TS 102 592-2, "Digital Video Broadcasting (DVB); IP Datacast: Electronic Service Guide (ESG) Implementation Guidelines; Part 2: IP Datacast over DVB-SH," January 2010.
- [12] ETSI EN 301 790, "Digital Video Broadcasting (DVB); interaction channel for satellite distribution systems," May 2009.
- [13] G. Fairhurst and B. Collini-Nocker, "Unidirectional Lightweight Encapsulation (ULE) for Transmission of IP Datagrams over an MPEG-2 Transport Stream (TS)," IETF RFC 4326, December 2005.
- [14] J. Cantillo, B. Collini-Nocker, U. De Bie, et al., "GSE: a flexible, yet efficient, encapsulation for IP over DVB-S2 continuous generic streams," *International Journal of Satellite Communications and Networking*, vol. 26, no. 3, pp. 231–250, 2008.
- [15] ETSI TS 102 606 (v1.1.1), "Digital Video Broadcasting (DVB); Generic Stream Encapsulation (GSE) Protocol," October 2007.
- [16] G. Fairhurst and B. Collini-Nocker, "Extension Formats for Unidirectional Lightweight Encapsulation (ULE) and the Generic Stream Encapsulation (GSE)," IETF RFC 5163, April 2008.
- [17] H. Schulzrinne, S. Casner, R. Frederick, and V. Jacobson, "RTP: A Transport Protocol for Real-Time Applications," RFC 3550, July 2003.
- [18] T. Paila, M. Luby, R. Lehtonen, V. Roca, and R. Walsh, "FLUTE—File Delivery over Unidirectional Transport," RFC 3926, October 2004.
- [19] L-E. Jonsson, K. Sandlund, G. Pelletier, and P. Kremer, "RObust Header Compression (ROHC): Corrections and Clarifications to RFC 3095," RFC 4815, February 2007.
- [20] C. Bormann, "RObust Header Compression (ROHC) over 802 networks," IETF work in progress, July 2009.
- [21] ATSC, "A/153: ATSC-Mobile DTV Standard, Part 1-ATSC Mobile Digital Television System," October 2009.
- [22] G. Fairhurst and M.-J. Montpetit, "Address Resolution Mechanisms for IP Datagrams over MPEG-2 Networks," IETF RFC 4947, July 2007.
- [23] A. Gulbrandsen, P. Vixie, and L. Esibov, "A DNS RR for specifying the location of services (DNS SRV)," RFC 2782, February 2000.
- [24] ETSI TS 102 034, "Digital Video Broadcasting (DVB); Transport of MPEG-2 TS Based DVB Services over IP Based Networks," 2007.
- [25] A. Adolf and P. MacAvock, "A Uniform Resource Name (URN) Namespace for the Digital Video Broadcasting Project (DVB)," IETF RFC 5328, September 2008.
- [26] UPnP Forum, UPnP Device Architecture 1.1, October 2008.
- [27] OIPF Functional Architecture [v1.2], March 2008.
- [28] ETSI TS 102 809, "Digital Video Broadcasting (DVB); signalling and carriage of interactive applications and services in Hybrid broadcast/broadband environments," January 2010.
- [29] World Wide Web Consortium (W3C), "Extensible Markup Language (XML) 1.0 (Fifth Edition)," <http://www.w3.org/TR/REC-xml/REC-xml-20081126.xml>.
- [30] Y. Nomura, R. Walsh, J.-P. Luoma, H. Asaeda, and H. Schulzrinne, "A Framework for the Usage of Internet Media Guides (IMGs)," RFC 4435, April 2006.
- [31] M. Handley, V. Jacobson, and C. Perkins, "SDP: Session Description Protocol," RFC 4566, July 2006.

- [32] SDPng, <http://www.dmn.tzi.org/ietf/mmusic/sdp-ng/index.html>.
- [33] Repository of DVB Metadata Related Documents, <http://www.dvb.org/metadata>.
- [34] H. Foellscher, "Transmission of media content on IP-based digital broadcast platforms," dissertation, Institute for Communications Technology, Technical University of Braunschweig, July 2007.
- [35] P. Deutsh, "GZIP file format specification version 4.3," IETF RFC 1952, May 1996.
- [36] ISO/IEC 23001-1 (MPEG-B), "Information Technology—MPEG Systems Technologies—Binary MPEG format for XML".
- [37] World Wide Web Consortium (W3C), "Efficient XML Interchange (EXI) Format 1.0," <http://www.w3.org/TR/exi/>.

Research Article

On the QoS of IPTV and Its Effects on Home Networks

Dongyu Qiu

Department of Electrical and Computer Engineering, Concordia University, Montreal, QC, Canada H3G 1M8

Correspondence should be addressed to Dongyu Qiu, dongyu@ece.concordia.ca

Received 2 October 2009; Accepted 20 May 2010

Academic Editor: Georgios Gardikis

Copyright © 2010 Dongyu Qiu. This is an open access article distributed under the Creative Commons Attribution License, which permits unrestricted use, distribution, and reproduction in any medium, provided the original work is properly cited.

In Internet Protocol Television (IPTV) systems, Quality-of-Service (QoS) is a critical factor for user satisfaction. In this paper, we first propose a queueing model for IPTV systems and discuss how to ensure the QoS of IPTV. We then use the model to analyze the effects of IPTV traffic on other applications in home networks. We find that TCP congestion control may not work well under this circumstance and propose a new approach to improve the performance of TCP. We also verify our results through *ns2* simulations.

1. Introduction

In recent years, we have seen a tendency of various services converging to the ubiquitous Internet-Protocol- (IP-) based networks. Besides traditional Internet applications such as web browsing, email, file transferring, and so forth, new applications have been developed to replace old communication networks. For example, Voice over IP (VoIP) can be used as an alternative to traditional telephone network. There are also efforts to provide digital television service over IP networks. IPTV is one of the solutions. In the future, we expect a single network, the IP network, to provide services that have been carried by different networks today.

Transmitting video over IP networks is not a new idea. People have been interested in it since the very early stage of the Internet. However, there are major technical difficulties that prevent transmitting video over IP with satisfactory quality. The IP network is designed to be a best-effort network, which means that it does not provide any QoS guaranty. QoS, on the other hand, is essential to the quality of video. To get good quality, the network has to satisfy certain requirements on bandwidth, end-to-end delay, and jitter, and so forth. Another important issue is scalability. Many systems perform well when the number of users is small. However, when there are thousands of users accessing the service at the same time, which is typical in a broadcasting TV system, it will stress the servers.

With the advances of video encoding and the quick development of communication networks, transmitting video

with at least VHS-quality has become possible in recent years. Digital video encoded with MPEG-1 around 1.5 Mbps can provide VHS-quality and MPEG-2 can offer High-Definition TV-quality video around 20 Mbps or higher. The next generation codecs, such as H.264 and VC1, can offer DVD- and HD- quality stream under 10 Mbps. At the same time, Internet access technology has been improved significantly. For example, ADSL can provide upto 8 Mbps download rate and the newest VDSL has up-to 52 Mbps download rate. Cable Modem can provide similar or even higher download bandwidth. With the recent deployment of Fiber to the premises (FTTP), we can expect higher Internet access bandwidth to be provided to home users. Hence, transmitting VHS-quality or even HDTV- quality video over the Internet becomes technically feasible.

In the current Internet, there are basically two solutions to deliver digital television service. The first one is Peer-to-Peer (P2P) video streaming. In [1], a P2P media streaming system called DONet has been proposed. Basically, all P2P video streaming systems work similarly. In such a system, the video is divided into many pieces. When a user obtains a piece, it will serve other peers by uploading this piece. Hence, each user serves as a client and a server at the same time. P2P systems have been proved to have very good scalability [2]. Hence, there is no need for expensive servers and high upload bandwidth to provide P2P video streaming. Due to the low setup cost and excellent scalability, P2P video streaming applications, such as PPLive, PPStream, and socpcast and so forth, have become very popular recently. However, since

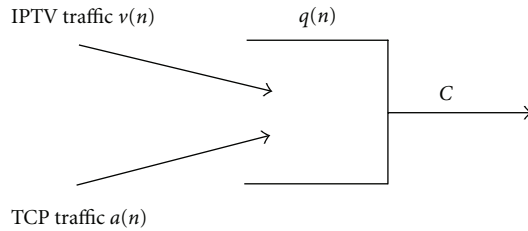


FIGURE 1: The queueing model.

P2P video streaming traffic may cross the whole public Internet, it is very hard to guarantee the QoS in such a system. There is normally little or no QoS management in P2P video streaming. IPTV, on the other hand, takes a different approach to solve the scalability and QoS issues. IPTV has been developed and deployed mainly by large telecommunication providers as a competitive replacement product for digital cable and satellite services. Hence, IPTV systems normally use a closed network infrastructure. In such a system, the IPTV service provider is also the Internet service provider. Since the video streaming traffic is transmitted in a closed network, the QoS management is much easier than that in a P2P system. IPTV uses the multicast technology to solve the scalability issue. When more than one user are watching the same TV channel, the service provider will multicast the video to the users. Hence, only one copy of the video is transmitted and the system has good scalability.

In this paper, we will focus on IPTV systems. The paper is organized as follows. In Section 2, we will propose a queueing model for IPTV systems and discuss how to ensure the QoS of IPTV in such systems. We will also discuss how this will affect other Internet applications in home networks. In Section 3, we will analyze the model and discuss how the system performance can be optimized. Simulation results using *ns2* simulator will be shown in Section 4. Finally, we conclude this paper in Section 5.

2. QoS of IPTV

IPTV is a new technology to delivery digital television service over IP networks. In contrast to the popular P2P video streaming, IPTV systems are normally closed and proprietary. It has been deployed by major telecommunication providers to compete with traditional digital cable service. In an IPTV system, users subscribe to the IPTV service through their Internet service provider. The service provider sometimes also offers VoIP, service as an alternative to traditional telephone service. The combination of IPTV, VoIP, and Internet access is referred to as “Triple-Play” service. IPTV has some significant advantages over digital cable service. For example, it can make the TV viewing experience more interactive and personalized. IPTV also offers Video on Demand (VoD), in which a user can choose movies from a database and play it immediately. However, IPTV also has its own limitations. Since video quality is very

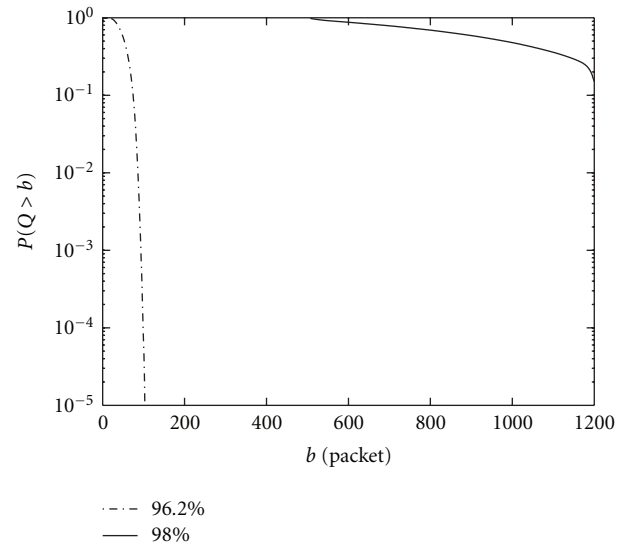


FIGURE 2: The effect of target utilization.

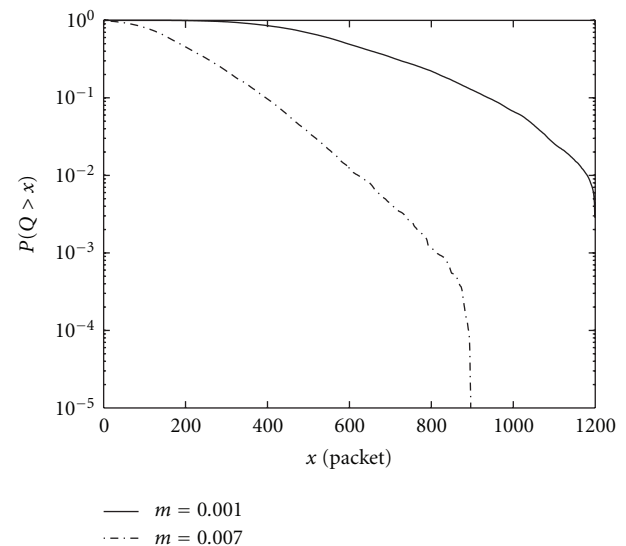


FIGURE 3: Queue distribution.

sensitive to packet loss and delay, how to ensure the QoS in a best-effort network like an IP network is a challenge topic.

Internet is a distributed system and there is no centralized control of it. This makes the QoS management extremely hard. The video traffic may travel through some segments of the Internet, where the service provider may have no control at all. In such a scenario, it is very difficult to ensure QoS. Fortunately, in IPTV systems, QoS management is significantly simplified. IPTV is a closed network, in which the service provider not only controls the IPTV system, but also controls the Internet access of the users. In the current Internet, the bottleneck for most connections is normally at the user’s Internet access link, which is sometimes called the last mile. In the core of Internet, optical fibers have been deployed to provide tens of Gbps bandwidths and hence

are unlikely to be the bottleneck. In an IPTV system, since the service provider also has control of the Internet access links, it can over provision the network to ensure the QoS of IPTV. For example, if the IPTV's bit rate is 3 Mbps, the service provider may over provision the capacity to ensure that the download bandwidth of the user is at least 5 Mbps, thus guaranteeing a minimum QoS level.

However, the simple over provision itself is not enough for IPTV QoS. Besides the IPTV application, there may be many other Internet applications running in the home network. For example, people may watch TV and browse the web at the same time. The traffic from other applications then will compete with the IPTV for the access bandwidth. If the total download rate exceeds the download bandwidth, packets will be dropped and hence it will degrade the video quality of IPTV. The solution to this problem is to give IPTV packets priority over other packets. This mechanism can be implemented in the network layer (e.g., Diffserv [3]) or in the MAC layer (e.g., IEEE802.1p). In either cases, when packets are competing for the output link, packets from IPTV flows will be processed with higher priority. Hence, although there may be other Internet applications, their traffic will not affect the QoS of IPTV. Combined with an appropriate over provision scheme, this mechanism can be used to ensure the QoS of IPTV and it is widely used in current IPTV systems.

Since IPTV traffic is given high priority, other Internet applications have to compete for the residual bandwidth and their performance may be affected. Different with IPTV, where UDP is used to carry the traffic, most other Internet applications such as HTTP, FTP, and SSH, and so forth, use TCP as the transport layer protocol. TCP itself has a built-in congestion control mechanism [4], which means that when TCP detects that the network is congested it will decrease its data rate. This kind of traffic is called elastic traffic and it can adapt to the available bandwidth in the network. Since many advanced video codecs produce variable-bit-rate (VBR) outputs, the available bandwidth for TCP will be time varying. Studying the impact of IPTV traffic on the performance of TCP is an interesting topic. Next, we use a simple queueing model to study it.

As we discussed before, the bottleneck normally happens at the Internet access link. Here, we use a queue to model this link that serves both IPTV and TCP traffics (Figure 1). In this model, C is the link capacity. For example, if the user's download bandwidth is 8 Mbps, then $C = 8$ Mbps. There are both IPTV traffic and TCP traffic on this link. Without loss of generality, we use a discrete time model. $v(n)$ is the data rate of IPTV traffic at time n and $a(n)$ is the data rate of TCP traffic. $q(n)$ is the queue length at time n . In the IPTV system, to ensure the QoS of IPTV, the data rate of IPTV traffic should not exceed the link capacity and hence $v(n) \leq C$. The link capacity available for TCP traffic is then $C - v(n)$, which is normally time varying as we discussed before. The queue length can be expressed as

$$q(n) = [q(n-1) + a(n) + v(n) - C]^+, \quad (1)$$

where $[x]^+ = x$ if $x \geq 0$ and $[x]^+ = 0$ if $x < 0$.

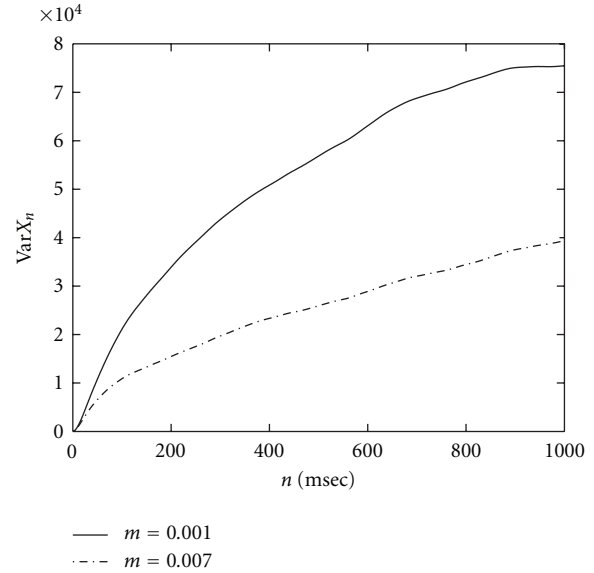


FIGURE 4: $\text{Var}X_n$.

Note that $a(n)$ is the data rate of TCP traffic and hence it can be controlled by TCP. Ideally, we would like to have $a(n) = C - v(n)$ for all time n . If so, the link capacity is fully utilized and the queue length is always 0. However, this is impossible to achieve in real networks due to network delays, estimation errors, and so forth. Next, we discuss how to control $a(n)$ based on information about $v(n)$.

3. Effects of IPTV Traffic on TCP Performance

The objectives of TCP congestion control are high link utilization and small packet loss probability. However, these two objectives are generally conflicting. TCP congestion control always tries to fully utilize the link capacity. In Section 4, we will see that this may cause unnecessary workload to the queue and hence does not work well in practice. Motivated by this, we define $\rho < 1$ to be the target link utilization. Then $u(n) = \rho C - v(n)$ is the residual link capacity that we want TCP traffic to utilize. For the simplicity of analysis, we will first use an explicit-rate control model, in which we assume that we can explicitly set the TCP data rate $a(n)$. Later, we will discuss how the result can be applied to real TCP networks. We also assume that the $a(n)$ is controlled by a linear system, in which

$$a(n) = L[u(n)]. \quad (2)$$

A linear feedback control has been found to give good results when we have video traffic as uncontrollable traffic [5], which is exactly what we have in an IPTV system. Let $a(z)$ and $u(z)$ be the Z-transforms of $a(n)$ and $u(n)$, respectively. We have

$$a(z) = H(z)u(z), \quad (3)$$

where $H(z)$ represents a linear time-invariant system. For example, if $a(n) = u(n-5)$, where 5 is the round trip delay of

the TCP connection, then $H(z) = z^{-5}$. This system has been studied in [6] and we list the main results here.

In [6], it has been found that when $H(1) = 1$ the system has some desirable properties. First, the actual utilization of the system will be equal to the target utilization ρ . Secondly, the queue length distribution decays very fast. The tail probability of the queue length can be approximated by

$$\mathbb{P}\{Q > x\} \approx e^{-x^2/2D}, \quad (4)$$

where $D = \sup_n \text{Var} X_n$ is a constant and

$$X_n = \sum_{j=-n+1}^0 (a(j) - u(j) - (1 - \rho)C) \quad (5)$$

is the net input to the queue over a given time period with length n . So, under a given target link utilization, the system performance can be optimized if we can minimize D . Next, we discuss how this can be done in a TCP network.

TCP has been widely used in the current Internet and its congestion control scheme has been shown to work well in many cases. However, it also has some drawbacks. For example, it has no provision for the detection of incipient congestion. When a queue overflows, packets are simply dropped. In past years, many Active Queue Management (AQM) schemes have been proposed [7–9] to improve the performance of TCP. In these schemes, the routers try to detect incipient congestion and mark packets accordingly to control the data rate of TCP flows. In this paper, we choose Random Exponential Marking (REM) [8] as an example to show how our result can be applied to real TCP networks.

In REM, the router maintains a price information, which is calculated based on the TCP data rate and the available bandwidth. The price at time n is given by

$$p(n) = p(n-1) + m(a(n) - u(n)), \quad (6)$$

where $m > 0$ is the step size and is the parameter that we need to choose. Note that here we slightly modified the REM algorithm by replacing the link capacity with the time-varying residual link capacity $u(n)$ to reflect the presence of IPTV traffic. This price information is then sent back to the TCP source through packet marking and TCP will adjust its data rate accordingly. Basically, when the price increases, the data rate will be decreased, and vice versa. This control is normally not linear. However, as an approximation, we can linearize the data rate control around its average value (see [10] for details on how the linearization can be done). Let τ be the round trip delay of the TCP flows. For the simplicity of analysis, we assume that all TCP flows have the same delay. Then the TCP data rate at time n can be expressed as

$$a(n) = -kp(n - \tau), \quad (7)$$

where $k > 0$ is a constant related to the utility function used by TCP. Note that the only approximation we made here is the linearization. The TCP data rate is not reacting

instantaneously to the price due to the delay τ . In Z-domain, we then have

$$\begin{aligned} p(z) &= \frac{m}{1 - z^{-1}}(a(z) - u(z)), \\ a(z) &= -kz^{-\tau}p(z). \end{aligned} \quad (8)$$

Solving these equations, we have

$$a(z) = \frac{kmz^{-\tau}}{1 - z^{-1} + kmz^{-\tau}}u(z), \quad (9)$$

and hence

$$H(z) = \frac{kmz^{-\tau}}{1 - z^{-1} + kmz^{-\tau}}. \quad (10)$$

We can easily verify that the system satisfies $H(1) = 1$ and hence has the desirable properties we discussed before. Note that in this system, since k is a constant related to TCP and cannot be changed, we need to choose an appropriate m to optimize the performance. Recall that the system performance is optimized when $D = \sup_n \text{Var} X_n$ is minimized. Hence, the problem becomes one of choosing the optimal m such that D is minimized. It is very hard to find a closed-form relation between D and m . However, in a real network, once we obtain the stochastic property of $u(n)$ (which is equivalent to that of $v(n)$, the data rate of IPTV traffic), it is relatively easy to find the optimal m numerically. Next, we show how this can be done through *ns2* simulations.

4. Simulation Results

We use the *ns2* simulator to simulate the Internet access link of a home network. The link capacity (or the download bandwidth) of the link is $C = 200$ Mbps. Note that the link capacity we use here is higher than that of most home networks due to two reasons. First, different link capacities should give the similar results if we scale all system parameters accordingly [11]. Hence, the absolute value of C is not essential here. Secondly, when C is larger, we can see the performance difference more clearly. The round trip delays of all TCP flows are $\tau = 10$ msec. We use TCP-Reno and the modified REM (see Section 3) as the AQM scheme. All TCP packets have the length of 1000 bytes.

In the first simulation, the link serves 100 TCP flows and there is no IPTV traffic. The REM parameter $m = 0.007$. The target link utilization is set to be 98% and 96.2% respectively. We measure the actual link utilization and find that it is 96.2%, in both cases. Under the same actual link utilization, we compare their queue distributions in Figure 2. We can see that, when the target link utilization is set to 98%, the tail probability is much higher than the other one and hence will have much higher packet loss rate. This tells us that setting a very high target link utilization does not guarantee that the actual link utilization is high and may only cause unnecessary workload.

In the next simulation, we add IPTV traffic into the network. The mean rate of the IPTV traffic is 100 Mbps. The IPTV traffic is generated by using a Gaussian process and is

carried by UDP packets. The target link utilization is set to be 96%. The REM parameter m is set to be 0.001 and 0.007, respectively, where $m = 0.001$ is chosen according to the guidelines in [10] and $m = 0.007$ is chosen by our algorithm to minimize D . Our simulation results are shown in Figures 3 and 4. From Figure 3, we can see that, with different REM parameters, the queue distribution can be quite different. In Figure 4, we show the corresponding $\text{Var } X_n$. We can see that the smaller the $\text{Var } X_n$ (in the case $m = 0.007$), the smaller the queue length. Hence, in a TCP network, minimizing $\text{Var } X_n$ will be an effective way to control the loss rate.

5. Conclusion

In this paper, we first discuss how over provisioning and differentiated services can be used to ensure QoS of IPTV. We then use a queueing model to study the effects of IPTV traffic on home networks. Using this model, we analyze the performance of TCP when there is IPTV traffic in the network. Based on the analysis, we give some guidelines on how the system performance can be optimized. We then use REM as an example to show how the results can be applied to real TCP networks. We also verify our results by *ns2* simulations.

References

- [1] X. Zhang, J. Liu, B. Li, and T.-S. P. Yum, "CoolStreaming/DONet: a data-driven overlay network for peer-to-peer live media streaming," in *Proceedings of the Annual Joint Conference of the IEEE Computer and Communications Societies (INFOCOM '05)*, Miami, Fla, USA, March 2005.
- [2] D. Qiu and R. Srikant, "Modeling and performance analysis of BitTorrent-like peer-to-peer networks," in *Proceedings of the ACM Conference on Applications, Technologies, Architectures, and Protocols for Computer Communication (SIGCOMM '04)*, pp. 367–377, August 2004.
- [3] I. Stoica and H. Zhang, "Providing guaranteed services without per flow management," in *Proceedings of the ACM Conference on Applications, Technologies, Architectures, and Protocols for Computer Communication (SIGCOMM '99)*, pp. 81–94, 1999, <http://citeseer.ist.psu.edu/article/stoica99providing.html>.
- [4] V. Jacobson, "Congestion avoidance and control," in *Proceedings of the ACM Conference on Applications, Technologies, Architectures, and Protocols for Computer Communication (SIGCOMM '88)*, pp. 314–329, 1988.
- [5] Y. Zhao, S. Q. Li, and S. Sigarto, "A linear dynamic model for design of stable explicit-rate ABR control schemes," in *Proceedings of the Annual Joint Conference of the IEEE Computer and Communications Societies (INFOCOM '97)*, pp. 283–292, April 1997.
- [6] D. Qiu and N. B. Shroff, "Queueing properties of feedback flow control systems," *IEEE/ACM Transactions on Networking*, vol. 13, no. 1, pp. 57–68, 2005.
- [7] S. Floyd and V. Jacobson, "Random early detection gateways for congestion avoidance," *IEEE/ACM Transactions on Networking*, vol. 1, no. 4, pp. 397–413, 1993.
- [8] S. Athuraliya and S. H. Low, "Optimization Flow Control II: Implementation," Internal report, Melbourne University, 2000.
- [9] S. Kunniyur and R. Srikant, "Analysis and design of an adaptive virtual queue (AVQ) algorithm for active queue management," in *Proceedings of the ACM Conference on Applications, Technologies, Architectures, and Protocols for Computer Communication (SIGCOMM '01)*, San Diego, Calif, USA, August 2001.
- [10] F. Paganini, J. Doyle, and S. Low, "Scalable laws for stable network congestion control," in *Proceedings of the 40th IEEE Conference on Decision and Control (CDC '01)*, vol. 1, pp. 185–190, December 2001.
- [11] P. Tinnakornsrisuphap and A. M. Makowski, "Limit behavior of ECN/RED gateways under a large number of TCP flows," in *Proceedings of the Annual Joint Conference of the IEEE Computer and Communications Societies (INFOCOM '03)*, pp. 873–883, April 2003.

Research Article

Performance Evaluation of Triple Play Services Delivery with E2E QoS Provisioning

Nikolaos Zotos, Evangelos Pallis, and Anastasios Kourtis

*NCSR Demokritos, Institute of Informatics & Telecommunications, Partiarxou Grigoriou & Neapolews,
Agia Paraskevi, Attiki, 15310 Athens, Italy*

Correspondence should be addressed to Nikolaos Zotos, nzotos@iit.demokritos.gr

Received 20 November 2009; Revised 30 March 2010; Accepted 21 June 2010

Academic Editor: Daniel Negru

Copyright © 2010 Nikolaos Zotos et al. This is an open access article distributed under the Creative Commons Attribution License, which permits unrestricted use, distribution, and reproduction in any medium, provided the original work is properly cited.

The creation and wide use of new high quality demanding services (VoIP, High Quality Video Streaming) and the delivery of them over already saturated core and access network infrastructures have created the necessity for E2E QoS provisioning. Network Providers use at their infrastructures several kinds of mechanisms and techniques for providing QoS. Most known and widely used technologies are MPLS and DiffServ. The IEEE 802.16-2004 standard (WiMAX) refers to a promising wireless broadband technology with enhanced QoS support algorithms. This document presents an experimental network infrastructure providing E2E QoS, using a combination of MPLS and DiffServ technologies in the core network and WiMAX technology as the wireless access medium for high priority services (VoIP, High Quality Video Streaming) transmission. The main scope is to map the traffic prioritization and classification attributes of the core network to the access network in a way which does not affect the E2E QoS provisioning. The performance evaluation will be done by introducing different kinds of traffic scenarios in a saturated and overloaded network environment. The evaluation will prove that this combination made feasible the E2E QoS provisioning while keeping the initial constrains as well as the services delivered over a wireless network.

1. Introduction

The increased use of the Internet and the creation of new high quality (bandwidth, loss, and delay sensitive) services (Internet telephony, High-quality video, and time critical data) have created an extremely large capacity problem to the core and access network infrastructures. In order to transfer such kinds of services, the networks should support high bandwidth, low-delay and low-jitter (Delay variation) transmission. In order to achieve a transmission keeping these constrains, the core networks should support service separation and service prioritization, in order to transfer different kinds of traffic with different behaviour aggregates. Such solutions are provided by the well-known Multiprotocol Label Switching mechanism and Differential Services protocol which are used for traffic engineering and QoS provisioning in the core networks. The promising WiMAX technology includes features that support QoS algorithms which could be used for the expansion of QoS constrains used by a wired QoS-enabled network to a wireless access network.

Despite the QoS perspective investigation regarding the MPLS, DiffServ technologies have been analysed in deep, and the performance of these technologies with the WiMAX technology fusion has been not tested yet. This document presents an experimental E2E network architecture and topology combining MPLS mechanism and DiffServ technology as a solution for enhanced QoS provisioning over core network infrastructures. Considering that the problem of inadequate service prioritisation still exists also inside the access network infrastructures, the paper describes how to use the WiMAX technology in order to provide the QoS guarantees keeping the same traffic behaviour until the end user. The main objective of this work is to test how the combination of MPLS traffic engineering mechanism and DiffServ technology with WiMAX technology helps to solve the network debility to transmit new high-priority services (internet telephony, video, time critical data) with an acceptable level of delay (according to the service characteristics), without distortion and with the predefined and guarantee quality of service until the end user. Another

important objective is to show how to configure such network in order to optimise its performance in sensitive (bandwidth, delay) data transmission. Therewithal, tests will be performed of how the access network environment can affect the network performance. The rest of the paper is organized as follows: in Section 2, a survey of MPLS, DiffServ, and WiMAX QoS approaches is provided as a way of solving the network congestion problem, providing service priority and an efficient way for service allocation. Section 3 presents the proposed experimental network architecture design and configuration. Section 4 describes the proposed evaluation scenarios, including different kind of services, passing through the network, with different quality and priority constrains. Mainly, in this section the experimental results of the applied scenarios are presented. Finally, in Section 5 the results are summarised and suggestions for future improvement and discussion are provided.

2. MPLS, DIFFSERV, and WiMAX QoS Perspective

2.1. QoS Definition. There are many QoS definitions and everyone can give a different definition for QoS. In this paper, the definition below is of the QoS perspective that is used to test and evaluate the performance of the experimental network infrastructure, in “high quality” services transmission. ITU-T (Recommendation E.800 [ITU-TE.800]) and ETSI [ETSI-ETR003] basically define Quality of Service (QoS) as “the collective effect of service performance which determines the degree of satisfaction of a user of the service” [1]. Mainly, QoS is the ability to differentiate between traffic types in order for the network to treat certain traffic flows differently from others and keep to acceptable level the service categorization and the overall network performance [1].

2.2. QoS Need Applications Overview. The applications that require a specific level of assurance from the network are the applications that need QoS, namely, applications which are sensitive in packet loss and delay. There is a big amount of applications that need a level of assurance but it is difficult to define a specific level for each one of them. For that reason, there exist several categories which called “QoS classes” in which the applications have been classified. The way that the application classification has been done related to the applications attributes. More specific, the attributes of applications which need quality assurance are

- (i) real-time, jitter sensitive, highly interactive,
- (ii) real-time, jitter sensitive, interactive,
- (iii) transaction data, highly interactive,
- (iv) transaction data, interactive,
- (v) low loss only (short transactions, bulk data, video streaming),
- (vi) traditional applications of default IP networks.

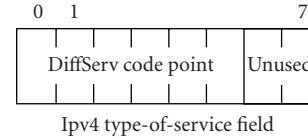


FIGURE 1: TOS field [2].

2.3. DiffServ QoS Approach Overview. Differentiated Services are a computer networking architecture that specifies a simple, scalable, and coarse-grained mechanism for classifying, managing network traffic and providing quality of service (QoS) guarantees on modern IP networks.

The DiffServ architecture is based on a simple model. When traffic entering a network is classified and conditioned at the boundaries of the network, and assigned to different Behaviour Aggregates (BAs), with each BA being identified by a single DiffServ Code-Point (DSCP). Within the core of the network, packets are forwarded according to a Per-Hop Behaviour (PHB) associated with the DSCP [2]. The smallest autonomic unit of DiffServ is called a DiffServ domain, where services are assured by identical principles. A domain consists of two types of nodes: Boundary (or Edge) routers and Core routers. Core nodes only forward packets; they do no signalling. Each router packets traverse is called a “hop” Packets, classified at the edge of the network, and forwarded according to a specific PHB throughout the core of the network. Packets may be forwarded across multiple networks on their way from source to destination. Each one of those networks is called a DiffServ Domain. More specific, a DiffServ Domain is a set of routers implementing the same set of PHBs. The DiffServ PHB class selector offers three forwarding priorities:

- (1) Expedited Forwarding (EF) characterized by a minimum configurable service rate, independent of the other aggregates within the router, and oriented to low-delay and low-loss services [1],
- (2) Assured Forwarding (AF) group, recommended in [RFC 2597] for 4 independent classes (AF1, AF2, AF3, AF4) although a DiffServ domain can provide a different number of AF classes. Within each AF class, traffic differentiated into 3 “drop precedence” categories [1],
- (3) Best Effort (BE), which does not provide any performance guarantee and does not define any QoS level.

2.4. MPLS QoS Approach Overview. Multiprotocol Label Switching (MPLS) as known in computer networking and telecommunications is a data-carrying mechanism which emulates some properties of a circuit-switched network over a packet-switched network. This mechanism lies between traditional definitions of Layer 2 (Data Link layer) and Layer 3 (Network layer) of the OSI Model and thus is often referred to as a “Layer 2.5” protocol. It was designed to provide a unified data-carrying service for both circuit-based clients and packet-switching clients. It can be used to carry many different kinds of traffic [3]. MPLS basic idea is to

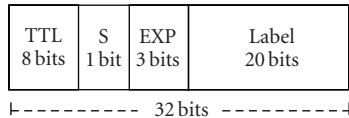


FIGURE 2: MPLS Header [4].

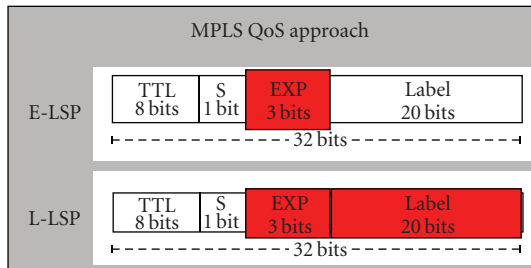


FIGURE 3: MPLS QoS-based Label distribution.

append a small fix length label before each packet in order to forward it inside the MPLS network. This label with some other attributes which also appended in front of the packets consists of the 32-bit length MPLS header. Figure 1 depicts the MPLS header and the use of each field. MPLS header entry contains four fields:

- (i) a 20-bit label value,
- (ii) a 3-bit field for QoS priority,
- (iii) a 1-bit bottom of stack flag. If this is set, it signifies the current label is the last in the stack,
- (iv) an 8-bit TTL (time to live) field.

MPLS has the capability to combine with DiffServ in order to enhance the QoS support inside the MPLS core network [5]. More specific there are two approaches of how LER [4] router can attach a label to packet in order to keep the predefined priorities: (a) the EXP-Inferred approach and (b) the Label-Inferred approach. Figure 2 shows how these two approaches work.

(i) **E-LSP**

Queue inferred EXP field
Drop priority inferred EXP field
8 Classes maximum (like IP TOS)

(ii) **L-LSP**

Queue inferred exclusively from label
(IP+ATM multi vc)
Drop priority inferred from EXP field
Combination will allow up to 64 classes
(DiffServ)

2.5. WiMAX QoS Approach Overview. WiMAX is defined as Worldwide Interoperability for Microwave Access by the WiMAX Forum, formed in April 2001 to promote conformance and interoperability of the standard IEEE 802.16. The

original WiMAX standard, IEEE 802.16, specifies WiMAX in the 10 to 66 GHz range. 802.16a, updated in 2004 to 802.16-2004, added support for the 2 to 11 GHz range, of which most parts are already unlicensed internationally and only very few still require domestic licenses. Most business interest will be in the 802.16-2004 standards, as opposed to licensed frequencies. 802.16-2004 is often called 802.16d, since that was the working party that developed the standard. It is also frequently referred to as “fixed WiMAX” since it has no support for mobility [6, 7]. 802.16e-2005 is an amendment to 802.16-2004 and is often referred to in shortened form as 802.16e [6–8]. It introduced support for mobility, among other things and is therefore also frequently called “mobile WiMAX”. The WiMAX specification improves upon many of the limitations of the Wi-Fi standard by providing increased bandwidth and stronger encryption. It also aims to provide connectivity between network endpoints without direct line of sight in some circumstances.

WiMAX systems support a wide range of network services: IP Access, IP VPN, VOIP, PPPoE, tunneling and of course give the ability to operators to provide differentiated SLAs with committed QoS for each service profile. The 802.16 standard provides powerful tools in order to achieve different QoS constrains [8]. The QoS support on 802.16 networks is defined by providing four different scheduling services for different service classification. The four scheduling services defined in 802.16 are

- (1) Unsolicited Grant Service (UGS),
- (2) real-time Polling Service (rtPS),
- (3) nonreal-time Polling Service (nrtPS),
- (4) Best Effort (BE).

2.6. UGS Scheduling. The UGS is designed to support real-time service flow of fixed-size data packets on a fixed interval. In UGS, there is no bandwidth sharing of multiple connections and each connection (service flow) is allocated with a dedicated channel (time slot) [6]. An example for UGS scheduling is the VOIP service.

2.7. rtPS Scheduling. The rtPS scheduling is designed to support real-time data streams consisting of variable-sized data packets that are issued at periodic intervals [8]. This would be the case for MPEG (Moving Pictures Experts Group) video transmission for example, nrtPS Scheduling.

The nrtPS scheduling is designed to support delay-tolerant data streams consisting of variable-size data packets for which a minimum data rate is required. The standard considers that this would be the case for an FTP transmission for example [8].

2.8. BE Service. The BE service is designed to support data streams for which no minimum service guarantees are required and therefore may be handled on a best available basis. The packets fitted in BE service in network congestion state cannot be transmitted for a long period [8].

The 802.16e also supports a fifth scheduling service called extended real-time Polling Service (ertPS) which is

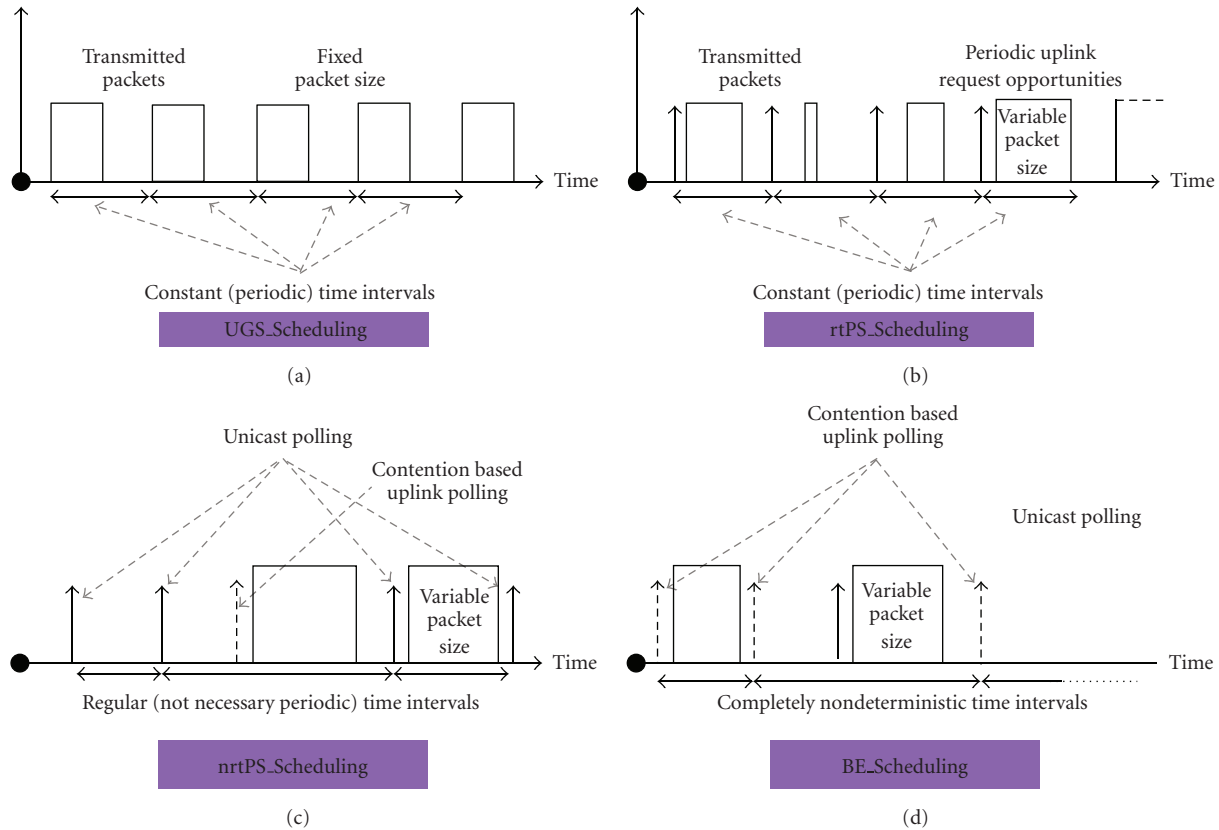


FIGURE 4: WiMAX scheduling algorithms [6].

a scheduling mechanism combining the efficiency of both UGS and rtPS [8].

3. QoS Architecture and Configuration

As shown in Figure 5, the implemented MPLS-DiffServ-WiMAX network infrastructure consists of: (i) a Service Provider Network, (ii) an MPLS-DiffServ capable domain, and (iii) a WiMAX Access Network where End-Users reside.

Service Provider network contains an A/V content server, a VoIP server, and Internet access (HTTP, FTP, mail, etc.). Also for test purposes, a traffic generator has been installed and configured in service provider network.

At the Core network, the traffic coming from the service providers reaches the ingress LER (Label Edge Router). The ingress LER router is responsible for mangling, marking the incoming traffic, and separating it into different traffic trunks with different QoS requirements. Also, ingress LER is attended to attach a short length label to each incoming packet. The decision on what label should be chosen at the ingress LER is based on the marked DSCP field in the packet header and on a predetermined policy and current-state information. For the needs of the experiment, the labels are predefined for each service and allocated to each traffic trunk with a static way. At the core of the network, there are the Label Switch Routers (LSR 1, LSR 2) which check the labels of the incoming packets and change them in order to

keep the same QoS requirements as the initial traffic. After the packets are forwarded to the egress LER, the labels will be removed and the packets will be forwarded according to the original network-layer routing scheme to the access network.

The WiMAX technology is used as the Access medium for the end user/s. The selection of WiMAX technology has been done in order to support hard QoS guarantees in the access network in contrast to the lack of QoS provision in 802.11 wireless network environments. The WiMAX Base station has the responsibility to map the traffic based on DSCP field to WiMAX QoS classes.

3.1. Network QoS Configuration. As mentioned before, the whole network consists of three parts. The first part deals with the high-quality services (VoIP and Video) creation. For the voice service, a Linux OS- (Operating System) based VoIP (Asterisk PBX) server is installed and configured in Service Provider's premises. For Video service creation, an H-264 encoder has also been installed and configured. The encoder has the ability to encode in H-264 video format two video streams simultaneously. For time critical data and background traffic, a traffic generator (using MGEN software) has been installed, which generates the traffic and allocates it into different QoS classes (based on DSCP field).

The second part is the core network infrastructure which consists of 4 Linux OS- (Debian testing with 2.6.21 kernel) based routers. Linux OS has been chosen because of its

TABLE 1: Traffic classes by flow.

EF (DSCP-0x2e)	VoIP
AF11(DSCP-0x0a)	A/V Content
AF22, BE	Other internet services

enhanced network implementation in contrast with other OS and because it is capable to support inside its kernel the MPLS and DiffServ technologies. The MPLS and DiffServ support in Linux achieved by installing the modules for each one technology separately inside Linux Kernel. The layered structure of the MPLS and DiffServ modules inside Linux kernel are shown in Figure 6. Based on this Linux kernel implementation and according to the architecture proposed in Figure 5, different packets are arriving from the SP and the traffic generator to the MPLS-DiffServ network.

The packets throughout the MPLS-DiffServ network are marked and assigned into different traffic classes by attaching to each class a different DSCP classifier value and by using HTB packet scheduler [9], at the Label Edge Router 1 (LER 1). The supported traffic classes are EF, AFxx, and BE. The following table shows the assignation of corresponding DSCP values to the services (VoIP, A/V, and Internet).

A Hierarchical Token Bucket (HTB) packet scheduler used for the DiffServ supported PHB. Specifically, a pFIFO queuing discipline is adopted for the EF class. Three GRED virtual queues with different drop precedence (2% for AF11, 4% for AF22) are implemented for the AFxx [9, 10]. The BE class served through a RED queuing discipline with 40% drop precedence. The maximum bandwidth allocated at the parent HTB class is 4 Mbps. The EF class guarantees 0.9 Mbit with maximum rate 1 Mbit for VoIP service. The AF11 provide 0.9 Mbit for video service. The AF22 provide 0.9 Mbit and the BE 0.9 Mbit. Figure 7 shows how the different flows classified and assigned to different traffic classes.

GRED queues were configured adjusting the following parameters:

(1) Q_{max} : maximum average queue size after which all packets get dropped, BS: percentage of the expected bandwidth share, L: maximum desired latency, BW: total network bandwidth,

(2) Q_{min} : minimum average queue length after which packets get dropped, AvPkt: average packet size,

(3) B: burst value in number of packets, and

(4) Q_{limit} : actual queue length which should never be exceeded.

Also, in LER 1 attached a short fixed length label to each incoming packet. The decision on what label to choose at the LER 1 based on the marked DSCP field in the packet header and on a predetermined policy and current-state information. One way of selecting labels is to aggregate different flows into trunks. A trunk is an aggregate of traffic flows that belongs to the same class, which means that all packets flowing in a trunk have the same MPLS header, including the 3-bit class of service field (currently experimental field or EXP), which it matched with a DSCP value.

TABLE 2: GRED queuing.

$$Q_{max} = \frac{0.01 * BS * L * BW}{8 \text{ bits/bytes} * 1000 \text{ ms/sec}} \quad (1)$$

$$Q_{min} = \frac{1}{2} * Q_{max} \quad (2)$$

$$B = \frac{2 * Q_{min} + Q_{max}}{3 * AvPkt} \quad (3)$$

$$Q_{liml} = 4 * Q_{max} \quad (4)$$

TABLE 3: Traffic class mapping.

CLASSES	DSCP	EXP
EF	0x2e	0x01
AF11	0x0a	0x02
AF12	0x0c	0x03
AF13	0x0e	0x04
AF21	0x12	0x05
AF22	0x14	0x06
AF23	0x16	0x07
BE	0x00	0x00

TABLE 4: Mapping with WiMAX traffic classes.

Service	Core network	Access network
VoIP	EF (DSCP-0x2e)	UGS Scheduling
A/V Content	AF11 (DSCP-0x0a)	rtPS Scheduling
High priority Services	AF22 (DSCP-0x14)	nrtPS Scheduling
Other internet services	BE	BE Scheduling

Different trunks can be routed along the same LSP, the only thing that distinguishes flows in different trunks is the class of service field. The following table shows how the EXP field matches with the correspondence DSCP values.

At each Label Switch Router (LSR 1, LSR 2), the label on the incoming packet is used as index in a table that contains the outgoing interface and a new label that is to replace the incoming label before it is transmitted to the next hop. Also the LSR routers take care of keeping the same PHB for each trunk. When a packet reaches the LER 2, the label will be removed and the packet will be forwarded to the access network.

At the access network, the WiMAX BS (Base Station) is configured to receive each service and map its predefined policy with core network similar one in order to keep the same quality until it reaches the end user. Table 4 shows the WiMAX scheduling services mapped with the different support traffic classes of the core network.

The way in which this allocation has been done is that the WiMAX base station takes into account the DiffServ traffic classes attributes, and comparing these attributes with the WiMAX scheduling algorithms characteristics (as reported in Section 2), it maps the corresponding traffic (based on DSCP field) to the WiMAX appropriate scheduling algorithm.

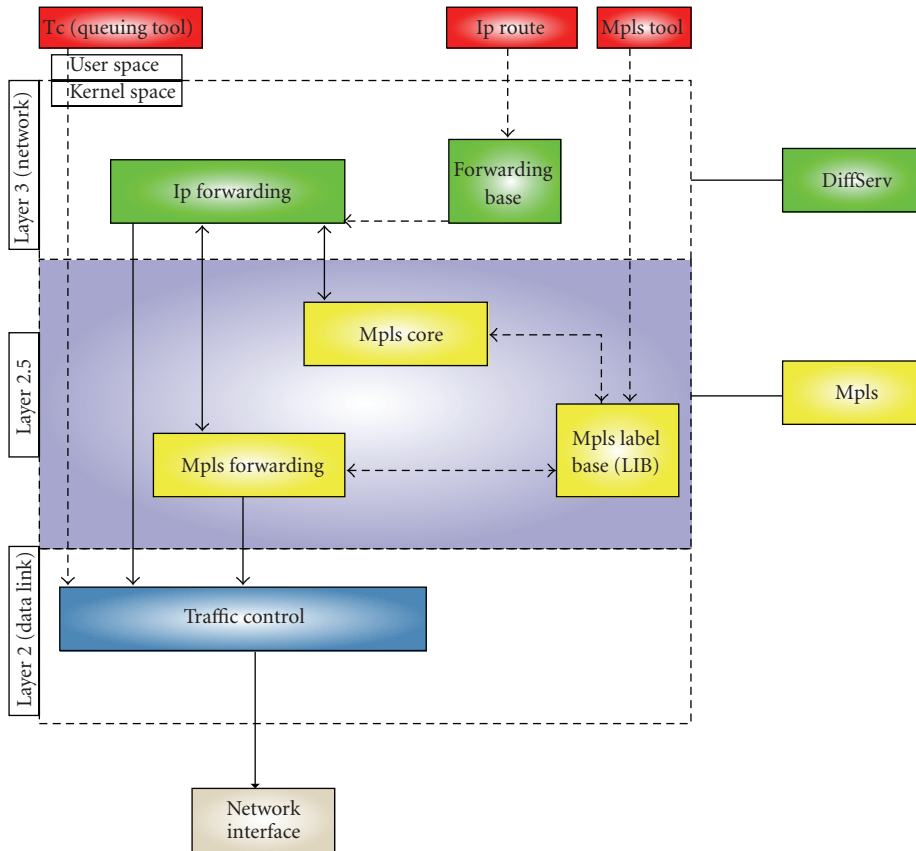


FIGURE 6: MPLS and DiffServ modules inside Linux Kernel.

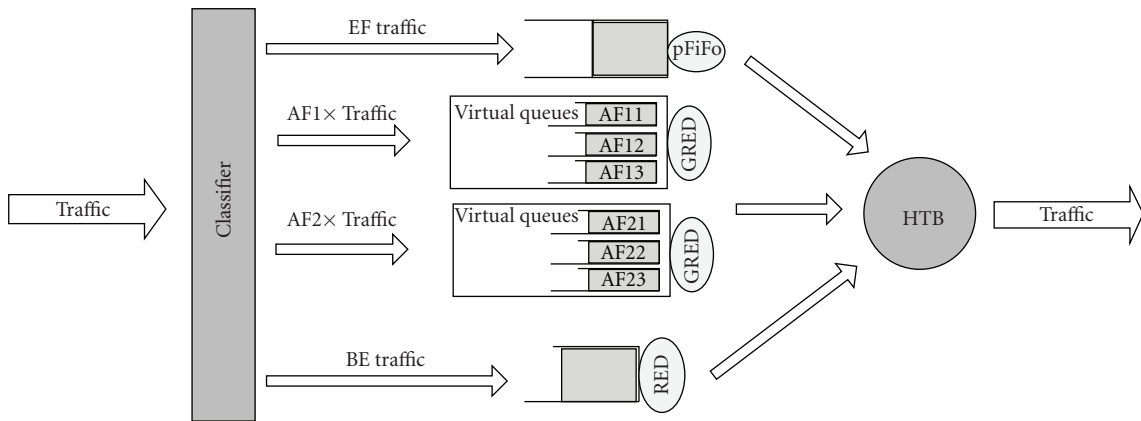


FIGURE 7: HTB packet scheduler and DiffServ supported classes [10].

TABLE 5: Initial test scenario.

Traffic class and packet size	Periodic traffic type				Poisson traffic type			
	EF (214 Bytes fixed)	AF11	AF22	BE	EF	AF11	AF22	BE
512	1Mbit Traffic per class							
768	make the total ingress traffic of the network							
1024	reach the upper capacity threshold which is 4 Mbits.							
1312	The BE class increase its traffic from 1 Mbps up to 2 Mbps.							
1472	The network load increases from 4 Mbps up to 5 Mbps but the network capacity still 4 Mbps							

server and from the H-264 encoder reaches the network via passing through the measurement server first. This happens because the measurement server needs to collect all data in order to produce the results for the one-way delay, data loss, and the jitter (delay variation). The network capacity at this phase is limited to 4 Mbps (by applying a filter at ingress LER) in order to realize how this can affect the 4 flows. The measurement server is going to increase gradually the bulk data flow (BE class) up to 2 Mbits. The network setup is shown in Figure 5.

4.4. QoS Provisioning over MPLS-DiffServ. During the second phase, the core network is configured again adapting the MPLS DiffServ QoS mechanism support. The four flows entering the network are marked (EF, AF11, AF22, BE) and allocated into two LSP's according to the DSCP and EXP field mapping. The EF (exp-0x01) and AF11 (exp-0x02) traffic classes are forwarded inside the same LSP (LSP1) in which label 10000 is assigned. In the second LSP (LSP2), the AF22 (exp-0x05) and BE (exp-0x0) traffic classes are forwarded marked with the label 20000. The measurement server generates three flows of 3 Mbps (1 Mbps each), and one flow of 1 Mbps is reaching the network from the VoIP server. The traffic from VoIP server and from the real time H-264 encoder reaches the network passing through the measurement server in the first place. This is happening because the measurement server needs to collect all data in order to produce the results for the one-way delay, data loss, and the jitter (delay variation). The network capacity at this phase is limited to 4 Mbits in order to be cleared out; how this can affect the four flows and how it could be compared to the previous setup results. The measurement server is going to increase gradually the bulk data flow (BE) up to 2 Mbits. Figure 8 shows the network setup.

4.5. QoS Provisioning over MPLS-DiffServ-WiMAX. The final step is to expand the same scenario into the WiMAX access network. Egress LER connects with the WiMAX BU (Base Unit) which is configured in order to keep the same quality constrains as the core network. The WiMAX access network capacity is limited up to 4 Mbps and maps each traffic class with the corresponding WiMAX classes. The EF mapped as UGS class, the AF11 as rtBS, the AF22 as nrtBS, and the BE as BE. The four flows are forwarded to the WiMAX SU (Subscriber Unit) and to the end user via the measurement server which collects data in order to provide the measurement results. The figure below shows the setup of the entire experiment and the role of each network entity.

5. Experimental Results

At this Section, the experimental results for each scenario are presented analytically and they will be discussed in order to introduce how the network changes can affect its performance. For each network, setup will be the graphs of average one way delay; jitter and packet loss will be included. The values that all graphs will show are the mean values of all used packet sizes (512, 768, 1024, 1312, and 1472). It is

TABLE 6: IP QoS classes and objective performance-metric upper limits (U-Unspecified) [1].

QoS Class	Characteristics	IPTD	IPDV	IPLR	IPER
0	Real time, jitter sensitive, highly interactive	100 ms	50 ms	1×10^{-3}	1×10^{-4}
1	Real time, jitter sensitive, interactive	400 ms	50 ms	1×10^{-3}	1×10^{-4}
2	Transaction data, highly interactive	100 ms	U	1×10^{-3}	1×10^{-4}
3	Transaction data, interactive	400 ms	U	1×10^{-3}	1×10^{-4}
4	Low loss only (short transactions, bulk data, video streaming)	1 s	U	1×10^{-3}	1×10^{-4}
5	Traditional applications of default IP networks	U	U	U	U

very important to mention that the packet size for EF flow is constant at 214 bytes during the whole experiment in order to take measurements which correspond better to the real applications. The network was tested at a 100% of network capacity traffic load (4 Mbps–1 Mbps per flow), with 112.5% traffic load (4.5 Mbps–3 flows of 1 Mbps and 1.5 Mbps BE) and finally 125% (5 Mbps–3 flows of 1 Mbps and 2 Mbps BE). The next paragraph refers to the QoS metrics which the experimental results depended on.

5.1. QoS Metrics. The QoS metrics mostly used [ITU-T-Y.1540] in an IP-based environment are as follows:

- (i) IPLR-IP Packet Loss Ratio,
- (ii) IPTD-IP Packet Transfer Delay,
- (iii) IPDV-IP Packet Delay Variation (Jitter),
- (iv) IPER-IP Packet Error Ratio.

The following table shows the upper bound of the acceptable values for each QoS class for each one of these metrics [1].

5.2. Core Network without QoS Support Experimental Results. At the first scenario, the analysis focused on the core network without QoS support. It is very important to understand how the network corresponds to any network change in order to state the metrics for the next experiment stages. After finishing the first stage of the experiment, the results, regarding the average one way delay and average packet loss ratio, are shown in the following figures.

Figure 11 shows the average one way delay for the four flows including all different traffic loads. The average delay values are very low, less than 1 msec. This seems to be very logical when considered that no queues have been installed but only the filter which limits the network capacity at 4 Mbps and just drops the packets which exceed this capacity. Figure 12 shows the average packet loss ratio. Observing Figure 11, it is clearly shown that when the traffic flows have a

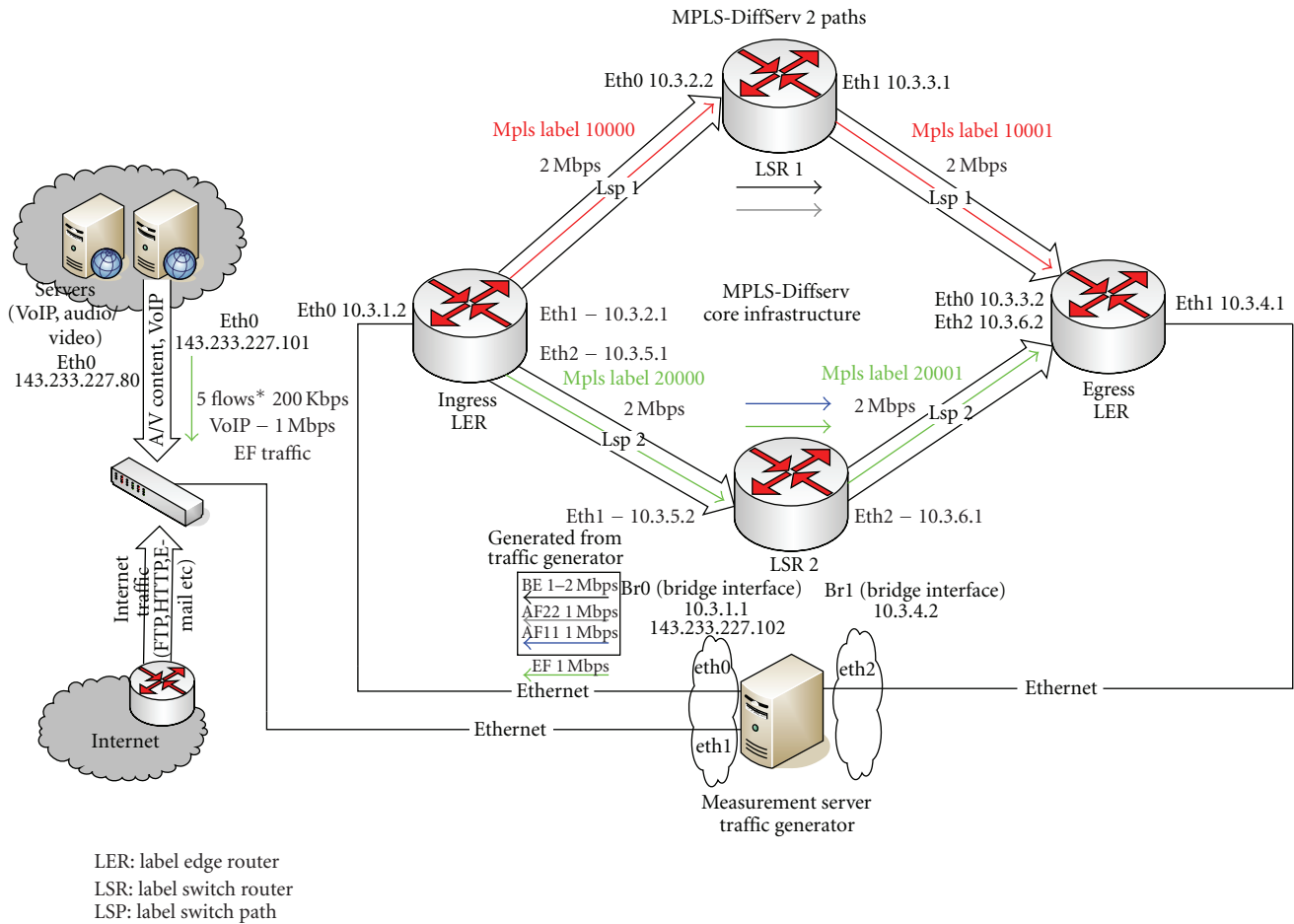


FIGURE 8: Core network with MPLS-DiffServ QoS enabled 2 paths.

PERIODIC transmission type, the packet loss can be detected in BE traffic only (bulk internet data). This is happening because the flows are separately transmitted and separately captured and the filter drops the packets inside the flow which exceeds the network capacity load (even when the flows carry the data unmarked).

It is ideal that data are created and they travel through core networks. In the real world systems, the way that a data transmission can occur is like POISSON transmission. That means that data have not a constant bit rate, but as the transmission continues there is a deviation between a minimum rate and a maximum rate. The most important observation from Figures 4–6 is that in POISSON transmission type even though that the increased traffic comes from BE class there is a high percentage of packet loss in AF11 and AF22 traffic classes (high quality video streaming, high priority internet service). That causes video transmission interruption and content distortion in a way that it is infeasible for the user to see it. The average packet loss percentage for EF class (Internet telephony-VoIP service) is lower than AF11 class, but by an average percentage of 2.636% for traffic load 112.5% (POISSON) and a 3.322% for traffic load 125% (POISSON), it is enough to distort the voice traffic (acceptable value 0.1% and in some special conditions until

1%). So it is imperative to add QoS support in order to protect the transmitted data.

Figure 13 above shows the average delay variation which has no special meaning to discuss because the values in all different circumstances are too low to affect the data transmission.

5.3. Core Network with QoS Support—2 LSP’s—Experimental Results. The MPLS traffic engineering capabilities are introduced to the network by separating the traffic classes into two different LSP’s with different routes inside the core network. The 1st LSP comprised of the EF and AF11 traffic classes in order to protect the most sensitive data from the BE class rate increase. The AF22 and BE traffic class comprised the 2nd LSP which also has a different route from the 1st LSP. Figure 14 below depicts the average one-way delay.

Regarding Figure 14, the most important observation is that the one-way delay of AF11 class decreased for approximately 10% from previous set up for traffic scenarios. The same decrease observed also for AF22 traffic class. The approximately 100 msec average one way delay decrease is the result of the different LSPs that the traffic classes are assigned. Data inside LSP 1 travels through the network in a different route from LSP 2 and the delay of EF and AF11 traffic classes

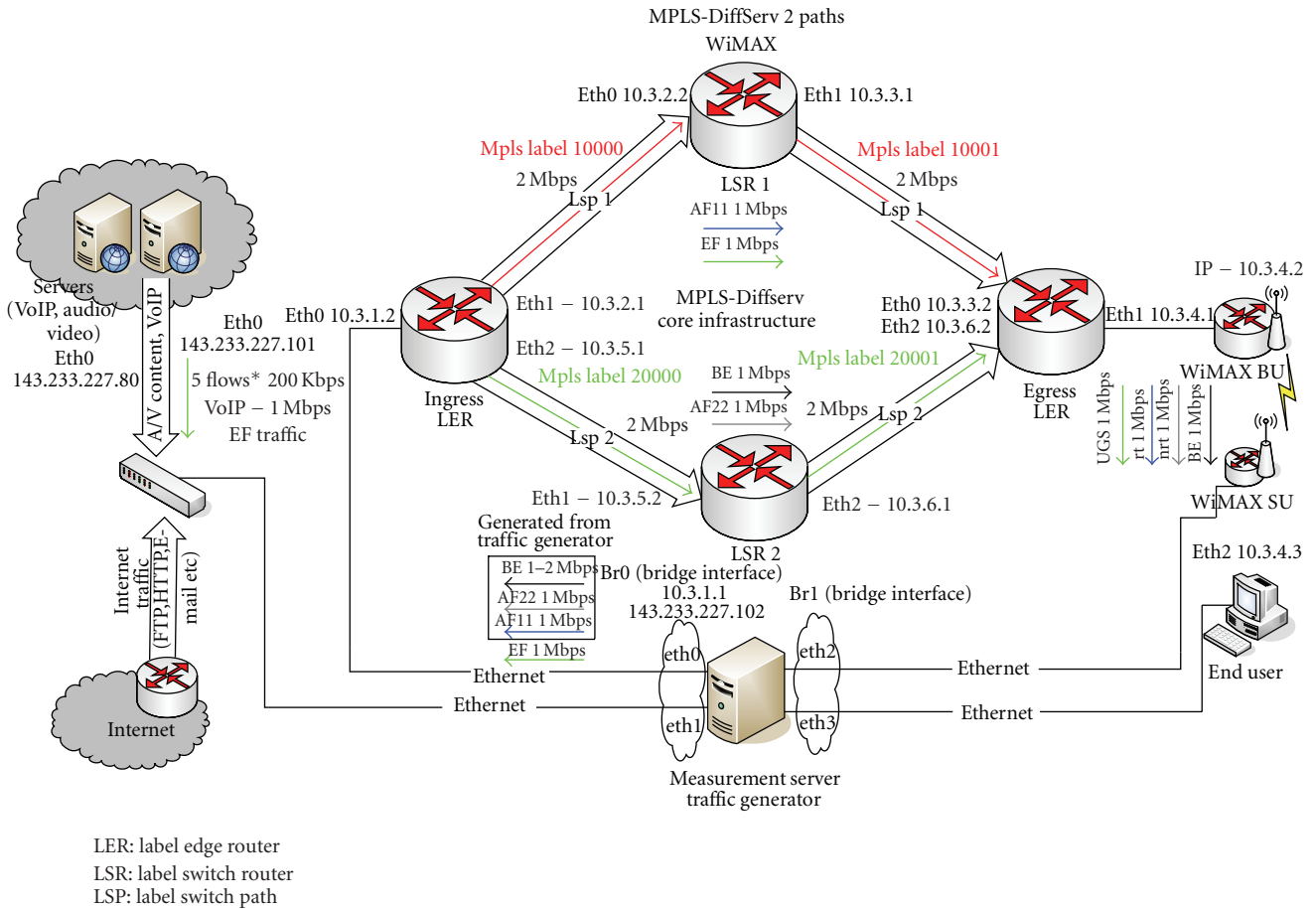


FIGURE 9: Core network with MPLS-DiffServ QoS enabled 2 paths with WiMAX access network.

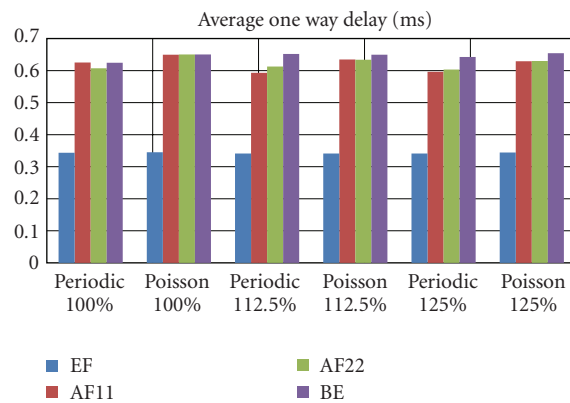


FIGURE 10: Average one way Delay graph.

affected only each other. Whereas the LSP 1 route is limited to 2Mbps, the EF and AF11 traffic classes affect each other and the result is the increase of EF traffic delay for about 2% which is still an acceptable value for voice transmission. The delay of AF11 traffic decreases as much as to increase the quality of the data transmission. The fact that the AF22 is the class with the highest priority inside LSP 2 is the cause of the average delay decrease for this class.

Observing Figure 15, it is easy to understand that the results regarding the packet loss are the same as the previous setup for the EF and BE traffic with small differences. The AF11 and AF22 classes have a decrease packet loss ratio about 0.5% because when the BE rate increases this affect less the AF11 than before because of the different LSP and different route that the classes follow. AF22 has decreased packet loss because in the second LSP is the

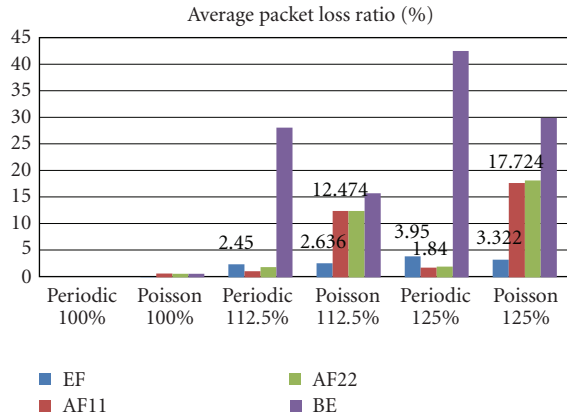


FIGURE 11: Average packet loss ratio.

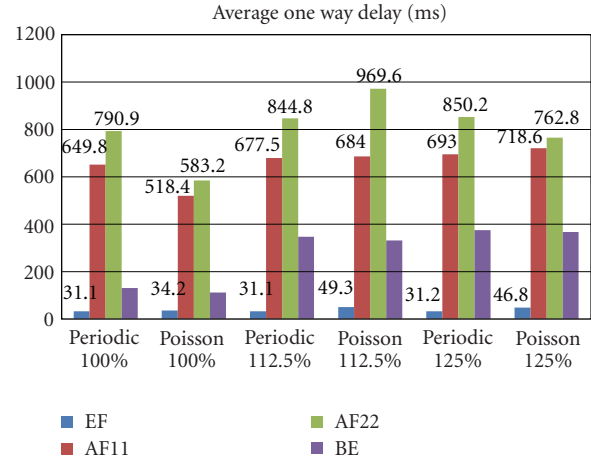


FIGURE 13: Average one way Delay graph.

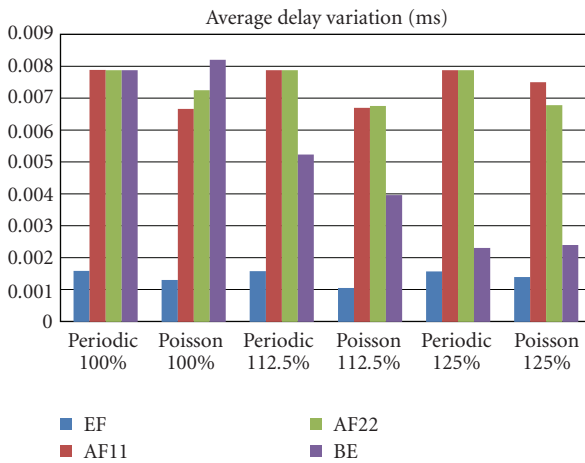


FIGURE 12: Average delay variation.

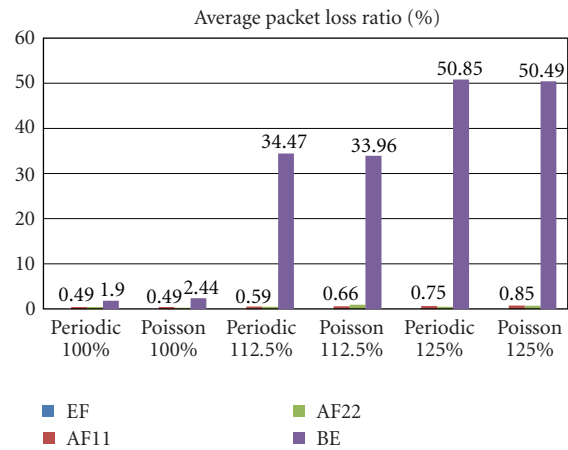


FIGURE 14: Average packet loss ratio.

traffic with the highest priority. Also the 95% of the whole average loss ratio are detected in BE class which is the class causing the network to exceed the capacity for about the 12.5% and 25%, respectively. Also, the average packet loss ratio between different traffic loads increased but with a rate of 0.1% every 12.5% traffic load increase. That means that the network will respond successfully in difficult congestion circumstances protecting the loss sensitive flows. Figure 16 below depicts the average delay variation which is still very small as at the initial stage for all the different traffic scenarios. That means that the packets are transmitted and received with constant ratio which does not affect the network performance and the service initial quality.

5.4. Core Network with QoS Support in 2LSP's and WiMAX Access Network. Completing the evaluation of the core network, it is shown that the provided level of quality was as high as to protect the services from distortion and transmission failure. The average one-way delay of the whole Core and Access networks infrastructure (including all traffic scenarios) are shown below in Figure 17.

Regarding the average one way delay, the WiMAX entity affects the delay by increasing it for about 10% (including all traffic scenarios) comparing with the results in the setup without WiMAX network (previous paragraph). Taking into account that it is a wireless technology, the delay increase is the physical cause for the network. Also this change lets the average one way delay values inside the acceptable limits that the initial data transmitted without distortion. The results are similar to the MPLS-DiffServ with the single-path network setup which means that the addition of a new LSP to the network helped to keep the delay in the acceptable limits. The EF class which is very sensitive (because it carries the voice service) exceeds the acceptable threshold of 50 msec for 12 msec (62 msec) in the case of the 125% traffic load which may cause a delay for the voice service. The delay would be understandable from human ear but in such an affordable level. Comparing with the results in Figure 15, the loss ratio for the EF traffic is 0.1% so the quality is still in high level.

For the AF11 class of service, the delay in whole range of data increases about 10% also, and loss ratio is about 1% for all traffic scenarios; the result is that the level of providing

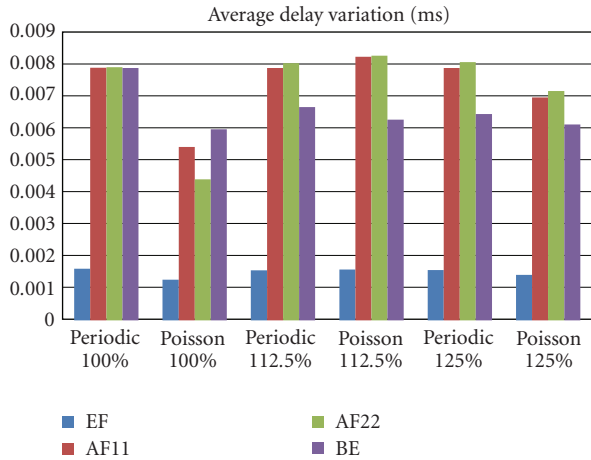


FIGURE 15: Average delay variation.

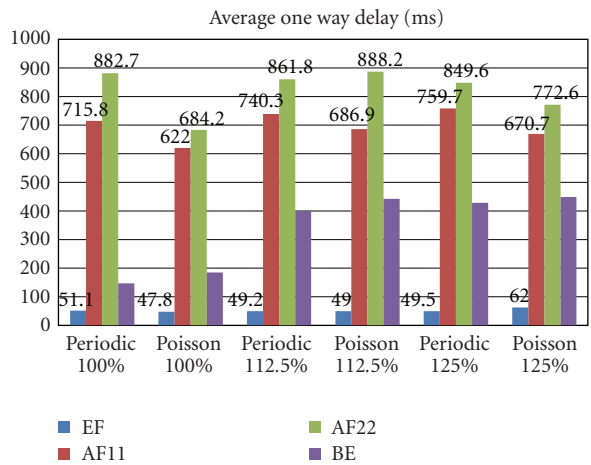


FIGURE 16: Average one way Delay graph.

quality is high considering the wireless medium and the high traffic load. The same results are for AF22 class which stays also inside the acceptable levels of quality. Below, Figure 19 shows the average delay variation for the whole experimental infrastructure. The values for all traffic scenarios are very low to affect the quality level and also the network performance.

5.5. Core versus E2E (Average Delay and Loss). Summarizing the experimental results will prove that overall E2E QoS provisioning succeeds even after the addition of the WiMAX access network.

(i) Loss

The figures below depict the difference and the average loss percentage addition; that WiMAX QoS enabled access network adds to the existing loss percentage of the core network.

As shown from the Figures 20 and 21, the level of loss percentage addition does not affect the E2E QoS provision. The services reach the end-user keeping the initial constrains even the traffic load exceeds the network capacity 25%.

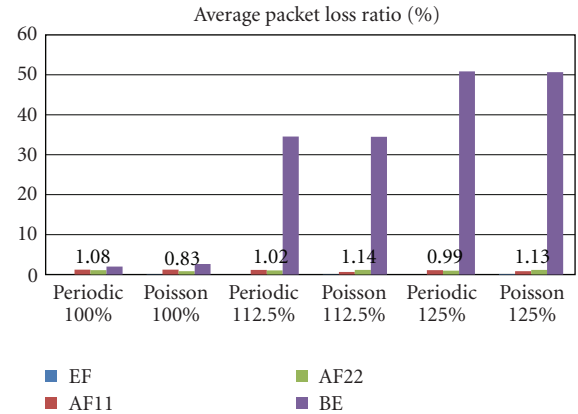


FIGURE 17: Average packet loss ratio.

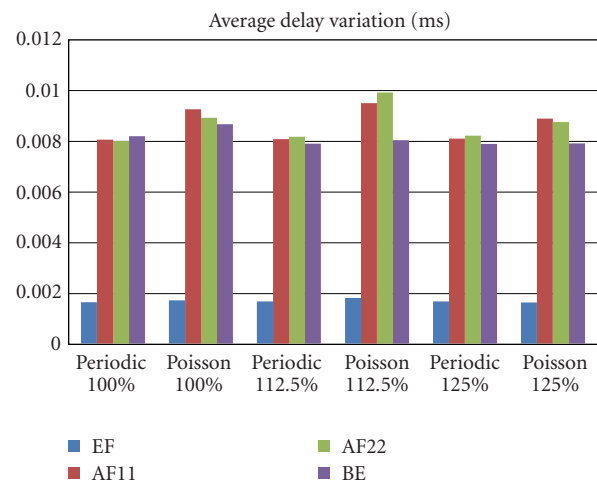


FIGURE 18: Average Delay variation.

(ii) Delay

The figures below depict the difference and the average delay (ms) addition; that WiMAX QoS enabled access network appends to the existing delay percentage of the core network.

As shown from the above delay comparison figures, the level of delay addition does not affect the E2E QoS provision. The services reach the end-user keeping the initial constrains; even the traffic load increases 25% higher than the network capacity.

6. Conclusions

Completing the evaluation of the core network, it is shown that the MPLS-DiffServ combination regarding the QoS provisioning (in delay and loss sensitive services) improved the core network performance. The provided level of quality was high enough to protect the transmitted services from distortion and transmission failure. The network responds impeccably to the dramatical change of network traffic load which initially was on saturation until the traffic load reaches the 125% of the configured network capacity.

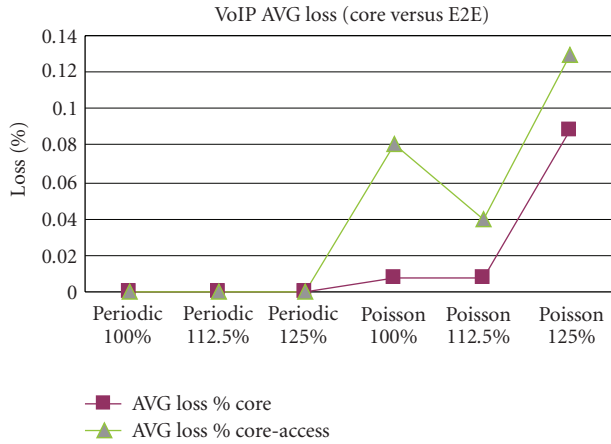


FIGURE 19: VoIP loss percentage AS addition.

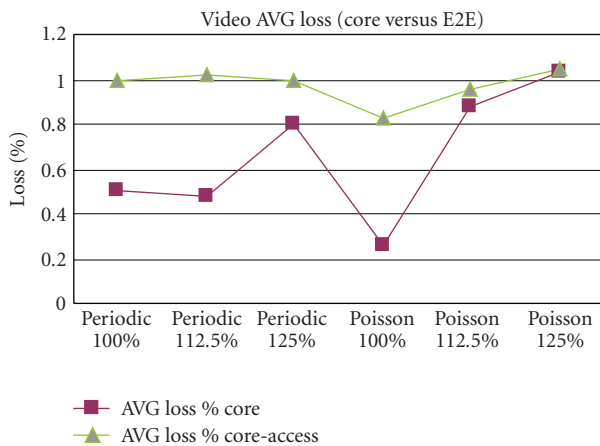


FIGURE 20: Video loss percentage AS addition.

The DiffServ architecture provided the expected quality guarantees by classifying the services into different BA's (Behavior Aggregates).

The delay inside core network was increasing and remaining in acceptable levels for a high quality services transmission, but the most important aspect is that the packet loss was decreasing dramatically giving to the voice service and to video streaming service a level of quality familiar with the initial. The MPLS traffic engineering capabilities are shown by the addition of a second LSP to the core network which decreased more than the average one way delay, improving the network performance and the QoS provisioning over the core infrastructure.

The expansion of the same QoS requirements into the access network using WiMAX technology has been tested successfully, providing results that prove the QoS provisioning over a wireless technology keeping the initial QoS constrains for sensitive services as VoIP and high quality video streaming. The average one way delay after the WiMAX addition was similar with delay average of the core network with a single LSP. This fact is shown as follows.

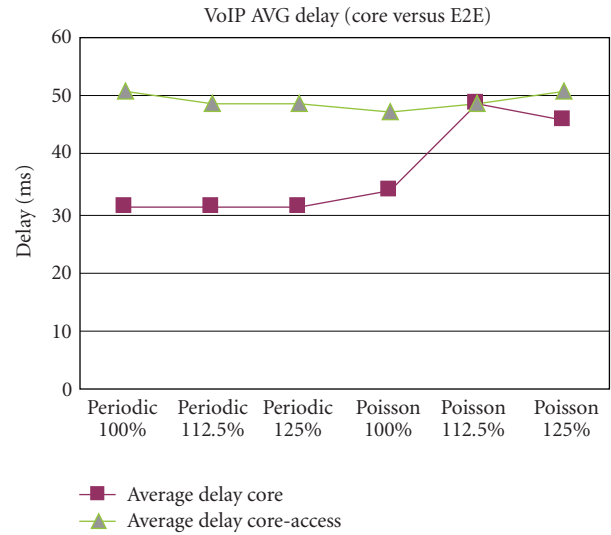


FIGURE 21: VoIP delay (ms) AS addition.

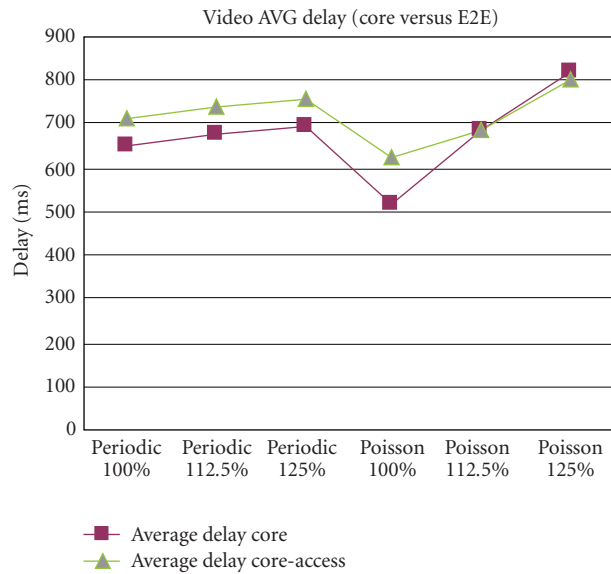


FIGURE 22: VoIP delay (ms) AS addition.

- (1) The integration of the WiMAX as Access medium and the Core network infrastructure show that the QoS provisioning inside wireless network is feasible even when the transmitted services are high quality services (VoIP, H-264 Video).
- (2) The evaluation of the infrastructure with the different proposed test scenarios shows that the MPLS-DiffServ-combined mechanism provides QoS to core network with low-packet loss ratio and with an acceptable level of one way delay when the MPLS traffic engineering capabilities have been used.
- (3) The WiMAX as access network technology successfully provides QoS guarantees to loss- and delay-sensitive services and affects the core network

performance only by adding a small ratio of loss and an acceptable level of delay (for wireless networks).

- (4) The Network Operators and Service Providers have another perspective of how a similar network can be attached in their premises (and with which type of format in their services) in order to provide triple play services with QoS guarantees.

Acknowledgment

The concept reported in this paper is been carried out in the frame of the EU-funded ENTHRONE (End-to-End QoS through Intergrated Management of Content, Networks and Terminals) research project (IST-FP6-038463).

References

- [1] M. Marchese, *QoS over Heterogeneous Networks*, John Wiley & Sons, New York, NY, USA, 2007.
- [2] Z. Wang, *Internet QoS: Architectures and Mechanisms for Quality of Service*, Morgan Kaufmann, San Francisco, Calif, USA, 2001.
- [3] B. S. Davie and Y. Rekhter, *MPLS: Technology and Applications*, Morgan Kaufmann, San Francisco, Calif, USA, 2000.
- [4] I. Minei and J. Lucek, *MPLS-Enabled Applications: Emerging Developments and New Technologies*, John Wiley & Sons, New York, NY, USA, 2005.
- [5] IETF RFC 3270, L. Wu, B. Davie, and S. Davari, "Multi-protocol Label Switching (MPLS) Support of Differential Services," May 2002, <http://www.ietf.org/rfc/rfc3270.txt>.
- [6] L. Nuaymi, *WiMAX Technology for Broadband Wireless Access*, John Wiley & Sons, New York, NY, USA, 2007.
- [7] N. Zotos, G. Xilouris, E. Pallis, and A. Kourtis, "An MPLS-DiffServ experimental core network infrastructure for E2E QoS content delivery," in *Proceedings of the 6th IEEE/ACS International Conference on Computer Systems and Applications (AICCSA '08)*, pp. 947–951, Doha, Qatar, April 2008.
- [8] D. Sweeney, *WiMAX Operator's Manual: Building 802.16 Wireless Networks*, Apress, New York, NY, USA, 2006.
- [9] G. Xilouris, T. Pliakas, and A. Kourtis, "Enthrone experimental infrastructure for E2E QoS provisioning," in *Proceedings of the 18th Annual IEEE International Symposium on Personal, Indoor and Mobile Radio Communications (PIMRC '07)*, pp. 1–6, Greece, Athens, September 2007.
- [10] D. Miras, et al., *A Survey of Network QoS Needs of Advanced Internet Applications*, Internet2 QoS Working Group, November 2002.
- [11] MGEN: Multi-Generator, <http://cs.itd.nrl.navy.mil/work/mgen/>.

Research Article

Network Performance Evaluation of Abis Interface over DVB-S2 in the GSM over Satellite Network

S. B. Musabekov,^{1,2} P. K. Srinivasan,³ A. S. Durai,³ and R. R. Ibraimov⁴

¹ZTE Investment LLC, Oybek Street 14, Tashkent 100015, Uzbekistan

²Ahmadabad Earth Station, Space Applications Centre (SAC), Headquarters, 4 Kalidas Road, Dehradun, 248001, India

³Indian Space Research Organization (ISRO), Ahmedabad, 380015, India

⁴Tashkent University of Information Technology (TUIT), 108, Amir Temur Street, Tashkent 100084, Uzbekistan

Correspondence should be addressed to S. B. Musabekov, smusabekov@yahoo.com

Received 30 September 2009; Revised 14 May 2010; Accepted 21 July 2010

Academic Editor: George Xilouris

Copyright © 2010 S. B. Musabekov et al. This is an open access article distributed under the Creative Commons Attribution License, which permits unrestricted use, distribution, and reproduction in any medium, provided the original work is properly cited.

This paper deals with establishing a GSM link over Satellite. Abis interface, which is defined between Base Transceiver Station (BTS) and Base Station Controller (BSC), in a GSM network is considered here to be routed over the Satellite. The satellite link enables a quick and cost-effective GSM link in meagerly populated areas. A different scenario comparison was done to understand the impact of Satellite environment on network availability comparing to terrestrial scenario. We have implemented an Abis interface over DVB S2 in NS2 and evaluated the performance over the high delay and loss satellite channel. Network performance was evaluated with respect to Satellite channel delay and DVB S2 encapsulation efficiency under different amount of user traffic and compared with the terrestrial scenario. The results clearly showed an increased amount of SDCCH and TCH channels required in the case of satellite scenario for the same amount of traffic in comparison to conventional terrestrial scenario. We have optimized the parameters based on the simulation results. Link budget estimation considering DVB-S2 platform was done to find satellite bandwidth and cost requirements for different network setups.

1. Introduction

The success story of second-generation (2G) terrestrial mobile systems (GSM) and the relative demise of 2G mobile satellite systems (MSS) such as, Iridium and Globalstar have influenced the future of MSS. These two distinct but interrelated events demonstrate the importance of proper market and business strategies for the success of the future mobile satellite industry. Global System for Mobile communications (GSM) is the most popular means for voice and data communication having more than 2 billion subscribers all over the world. Still 3/4 of the globe is not covered by GSM networks. Despite growing demand for GSM services in rural areas, it is not cost-effective for GSM service providers to cover areas with meager population density. Poor terrestrial infrastructure in remote areas leads to high capital expenditures for establishing new links by means of fiber optic cables or microwave links, leading to an alternate

and cost-effective solution like Satellite interface. Proposed work considers DVB-S2 [1] as a physical interface between Earth station and Satellite due to its highly spectrum efficient Modulation and powerful FEC schemes (ModCode). DVB-S2 has two different frames, long (64800 bit) and short (16200 bit) frames. Hence encapsulation efficiency and Network bandwidth utilization should be evaluated for different scenarios.

Presently there are no clear specifications on Abis interface over satellite technology. Still there are many proprietary solutions present at the world market. There is a lack of open standard definition in this area. Issues like change in signaling protocol on Abis interface while routing through Satellite are not addressed. Questions about implications on network availability and integrity while switching to GSM over satellite technology are not discussed elsewhere, which lead to a definition of an open standard architecture for an Abis interface over Satellite. We had proposed in [2] a novel

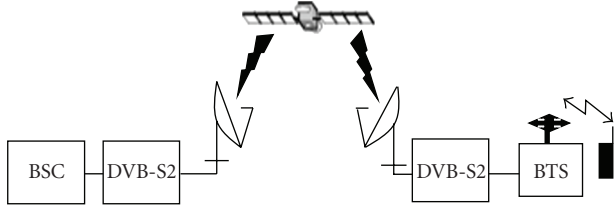


FIGURE 1: Abis interface over Satellite [4].

OSI architecture for Abis over satellite interface but there is a requirement of network performance evaluation, which is attempted in this paper.

We have proposed a new protocol architecture called Abis over IP over DVB-S2 in which the signaling and Transcoding Rate and Adaptation Unit (TRAU) frames are formatted over UDP/IP and RTP/UDP/IP, respectively, and encapsulated in Generic Stream (GS) stream of DVB-S2 over the forward and return link. Simulation is performed using standard network simulator NS-2.33 [3] under delay and different loss scenarios of the Satellite and the results are analyzed.

The following sections are organized as follows. Section 2 provides NS2 network (OSI) model; Section 3 gives the mathematical analysis for the traffic, subscriber density, and BTS capacity requirements for Abis over Satellite and terrestrial Abis. Section 4 describes Simulation Parameters, Results, and Analysis. Section 5 presents link budget estimations for Abis over DVB-S2 platform. Section 6 concludes this paper.

2. Proposed Abis over IP over DVB-S2 Network Performance Evaluation

The system setup for Abis interface over IP over DVB-S2 is shown in Figure 1, where the proposed protocol architecture lies between the BTS and BSC.

Figure 2 shows the proposed signaling protocol architecture for Abis interface over Satellite, and Figure 3 shows framing format. Frames on Abis interface are separated into TRAU frames and Signaling frames. The signaling frames is formatted over UDP/IP and encapsulated into Data Field Length (DFL) of DVB-S2 frame. The traffic in TRAU frames are formatted over RTP/UDP/IP and encapsulated over DVB-S2. Before IP encapsulation timeslot elimination technique may be applied to save bandwidth to considerable amount [5].

In the forward link, that is, from BSC to BTS, these messages describe the link establishment and release information and its acknowledgment to all its BTS [6]. The messages with added UDP and IP header form a multiple transport stream of the DVB-S2 system. The Base Band (BB), FEC and Physical Layer (PL) headers of DVB-S2 frame are added and modulated before given to the RF Satellite channel. The signaling links over the Abis interface are addressed to the different units by Terminal Endpoint Identifiers (TEIs) [7]. UDP header will represent destination port address of LAPD frame. Each of the physical link time slots of E1 [8] is now

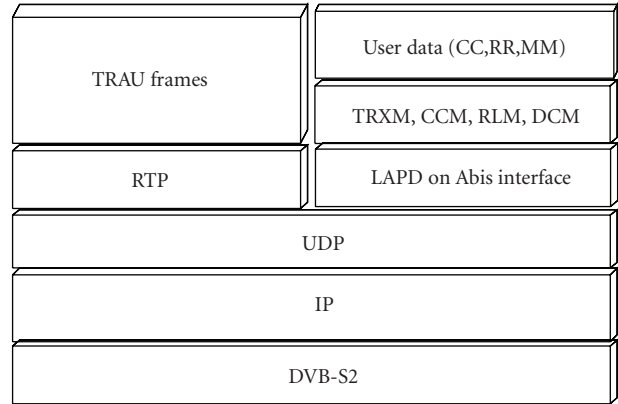


FIGURE 2: Abis interface over Satellite protocol architecture.

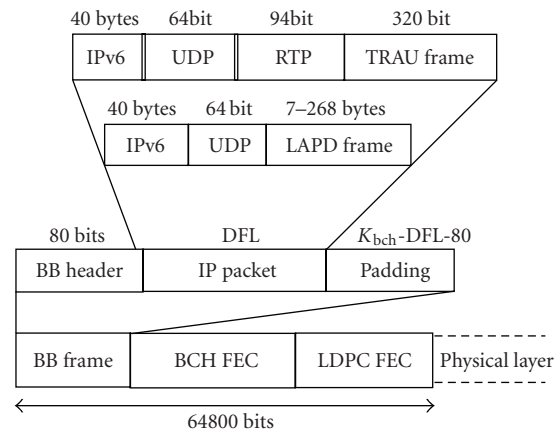


FIGURE 3: Framing format.

distinguished by each stream of the multiplexed GS stream fed to the DVB-S2 system.

TRAU frames [9] which carry voice are encapsulated into Real-Time Protocol (RTP) packets with time stamp of playback to prevent jitter while receiving, then encapsulated into UDP packets. Resulting UDP packets are IP encapsulated and formed Generic stream for the DVB-S2 system. DVB-S2 has inherent bandwidth efficient modulation modes and power efficient coding.

3. Traffic Analyses

This section gives the mathematical analysis for the traffic and subscriber density for the satellite scenario compared with the terrestrial scenario [10]. Each BTS has three sectors (cells). Each cell has one TRX containing one time slot (TS) for BCCH (Broadcasting Control Channel) to broadcast information about serving BTS, SDCCH (Stand Alone Dedicated Control Channel) for signaling during MOC, MTC, and Location Update, FACCH (Fast Associated Control Channel) for transferring measurements results and handover. Other TRX within this cell will have only TCH. If the number of TRX is more than three, then one more SDCCH TS should be added. Traffic refers to the numbers

of subscribers the network can support and is described as follows:

$$A = n \times \frac{T}{3600}, \quad (1)$$

where n -Calls are made by a subscriber within an hour, T is Average duration of each call (in seconds), and A is Traffic, in Erlang.

If one call is made by a subscriber within an hour and last 120 seconds, the traffic is calculated as $A = 1 \times 120/3600 = 33$ mErl. For convenience of engineering calculation, the traffic is defined as 25 mErl per subscriber. The SDCCH average process time for MOC, MTC is considered as 3 seconds. Location updating process takes 9 seconds, BHCA (Busy Hour Call Attempts) = 2.

The traffic of SDCCH per subscriber is

$$\frac{3 \times 2 + 9}{3600} = 0.0042 \text{ Erlang.} \quad (2)$$

For 4 SDCCH and blocking probability of 2%, we can support 1.092 Erlang (from Erlang B table). SDCCH/8 has 8 SDCCH logical channels within one time slot. Hence,

$$\left(\frac{1.092}{0.0042} = 260 \text{ sub} \right) \times 0.025 \text{ Erlang} = 6.5 \text{ Erlang.} \quad (3)$$

In Erlang-B with blocking probability of 2%, 6.5 Erlang needs 12TCH (2TRX). During the establishment and terminating of MOC and MTC, 29 commands and response I frames are transferred between BTS and BSC. Each frame will be delayed by $t \approx 240$ ms while propagating through Satellite. For Satellite communication, SDCCH average process time for MOC and MTC approximately will be 7 seconds due to Satellite delay; location updating process will be 20 seconds. Assuming 2 BHCA, we have the traffic of SDCCH per subscriber as

$$\frac{7 \times 2 + 20}{3600} = 0.0094 \text{ Erlang.} \quad (4)$$

By 4SDCCH with blocking probability of 2%, we can support 1.092 Erlang (from Erlang B table).

$$\left(\frac{1.092}{0.0094} = 116 \text{ sub} \right) \times 0.025 \text{ Erl} = 2.9 \text{ Erl.} \quad (5)$$

In Erlang-B with blocking probability of 2%, 2.9 Erlang need 7 TCH (1TRX) channels.

From above calculations, it can be concluded that for Abis over Satellite the same amount of Erlangs on SDCCH channel can support less number of subscribers than in terrestrial communication.

The same amount of subscribers is taken into account for Satellite Abis and terrestrial Abis 200 subscribers. Every time when MS initiates a call, there will be delay during call setup and also during conversation. Since each message signaling and traffic will be delayed while sending over satellite channel, it is considered that after call set-up phase subscriber needs to deliver 40 messages, and message

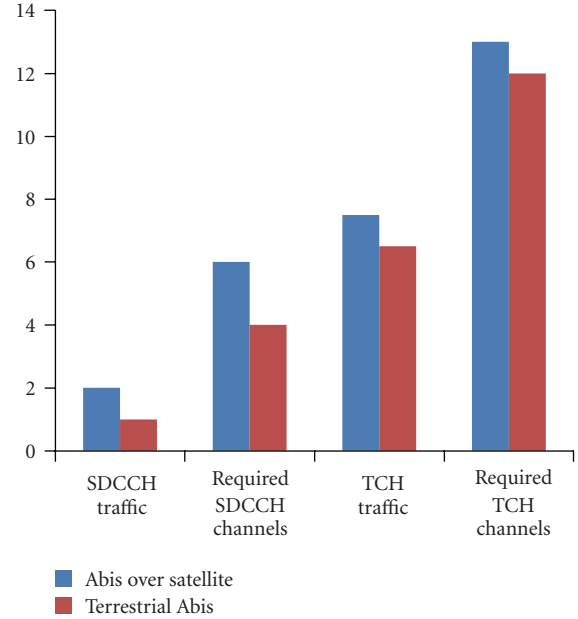


FIGURE 4: Traffic for Abis over Satellite and Terrestrial Abis.

duration is 3 seconds. Hence one conversation time will be $40 \times 3 = 120$ seconds. In case of Abis over Satellite, conversation time will increase to 129.6 seconds. Hence mErl per subscriber will increase. Figure 4 shows comparison of Satellite Abis and Terrestrial Abis for the above described scenario. This shows that to support same amount of traffic a number of SDCCH and TCH channels are required in Abis over Satellite scenario. This calculation will give the number of TRX's or TS required for the same amount of the traffic.

4. Simulations

4.1. Simulation Description and Parameters. Simulation of the proposed OSI stack was performed using the NS version 2.33. The LAPD generation was based on the source code found under over which the rest of the OSI stack is incorporated. During simulation, two signaling frames from Um interface are considered Channel request and Connection acknowledgment messages. SABM frame to BSC to establish signaling link between BSC and BTS and sent over UDP/IP and over DVB-S2 frame. Corresponding UA frame will be sent to BTS. When LAPD link is established, Chan_Req message will be forwarded and 27 consecutive command response frames are sent in both directions to simulate call setup scenario. Call is established when connection acknowledgment frame is received. Table 1 shows simulation parameters.

Simulation is done for various scenarios where configuration of BTS varied from 1 TRX to 12 TRX. Each scenario considers different number of users and data rates for Abis interface and Satellite channel. Only CS traffic is considered during simulation over the fixed DVB-S2 frames. Simulation is done to monitor the encapsulation efficiency of Abis interface over IP over DVB-S2 platform.

TABLE 1: Simulation parameters.

Sr. No	Simulation parameter	Value
1	No. of MS/BTS	1–150
2	No. of time slots/BTS	8–168
3	Call duration	120 sec
4	N200	3
5	T200	200 ms–900 ms
6	I-Frame length	7–268 bytes
7	Data rate for one voice channel	16 Kbps
8	DVB-S2 frame	64800/16200 bits
9	DVB-S2 FEC	3/4
10	DVB-S2 DFL	48408/11712 bits
11	Channel delay	250 msec
12	Channel loss Probability	93% Good,7% Bad

4.2. *Simulation Results.* Three scenarios are considered with different timer $T200$ [11] values of 200 ms and 900 ms and with channel error probability to understand the performance of Abis interface. Figure 5 shows the simulation trace file generated over the NS2 for $T200 = 900$ ms.

Following piece of trace file shows the performance of Abis over Satellite with $T200 = 900$ ms: + enqueue, – dequeue, r - received, 1- BTS, 0- Satellite, 2- BSC. Trace file is depicted in the following sequence.

Frame state – time – from – to – LAPD – byte – via – source – destination - N(S) - N(R) – longitude – latitude – frame

The call set-up time is given by

$$t = N * t' = 30 * 0.334 = 10.02. \quad (6)$$

N : number of command and response I frames, and t' = Satellite delay + processing delay. Typical values obtained from the simulation are $N = 30$, $t' = 33$ msec, which amounts to $t = 10.02$ sec.

Figure 6 shows that for lower timer values, the continuous retransmission may cause link congestion and will delay call set-up time $t = 10.03$ for $T200 = 900$ ms and $t = 10.42$ for $T200 = 200$ ms.

Hence the optimum value of the $T200$ retransmission timer has to be setup based on the actual network (satellite + processing) delay experienced.

The call set-up time delay due to lost I frame is given by

$$t = Nl * T200 = 1 * 900 \text{ ms}. \quad (7)$$

Nl : Number of lost I-frame.

The General equation for call set-up time can be written as

$$t = N * t' + Nl * T200. \quad (8)$$

Figure 7 shows the trace generated in NS2 under channel error probability of 7%. From the figure, it can be concluded that continuous retransmission will cause high link congestion, and service availability will be reduced as the TCH call set-up time will not increase dramatically. This

```
+01 0 LAPD 2025 ----- 0 1.0 2.0 -1 0 42.30 -71.10 0.00 -95.00[1 2 U SABME]
-01 0 LAPD 2025 ----- 0 1.0 2.0 -1 0 42.30 -71.10 0.00 -95.00[1 2 U SABME]
r0.16811 0 LAPD 2025 ----- 0 1.0 2.0 -1 0 42.30 -71.10 0.00 -95.00[1 2 U SABME]
+0.16810 2 LAPD 2025 ----- 0 1.0 2.0 -1 0 0.00 -95.00 30.90 -122.30[1 1 U SABME]
-0.16810 2 LAPD 2025 ----- 0 1.0 2.0 -1 0 0.00 -95.00 30.90 -122.30[1 1 U SABME]
r0.33420 2 LAPD 2025 ----- 0 1.0 2.0 -1 0 0.00 -95.00 30.90 -122.30[1 1 U SABME]
+0.33422 0 LAPD 2025 ----- 0 2.0 1.0 -1 1 30.90 -122.30 0.00 -95.00[2 1 U UA]
-0.334220 LAPD 2025 ----- 0 2.0 1.0 -1 1 30.90 -122.30 0.00 -95.00[2 1 U UA]
-CHAN_REQ message
r0.50022 0 LAPD 2025 ----- 0 2.0 1.0 -1 1 30.90 -122.30 0.00 -95.00[2 1 U UA]
+0.50020 1 LAPD 2025 ----- 0 2.0 1.0 -1 1 0.00 -95.00 42.30 -71.10[1 2 U UA]
-0.50020 1 LAPD 2025 ----- 0 2.0 1.0 -1 1 0.00 -95.00 42.30 -71.10[1 2 U UA]
r0.668301 LAPD 2025 ----- 0 2.0 1.0 -1 1 0.00 -95.00 42.30 -71.10[1 2 U UA]- round
trip delay t = 669 ms, T200 > 669 ms
-9.689 2 0 HDLC 28 ----- 0 2.0 1.0 -1 1 15 30.90 -122.30 0.00 -95.00[29 1 S 14 RR]
r9.8551 2 0 LAPD 2025 ----- 0 2.0 1.0 -1 1 15 30.90 -122.30 0.00 -95.00[29 1 S 14 RR]
+9.8551 0 1 LAPD 2025 ----- 0 2.0 1.0 -1 1 15 0.00 -95.00 42.30 -71.10[1 30 S 14 RR]
-9.8551 0 1 LAPD 2025 ----- 0 2.0 1.0 -1 1 15 0.00 -95.00 42.30 -71.10[1 30 S 14 RR]
r10.023201 LAPD 2025 ----- 0 2.0 1.0 -1 1 15 0.00 -95.00 42.30 -71.10[1 30 S 14
RR] - CON_ACK frame received. Time taken to establish a call t = 10.03 seconds.
```

FIGURE 5: Shows the TCH call set-up time for $T200 = 900$ ms.

```
+ 0.0000 1 0 HDLC 28 ----- 0 1.0 2.0 -1 0 42.30 -71.10 0.00 -95.00[1 2 U SABME]
-0.0000 1 0 HDLC 28 ----- 0 1.0 2.0 -1 0 42.30 -71.10 0.00 -95.00[1 2 U SABME]
r0.1281 1 0 HDLC 28 ----- 0 1.0 2.0 -1 0 42.30 -71.10 0.00 -95.00[1 2 U SABME]
+ 0.1281 0 2 HDLC 28 ----- 0 1.0 2.0 -1 0 0.00 -95.00 30.90 -122.30[1 1 U SABME]
- 0.1281 0 2 HDLC 28 ----- 0 1.0 2.0 -1 0 0.00 -95.00 30.90 -122.30[1 1 U SABME]
+ 0.2000 1 0 HDLC 28 ----- 0 1.0 2.0 -1 1 42.30 -71.10 0.00 -95.00[1 2 U SABME]
- 0.2000 1 0 HDLC 28 ----- 0 1.0 2.0 -1 1 42.30 -71.10 0.00 -95.00[1 2 U SABME]-
T200 = 200 ms timer expired
+ 10.1720 2 0 HDLC 28 ----- 0 2.0 1.0 -1 45 30.90 -122.30 0.00 -95.00[82 1 S 13 RR]
-10.1720 2 0 HDLC 28 ----- 0 2.0 1.0 -1 45 30.90 -122.30 0.00 -95.00[82 1 S 13 RR]
r10.2262 0 1 HDLC 28 ----- 0 2.0 1.0 -1 44 0.00 -95.00 42.30 -71.10[1 83 S 13 RR]
r 10.2981 2 0 HDLC 28 ----- 0 2.0 1.0 -1 45 30.90 -122.30 0.00 -95.00[82 1 S 13 RR]
+ 10.2981 0 1 HDLC 28 ----- 0 2.0 1.0 -1 45 0.00 -95.00 42.30 -71.10[1 84 S 13 RR]
-10.2981 0 1 HDLC 28 ----- 0 2.0 1.0 -1 45 0.00 -95.00 42.30 -71.10[1 84 S 13 RR]
r10.4262 0 1 HDLC 28 ----- 0 2.0 1.0 -1 45 0.00 -95.00 42.30 -71.10[1 84 S 13 RR]
```

FIGURE 6: TCH call set up time $T200 = 200$ ms.

is because retransmitted I frame will receive response of the first sent I frame. However, under the channel errors, the call set-up time increases due to the actual loss of I frames. Table 2 below gives call set-up time obtained from the simulation under various scenarios.

4.2.1. *Comparison of Various Network Scenarios and Network Optimizations.* Different scenarios are considered to find optimal network configuration for Abis over DVB-S2 platform Table 3. The number of TRX is varied from 1 to 21. Subsequently, the number of users and data rates on Abis interface and Satellite channel is changed. During simulation FEC 3/4 is considered.

Data rate evaluation is done under different data rate definitions.

- (1) *Abis data rate.* Abis data rate corresponds to the data rate after idle time slot elimination. It depends on TRX quantity.
- (2) *Useful data rate.* This is the occupied TS of Abis data by one user. This corresponds to one occupied voice channel by each subscriber.
- (3) *Satellite data rate.* This is the time interval between consecutive sent DVB-S2 frames. DVB-S2 frame is 16200 bit. For, for example, sending DVB-S2 frame, each 40 ms will give 405 Kbps satellite data rate.

TABLE 2: Call set-up time for different scenarios.

Scenario	Value (seconds)
$T = 900$ ms	10.02
$T = 200$ ms	10.42
$T = 900$ ms + 7% loss	10.92

```

+01 0 LAPD 2025 ----- 0 1.0 2.0 -1 0 42.30 -71.10 0.00 -95.00[1 2 U SABME]
-01 0 LAPD 2025 ----- 0 1.0 2.0 -1 0 42.30 -71.10 0.00 -95.00[1 2 U SABME]
r0.16811 0 LAPD 2025 ----- 0 1.0 2.0 -1 0 42.30 -71.10 0.00 -95.00[1 2 U SABME]
+0.16810 2 LAPD 2025 ----- 0 1.0 2.0 -1 0 0.00 -95.00 30.90 -122.30[1 1 U SABME]
-0.16810 2 LAPD 2025 ----- 0 1.0 2.0 -1 0 0.00 -95.00 30.90 -122.30[1 1 U SABME]
r0.33420 2 LAPD 2025 ----- 0 1.0 2.0 -1 0 0.00 -95.00 30.90 -122.30[1 1 U SABME]
+0.33422 0 LAPD 2025 ----- 0 2.0 1.0 -1 1 30.90 -122.30 0.00 -95.00[2 1 U UA]
-0.33422 0 LAPD 2025 ----- 0 2.0 1.0 -1 1 30.90 -122.30 0.00 -95.00[2 1 U UA]
r0.50022 0 LAPD 2025 ----- 0 2.0 1.0 -1 1 30.90 -122.30 0.00 -95.00[2 1 U UA]
+0.50020 1 LAPD 2025 ----- 0 2.0 1.0 -1 1 0.00 -95.00 42.30 -71.10[1 2 U UA]
-0.50020 1 LAPD 2025 ----- 0 2.0 1.0 -1 1 0.00 -95.00 42.30 -71.10[1 2 U UA]
r0.66830 1 LAPD 2025 ----- 0 2.0 1.0 -1 1 0.00 -95.00 42.30 -71.10[1 2 U UA]
+9.689 2 0 LAPD 2025 ----- 0 2.0 1.0 -1 15 30.90 -122.30 0.00 -95.00[29 1 S 14 RR]
-9.689 2 0 LAPD 2025 ----- 0 2.0 1.0 -1 15 30.90 -122.30 0.00 -95.00[29 1 S 14 RR] -1
frame 15 sent
r9.8551 2 0 LAPD 2025 ----- 0 2.0 1.0 -1 15 30.90 -122.30 0.00 -95.00[29 1 S 14 RR]
+9.8551 0 1 LAPD 2025 ----- 0 2.0 1.0 -1 15 0.00 -95.00 42.30 -71.10[1 30 S 14 RR]
-9.8551 0 1 LAPD 2025 ----- 0 2.0 1.0 -1 15 0.00 -95.00 42.30 -71.10[1 30 S 14 RR]
e10.0232 0 1 LAPD 2025 ----- 0 2.0 1.0 -1 15 0.00 -95.00 42.30 -71.10[1 30 S 14 RR]
error
+10.589 2 0 LAPD 2025 ----- 0 2.0 1.0 -1 15 30.90 -122.30 0.00 -95.00[29 1 S 14 RR]
-10.589 2 0 LAPD 2025 ----- 0 2.0 1.0 -1 15 30.90 -122.30 0.00 -95.00[29 1 S 14 RR] -
T200 = 900 ms expired
r10.7551 2 0 LAPD 2025 ----- 0 2.0 1.0 -1 15 30.90 -122.30 0.00 -95.00[29 1 S 14 RR]
+10.7551 0 1 LAPD 2025 ----- 0 2.0 1.0 -1 15 0.00 -95.00 42.30 -71.10[1 30 S 14 RR]
-10.7551 0 1 LAPD 2025 ----- 0 2.0 1.0 -1 15 0.00 -95.00 42.30 -71.10[1 30 S 14 RR]
r10.9232 0 1 LAPD 2025 ----- 0 2.0 1.0 -1 15 0.00 -95.00 42.30 -71.10[1 30 S 14 RR]

```

FIGURE 7: TCH call set-up time with channel error probability 7%.

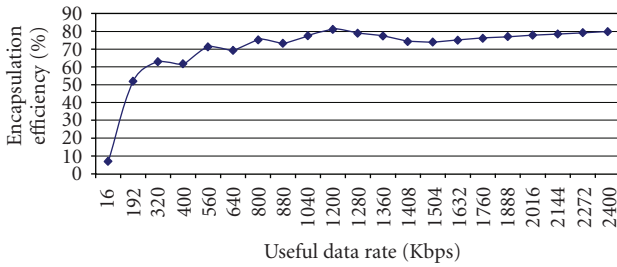


FIGURE 8: Encapsulation efficiency versus useful data rate for DVB-S2 short frames.

From Figure 8, we can observe that configuration of one TRX will have poor encapsulation efficiency. With increasing of Abis data rate encapsulation efficiency improves and varies for different data rates. Figure 9 shows Encapsulation efficiency versus useful data rate for DVB-S2 long frames.

In comparison to DVB-S2 short frames, long frames have almost the same encapsulation efficiency. One disadvantage of DVB-S2 long frames is higher delay.

Figure 10 shows delay versus useful data rate for DVB-S2 short and long frames.

From Figure 10, we can see that in case of one TRX and one occupied TCH delay between transferring DVB-S2 frame will reach 200 ms for long and 50 ms for short frames. Delay between transmissions of DVB-S2 frames will reduce with increase of data rate on Satellite channel and on Abis interface.

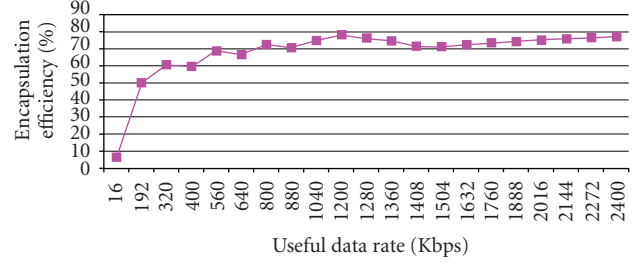


FIGURE 9: Encapsulation efficiency versus useful data rate for DVB-S2 long frames.

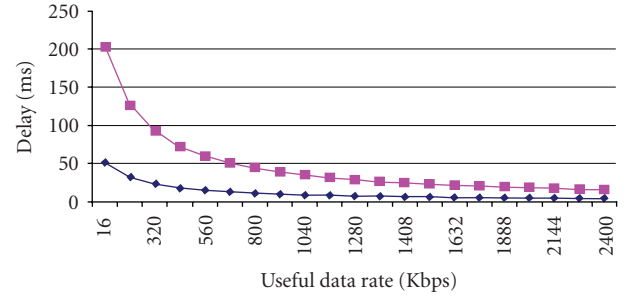


FIGURE 10: Delay versus useful data rate for DVB-S2 short and long frames.

5. Link Budget Estimations for DVB-S2 Platform

Link budget estimations are done considering GSAT-3 (<http://www.isro.org/>) satellite parameters. DVB-S2 platform has 28 modulation coding (ModCode) modes. Table 4 shows required energy per transmitted symbol E_s/N_0 (dB) is the figure obtained from computer simulations.

From (9), the required E_b/N_0 for each ModCode can be calculated

$$\frac{E_b}{N_0} = \frac{E_s}{N_0} - 10 \log(\eta_{\text{tot}}), \quad (9)$$

where η_{tot} is spectral efficiency.

C/N_0 total can be found from (10).

$$\left(\frac{C}{N_0}\right) = \frac{E_b}{N_0} + 10 \log(R_b) \text{ (dBHz)}. \quad (10)$$

R_b is Information rate (Bits/s).

DVB-S2 platform can support three Roll Off factor modes 0.35, 0.25, and 0.20. During Link Budget estimation, value of 0.25 is considered.

Different scenarios are evaluated with different numbers of BTS and TRX's within BTS. Table 5 shows all three scenarios.

Link Budget Estimations are done considering idle time slot elimination technique.

5.1. Results and Analysis. Table 6 shows obtained results for all DVB-S2 modulation modes with FEC 3/4, for a single BTS connection point-to-point SCPC link.

TABLE 3: Different network parameters during simulation.

Number of TRX	DFL short frame bit	DFL long frame bit	Abis DR Kbps	MS	Useful data rate Kbps	Satellite data rate Kbps
1	11712	48408	320	1	16	400
2	11712	48408	512	12	192	592
3	11712	48408	704	20	320	784
4	11712	48408	896	25	400	976
5	11712	48408	1088	35	560	1168
6	11712	48408	1280	40	640	1360
7	11712	48408	1472	50	800	1552
8	11712	48408	1664	55	880	1744
9	11712	48408	1856	65	1040	1936
10	11712	48408	2048	75	1200	2128
11	11712	48408	2240	80	1280	2320
12	11712	48408	2432	85	1360	2512
13	11712	48408	2624	88	1408	2704
14	11712	48408	2816	94	1504	2896
15	11712	48408	3008	102	1632	3088
16	11712	48408	3200	110	1760	3280
17	11712	48408	3392	118	1888	3472
18	11712	48408	3584	126	2016	3664
19	11712	48408	3776	134	2144	3856
20	11712	48408	3968	142	2272	4048
21	11712	48408	4160	150	2400	4240

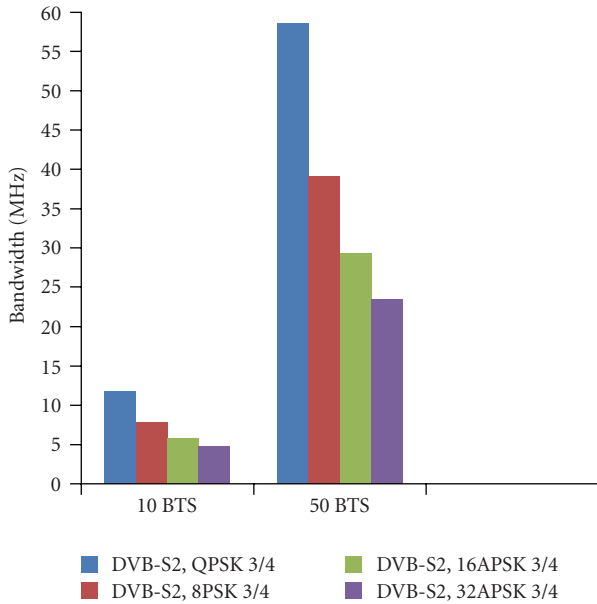


FIGURE 11: Required bandwidth for 10 and 50 BTS.

Figure 11 gives a comparison between two scenarios considering 10 and 50 BTS for DVB-S2 platform.

The cost of bandwidth on Satellite is taken as 4000 US \$ per 1 MHz per month [12]. Since Satellite is distance insensitive, this cost will be constant, in comparison to terrestrial scenario where cost of the 2.048 Mbps E1 channel is distance-dependent.

TABLE 4: E_s/N_0 performance at Quasi-Error-Free PER = 10^{-7} (AWGN channel).

Mode	Spectral efficiency (η_{tot})	Ideal E_s/N_0 (dB) for FECFRAME length = 64 800 bit
QPSK 3/4	1,487473	4,03
8PSK 3/4	2,228124	7,91
16APSK 3/4	2,966728	10,21
32APSK 3/4	3,703295	12,73

TABLE 5: Number of TRX for each case.

	Single BTS	10 BTS	50 BTS
No of TRX	8,4,1	3	3

Figure 12 illustrates cost of bandwidth per month for single BTS configuration with different number of TRX.

Figure 13 shows a comparison of different scenarios of 10 and 50 BTS configuration with 3 TRX in each BTS.

6. Conclusions

During studies of Abis interface, it was found that one of the weaknesses of this interface is that there is no network layer to serve number of BTSs which are located in different areas within the network and connected via Geostationary Satellite.

TABLE 6: Required bandwidth for all modulation modes of DVB-S2 for single BTS configuration.

		SCPC, 8TRX	SCPC, 4TRX	SCPC, TRX
Information Rate	kbps	1664	896	320
Occupied RF bandwidth (QPSK)	KHz	1386,6	746,6	266,6
Occupied RF bandwidth (8PSK)	KHz	924,44	497,77	177,77
Occupied RF bandwidth (16APSK)	KHz	693,33	373,33	133,33
Occupied RF bandwidth (32APSK)	KHz	554,66	298,66	106,66

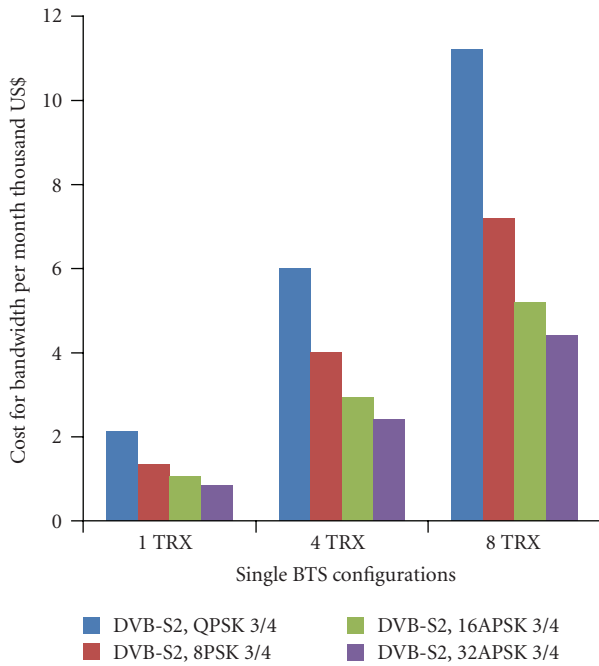


FIGURE 12: Required cost for bandwidth for single BTS configuration.

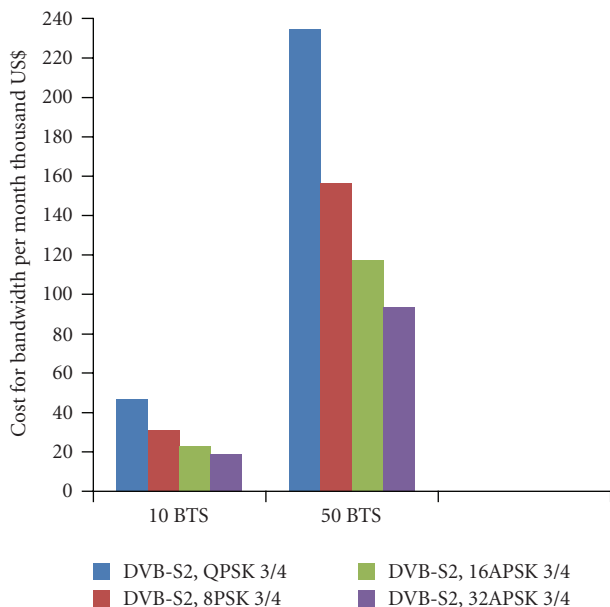


FIGURE 13: Required cost for bandwidth with more number of BTS.

Traffic and subscriber density calculations show that more numbers of SDCCH and TCH channels should be configured to serve the same amount of MS's as in terrestrial scenario.

From the above results, it can be concluded that continuous retransmission of LAPD frames will cause high link congestion which is due to small value of T_{200} . Frame loss will delay call set-up time. From simulation, it is observed that round trip delay for DVB-S2 short frames will reach 334 ms. It is suggested to set the number of retransmissions counter N_{200} to the maximum value in Abis over Satellite to overcome losses on Satellite channel. It is observed that increase of number of TRX and useful data rate will improve encapsulation efficiency, and Satellite resources will be utilized more efficiently while using DVB-S2 platform. It is also observed that DVB-S2 long frames are not suitable because of higher delay between retransmissions. When the number of TRX reaches 10 and the number of MS 75 encapsulation efficiency reaches to 80%, delay between transmitting DVB-S2 short frames will reach 8 ms which is acceptable for Satellite environment.

Simulation results on DVB-S2 encapsulation show that different ModCode modes will give different encapsulation efficiencies. For efficient encapsulation into DVB-S2 frame, appropriate ModCode mode should be chosen; however, the selection of the ModCode is dependent on the channel fades encountered. It is concluded that DVB-S2 will provide several advantages like improved Roll-Off factor, different power and bandwidth efficient modulation modes. For efficient utilization of frequency spectrum parameters such as padding efficiency and overall encapsulation efficiencies should be evaluated.

Present development of 3G and 4G systems in the world market shows that requirement for new services and higher data rates will grow. 3G (WCDMA/UMTS) which offers 2M of data rate per subscriber is a good gateway in the world of Data and Internet. Hence it is important to know how these technologies may be provided in the remote areas efficiently for 24 hours in a day.

Paper addressed only GSM technology. Future work for 3G, 4G technologies should be done.

References

[1] ETSI EN 302 307 version1.1.1, "Digital Video Broadcasting (DVB); Second generation framing structure, channel coding and modulation systems for Broadcasting, Interactive Services, News Gathering and other broadband satellite applications," 2004.

- [2] S. B. Musabekov, P. K. Srinivasan, A. S. Durai, and R. R. Ibroimov, "Simulation analysis of abis interface over IP over DVB-S2-RCS in a GSM over satellite network," in *Proceedings of the 4th IEEE/IFIP International Conference in Central Asia on Internet (ICI '08)*, September 2008.
- [3] The VINT Project, "The ns Manual (formerly ns Notes and Documentation)," July 2008.
- [4] DVB Document A134, "Generic Stream Encapsulation (GSE) Implementation Guidelines," February 2009.
- [5] Ses New Skies B.V., "GSM Over Satellite," 2006.
- [6] 3GPP TS 08.58 version 8.6.0, "Base Station Controller—Base Transceiver Station (BSC-BTS) Interface Layer 3 Specification," <http://www.3gpp.org/>.
- [7] 3GPP TS 08.56 version 8.0.1, "BSC-BTS Layer 2; Specification," <http://www.3gpp.org/>.
- [8] 3GPP TS 08.54 version 8.0.1, "BSC-BTS Layer 1; Structure of Physical Circuits," <http://www.3gpp.org/>.
- [9] ETSI EN 300 737, "Digital cellular telecommunication systems (Phase2+) In-band control of remote transcoders and rate adaptors for full rate traffic channels," V7.2.1, September 2000.
- [10] S. B. Musabekov and R. R. Ibraimov, "NS-2 network performance evaluation of abis interface over DVB-S2 in the GSM over satellite network," in *Proceedings of the 1st Asian Himalayas International Conference on Internet (AH-ICI '09)*, pp. 1–5, 2009.
- [11] ETS 300 125, "Integrated Services Digital Network (ISDN); User-network interface data link layer specification; Application of CCITT Recommendations Q.920/I.440 and Q.921/I.441," part-2, subclause 5.9.1, September 1991.
- [12] Globecom, "Optimizing GSM Abis Extensions Via Satellite," 2006.